

Proposed Automobile Steering Wheel Test Method for Vibration

A thesis submitted for the Degree of Doctor of Philosophy

by

Byung Ho Jeon

School of Engineering and Design

Brunel University

August 2010

Abstract

This thesis proposes a test method for evaluating the perceived vibration which occurs at the driver's hand in automotive steering wheel interface. The objective of the research was to develop frequency weightings for quantifying the human perception of steering wheel hand-arm vibration. Family of frequency weightings were developed from equal sensation curves obtained from the psychophysical laboratory experimental tests.

The previous literature suggests that the only internationally standardised frequency weighting W_h is not accurate to predict human perception of steering wheel hand-arm vibration (Amman et. al, 2005) because W_h was developed originally for health effects, not for the human perception. In addition, most of the data in hand-arm vibration are based upon responses from male subjects (Neely and Burström, 2006) and previous studies based only on sinusoidal stimuli. Further, it has been continuously suggested by researchers (Gnanasekarna et al., 2006; Morioka and Griffin, 2006; Ajovalasit and Giacomini, 2009) that only one weighting is not optimal to estimate the human perception at all vibrational magnitudes.

In order to address these problems, the investigation of the effect of gender, body mass and the signal type on the equal sensation curves has been performed by means of psychophysical laboratory experimental tests. The test participants were seated on a steering wheel simulator which consists of a rigid frame, a rigid steering wheel, an automobile seat, an electrodynamic shaker unit, a power amplifier and a signal generator. The category-ratio Borg CR10 scale procedure was used to quantify the perceived vibration intensity. A same test protocol was used for each test and for each test subject.

The first experiment was conducted to investigate the effect of gender using sinusoidal vibration with 40 test participants (20 males and 20 females). The results suggested that the male participants provided generally lower subjective ratings than the female participants. The second experiment was conducted using band-limited random vibration to investigate the effect of signal type between sinusoidal and band-limited random vibration with 30 test participants (15 males and 15 females). The results

suggested that the equal sensation curves obtained using random vibration were generally steeper and deeper in the shape of the curves than those obtained using sinusoidal vibration. These differences may be due to the characteristics of random vibration which produce generally higher crest factors than sinusoidal vibration. The third experiment was conducted to investigate the effect of physical body mass with 40 test participants (20 light and 20 heavy participants) using sinusoidal vibration. The results suggested that the light participants produced generally higher subjective ratings than the heavy participants. From the results it can be suggested that the equal sensation curves for steering wheel rotational vibration differ mainly due to differences of body size rather than differences of gender. The final experiment was conducted using real road signals to quantify the human subjective response to representative driving condition and to use the results to define the selection method for choosing the adequate frequency weightings for the road signals by means of correlation analysis. The final experiment was performed with 40 test participants (20 light and 20 heavy participants) using 21 real road signals obtained from the road tests. From the results the hypothesis was established that different amplitude groups may require different frequency weightings. Three amplitude groups were defined and the frequency weightings were selected for each amplitude group.

The following findings can be drawn from the research:

- the equal sensation curves suggest a nonlinear dependency on both the frequency and the amplitude.
- the subjective responses obtained from band-limited random stimuli were steeper and the deeper in the shape of the equal sensation curves than those obtained using sinusoidal vibration stimuli.
- females provided higher perceived intensity values than the males for the same physical stimulus at most frequencies.
- light test participants provided higher perceived intensity than the heavy test participants for the same physical stimulus at most frequencies.
- the equal sensation curves for steering wheel rotational vibration differ mainly due to differences in body size, rather than differences of gender.
- at least three frequency weightings may be necessary to estimate the subjective intensity for road surface stimuli.

Acknowledgments

First of all I would like to thank God who allows to accomplish this thesis.

I would like to give my special gratitude to my supervisor Professor Joseph A. Giacomini who has provided great effort and constant support. I would like also to thank him for his valuable contributions of scientific knowledge and criticism that helped this research work to be completed professionally.

I am indebted to my colleagues of the PES (Perception Enhancement Systems) research group, Dr. Marco Ajovalasit and Dr. Tania Paloma Berber-Solano, for their support, friendship, feedback and contribution to my work.

This thesis would not have been possible unless more than a hundred of people who were the staff or students of Brunel University and friends of mine participated voluntarily in the several experiments. I appreciate them once again for their willingness.

I am specially acknowledge my former professors, Prof. Sung Kyun Kim and Prof. Jae Hyo Lee in Konkuk University for their kind recommendation letters, and my former manager, Mr Sung Kyu Kim, and many former colleagues in Hyundai Motor Company for their invaluable comments while corresponding of mails.

I am grateful to my family and parents of both families, who gave me the constant support with their love and prayer. They provided the moral support when I am in distressed circumstances and the economical support when I am in financial difficulties. Most of all I owe my deepest gratitude to my wife, Ho-Kyoung, who stood behind me all the time and encouraged me even in a weak moment. My special thanks go to my only daughter, Ha-Eun, who always cheered me up and never lost her smile by my side.

List of Contents

Abstract	II
Acknowledgments	IV
List of Contents	V
List of Figures	VIII
List of Tables	XIII
Nomenclature	XVI
1. Introduction	1
1.1 Steering Wheel Vibration	1
1.2 Quantifying the Human Subjective Response to Steering Wheel Vibration.....	5
1.3 Research Objectives.....	9
2. Psychophysics	11
2.1 Psychophysical Scaling.....	13
2.2 Indirect Scaling Methods	15
2.2.1 The Method of Constant Stimuli	15
2.2.2 The Method of Limits	15
2.2.3 The Method of Adjustment	16
2.2.4 The Paired-Comparisons Method Using Thurstone's Model.....	16
2.3 direct Scaling Methods	17
2.3.1 The Method of Magnitude Estimation	17
2.3.2 The Method of Magnitude Production	18
2.3.3 Category Scaling	18
2.3.4 Category-Ratio Scaling (Borg CR10 Scale).....	19
3. Hand-arm vibration	21
3.1 Biomechanical Response of the Hand-Arm System	21
3.1.1 Mechanical Impedance of the Hand-Arm System.....	21
3.1.2 Vibration Transmissibility through the Hand-Arm Vibration	24
3.2 Human Subjective Response to Hand-Arm Vibration	26
3.2.1 The Mechanoreceptors of Human Skin.....	27
3.2.2 Effect of Vibration Frequency on Subjective Response.....	29
3.2.3 Effect of Vibration Magnitude on Subjective Response	32
3.2.4 Effect of Vibration Direction on Subjective Response.....	35
3.2.5 Effect of Vibration Duration on Subjective Response	36
4. A Review of Digital Signal Processing	39
4.1 Introduction.....	39
4.2 Classification of Signals	39
4.2.1 Continuous and Discrete Signals.....	40
4.2.2 Deterministic and Random Signals	42
4.3 Global Signal Statistics	44
4.3.1 Root Mean Square Value	44
4.3.2 Skewness	45
4.3.3 Kurtosis	45
4.3.4 Root Mean Quad Value.....	45
4.3.5 Crest Factor Value.....	46
4.4 Frequency Domain Analysis.....	46
4.4.1 The Fourier Transform.....	46
4.4.2 The Discrete Fourier Transform (DFT).....	47
4.4.3 The Fast Fourier Transform (FFT)	47

4.5 Digital Filters	49
4.5.1 Finite Impulse Response (FIR) Filters	50
4.5.1.1 FIR Filter Design	52
4.5.2 Infinite Impulse Response (IIR) Filters	55
4.5.2.1 IIR Filter Design	56
4.5.2.2 Some Typical IIR Filters.....	57
5. Steering Wheel Vibration Measurement from Road Testing.....	60
5.1 Introduction.....	60
5.2 Experimental Vibration Tests	61
5.2.1 Mira Tests.....	62
5.2.2 Michelin Tests	67
5.2.3 Honda Tests.....	71
5.2.4 Uxbridge Tests	75
5.2.5 Summary of the Road Testing Data	80
6. Human Subjective Response to Steering Wheel Hand-Arm Vibration consisting of Sinusoidal Vibration	83
6.1 Introduction.....	83
6.2 Experimental Apparatus.....	86
6.2.1 Test Facility.....	86
6.2.2 Accuracy of Signal Reproduction	87
6.3 Laboratory Based Experimental Testing using Sinusoidal Vibration	89
6.3.1 Test Stimuli	89
6.3.2 Test Subjects	92
6.3.3 Test Protocol	92
6.3.4 Multivariate Regression Methods	92
6.3.4.1 MethodI: Least Squares Regression Procedure.....	96
6.3.4.2 MethodII: All Possible Regressions Procedure	96
6.3.4.3 MethodIII: Backward Elimination Procedure.....	96
6.3.4.4 MethodIV: Stepwise Regression Procedure	96
6.3.5 Results	98
6.3.5.1 Effect of the Multivariate Regression Approach	98
6.3.5.2 Effect of Gender	101
6.4 Discussion.....	103
6.3 Summary.....	105
7. Human Subjective Response to Steering Wheel Hand-Arm Vibration consisting of Random Vibration	107
7.1 Introduction.....	107
7.2 Laboratory Based Experimental Testing using Random Vibration	108
7.2.1 Test Stimuli	108
7.2.2 Test Subjects	111
7.2.3 Results	112
7.2.3.1 Effect of the Signal Type	115
7.2.3.2 Confirming of the Effect of Gender.....	116
7.3 Discussion.....	117
7.4 Summary.....	118
8. Effect of Physical Body Mass Difference on the Subjective Perceived Intensity of Steering Wheel Vibration	120
8.1 Introduction.....	120
8.2 Laboratory Based Experimental Testing for Effect of the Physical Body Mass	121
8.2.1 Test Subjects	121
8.2.2 Results	122

8.2.2.1 Effect of Physical Body Mass	124
8.3 Discussion.....	127
8.4 Summary	128
9. Human Subjective Response to Steering Wheel Hand-Arm Vibration using the Real Road Stimuli.....	130
9.1 Introduction.....	130
9.2 Laboratory Based Experimental Testing using Real Road Stimuli.....	131
9.2.1 Test Stimuli	131
9.2.2 Test Subjects	133
9.2.3 Results	134
9.3 Discussion.....	135
9.4 Frequency Weightings developed from the Equal Sensation Curves	136
9.4.1 Estimates obtained by means of the Frequency Weightings	138
9.4.2 Selection of the Frequency Weightings.....	140
9.5 Summary.....	144
10. Conclusions and Recommendations for Future Research.....	146
10.1 Summary of the Research Findings	146
10.2 Recommended Test Protocol for Evaluating Automotive Steering Wheel Rotational Vibration.....	151
10.3 Suggested Future Research	153
References	155
Appendix A. Technical Specifications of Experimental laboratory tests.....	169
Appendix B. Geometrical Dimension of Clamp for Vibration Measurement	179
Appendix C. Laboratory Test Sheets	183
Appendix D. Weighting Filters	188

List of Figures

Figure 1.1	Vibration stimuli arriving at the driver of a road vehicle.	2
Figure 1.2	Three axes of vibration measured on a steering a wheel.	3
Figure 1.3	Mean acceleration power spectral densities for steering wheel vibrations of petrol and diesel automobiles in all three axes (x, y and z) measured on large, medium and small automobiles.	4
Figure 1.4	Mean acceleration power spectral densities for seat vibrations of petrol and diesel automobiles in all three axes (x, y and z) measured on large, medium and small automobiles.	5
Figure 1.5	W_h frequency weighting curve for hand-transmitted vibration defined in ISO 5349-1.	7
Figure 1.6	Comparison between the proposed frequency weighting W_s for rotational steering wheel vibration and frequency weighting W_h .	8
Figure 2.1	Relationship between the perceived sensation and the stimulus intensity according to Fechner's law.	12
Figure 2.2	Relationship between stimulus intensity and perceived sensation according to Stevens' power law.	13
Figure 2.3	Four main types of measurement scale.	14
Figure 2.4	The Borg CR10 scale.	20
Figure 3.1	Mechanical driving point impedance of the hand-arm system in the three orthogonal directions as defined in ISO 5349, the dotted line indicates the mean value, the dark lines indicate the maximum value, and the dashed line represents impedance values of a 4-degree-of-freedom biodynamic model: X_h direction, Y_h direction and Z_h direction.	23
Figure 3.2	Mean transmissibility curves for vibration in the vertical direction, horizontal direction and axial direction, to the hand and arm positions [middle phalanx; proximal phalanx; third metacarpal; triquetrum carpal; styloid process of ulna; olecranon; medial epicondyle; acromoin].	25
Figure 3.3	Location of the mechanoreceptors in hairy and glabrous skin of the human hand.	27
Figure 3.4	Properties of the four-channel model of mechanoreception.	28

Figure 3.5	Detection threshold as a function of frequency and of contactor area for the four individual tactile channels.	29
Figure 3.6	Equal sensation magnitude contours. Each curve describes the combinations of frequency and intensity that give rise to equal sensation magnitudes.	30
Figure 3.7	Equal sensation data from studies of translational and rotational vibration.	31
Figure 3.8	Subjective magnitude of suprathreshold vibration presented at the fingertip at frequencies of 25, 100, 250 and 500 Hz.	33
Figure 3.9	Subjective response to sinusoidal hand-arm vibration of 30 Hz and 75 Hz. Data was determined for engineers with experience in analysing vibration and individuals with no specific experience in analysing vibration.	34
Figure 3.10	Standardised anatomical and basicentric co-ordinate system for the directions of vibration for the hand.	35
Figure 3.11	Temporal summation effects on vibrotactile perception threshold.	37
Figure 4.1	Classification of signals.	40
Figure 4.2	Effect of the aliasing appeared by improper sampling.	41
Figure 4.3	Effect of the quantization appeared by converting the values of each sample from continuous (analog input) to discrete (digital output)	41
Figure 4.4	The Gaussian distribution.	43
Figure 4.5	Examples of a stationary and non-stationary time histories: Stationary Gaussian signal (Highway Surface), Mildly non-stationary signal (Speed Circuit Surface) and Heavily non-stationary signal (Bump).	44
Figure 4.6	Sampling a continuous function of time at regular intervals.	47
Figure 4.7	Partitioning the sequences x_r into two half sequences y_r and z_r .	48
Figure 4.8	A transfer function of input and output.	49
Figure 4.9	The four typical frequency responses; A low-pass, high-pass, band-pass and a band-stop responses.	51

Figure 4.10	Three parameters for evaluation frequency domain performance with comparisons between poor and good example of performance.	52
Figure 4.11	Input signal not periodic in time record.	53
Figure 4.12	Conversion from digital to analog frequencies.	57
Figure 5.1	Road surfaces used by MIRA for their steering wheel vibration tests.	64
Figure 5.2	A 7 second segments of the tangential acceleration time history measured at the steering wheel for each of the six road surfaces (The MIRA test).	65
Figure 5.3	Power Spectral Densities (PSD) calculated from the four tangential acceleration time histories of the 2 minute duration which were measured at the steering wheel.	67
Figure 5.4	Road surfaces used by Michelin for their steering wheel vibration tests.	68
Figure 5.5	A 7 second segments of the tangential acceleration time history measured at the steering wheel for each of the four road surfaces (The Michelin test).	69
Figure 5.6	Power Spectral Densities (PSD) calculated from the four tangential acceleration time histories of the 1 minute duration which were measured at the steering wheel.	70
Figure 5.7	Road surfaces used by Honda for their steering wheel vibration tests.	72
Figure 5.8	A 7 second segments of the tangential acceleration time history measured at the steering wheel for each of the six road surfaces (The Honda test).	73
Figure 5.9	Power Spectral Densities (PSD) calculated from the two tangential acceleration time histories of the 1 minute duration which were measured at the steering wheel.	74
Figure 5.10	Road surfaces for the Uxbridge steering wheel tests.	77
Figure 5.11	A 7 second segments of the tangential acceleration time history measured at the steering wheel for each of the five road surfaces (The Uxbridge test).	78

Figure 5.12	Power Spectral Densities (PSD) calculated from the four tangential acceleration time histories of the 1 minute duration which were measured at the steering wheel.	79
Figure 5.13	Comparison between the root mean square value and the root mean quad value of the 21 road surfaces.	80
Figure 5.14	Distribution of the statistical values of the 21 road surfaces: r.m.s. acceleration level against r.m.q. value.	81
Figure 5.15	The minimum, mean and the maximum vibrational magnitude for each frequency of the 21 road surfaces.	82
Figure 6.1	Steering wheel vibration test rig and associated electronics.	87
Figure 6.2	Comparison the 86 sinusoidal rotational steering wheel vibration stimuli with the hand-arm vibration perception threshold and the hand-arm vibration annoyance threshold.	91
Figure 6.3	Equal sensation curves obtained for Borg subjective perceived intensity values from 0.5 to 8.0 using the four regression procedures in the experiment: Least-square regression procedure, All possible regressions procedure, Backward elimination regression procedure and Stepwise regression procedure.	100
Figure 6.4	Equal sensation curves obtained separately for the male test participants (n = 20) and for the female test participants (n = 20), obtained by means of the stepwise regression procedure.	102
Figure 6.5	Equal sensation curves obtained in the current study and those obtained in previous studies of hand-arm translational or rotational vibration.	104
Figure 7.1	Gaussian white noise signal used to be filtered by applying Butterworth band-pass filter	109
Figure 7.2	Three examples of the band-limited random signals used in the experiment: time series representation and power spectral density (PSD) representation.	110
Figure 7.3	Equal sensation curves obtained for Borg subjective perceived intensity values from 0.5 to 8.0 using the regression formula obtained for the band-limited random vibration.	114
Figure 7.4	Comparison of the equal sensation curves which were obtained using the band-limited random signals to those obtained using	115

the sinusoidal signals.

Figure 7.5	Equal sensation curves obtained separately for the male test participants and for the female test participants, obtained by means of the stepwise regression procedure using sinusoidal vibration stimuli and band-limited random vibration stimuli.	117
Figure 8.1	Equal sensation curves for the complete group of 40 participants obtained for Borg subjective perceived intensity values from 0.5 to 8.0 using the regression formula obtained for sinusoidal vibration.	124
Figure 8.2	Equal sensation curves obtained separately for the light test participants and the heavy test participants using the regression formulas obtained for sinusoidal vibration.	127
Figure 9.1	Comparisons the existing frequency weightings W_h (ISO 5349-1, 2001) and W_s (Giacomin et al., 2004) to the W_{ss_n} and W_{sr_n} frequency weightings obtained from the equal sensation curves using sinusoidal and band-limited random steering wheel rotational vibration respectively.	138
Figure 9.2	Comparison of the amplitude range of the steering wheel road vibration signals, the equal sensation curves obtained using band-limited random signals and the perception threshold curves defined by Miwa (1967) and by Morioka (2004).	141
Figure 10.1	Test method for evaluating steering wheel vibration in automobiles.	152

List of Tables

Table 5.1	Global statistical properties of the six road stimuli measured from Mira tests.	66
Table 5.2	Global statistical properties of the four Michelin road stimuli.	70
Table 5.3	Global statistical properties of the six Honda road stimuli.	74
Table 5.4	Global statistical properties of the five Uxbridge road stimuli.	79
Table 6.1	Test protocol parameters adopted in previous studies of human subjective response sinusoidal hand-arm vibration.	85
Table 6.2	Geometric dimensions of the steering wheel rotational vibration test rig.	87
Table 6.3	Bench steering vibration reproduction error defined as a percentage of the target r.m.s. acceleration level (n = 3 test subjects).	89
Table 6.4	Frequency and amplitude of the 86 sinusoidal rotational steering wheel vibration stimuli.	91
Table 6.5	Mean and standard deviation summary statistics for the test participants.	92
Table 6.6	Minimum and maximum angles of the wrist, elbow, shoulder and back which were found to guarantee postural comfort.	93
Table 6.7	Steering wheel rotational vibration testing protocol.	95
Table 6.8	Summary of the subjective responses to sinusoidal steering wheel vibration stimuli obtained by means of Borg CR10 scale (n = 40).	99
Table 6.9	Goodness of fit statistics obtained for overall data set in both experiments (n = 40).	100
Table 6.10	Goodness of fit statistics obtained separately for the male test participants data set (n = 20) and for the female test participants data set (n = 20).	102
Table 7.1	Frequency and amplitude of the 86 steering wheel rotational 1/3 octave band-limited random vibration stimuli.	111
Table 7.2	Mean and standard deviation summary statistics for the test participants.	112

Table 7.3	Summary of the subjective responses obtained by means of Borg CR10 scale.	113
Table 7.4	Goodness of fit statistics obtained for overall data set (n = 30).	113
Table 7.5	Goodness of fit statistics obtained by fitting to the data of the male test participants (n = 20) and the female test participants (n = 20) separately.	116
Table 8.1	Mean and standard deviation summary statistics for the test participants.	121
Table 8.2	Summary of the subjective response of the complete group of 40 test subjects to sinusoidal steering wheel vibration, obtained by means of Borg CR10 scale.	122
Table 8.3	Goodness of fit statistics obtained for overall data set (n = 40).	123
Table 8.4	Summary of the subjective response obtained separately for the light test participants data set (n = 20) and for the heavy test participants data set (n = 20) by means of Borg CR10 scale.	125
Table 8.5	Goodness of fit statistics obtained separately for the light test participants data set (n = 20) and for the heavy test participants data set (n = 20).	126
Table 9.1	Global statistical properties of the 21 road stimuli used the laboratory experimental testing.	132
Table 9.2	Steering wheel rotational vibration testing protocol.	133
Table 9.3	Mean and standard deviation summary statistics for the test participants.	134
Table 9.4	Mean and standard deviation Borg CR10 subjective intensity values obtained for the complete group of test participants and for the light and heavy subgroups, for each road stimuli.	135
Table 9.5	The r.m.s. acceleration magnitudes of the unweighted, the W_h weighted, the W_s weighted and both the W_{ss_n} and W_{sr_n} weighted signals along with the corresponding mean Borg CR10 subjective response value for the stimulus.	139
Table 9.6	Procedure used to define the adequate frequency weighting.	140
Table 9.7	The r.m.s. acceleration values of the steering wheel acceleration signals in each frequency range.	142

Table 9.8 The correlation coefficients results obtained between the weighted r.m.s. values of the road signals by both the W_{ss_n} and the W_{sr_n} filters and the subjective responses for each amplitude level group. 143

Nomenclature

a	r.m.s. acceleration magnitude [m/s^2]
$a(k)$	Coefficients of the non-recursive component of the filter
$a_{in}(f)$	Acceleration value at the input reference point [m/s^2]
$a_{out}(f)$	Acceleration value at the output reference point [m/s^2]
A	Sinusoidal motion amplitude
$b(k)$	Coefficients of the recursive component of the filter
$B_n(s)$	n_{th} order Bessel polynomial
c	Weber fraction constant
$C_n(\omega)$	Chebyshev polynomials
C_p	Total squared error
d_0	Normalizing constant of the Bessel filter
dB	Decibel
f	Frequency [Hz]
f_s	Sampling frequency
$F(f)$	Input force [N]
$h(k)$	Filter coefficient array
$H(k)$	Frequency response function of the FIR filter
$H(f)$	Transmissibility function
$H(s)$	Frequency response function of the filter in s-domain
$H_z(z)$	Frequency response function of the filter in z-domain
$H(\omega)$	Frequency response function of the IIR filter
G_{xx}	Auto-power spectral density of a time series [$(\text{m/s}^2)^2/\text{Hz}$]
I	Physical intensity of stimulus
j	Number of data in a time series
k	Constant determined from the measurement units
K_t	Kurtosis [dimensionless]
L	Ripple properties parameter
M, N	Number of taps of the filter
n_d	Number of averages
n_D	Number of test conditions of diesel cars
n_P	Number of test conditions of petrol cars
n_s	Number of test stimuli
N	Number of data points [samples]
N_s	Number of sample records in a time series
p	Number of parameters in a regression model
$p(x)$	Probability density function of a time series
$P(x)$	Probability distribution of a time series
r_{jk}	Coefficient of correlation between stimulus j and stimulus k
$r.m.s.$	Root mean square [m/s^2]
$r.m.q.$	Root mean quad [$\text{m/s}^{1.75}$]
R^2	Coefficient of determination
R_a^2	Adjusted coefficient of determination
$R_n(\omega L)$	Chebyshev rational function
R_{xx}	Auto-correlation function [$(\text{m/s}^2)^2$]
R_{xy}	Cross-correlation function [$(\text{m/s}^2)^2$]
s	Unit circle ($j\omega$) in s-domain

S	Borg CR10 subjective intensity value
S_j	Subjective response scale associate to stimuli j
S_k	Subjective response scale associate to stimuli k
S_{kew}	Skewness [dimensionless]
t	Time [s]
t_s	Student t-distribution
T	Sampling period
$v(f)$	Response velocity [m/s]
$w(n)$	Window function of the FIR filter
W_h	Weighting filter for hand-arm vibration according to ISO 5349
W_s	Weighting filter for steering wheel hand-arm vibration
W_{ss_n}	Weighting filters for steering wheel hand-arm vibration developed from equal sensation curves obtained using sinusoidal vibration
W_{sr_n}	Weighting filters for steering wheel hand-arm vibration developed from equal sensation curves obtained using band-limited random vibration
x_j	Instantaneous value of a time series at sample j
x_{jmax}	Maximum instantaneous value of a time series [m/s ²]
$x(n)$	Filter input for time n
$x[n]$	Sequence of discrete signal (n th sample)
$x_c(t)$	Continuous time signal
$x(t)$	Instantaneous value of a time series [m/s ²]
X	Steering wheel fore-and-aft measurement direction
X_{th}	Stimulus magnitude at threshold
$X(\omega)$	Fourier transform dataset
$y(n)$	Filter output for time n
Y	Steering wheel lateral measurement direction
\hat{Y}_i	Estimated value in a regression model
\bar{Y}_i	Mean value of the variables in a regression model
z	Unit circle ($e^{j\omega}$) in z-domain
z_{jk}	Normal deviate of the frequency percentage of preference
Z	Steering wheel vertical measurement direction
$Z(f)$	Driving point mechanical impedance [N/ms ⁻¹]
β	Stevens' power exponent
ε	Ripple parameter in the pass-band of the Chebyshev filter
ΔI	Difference threshold in the physical stimulus of intensity
$\theta(\omega)$	Phase response of the filter
μ	Mean value [m/s ²]
μ_x	Mean value of a time series [m/s ²]
μ_x^2	Mean square value of a time series [m/s ²]
σ_j	Standard deviation of the discriminial distribution of stimulus j
σ_k	Standard deviation of the discriminial distribution of stimulus k
σ^2	Estimate of the error variance
σ_x^2	Variance of a time series [m/s ²]
Ψ	Sensation magnitude
Ψ_0	Sensation magnitude at threshold
ω	Angular frequency [s ⁻¹]
ω_a	Analog cut-off frequency
ω_c	Desired filter cut-off frequency

Ω_d	Digital cut-off frequency
ASTM	American Society for Testing and Materials
BS	British Standards
CR	Category-ratio
CF	Crest Factor
DAT	Digital Audio Tape
DFT	Discrete Fourier transform
dTi	Turbocharged diesel direct injection system
EFi	Electronic Fuel injection system
FA	Fast acting receptors
FHC	Fixed-Head Coupé
FIR	Finite Impulse Response
FFT	Fast Fourier transform
IIR	Infinite Impulse Response
ISO	International Organization for Standardization
JND	Just noticeable difference in sensation
LIVM	Low Impedance Voltage Mode
LMS	Leuven Measurement Systems
MSE	Residual Mean Square
MIRA	Motor Industry Research Association
NPI	Non-Pacinian channel typel
NPll	Non-Pacinian channel typell
NPlll	Non-Pacinian channel typelll
OICA	International Organization of Motor Vehicle Manufacturers
P	Pacinian channel
PAS	Power Assist Steering
PSD	Power spectral density
R	Radial
RSS	Residual sum of squares
SA	Slow acting receptors
SAL	Saloon Sedan
SAE	Society of Automotive Engineers
SD	Standard deviation
TDF	Test Data File
THD	Total harmonic distortion
TSS	Total sum of squares
WF	Weber fraction

Chapter 1

Introduction

1.1 Steering Wheel Vibration

The number of households possessing a car has been steadily increasing since the 1960s in most countries. For example, according to U.K. National Statistics (2006), 74 % of households possessed at least one car in 2003 whereas only 31 % of households owned a car in 1961. In addition, the importance of the car is reflected by the fact that 80 % of annual travels are made by car rather than by public transportation such as bus or train (National Travel Survey, 2005).

While driving or when the engine is at idle automobile drivers are continuously exposed to vibrational stimuli. Drivers perceive vibration through different vibrating surfaces including the floor panel, pedals, seat, gearshift lever and the steering wheel as shown in Figure 1.1. Of these, the steering wheel is particularly important due to the great sensitivity of the skin tactile receptors of the hand (Gescheider et al., 2004) and due to the lack of intermediate structures such as shoes or clothing which can attenuate vibration.

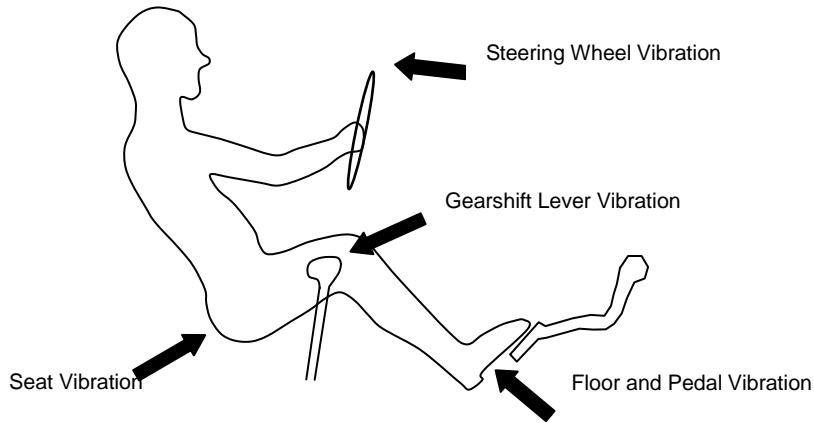


[Figure 1.1] Vibration stimuli arriving at the driver of a road vehicle.

Automobile steering wheel vibration is affected by various internal and external vibrational sources. The internal sources are the rotational irregularity of the engine which is caused by both the stochastic combustion forces and the dynamic unbalance of components such as the translating pistons. The external sources include the road surface irregularities and the aerodynamic forces. (Kim et al., 1985; Ajovalasit and Giacomini, 2007). For both the internal and external sources the vibration which actually reaches the driver is moderated by the dynamic response of the automobile chassis components.

Figure 1.2 presents the three principal vibrational axes of the steering wheel defined by standard SAE J670e (1976). The vibration at the steering wheel is normally measured along these three axes:

- The X – axis is taken along the fore-and-aft direction of the automobile with the positive direction taken as forwards, i.e. from the driver towards the front bumper.
- The Y – axis is taken along the lateral direction of the automobile with the positive direction towards the left of the vehicle.
- The Z – axis is taken along the vertical direction of the automobile with the positive direction towards the roof of the vehicle.

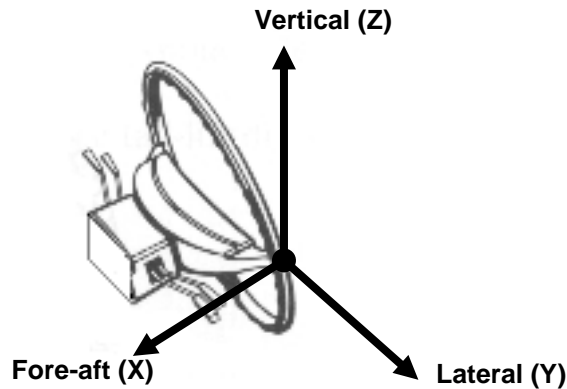


[Figure 1.2] Three axes of vibration measured on a steering a wheel.

Steering wheel vibration can reach frequencies of up to 300 Hz during driving (Giacomin et al., 2004) and vibrational modes of the wheel and column can produce large resonant peaks in the steering wheel power spectrum at frequencies from 20 to 50 Hz (Pottinger et al., 1986; Fujikawa, 1998). Although steering wheel vibrations do not normally exceed levels which present a health risk in automobiles (Masmеjean et al., 1999; Mansfield and Marshall, 2001), such vibrations nevertheless can cause discomfort, annoyance and physical or mental fatigue (Giacomin et al., 2004).

Research by Peruzzetto (1988) has shown that translational hand-arm vibration has equivalent discomfort levels to translational whole-body vibration when the acceleration level is 5 to 7 times larger. Similar results can also be found in a study performed by Bellmann (2002), which noted that the acceleration magnitudes measured at the steering wheel are several times higher, and also contain more energy, than vibrations measured at the seat or the floor panel.

Figures 1.3 and 1.4 present the acceleration power spectral densities measured along the three orthogonal directions for steering wheel and seat vibration on examples of large, medium and small automobiles. Given the acceleration levels normally measured at the steering wheel and at the seat in road vehicles, the steering wheel vibration should be considered an important source of discomfort, annoyance and fatigue during driving (Giacomin et al., 2004).

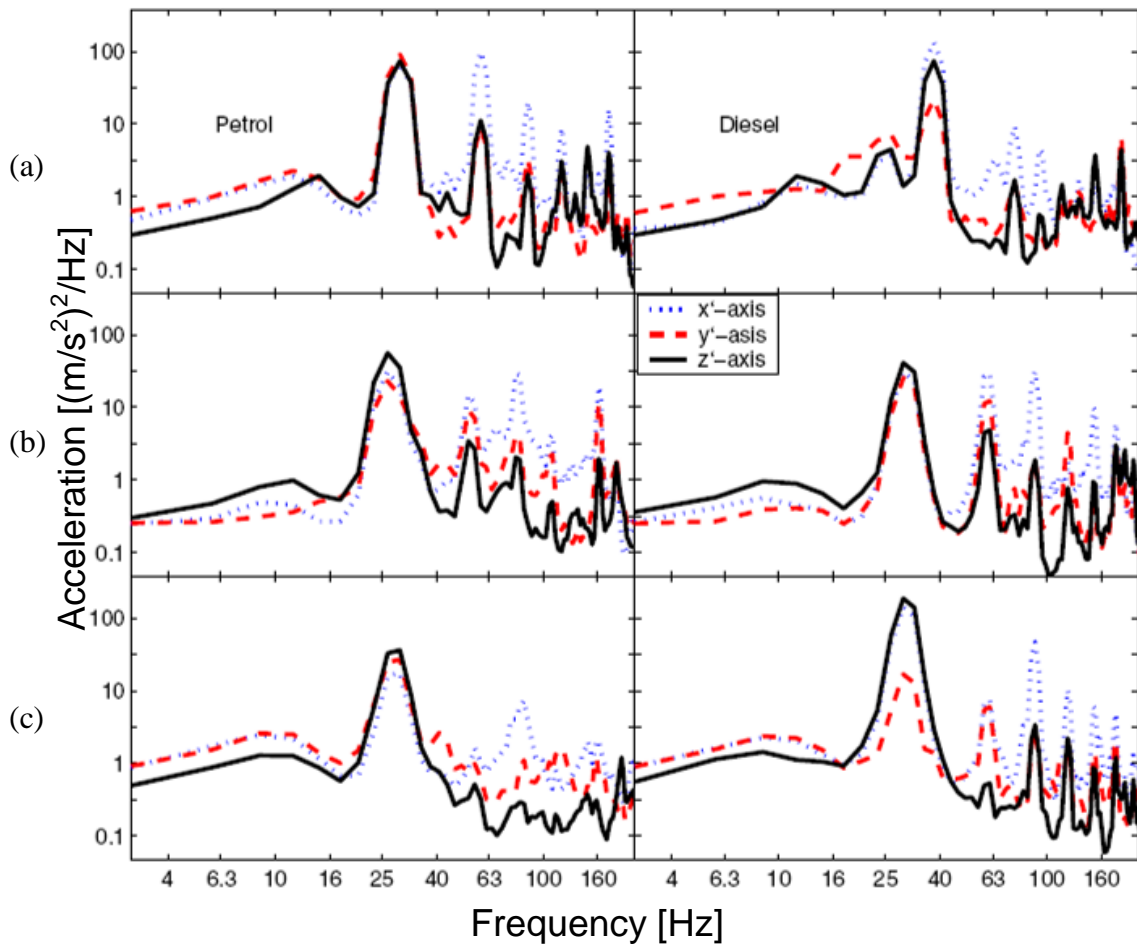


[Figure 1.3] Mean acceleration power spectral densities for steering wheel vibrations of petrol (left) and diesel (right) automobiles in all three axes (x, y and z) measured on (a) large ($n_P^* = 9$, $n_D^{**} = 26$), (b) medium ($n_P = 18$, $n_D = 27$) and (c) small ($n_P = 21$, $n_D = 22$) automobiles (adapted from Bellman, 2002).

* n_P denotes the number of test conditions of petrol cars.

** n_D denotes the number of test conditions of diesel cars.

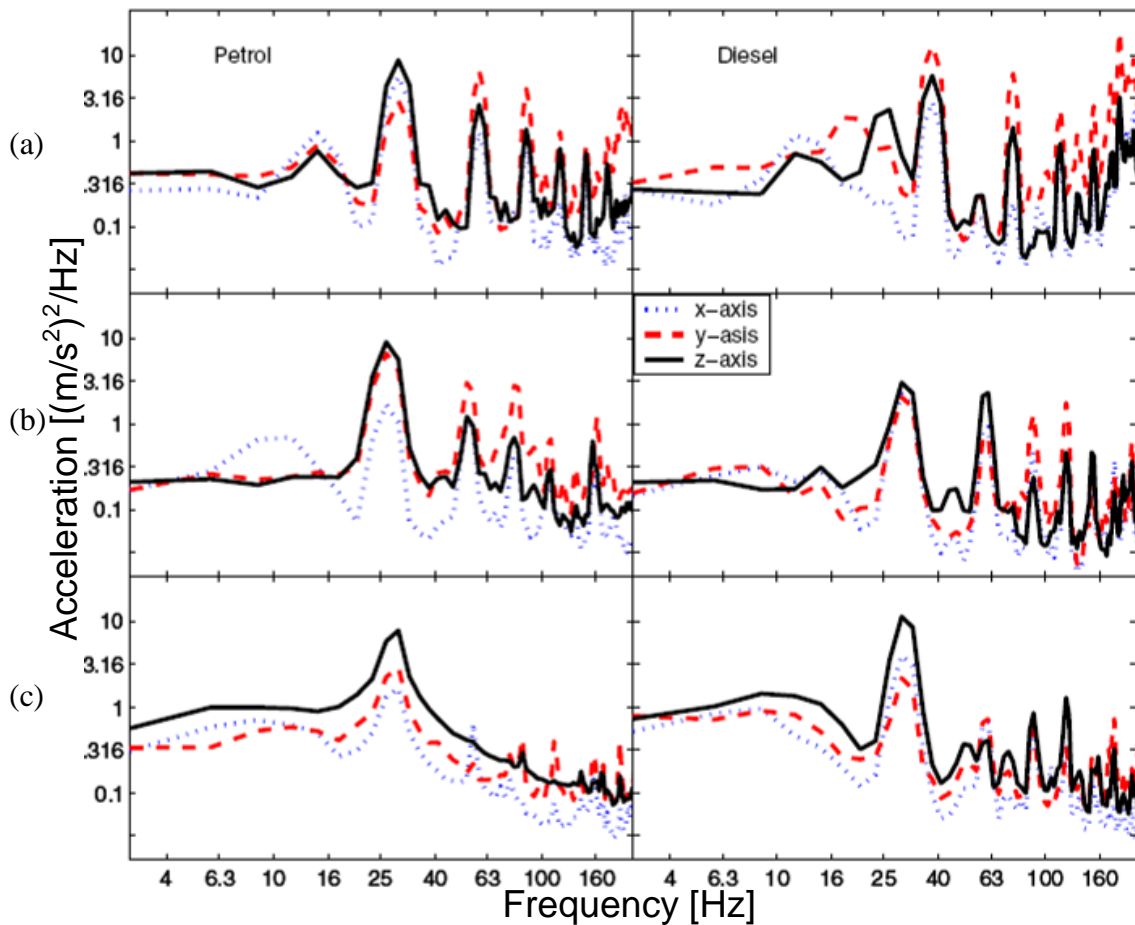


[Figure 1.4] Mean acceleration power spectral densities for seat vibrations of petrol (left) and diesel (right) automobiles in all three axes (x, y and z) measured on (a) large ($n_P^* = 9$, $n_D^{**} = 26$), (b) medium ($n_P = 18$, $n_D = 27$) and (c) small ($n_P = 21$, $n_D = 22$) automobiles (adapted from Bellman, 2002).

* n_P denotes the number of test conditions of petrol cars.

** n_D denotes the number of test conditions of diesel cars.

1.2 Quantifying the Human Subjective Response to Steering Wheel Vibration

Driver's subjective response to steering wheel vibration can be investigated from several different points of view. Research findings have been reported concerning the perceived intensity of short-term steering wheel vibration (Giacomin et al., 2004), concerning the long-term fatigue that is induced in the human upper body by steering wheel vibration (Giacomin and Screti, 2005) and concerning the cognitive information carried by

steering vibration stimuli (Giacomin and Woo, 2004). Given the importance of the perceived intensity towards both intensity and information, it is useful to know what values of the quantity are associated by drivers with various operating conditions of the automobile.

The Cambridge advanced learner's dictionary (2008) defines intensity as "the strength of something which can be measured such as light, sound, etc." With similar meaning, the term intensity is used in this research to refer to the sensation magnitude of steering wheel hand-arm vibration. This is in line with standard practice in the field of psychophysics since Fechner, the founder of psychophysics, used the term intensity when expressing psychological magnitude (Warren, 1981).

In order to quantitatively assess the perceived intensity of steering wheel vibration the recorded acceleration values are traditionally weighted according to the frequency, so as to represent the differences in human sensitivity with respect to frequency (Mansfield, 2005). A frequency weighting, commonly used for the assessment of perceived human vibration, is a transfer function which models the frequency dependency of the human subjective response (Griffin, 1990). Frequency weightings are applied to convert the physical (objective) input acceleration into perceived (subjective) human response. A frequency weighting expresses the human sensitivity by attenuating according to the frequency range (Mansfield, 2005).

The mostly commonly used hand-arm vibration standards are the International Organization for Standardization 5349-1 (2001) and British Standards Institution 6842 (1987) which both numerically specify the frequency weighting W_h . Both standards use the same frequency weighting, W_h , for each of the three translational axes of vibration at the point of entry to the hand. Figure 1.5 shows the ISO 5349-1 W_h frequency weighting curve for hand-transmitted vibration.

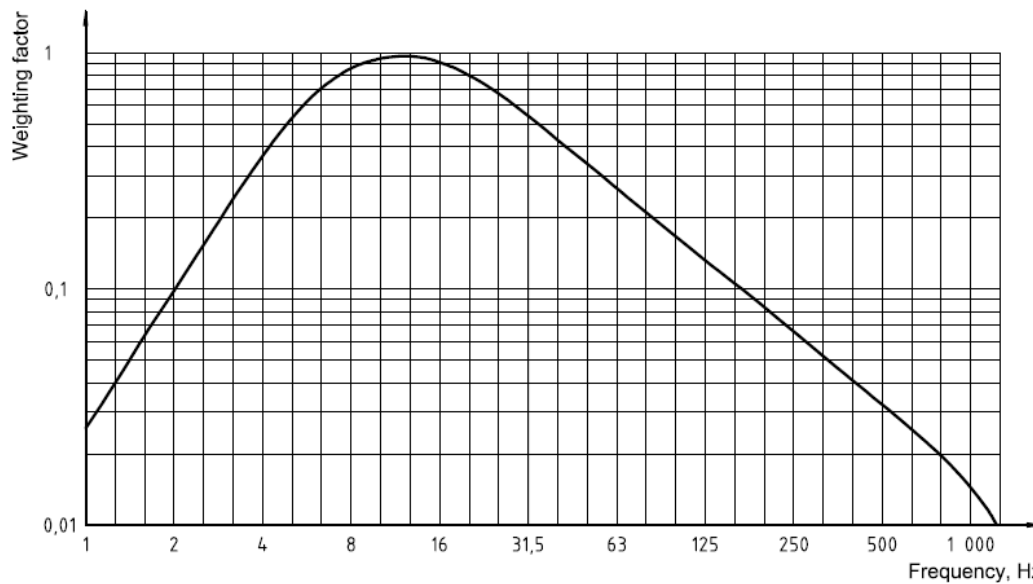


[Figure 1.5] W_h frequency weighting curve for hand-transmitted vibration defined in ISO 5349-1 (reproduced from ISO 5349-1, 2001).

The W_h weighting, the standardising of which was mainly based on the work of Miwa (1967) who measured hand-arm perception threshold curves and hand-arm equal sensation curves for both vertical and horizontal sinusoidal vibration, was primarily defined for use in measuring and reporting hand-arm exposures for the purpose of quantifying health effects and risk of injury over the frequency range from 8 to 1000 Hz. As the only internationally standardised frequency weighting for the hand-arm system, the W_h weighting has been applied to the evaluation of the perception of hand-arm vibration and has even been used in the automotive industry (Peruzzetto, 1988; Pak et al., 1991; Isomura et al., 1995).

Several criticisms have been raised, however, regarding the use of W_h for modeling the human perception of vibration at magnitudes lower than the vibration exposures limits, or in the case of vibration having significant energy at frequencies below 8 Hz or above 1000 Hz. In fact, studies of the subjective response to hand-arm vibration (Neely and Burström, 2006) have suggested that the W_h frequency weighting underestimates the perceived intensity of hand-arm vibration, and Morioka and Griffin (2006) have also suggested that W_h does not appear to be optimum for predicting the perception of steering wheel vibration.

Further, in the steering application, it is not obvious whether W_h is appropriate in the case of steering wheel rotation. Giacomini et al. (2004) have proposed a new hand-arm frequency weighting for steering wheel rotational vibration, called W_s , which presents significant differences with respect to the W_h weighting at low (3 to 6.3 Hz), intermediate (6.3 to 50 Hz) and high (above 50 Hz) frequencies. An important difference is the higher human sensitivity to hand-arm vibration indicated by W_s at frequencies below 6.3 Hz, and the constant velocity weighting from 6.3 to 50 Hz as opposed to the constant acceleration weighting from 8 to 16 Hz of W_h . The constant velocity contour of W_s has been found to be in agreement with the equal sensation curves for steering wheel rotational vibration developed by Amman et al. (2005), who suggest a constant velocity weighting in the frequency range from 8 to 20 Hz. Figure 1.6 presents comparisons between the frequency weighting W_s and W_h curves.

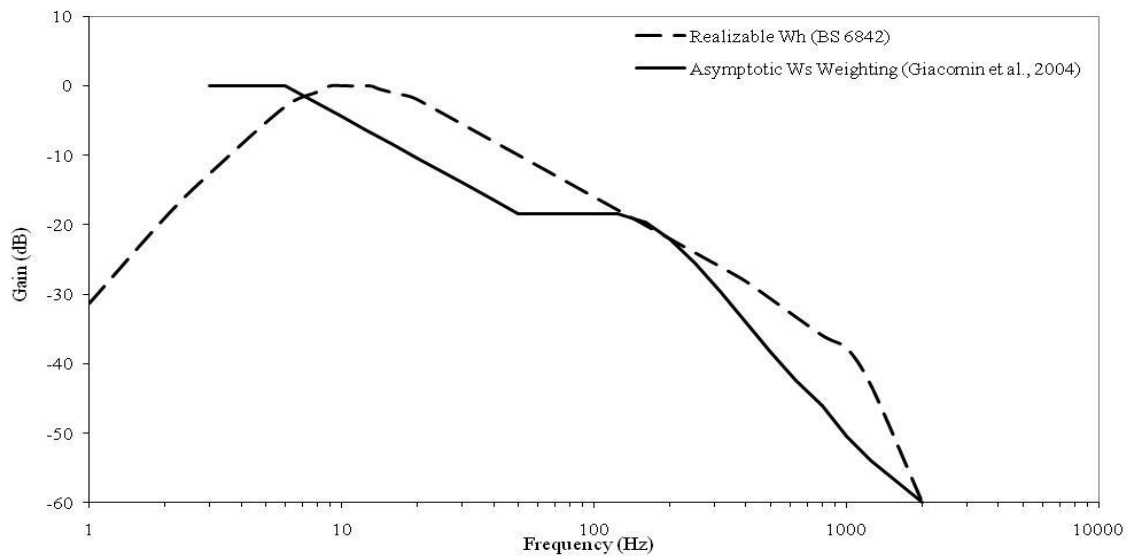


[Figure 1.6] Comparison between the proposed frequency weighting W_s for rotational steering wheel vibration and frequency weighting W_h .

Gnanasekaran et al. (2006) have evaluated the correlation between the weighted acceleration obtainable when applying the W_h or W_s weightings and the subjective perceived intensity responses provided by test participants for eight different types of steering vibration stimuli. The results suggest that the W_s weighting provides a slightly better correlation than the W_h weighting. The results also suggest, however, that more accurate vibration perception weightings are required, analogous to psychoacoustics

weightings, due to the variable vibration perception according to the amplitude ranges of steering wheel rotational vibration. Ajovalasit and Giacomini (2009) also insist that a range of weightings are useful in some work environments where a wide range of vibration amplitudes occur.

1.3 Research Objectives

Several new frequency weightings of hand-arm vibration (Thomas and Beaucamp, 1998; Tominaga, 2005; Dong et al. 2006) have been recently proposed. However, the studies have investigated the health effects produced by human hand-arm vibration. Only a few research studies dealt with steering wheel hand-arm vibration (Hong et al., 2003; Giacomini et al., 2004).

In addition, a single frequency weighting may not provide accurate estimations of subjective response of hand-arm vibration since the results of previous studies (Morioka and Griffin, 2006; Ajovalasit and Giacomini, 2009) have suggested that no one weighting may not be suitable at all magnitudes of vibration. Further, the current frequency weighting is based mainly upon the subjective response from male participants despite the fact that since the 1970s the percentage of female drivers has increased in most countries (National Travel Survey, 2005), thus the availability of only the current W_h frequency weighting appears problematic.

The general objective of the research presented in this thesis was to quantify the human subjective response to steering wheel rotational vibration in order to develop frequency weightings for automotive drivers. The general objective was achieved by means of a set of intermediate objectives, which subdivided the research activity into separate phases. The intermediate objectives were:

- To quantify the human subjective response to steering wheel rotational vibrational stimuli by means of laboratory experiments involving a steering wheel vibration test facility and test subjects.
- To determine the effect of signal differences between sinusoidal and narrow band-

limited random vibration on the human perceived intensity.

- To determine the effect of gender differences on the human perceived intensity.
- To determine the effect of physical body mass differences on the human perceived intensity.
- To select the adequate frequency weightings for evaluating steering wheel rotational hand-arm vibration by establishing the level of correlation between the subjective responses and the analytical estimates of the human subjective responses.

The main questions which the research set out to answer were the following:

- How do the subjective responses change when the frequency changes?
- How do the subjective responses change when the amplitude changes?
- How nonlinear is the human response?
- Is the subjective response dependent on the signal type?
- Is the subjectively perceived intensity for males and females the same when the steering wheel vibration is the same?
- Is the subjectively perceived intensity for light and heavy individuals the same when the steering wheel vibration is the same?
- How many frequency weightings are necessary for quantifying human perception of steering wheel hand-arm vibration?

Chapter 2

Psychophysics

Psychophysics is the study of the relationship between the properties of physical stimuli and the psychological reactions to those properties (Coren et al., 2003). Psychophysical theory has shown that to discriminate two stimuli as different it is necessary that they present a specific difference, ΔI , in the magnitude of the physical stimuli. The value of ΔI represents the smallest increment of a stimulus that can be detected. The proportion by which stimulus intensity I must be changed in order to produce a just noticeable difference (JND) in sensation is referred to as the Weber fraction (WF):

$$\frac{\Delta I}{I} = c \quad (2.1)$$

where ΔI is the difference threshold in the physical stimulus of intensity I , and c is the Weber fraction constant. The ΔI difference threshold increases with increases in the magnitude of the vibration stimulus I , whereas c is a constant which depends on the type of stimulus. The smaller the Weber fraction value, the greater the sensitivity to stimulus differences along a sensory dimension. The Weber fraction for hand-transmitted vibration has been found to vary from a minimum of 0.05 as found by Knudson (1928) in a study for the detection of changes in vibration amplitude using needles indenting the skin of the fingertips, to a maximum of 0.15 to 0.18 as found by

Morioka (1999) in a study using sinusoidal vibration at frequencies from 8 to 500 Hz applied to a wooden handle.

Fechner, by assuming the validity of Weber's law of Equation 2.1, derived an indirect measure of sensory magnitude from the difference thresholds in the stimulus magnitude. The general assumption made by Fechner and co-workers (Gescheider, 1997) was that each JND was an equal psychological increment in sensation magnitude, regardless of the size of difference threshold ΔI . By counting an increase of 1 psychological unit of subjective response for each JND value, which increases with increasing stimulus intensity, a response curve is produced which is characterised by a linear abscissa being plotted against a logarithmic ordinate.

Given the shape of the response curve, Fechner proposed that the sensation magnitude increased with the logarithm of the stimulus intensity, deriving a general formula which is known as Fechner's law:

$$\Psi = c \log I \quad (2.2)$$

where Ψ is the sensation magnitude, I is the intensity of the stimulus in units above the absolute threshold, and c is the Weber fraction. Fechner's law is presented in Figure 2.1 where it can be seen that equal increments in sensation correspond to increasingly larger values of stimulus intensity as the stimulus intensity increases.

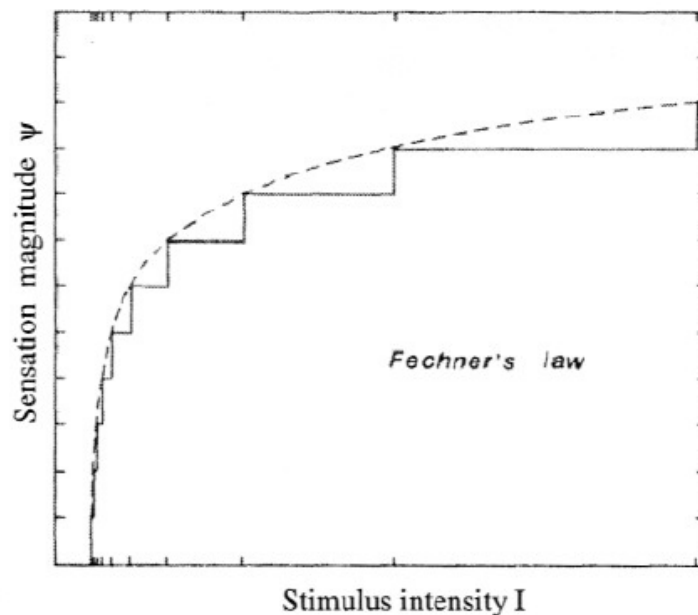


[Figure 2.1] Relationship between the perceived sensation and the stimulus intensity according to Fechner's law (adapted from Stevens, 1986).

Stevens (1986) later proposed that the perceived intensity of a stimulus was best related to the physical intensity by a power law relationship, which in its most general form is expressed as:

$$\Psi = \Psi_0 + k(X - X_{th})^\beta \quad (2.3)$$

where Ψ is the subjective perceived magnitude, k is a constant determined from the measurement units, Ψ_0 and X_{th} are constants which define the subjective and stimulus magnitudes at threshold, which indicate the starting point of the growth function on the response axis (y-axis) and on the stimulus axis (x-axis) respectively, and β is the power exponent defining the growth of the human response. The Stevens' power exponent β is useful since it provides a means for translating the measurable physical objective quantities into perceived subjective quantities. As shown in Figure 2.2, power function exponents have been found to be as small as 0.33 for brightness, and as large as 3.5 for electric shock on the fingertip.

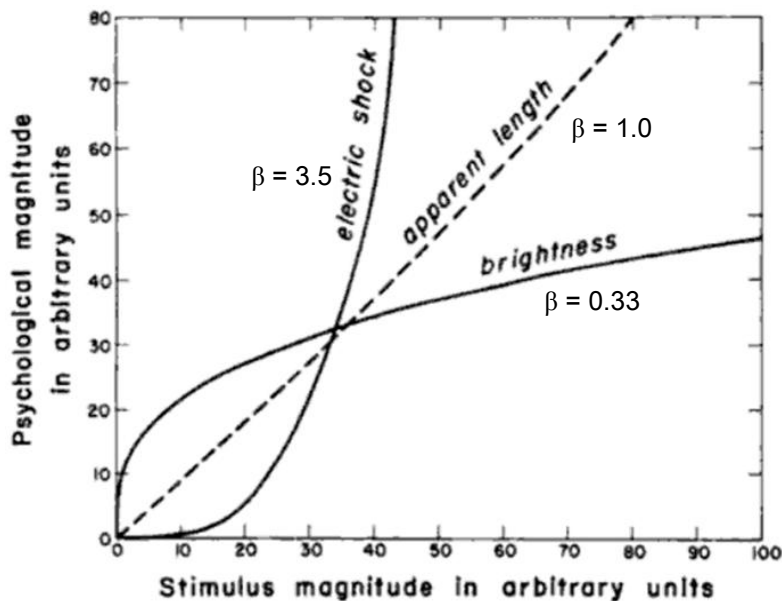


[Figure 2.2] Relationship between stimulus intensity and perceived sensation according to Stevens' power law (adapted from Stevens, 1986).

2.1 Psychophysical Scaling

Scaling is defined (Griffin, 1990) as “the process of determining a scale along a subjective or psychological dimension which has a continuous mathematical relation to

some physical dimension. As summarised in Figure 2.3, the four main types of scale are nominal scale, ordinal scale, interval scale and ratio scale. A nominal scale categorises objects, and the numbers reflect only that the objects are different from one another. An ordinal scale uses numbers to rank objects with respect to some characteristic such that different numbers have a greater-than-less-than relation between them. In an ordinal scale, the intervals between the assigned numbers are meaningless. In an interval scale, the size of the differences between numbers, as well as their ordinal relation, has meaning. However, the zero point of the scale can be set arbitrarily and therefore does not necessarily represent the zero amount of the property measured. A ratio scale, on the other hand, as well as having the properties of order and distance, has a natural origin to represent zero amount of the stimulus. The property of having a true zero value guarantees that the ratios which can be determined from different values of the scale values have meaning (Gescheider, 1997).

Scale	Operations we perform	Permissible transformations	Some appropriate statistics	Examples
Nominal	Identify and classify	Substitution of any number for any other number	Number of cases Mode Contingency correlation	Numbering football players Model numbers
Ordinal	Rank order	Any change that preserves order	Median Percentiles Rank-order correlation	Preference lists Hardness of minerals Rank lists
Interval	Find distances or differences	Multiplication by a constant Addition of a constant	Mean Standard deviation Product-moment correlation	Temperature Fahrenheit Temperature Celsius Calendar time Standard scores
Ratio	Find ratios, fractions, or multiples	Multiplication by a constant only	Geometric mean Percent variability	Length, weight, numerosity, duration, and most physical scales Temperature Kelvin Loudness in sones

[Figure 2.3] Four main types of measurement scale (adapted from Stevens, 1986).

According to Fechner, a subject can only perceive the relative difference between two stimuli with respect to a given attribute and, therefore, sensation can only be indirectly scaled. On the other hand, Stevens (1986) proposed that a subject can actually judge the strength of a given stimulus attribute, implying that sensation can be directly scaled.

The remaining sections of this chapter provide an overview of the most commonly used indirect and direct scaling methods. A brief summary is provided for each, as there are key bibliographic references which can be used to obtain more detailed explanation of the individual methods.

2.2 Indirect Scaling Methods

Indirect scaling is defined as those methods in which measurements of psychological magnitude are derived from data on how well observers can tell one stimulus from another. Fechnerian JND scales and Thurstonian scales are examples of indirect scaling (Gescheider, 1997). Fechner's indirect method, which is based on JND counting, is not considered suitable for constructing scales since it depends on only the distance between the stimuli on the psychological continuum, and does not take into account the statistical variability in the subjective estimates. Thurstone's law of comparative judgment (Thurstone, 1959) is the indirect scaling method that is most frequently used to construct a psychophysical scale, due to its generality and reliability.

2.2.1 The Method of Constant Stimuli

In the method of constant stimuli, stimuli of varied intensity are presented several times in a random order to an observer who, in the case of measuring absolute threshold, is required to report the presence or absence of the stimulus or who, in the case of measuring difference thresholds, must report which of two stimuli is more intense (Gescheider, 1997). The method of constant stimuli is frequently used when the threshold must be measured precisely, but it is time consuming because it requires many stimulus presentations and responses.

2.2.2. The Method of Limits

In the method of limits the intensity of the stimulus presented to the observer is increased or decreased on successive trials until the stimulus is no longer detected or, in the case of measuring difference thresholds, until a stimulus difference is no longer noticed (Gescheider, 1997). The experimenter presents successively lower levels of the

stimulus or successively higher levels of the stimulus, and on each trial the observer indicates whether the stimulus is above threshold or not. The observer is asked to say ‘yes’ if the stimulus is detected or ‘no’ if it is not.

2.2.3 The Method of Adjustment

In the method of adjustment the test subject is required to adjust the test stimuli until it produces the same perceived sensation as was produced by the reference stimuli in the case of measuring difference thresholds, while the test subject is required to ask the observer either to increase the intensity level until it is just perceptible, or to decrease the intensity until the sensation just disappears in the case of measuring absolute thresholds. (Gescheider, 1997).

2.2.4 The Paired-Comparisons Method Using Thurstone’s Model

In the method of paired-comparisons (Thurstone, 1959; David, 1988) all stimuli are presented to the test subjects in all possible pairs. The subjects are required to make comparative judgments for all the pairs, so as to state which of the two stimuli is greater than the other with respect to a chosen semantic attribute (e.g. unpleasantness, intensity, etc.). The test subject is not required to directly judge the magnitude of the stimulus. The method of paired-comparisons is not suitable when large numbers of stimuli are to be tested since the number of comparisons required by the method is equal to the number of possible combinations, which for a number n_s of stimuli is given by:

$$n_s(n_s - 1) = n_s^2 - n_s \quad (2.4)$$

Thus, the number of comparative judgments increases with the square of the number of the stimuli considered.

Thurstone (1959) developed a mathematical model for deriving subjective scale values from comparative judgment proportions. Thurstone’s model assumes that a given stimulus is capable of producing a range of momentary estimates of the position of the stimulus along the human internal psychological continuum. Variations in the human subjective response from one presentation to the next occur due to changes in human physiological sensitivity, contextual effects, fatigue and learning effects. In Thurstone’s

model the variations in the estimates are assumed to be normally distributed along the psychological continuum, and the standard deviation of each distribution is usually referred to as the discriminial dispersion. The difference between the means of two distributions, associated with two stimuli, specifies the difference on the psychological continuum between the sensations produced by the two stimuli. Thurstone's law of comparative judgments is:

$$S_j - S_k = z_{jk} \sqrt{\sigma_j^2 + \sigma_k^2 - 2r_{jk}\sigma_j\sigma_k} \quad (2.5)$$

where S_j and S_k are the subjective scale values of stimuli j and k respectively, z_{jk} is the normal deviate corresponding to the proportion of times the stimulus j is preferred over the stimulus k when they are compared, σ_j and σ_k are the standard deviations of the distribution of momentary estimates and r_{jk} is the coefficient of correlation between the pairs of discriminial processes. Thurstone (1959) presented five different cases of the law of comparative judgment which solve Equation 2.5. Each of the five cases involves a different set of assumptions that simplify the equation. Analytical procedures have been devised to give good estimates of the unknown terms when using one of thurstone's five cases (Torgerson, 1958). Thurstone's model has been widely used in several scientific disciplines (Stevens, 1966; Gescheider, 1997) because of its generality and ability to quantify numerous psychological qualities for which there are no obvious measurable, physical stimulus properties (Guilford, 1954).

2.3 Direct Scaling Methods

In direct scaling methods, the test subjects are assumed to be capable of estimating quantitative relations between subjective experiences, and are thus asked to assign numbers to stimuli to represent the magnitude of their subjective sensation (Stevens, 1986; Gescheider, 1997).

2.3.1 The Method of Magnitude Estimation

In the method of magnitude estimation, subjects are required to make direct numerical estimations of the sensory magnitudes produced by the various test stimuli. In the magnitude estimation procedure a subject is presented with a standard stimulus that the experimenter assigns an arbitrary subjective magnitude value such as 100. Other stimuli

are then presented, and the subject is asked to estimate the subjective magnitude of each of them as a multiple or ratio of the standard subjective value. Magnitude estimation thus offers the advantage of reducing the range effects that can be encountered when using fixed scale techniques such as semantic scales or numbered scales (Gescheider, 1997). However, a major disadvantage is that different subjects may give wildly different magnitude estimates (Teghtsoonian and Teghtsoonian, 1983; Stevens, 1986), which is referred to as the regression effect. Subject training is therefore required in order to minimise unwanted trends in the data.

2.3.2 The Method of Magnitude Production

The method of magnitude production is the inverse of the method of magnitude estimation. The subject is presented with a standard stimulus whose magnitude is described by an arbitrary number, then is asked to adjust the level of a comparison stimulus such that the subjective sensation it produces bears a given ratio to the sensation produced by the standard stimulus (Griffin, 1990). Unfortunately, this method can result in a bias towards low settings, since subjects do not like exposing themselves to uncomfortable stimuli (Stevens, 1986; Griffin, 1990), which is again a regression effect.

2.3.3 Category Scaling

Category scaling is a direct method for quantifying subject opinion about a certain attribute of the stimulus (Stevens, 1986; Gescheider, 1997). When the subject is presented with the stimulus, he or she is asked to assign it to a specified number category (such as 1, 2 or 3) or to an adjective (such as low, medium or high). The results obtained when using semantic scales depend on the question phrasing, and on the words actually chosen for the scale. It is important that the choice of the attribute to describe the sensation be appropriate to the application (Gescheider, 1997). The number of useful semantic labels has been found to be limited by the human ability to resolve differences between stimuli and situations. Research (Pollack, 1952) suggests that the optimum is from 5 to 9 levels. The use of semantic scales normally involves large inter-subject differences due to the fact that each subject attaches a slightly different meaning to the

descriptive label.

2.3.4 Category-Ratio Scaling (Borg CR10 Scale)

According to Borg (1998), ratio scaling procedures cannot actually provide information about the absolute levels of subjective impressions, and thus are not able to meaningfully compare the absolute values of magnitude estimations of individual observers. Borg therefore created a scaling procedure that had properties of both category and ratio scales. Category-ratio scaling is a method for controlling for individual differences in the use of numbers. Adjectives such as extremely strong, strong, moderate, weak, extremely weak and so on, are associated with specific numbers, forming a verbally labelled category scale. The numbers, however, are chosen so that the results are linearly related to magnitude estimation scales and, therefore, this type of scale is considered to be category-ratio scale.

Borg (1998) initially designed the category ratio scale to measure perceived exertion during exercise. He assumed that all observers share a common scale of perceived exertion, with a common anchor at the point of maximal exertion. Descriptive adjectives such as extremely strong, moderate, etc. were used to describe the various experiences of exertion. The major assumption was that a similar level of perceived exertion could be described by a particular adjective which would be experienced in the same way by different observers.

The Borg CR10 scale is a category-ratio scale for use in quantifying subjective perceptions of stimuli intensity anchored at the number 10, which represents the value of maximal perceived intensity. The Borg CR10 scale, shown in Figure 2.4, consists of a numerical scale from 0 (nothing at all) to 10 (extremely strong) with nine verbal anchors placed along the number scale in approximately logarithmic order. The “Extremely strong” 10 rating value is used to represent the strongest perception that has been previously experienced by the test subject. The rating “absolute maximum”, located below the value 10 and indicated by a dot “●”, provides an opportunity for estimating the intensity value of any test stimuli which is stronger than the personal experience of the test subject. Test subjects are instructed to use the scale by first finding the verbal

anchor which best fits the perceived sensation, and by then choosing an appropriate numerical value from those associated with the verbal anchor. Subjects are allowed to use any number, including fractions or decimals. If subjects experience the perceived intensity to be stronger than their own personal experience, they are allowed to choose a number greater than 10 in order to avoid ceiling effects (Gescheider, 1997).

The validity and reliability of the Borg CR10 scale when used to quantify the human subjective response to hand-arm vibration has been investigated by Wos et al. (1988b), who have claimed that the Borg CR10 scale is highly reliable, with reliability coefficients ranging from 0.841 to 0.986. Neely et al. (1992) have reported coefficients of determination (R^2) of 0.79 between Borg CR10 results and subjective data obtained by means of a visual analogue scale, and also reported typical retest coefficients of determination of 0.98.

0	Nothing at all	"No P"
0.3		
0.5	Extremely weak	Just noticeable
1	Very weak	
1.5		
2	Weak	Light
2.5		
3	Moderate	
4		
5	Strong	Heavy
6		
7	Very strong	
8		
9		
10	Extremely strong "Max P"	
11		
↔		
●	Absolute maximum	Highest possible

[Figure 2.4] The Borg CR10 scale (reproduced from Borg, 1998).

Chapter 3

Hand-Arm Vibration

3.1 Biomechanical Response of the Hand-Arm System

3.1.1 Mechanical Impedance of the Hand-Arm System

Mechanical impedance is the complex ratio of the force to the velocity, where force and velocity may be taken at the same or different points in the same system (Griffin, 1990). These measurements provide invaluable insights into the relative importance of different vibration frequencies (Stelling and Dupuis, 1996; Sörensson and Burström, 1997) and convenient tools for investigate the influence of variables such as hand-arm posture, body size, grip force and grip contact area on the likely effect of vibration at the hand (Reynolds and Soedel, 1972; Pyykkö et al., 1976; Lundström and Burström, 1989).

The driving point mechanical impedance is defined as:

$$Z(f) = \frac{F(f)}{v(f)} \quad (3.1)$$

where F is the input force measured at the driving point, v is the response velocity measured at the driving point, and f is the frequency of oscillation. The mechanical

impedance Z can be described as the resistance of a mechanical structure to an applied vibration (Pyykkö et al., 1976; Lundström and Burström, 1989). For the hand-arm system, the driving point mechanical impedance is usually measured using a T-bar handle which rigidly attached to a vibration exciter (e.g. an electrodynamic shaker) to produce the input stimulus into the hand. The handle is usually also equipped with strain gauges for measurements of both the grip and the feed forces applied by the subject to the handle over the frequency range from 10 to 1000 Hz (ISO 5349-1, 2001).

The driving point mechanical impedance characteristics of the hand-arm system have been investigated by several researchers (Reynolds and Soedel, 1972; Mishoe and Suggs, 1977; Lundström and Burström, 1989; Gurram et al., 1995). Considerable differences are known to exist among the impedance measurements reported by the different investigators. These differences may be due to variations in the experimental techniques used, the hand-arm postures used and the grip forces adopted.

Reynolds and Soedel (1972) studied the mechanical response of the hand-arm system to translational sinusoidal vibration in the frequency range from 20 to 500 Hz when gripping a handle. They concluded that arm position had only a minor effect on the impedance of the hand across the frequency range tested, but that grip tightness and hand pressure influenced the vibration response at frequencies greater than 60 Hz. They also suggested that once a method of grip had been established, the hand-arm system could be treated as a linear system.

Lundström and Burström (1989) investigated the mechanical impedance of the hand-arm system in the frequency range from 20 to 1500 Hz. Firmer grips as well as higher vibration levels resulted in higher impedance magnitudes for frequencies above 100 Hz. Below 100 Hz, increasing the vibration input lowered somewhat the hand-arm impedance, while the grip force had little or no influence. All impedance curves had a pronounced minimum in the frequency range from 50 to 150 Hz, while the overall tendency outside that frequency range was of increasing impedance with increasing frequency, indicating that remote elements of the arm become less active as the frequency rises, eventually reaching a situation where only the fingers vibrate with the handle.

Typical values of impedance have been defined by summarizing the values reported in the literature for similar measurement conditions. The mechanical impedance of the hand-arm system under conditions representative of power-tool operation is shown in Figure 3.1 (Gurram et al., 1995) for vibration along the directions X_h , Y_h and Z_h of the standardised coordinate system for the hand. Gurram et al., synthesised the dynamic impedance data obtained from the test data sets of the 9 other studies which each involved from 1 to 75 male adult subjects. The dotted line shows the mean value of the data, while the dark solid lines indicate the maximum and minimum values found in the data. Also shown is a dashed line which represents the impedance values of a 4-degree-of-freedom biodynamic model.

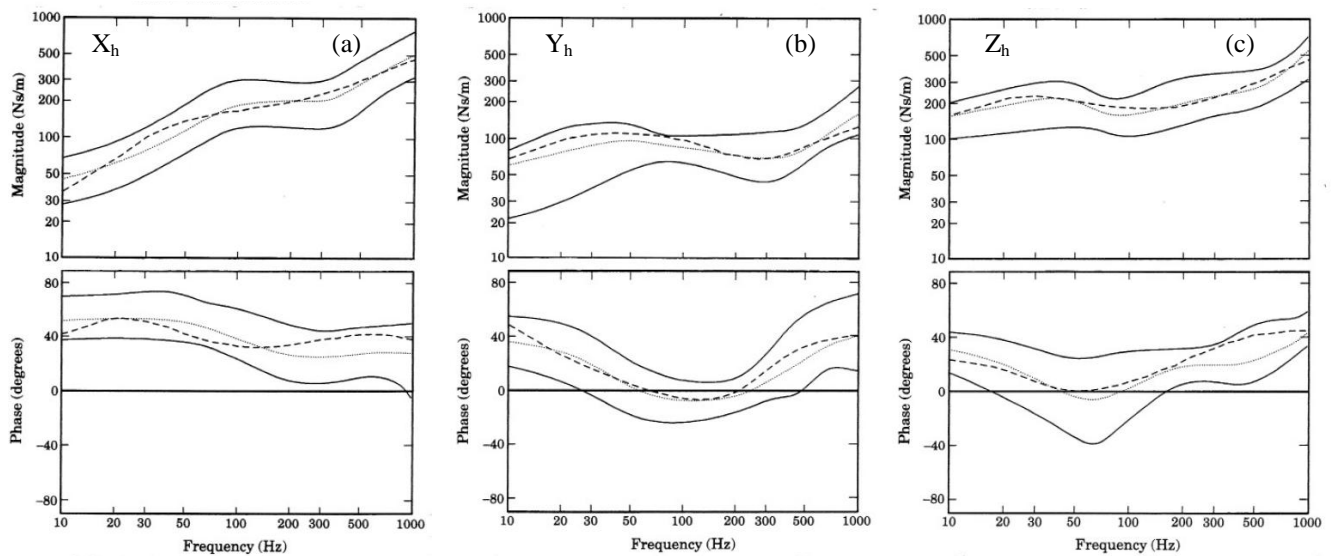


[Figure 3.1] Mechanical driving point impedance of the hand-arm system in the three orthogonal directions as defined in ISO 5349, the dotted line indicates the mean value, the dark lines indicate the maximum value, and the dashed line represents impedance values of a 4-degree-of-freedom biodynamic model: (a) X_h direction (b) Y_h direction (c) Z_h direction (reproduced from Gurram, 1995).

From Figure 3.1, it can be observed that the mechanical impedance of the hand-arm system in the X_h direction increases in magnitude with frequency, with a maximum from 20 to 70 Hz. The variation in the mean driving point impedance magnitude in the Y_h and Z_h directions is less pronounced, and more difficult to describe. The standard error in impedance magnitude approaches 30 to 37 percent at 1000 Hz. From the

analysis of their data Gurram et al. have suggested that changes in the grip force caused variations in the driving point mechanical impedance magnitude and phase estimates of less than 10 percent at all frequencies below 100 Hz.

3.1.2 Vibration Transmissibility through the Hand-Arm Vibration

The human mechanical response to hand-arm vibration is also commonly reported in terms of acceleration transmissibility. Transmissibility is the ratio of the force at one point to the force at another point, or the motion at one point to the same form of motion at another point. Transmissibility is normally expressed in terms of the measured acceleration since accelerometers are the most commonly used motion sensors (BS 6842, 1987; ISO 5349-1, 2001). When expressed in terms of acceleration, transmissibility is defined as:

$$H(f) = \frac{a_{out}(f)}{a_{in}(f)} \quad (3.2)$$

where the acceleration a is measured at reference points which represent the points of input and output to the system, and f is the frequency of the vibration. The acceleration at the input is usually measured by an accelerometer attached to the hand where the vibration enters, while the acceleration at the output is measured by one attached to a specific location along the body, such as the wrist, elbow, shoulder, neck, etc. (Pyykkö et al., 1976; Reynolds and Angevine, 1977).

Transmissibility results found in the research literature suggest a considerable attenuation of vibration from wrist to upper arm at frequencies above 100 Hz (Pyykkö et al., 1976), whereas vibration at frequencies below 40 Hz is generally found to be transmitted to the hand (from the tip of the finger to wrist) with little attenuation (Sörensson and Lundström, 1992). This suggests that the hand-arm system operates as a low-pass filter. Iwata et al. (1972) studied the properties of the hand-arm system by using varying psychophysical compression forces and an input acceleration level of 2 g in the frequency range from 6.3 to 100 Hz. They reported that at very low frequencies in the range from 6.3 to 20 Hz the hand-arm system operates like an amplifier due to the presence of resonances.

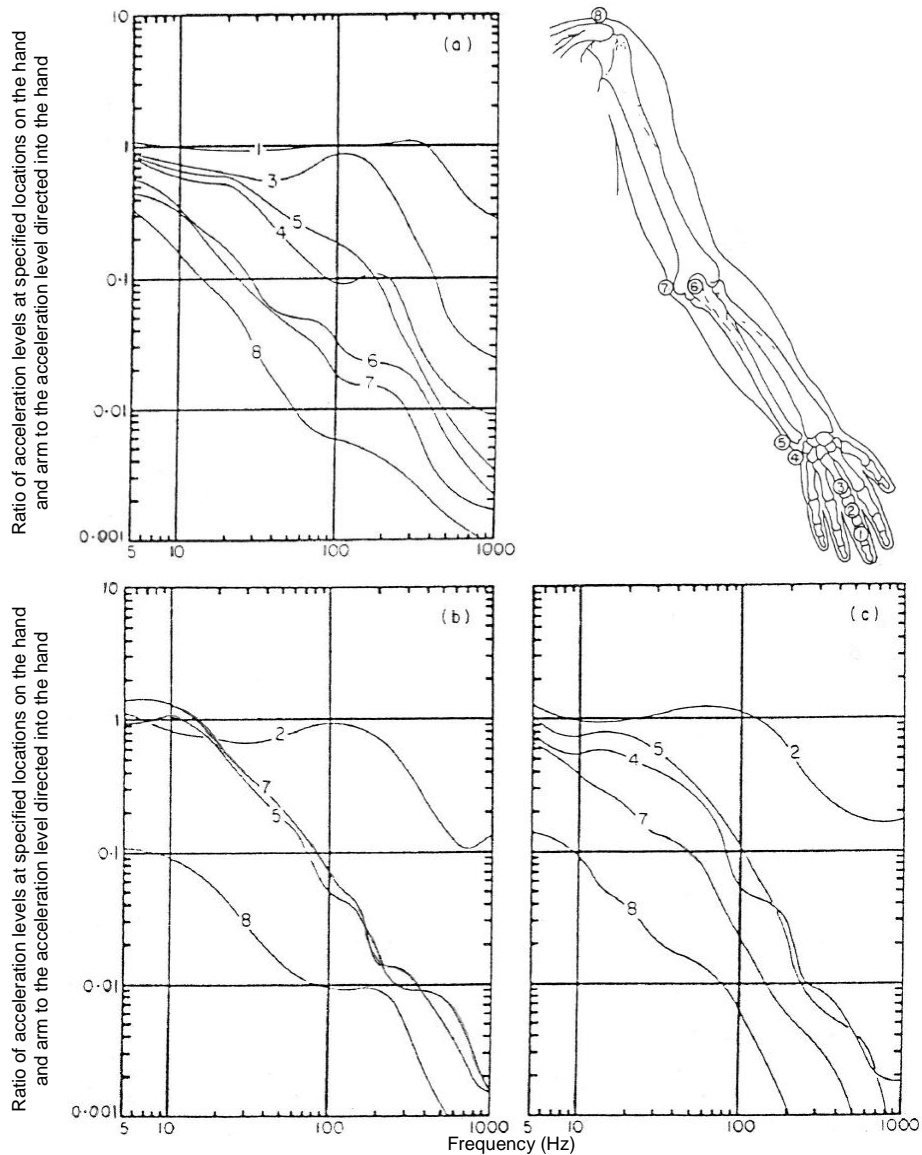


[Figure 3.2] Mean transmissibility curves for vibration in the (a) vertical direction, (b) horizontal direction and (c) axial direction, to the hand and arm positions [① middle phalanx; ② proximal phalanx; ③ third metacarpal; ④ triquetrum carpal; ⑤ styloid process of ulna; ⑥ olecranon; ⑦ medial epicondyle; ⑧ acromoin] (reproduced from Reynolds and Angevine, 1977).

Reynolds and Angevine (1977) placed small accelerometers at eight points along the hand-arm system and measured the transmissibility properties of the handle-induced vibration in the three orthogonal directions as shown in Figure 3.2. The locations of the accelerometers attached to the skin were: three measurement points on the middle finger

(① middle phalanx; ② proximal phalanx; ③ third metacarpal), two measurement points on the wrist (④ triquetrum carpal; ⑤ styloid process of ulna), two measurement points on the elbow (⑥ olecranon; ⑦ medial epicondyle) and on measurement point on the shoulder (⑧ acromion). From Figure 3.2 it can be observed that the vibration amplitude was greatly attenuated at frequencies above approximately 150 Hz between the location 1 (middle finger) and the location 3 (palm) suggesting that vibration at frequencies above 150 Hz tended to be concentrated in the areas of the hand and fingers directly in contact with the vibrating handle. From Figure 3.2 it can be also observed that the vibration amplitude was greatly decreased at locations 4 and 5 (wrist) at frequencies greater than 100 Hz, indicating that most of the vibration at frequencies above 100 Hz was limited to the hand and fingers. Another feature which can be noted is that the vibration amplitude was greatly decreased from locations 5 (wrist) to 7 (elbow) for the vertical and axial directions, while no reduction was found in horizontal direction. From this finding Reynolds and Angevine suggested that the amount of the transmitted vibration is very little from wrist to elbow when the vibration direction is perpendicular to forearm.

3.2 Human Subjective Response to Hand-Arm Vibration

The term subjective refers to something which is influenced by or based on personal beliefs or feelings, rather than based on facts (Cambridge advanced learner's dictionary, 2008) and the term response refers to an answer or reaction to something (Cambridge advanced learner's dictionary, 2008). Therefore, the term subjective response in this thesis refers to a reaction to something which is dependent on an individual (Griffin, 1990).

Reynolds et al. (1977) have stated that the human subjective response to hand-arm vibration is composed of four main parameters: quality, intensity, locus and affect. Quality is the subjective difference that allows a name to be associated with a sensation, i.e. heat, cold, taste or smell, etc. Intensity represents the strength or amplitude of perception. Locus indicates the position from which the sensation originates. Affect is the characteristic of the sensation that allows a subject to classify the sensation as

pleasant or unpleasant.

The subjective response to hand-arm vibration has been found to depend on several of the physical parameters of the vibration (Griffin, 1990). This section therefore provides an overview of the main independent physical variables which affect the subjective response to hand-arm vibration.

3.2.1 The Mechanoreceptors of Human Skin

The human skin acts as a sensor to various forms of external energy such as mechanical, thermal, chemical or electrical stimuli. The sensory effect of stimulation of the skin is termed cutaneous sensitivity (Martin and Jessell, 1999). Research has demonstrated that the glabrous (non-hairy) skin of the hand contains different types of mechanoreceptors, the cutaneous end organs responsible for transducing mechanical energy into neural signals. Bolanowski et al. (1988), in a series of experiments involving selective masking of the various tactile receptors, provided evidence for the existence of four main afferent fibre types in glabrous skin. These receptors are the Merkel's disks, Ruffini cylinders, Meissner's corpuscles and Pacinian corpuscles shown in Figure 3.3. The four receptors form the so-called four-channel model of mechanoreception which is currently accepted by most psychophysical researchers (Bolanowski et al., 1988; Hollins and Roy, 1996; Gescheider et al., 2001; Morioka, 2001).

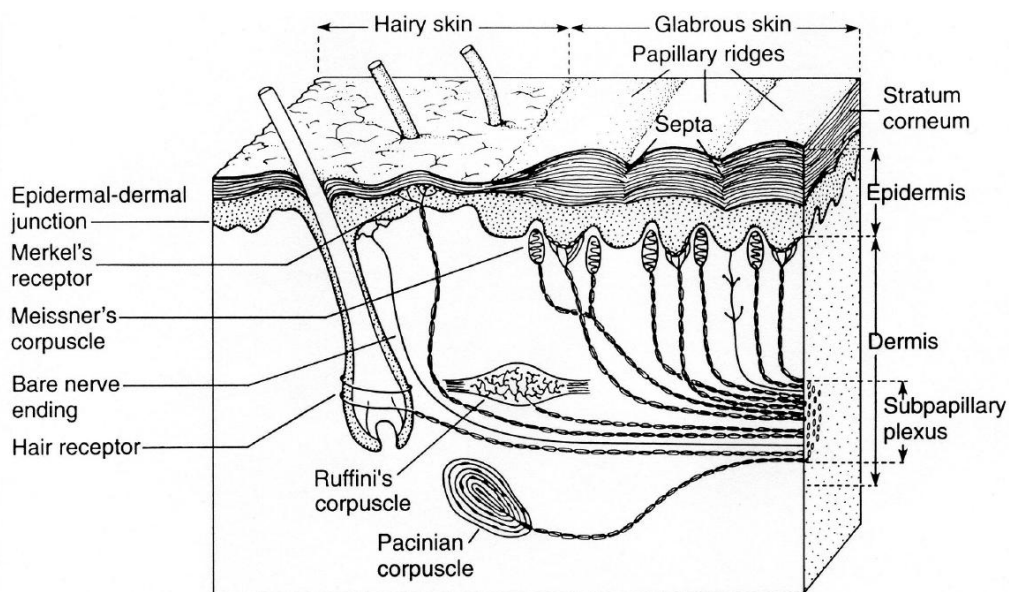


[Figure 3.3] Location of the mechanoreceptors in hairy and glabrous skin of the human

hand. (reproduced from Kandel et al., 1991).

Studies involving electrophysiological recording (Talbot et al., 1968; Mountcastle et al., 1972), direct recordings from human nerves (Knibestol and Vallbo, 1970; Johansson et al., 1982; Phillips et al., 1992) and psychophysics (Békésy, 1940; Verrillo, 1966; Gescheider, 1976; Verrillo, 1985; Bolanowski et al., 1988; Lamoré and Keemink, 1988; Hollins and Roy, 1996; Gescheider et al., 2001) have shown these mechanoreceptive fibres to possess distinct capacities to respond to specific frequency ranges of vibratory stimuli. The mechanoreceptive fibres are thus classified depending on how quickly they adapt to a steady stimulus, being defined as either fast acting (FA) or slow acting (SA). Slowly acting units continue to respond throughout the duration of the stimulus, whereas the response dies out quickly in the case of the fast acting units (Johansson et al., 1982).

The four-channel model consists of the high frequency Pacinian (P) channel and the high frequency non-Pacinian NP II channel, along with the two low frequency channels non-Pacinian NP I and non-Pacinian NP III. Research has suggested that stimuli detection may be performed within the individual channel that is most sensitive to the signal in question (Bolanowski et al., 1988; Hollins and Roy, 1996; Gescheider et al., 2001). Evidence to support the independence of the different sensory channels is found in studies of adaptation (Verrillo and Gescheider, 1977), of enhancement (Gescheider et al., 1977) and of masking (Labs et al., 1978; Hamer et al., 1983). Figure 3.4 shows the salient characteristics of the four channel model of mechanoreception, while Figure 3.5 illustrates the differences in area and frequency selectivity between the four tactile channels.

Type of tactile channel	Associated neural receptors	Physiological characteristics	Frequency range response small contactor (0.008 cm ²)	Frequency range response large contactor (2.9 cm ²)	Frequencies of max sensitivity	Shape of threshold function	Spatial summation	Temporal summation
Pacinian (P) *	Pacinian corpuscles	fast adapting (FA 2)	none	high freq. (40 ÷ 700 Hz)	250 ÷ 300 Hz	U-shape	YES	YES
Non-pacinian (NP I) **	Meissner corpuscles	fast adapting (FA 1)	low freq. (3 ÷ 100 Hz)	low freq. (3 ÷ 35 Hz)	30 ÷ 50 Hz	flat	NO	NO
Non-pacinian (NP II) ***	Merkel disks	slow adapting (SA 1)	high freq. (15 ÷ 400 Hz)	none	250 ÷ 300 Hz	U-shape	YES	YES
Non-pacinian (NP III) ****	Ruffini cylinders	slow adapting (SA 2)	low freq. (0.4 ÷ 3 Hz)	low freq. (0.4 ÷ 3 Hz)	0.4 ÷ 2 Hz	flat	NO	NO

* Verrillo (1985). ** (Talbot et al., 1968; Mountcastle et al., 1972). *** (Labs et al., 1978; Gescheider et al., 1985). **** (Bolanowski and Gescheider, 1988).

[Figure 3.4] Properties of the four-channel model of mechanoreception (reproduced

from Ajovalasit, 2005).

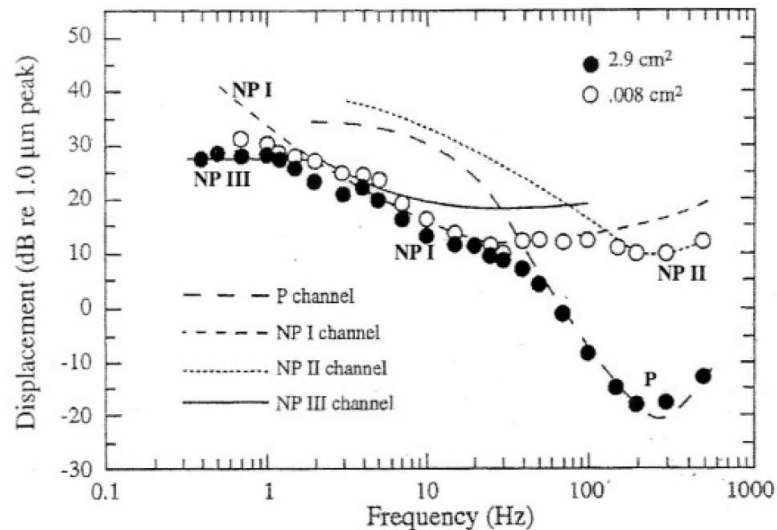


[Figure 3.5] Detection threshold as a function of frequency and of contactor area for the four individual tactile channels (reproduced from Gescheider et al., 2001).

3.2.2 Effect of Vibration Frequency on Subjective Response

Several researchers have measured perception thresholds and annoyance thresholds in response to stimuli of different frequency. Research has shown that a constant vibration magnitude does not produce the same intensity at all frequencies (Stevens, 1986; Griffin, 1990). Figure 3.6 presents a set of contours of equal sensation magnitude obtained by Verrillo et al. (1969) using sinusoidal vibration stimuli applied to the skin of the index finger by means of a vibrating needle. Each curve describes the combinations of frequency and amplitude that result in judgments of equal subjective intensity. At threshold, the curve is U-shaped, resembling the vibrotactile perception threshold of the hand (Verrillo, 1985), and has a flattened portion in the smoother shape over the high frequency range from 100 to 1000 Hz. The flatening of the equal sensation curves as the vibration intensity increases is analogous to the behaviour of the well-known equal loudness contours for hearing (Moore, 1997), indicating that high-intensity sounds appear equally loud regardless of the frequency.

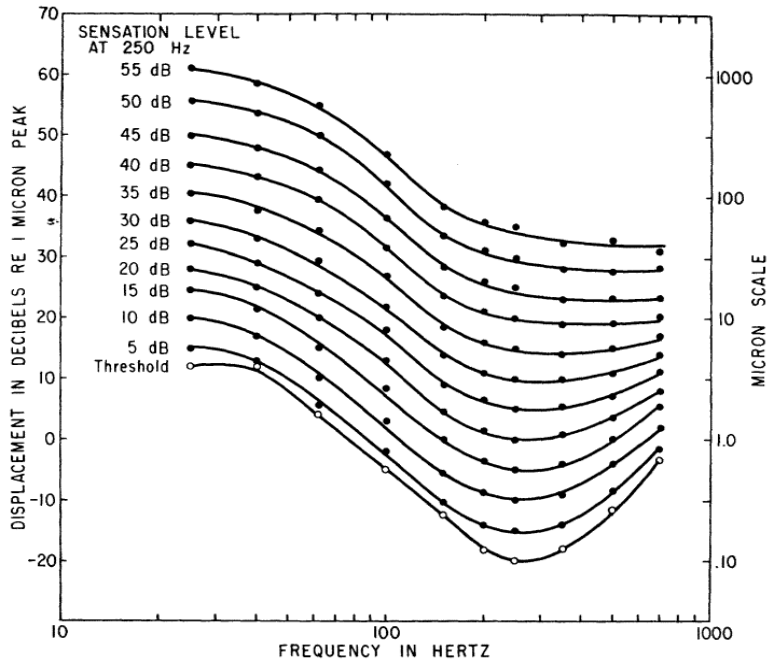


[Figure 3.6] Equal sensation magnitude contours. Each curve describes the combinations of frequency and intensity that give rise to equal sensation magnitudes (reproduced from Verrillo et al., 1969).

Research has suggested that, when plotted in terms of acceleration amplitude, human subjective response to hand-arm vibration decreases almost monotonically as a function of frequency (Miura et al., 1959; Miwa, 1967; Reynolds et al., 1977; Verrillo, 1985; Griffin, 1990; Giacomini et al., 2004). Miwa (1967), for example, performed equal sensation and perception threshold tests for 10 subjects holding their palm flat against a vibration plate, for vertical and horizontal vibration. Acceleration threshold was found to reach a maximum sensitivity at 100 Hz. Reynolds et al. (1977) studied the subjective response to vertical and axial direction translational handle vibration by measuring perception and annoyance threshold curves for eight test subject. For fixed acceleration amplitude, their results showed a general trend of reduced sensitivity with increasing frequency.

Giacomin and Onesti (1999) produced equal sensation curves for the frequency range from 8 Hz to 125 Hz using a sinusoidally rotating steering wheel at reference amplitudes of 1.86 and 5.58 m/s². From the results they suggested that the subjective response was found to be linear as a function of frequency over the frequency range considered, and that grip tightness did not have a great effect on the subjective response. Giacomin et al. (2004) have investigated the hand-arm perception of rotational steering wheel vibration by means of four equal sensation and one annoyance threshold tests. All equal sensation curves showed a decrease in human sensitivity to hand-arm vibration with increasing frequency. Giacomin et al. (2004) suggested that two characteristic transition points existed in the curves of equal subjective response, shown in Figure 3.7, at frequencies of 6.3 Hz and in the interval from 50 to 80 Hz. The first was stated to be due to mechanical decoupling of the hand-arm system, while the second was claimed to be due to the onset of Pacinian receptor output. The Giacomin et al. study also suggested that the human sensitivity decreased by 6 dB and 10 dB per octave in the frequency range from 6.3 to 50 Hz and from 160 to 315 Hz respectively while 0 dB per octave corresponding constant acceleration was observed in both frequency ranges from 0 to 6.3 Hz and from 50 to 160 Hz.

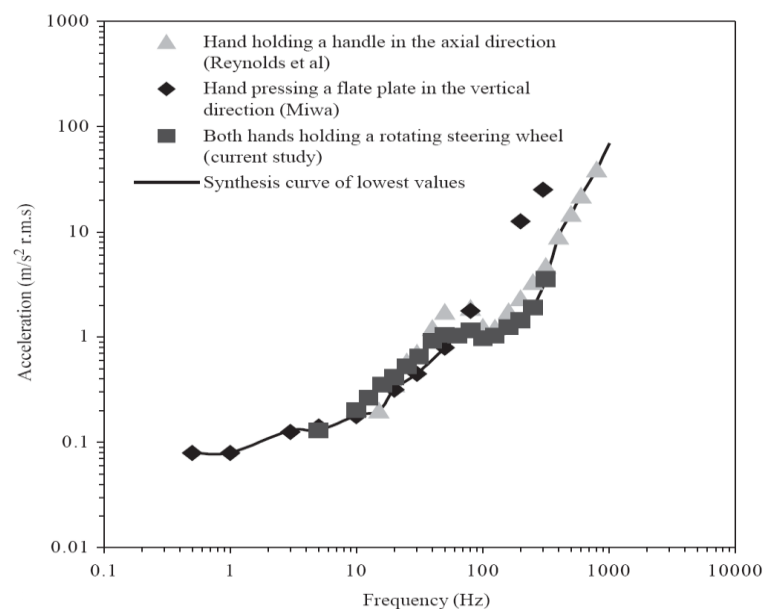


[Figure 3.7] Equal sensation data from studies of translational and rotational vibration (reproduced from Giacomin et al. 2004).

Regarding the effect of vibration frequency on subjective response it can be stated that:

- The subjective response magnitude is different at each vibrational frequency (Stevens, 1986).
- The shape of equal sensation magnitude contours has qualitative similarities to the well known equal loudness contours for hearing in terms of its frequency dependency (Moore, 1997); at low vibration magnitudes the curve is U-shaped, while at high vibration magnitude the curve is flat-shaped.
- The subjective response to steering wheel hand-arm vibration is characterised by two transition points, one at 6.3 Hz and the other in the interval from 50 to 80 Hz (Giacomin et al., 2004).
- The subjective sensitivity decreases by 6 dB per octave in the frequency range from 6.3 to 50 Hz while it decreases 10 dB per octave in the range from 160 to 315 Hz and 0 dB per octave in the rest of the frequency ranges from 0 to 6.3 Hz and from 50 to 160 Hz (Giacomin et al., 2004).
- From the results of the previous research studies it is observed that the use of a logarithmic transformation for the frequency values provided a more accurate description of the physical phenomena. (Miwa, 1967; Verrillo et al., 1969; Reynolds et al., 1977; Giacomin and Onesti, 1999; Giacomin et al., 2004).

3.2.3 Effect of Vibration Magnitude on Subjective Response

The magnitude of a mechanical vibration refers to the extent of its oscillatory motion. It can be measured in terms of either displacement, velocity or acceleration (Griffin, 1990). For practical convenience, the magnitude of vibration is usually expressed in terms of the acceleration, whose units are m/s^2 , and is normally measured by means of accelerometers (ISO 5349-1, 2001). Magnitude of hand-transmitted vibration is usually expressed in terms of the average power of the acceleration, namely the root-mean-square value (m/s^2 r.m.s.). Several studies have attempted to answer the question how the human subjective response to hand-arm vibration changes as a function of the magnitude of the vibration.

Verrillo et al. (1969) determined the rate at which the subjective intensity grows as a function of the vibration amplitude of sinusoidal stimuli which were applied to the skin of the index finger by means of a vibrating needle. The resulting curves, shown in

Figure 3.8, suggest that the subjective magnitude increased as the physical intensity of the vibration was increased. At low intensities, the subjective response was found to grow approximately linearly with respect to the intensity of the vibration at frequencies from 25 to 250 Hz. This result is in agreement with Zwislocki's theory of vibration sensitivity (Zwislocki, 1960) which states that sensory magnitude is approximately proportional to the stimulus intensity near threshold.

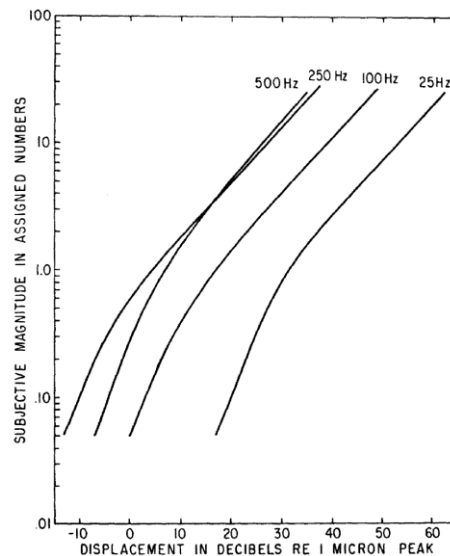


[Figure 3.8] Subjective response magnitude of suprathreshold vibration presented at the fingertip at frequencies of 25, 100, 250 and 500 Hz (reproduced from Verrillo et al., 1969).

The subjective response curves of Figure 3.8 are parallel at the upper intensities except for the 500 Hz stimuli which is steeper. This result was thought to be a reflection of the flattening of the equal sensation curves of Figure 3.6 as the vibration intensity increases.

Wos et al. (1988a) studied the subjective response to hand-arm vibration as a function of the vibration intensity using sinusoidal stimuli of frequencies of 30, 75 and 187 Hz at five amplitude values ranging from 26 to 5130 μm peak-to-peak values. The test subjects were asked to quantify their subjective responses by means of a Borg CR10 scale of perceived intensity (Borg, 1988). The function describing the relationship between the stimulus amplitude and the subjective response was determined for two different groups of test subjects. The first group consisted of engineers who were experienced in analysing vibrational phenomena, while the second group consisted of

individuals with no specific experience in analysing vibrational phenomena. Subjective response was found to be a negatively acceleration function of the vibration intensity. As shown in Figure 3.9, the experienced engineers were found to provide higher intensity ratings at the test frequencies of 30 and 75 Hz. Figure 3.9 also presents the line of best fit through the mean subjective response values, which is a power function with exponent ranging from 0.72 to 1.10.

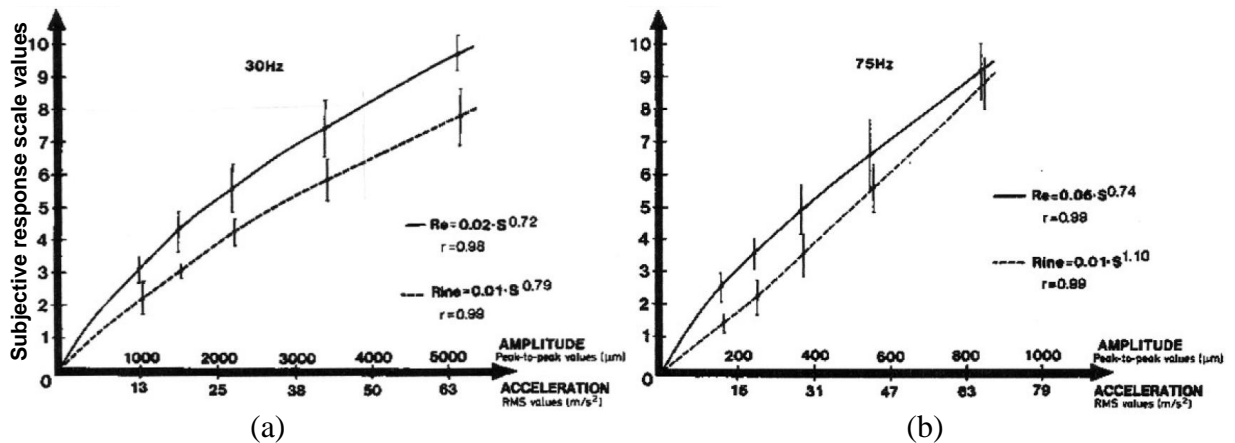


[Figure 3.9] Subjective response to sinusoidal hand-arm vibration of (a) 30 Hz and (b) 75 Hz. Data was determined for engineers with experience in analysing vibration (indicated as Re) and individuals with no specific experience in analysing vibration (indicated as Rine). Data was presented as mean value plus or minus one standard deviation (reproduced from Wos et al., 1988a).

Regarding the effect of vibration magnitude on subjective response it can be stated that:

- The subjective response magnitude increases as the physical intensity of the vibration is increased (Verrillo et al., 1969).
- The subjective response of experienced subjects produced higher intensity ratings than that of inexperienced subjects at test frequencies of 30 and 75 Hz. (Wos et al., 1988a).
- The subjective response magnitude increases at a rate of power function exponent 0.72 for experienced subjects and 0.79 for inexperienced subjects at a frequency of 30 Hz while it increases at a rate of 0.74 for experienced subjects and 1.10 for inexperienced subjects at a frequency of 75 Hz (Wos et al., 1988a).
- From the results of the previous research studies it is observed that the use of a logarithmic transformation for the vibration magnitude values provided a more

accurate description of the physical phenomena (Verrillo et al., 1969; Wos et al., 1988a).

3.2.4 Effect of Vibration Direction on Subjective Response

International Organization for Standardization 5349-1 (2001) and British Standards Institution 6842 (1987) define the directions along which the vibration is transmitted to the hand, referring to the anatomical and basicentric co-ordinate system, as presented in Figure 3.10. The anatomical co-ordinate system is defined in both standards as centred on the hand in the head of the third metacarpal bone while the basicentric co-ordinate system is defined as centred on (or adjacent to) the vibrating surface. In practice, vibration measurements are usually obtained with respect to basicentric co-ordinate system (ISO 5349-1, 2001).

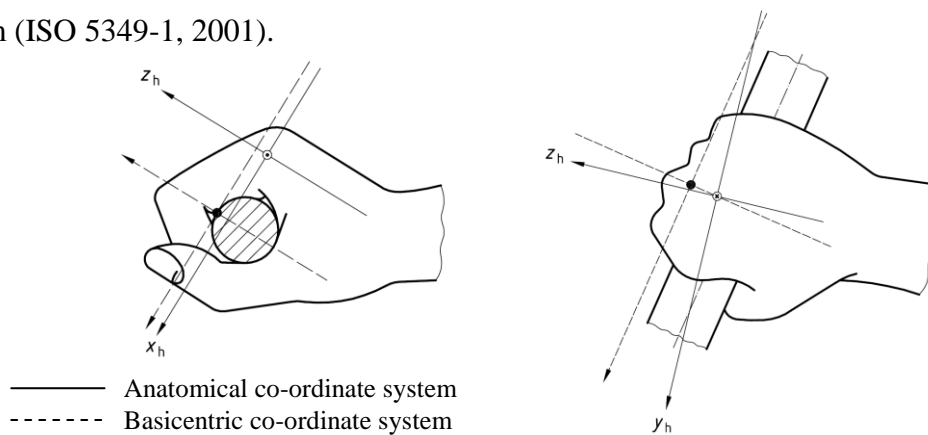


[Figure 3.10] Standardised anatomical and basicentric co-ordinate system for the directions of vibration for the hand (reproduced from ISO 5349-1, 2001)

In the studies of equal sensation and annoyance threshold reported by Miwa (1967), it was found that the subjective response to hand-arm vibration was the same in both the horizontal and vertical directions, for one or two hands pushing against the plate, and for various shapes of the handle grip. Reynolds et al. (1977) studied the subjective response to vertical and axial direction translational handle vibration for eight test subjects. For fixed acceleration amplitude, they observed that vibration along the vertical direction caused the greatest subjective intensity, while vibration along the tubular handle caused the least subjective intensity.

In the case of perceived intensity relative to an automobile steering wheel, Schröder and Zhang (1997) investigated the subjective response to steering wheel acceleration stimuli measured along the three orthogonal axes on a mid-sized European passenger car for different driving speeds ranging from 30 to 70 km/h over three different road surfaces. Comparison of the subjective ratings to the measured steering wheel acceleration values suggested that the vibration along the vertical direction of the steering wheel correlates best with the subjective ratings of the drivers in the frequency range from 30 to 90 Hz, which is the frequency range where most of the vibration energy is present at the steering wheel (Peruzzetto, 1988; Amman et al., 2001; Giacomini et al., 2004).

Regarding the effect of vibration direction on subjective response it can be stated that:

- The subjective response to hand-arm vibration appears to be the same in both the horizontal and vertical directions from the results of Miwa's study (1967) while Reynolds et al. (1977) observed that vibration along the vertical direction causes the greatest subjective intensity.
- The subjective response to hand-arm vibration appears to be the same when pressing the vibration table with and without handle grip in both the horizontal and vertical directions (Miwa, 1967).
- The subjective responses of test subjects appear to be best correlated with the level of vertical direction for a steering wheel (Schröder and Zhang, 1997).

3.2.5 Effect of Vibration Duration on Subjective Response

Research has shown that the stimulus duration affects both the vibrotactile sensitivity at threshold (Verrillo, 1965; Gescheider, 1976; Checkosky and Bolanowski, 1992) and at suprathreshold levels of stimulation (Verrillo et al., 1969; Gescheider, 1997). For stimuli frequencies greater than 40 Hz and stimuli durations shorter than approximately 1.0 second, the threshold amplitude for detection has been found to decrease monotonically with stimulus duration (Verrillo, 1965; Gescheider, 1976). The phenomenon is usually referred to as temporal summation or temporal integration. For stimuli frequencies greater than 40 Hz and stimuli durations longer than approximately 1.0 second the perception threshold does not change with increases in stimulus duration (Verrillo, 1965; Gescheider, 1976). For vibration frequencies less than 40 Hz, no temporal

summation has been observed (Gescheider, 1976).

Figure 3.11 illustrates the nature of the temporal summation effect in terms of perception thresholds for vibratory stimulation at 30 Hz and 200 Hz delivered to the hand. It can be seen that the non-Pacinian channels NP I and NP III have an approximately constant sensitivity at low frequencies below 40 Hz and thus do not present temporal integration properties (Verrillo, 1965; Gescheider, 1976; Bolanowski et al., 1988; Gescheider et al., 1994). Since increases in stimulus duration produce decreases in the thresholds of the Pacinian receptors (at 200 Hz) and the non-Pacinian NP II receptors (at 30 Hz), these two sensory systems are believed to be capable of temporal integration (Verrillo, 1965, 1966; Gescheider, 1976; Gescheider et al., 1985; Bolanowski et al., 1988).

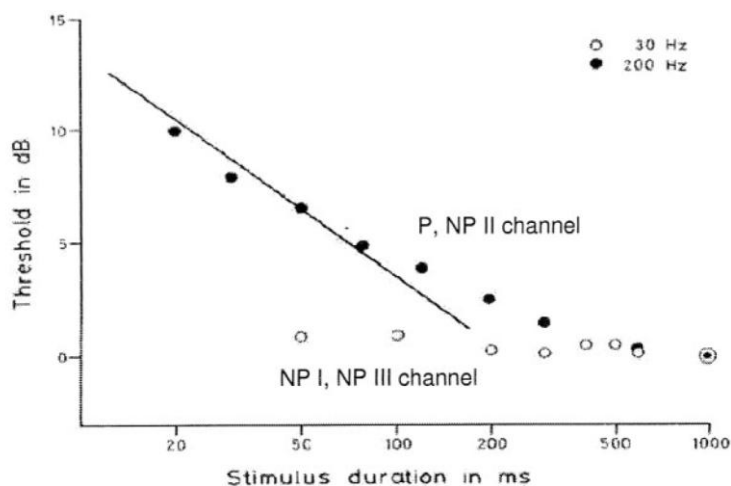


[Figure 3.11] Temporal summation effects on vibrotactile perception threshold (reproduced from Gescheider, 1976).

Cohen and Kirman (1986) have performed an experiment to measure the vibrotactile frequency discrimination at durations of 30, 50, 100 and 200 milliseconds (ms) with a standard frequency of 100 Hz. From the experimental results they suggested that 50 ms is the minimum vibratory duration for good frequency discrimination. Other research studies (Craig, 1985; Gescheider et al., 1990; Biggs and Srinivasan, 2002) have suggested that only a few ms are enough to perceive stimuli in human tactile vibration.

Most laboratory studies of hand-arm vibration have involved protocols in which the test subjects judged the subjective intensity of the vibration for brief exposures from 2 to 10 seconds (Miwa, 1968; Giacomini and Onesti, 1999; Giacomini et al., 2004; Morioka, 2004; Morioka and Griffin, 2006). Miwa (1968), for example, asked subjects to judge the relative subjective intensity produced by short periods of sinusoidal vibration, and pulsed sinusoidal vibration, for signal durations up to 6 seconds. From the test results Miwa suggested that for vibration in the frequency range from 2 to 60 Hz there is no further increase in sensation intensity for stimuli durations greater than approximately 2.0 seconds, whereas for vibration in the frequency range from 60 to 200 Hz the same limit is approximately 0.8 seconds.

Regarding the effect of vibration duration on subjective response it can be stated that:

- NPI and NPIII receptors do not present temporal summation properties at frequencies lower than 40 Hz (Verrillo, 1965; Gescheider, 1976; Bolanowski Jr et al., 1988; Gescheider et al., 1994) while Pacinian and NP receptors produce the temporal summation at 200 Hz and at 30 Hz respectively (Verrillo, 1965, 1966; Gescheider, 1976; Gescheider et al., 1985; Bolanowski Jr et al., 1988).
- A stimulus duration of 50 milliseconds is the minimum vibratory duration for good frequency discrimination (Cohen and Kirman, 1986).
- Most research studies for hand-arm vibration have involved brief vibration exposures of from 2 to 10 seconds (Miwa, 1968; Giacomini and Onesti, 1999; Giacomini et al., 2004; Morioka, 2004; Morioka and Griffin, 2006).
- Subjective intensity does not increase for stimuli durations greater than approximately 2.0 seconds in the frequency range from 2 to 60 Hz, while the same limit is approximately 0.8 seconds in the frequency range from 60 to 200 Hz (Miwa, 1968).

Chapter 4

A Review of Digital Signal Processing

4.1 Introduction

The main objective of signal processing analysis is to determine the statistical properties of a signal which can be used to identify and describe the nature of the signal which is being analysed (Bendat and Piersol, 1986; Piersol, 1992). The identified signal statistics provide objective metrics that can be used to quantify the overall effect of an individual signal condition, and to compare the signal properties of different sets of data. The effectiveness of a signal processing technique depends mainly on the type of signal being analyzed, and on the type of signal information that is to be determined (Bendat and Piersol, 1986; Piersol, 1992). This chapter provides an introduction to the definitions and techniques from the field of digital signal processing which are

fundamental towards the understanding of the experiments performed during the research which is described in this thesis.

4.2 Classification of Signals

Two broad classifications of signal are generally accepted by the scientific community (Bendet and Piersol, 1986): deterministic and random. If the excitation acting on the vibratory system can be described by a mathematical function at any given time, the motion is said to be predictable or deterministic. A deterministic signal can further be characterised as being periodic or nonperiodic. A signal is periodic if it repeats with a characteristic period for all time. A signal is nonperiodic, instead, if it only exists for a finite time range (transient signal) or when one or more of the signal statistical parameters change with time (aperiodic). Periodic signals can further be characterised by having one single frequency (sinusoidal signal) or being a superposition of two or more harmonic waves (complex periodic). A generally accepted system of signal classification is presented in Figure 4.1.

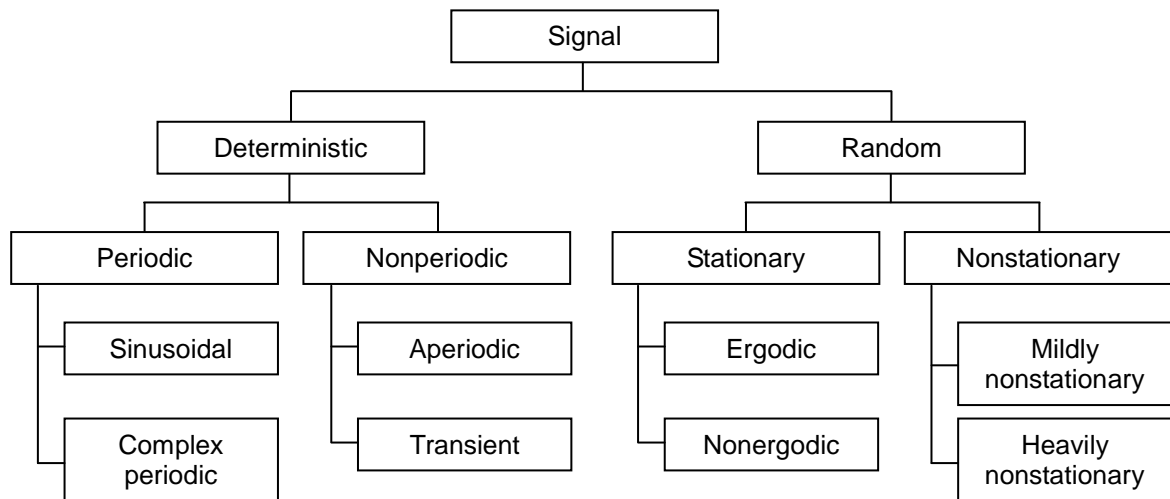


[Figure 4.1] Classification of signals (adapted from Bendat and Piersol, 1996).

4.2.1 Continuous and Discrete Signals

A signal is a description of how one parameter is related to another parameter. Since both parameters can assume a continuous range of values, it is called a continuous signal. In comparison, signals formed from parameters that are quantized are said to be

discrete signals or digitised signals. The nature of the two parameters must be clearly stated (Smith, 2003).

A typical method of obtaining a discrete signal from a continuous signal is through periodic sampling (Oppenheim et al., 1999; Wanhammer, 1999), i.e.,

$$x[n] = x_c(nT) \quad -\infty < n < \infty \quad (4.1)$$

where $x[n]$ is a sequence of samples, $x_c(t)$ is a continuous signal, T is a sampling period and its reciprocal is the sampling frequency or sampling rate ($f_s = 1/T$). However, if the sampling rate is less than twice the highest frequency of the input a phenomenon known as the aliasing which is the effect of appearing as a lower frequency signal in the sampled data will occur (Kester, 2003) shown in Figure 4.2.

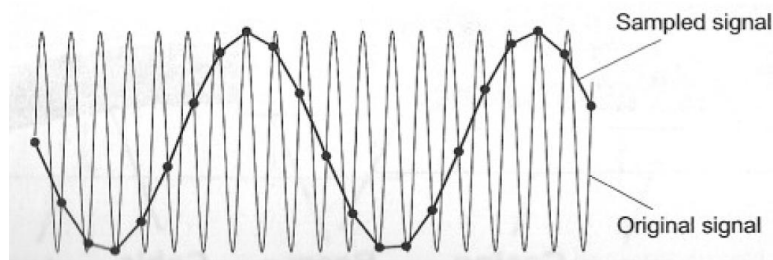


[Figure 4.2] Effect of the aliasing appeared by improper sampling (reproduced from Mansfield, 2005).

When converting the values of each sample from continuous to discrete, another phenomenon known as the quantization error or quantization uncertainty which is a difference between the actual analog input and the exact value of the digital output will occur (Kester, 2003) shown in Figure 4.3.

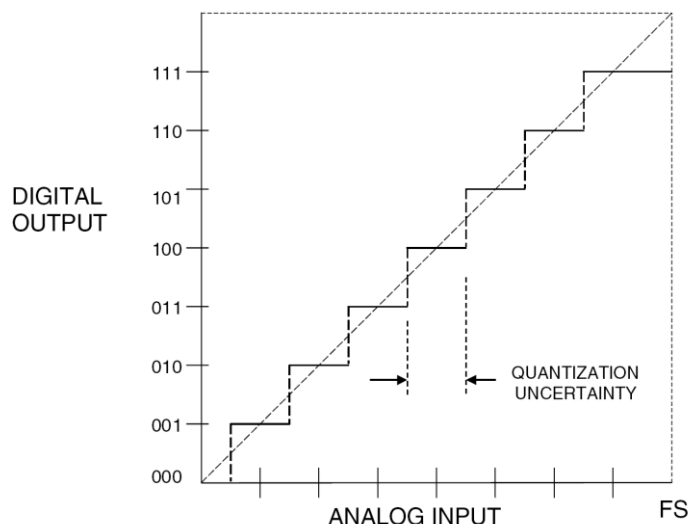


[Figure 4.3] Effect of the quantization appeared by converting the values of each sample from continuous (analog input) to discrete (digital output) (reproduced from Kester, 2003).

4.2.2 Deterministic and Random Signals

When the value of the excitation at a given time cannot be predicted, the excitation is instead said to be random. In this case, the signal can be described only in terms of probability distributions and statistical averages computed over the ensemble of the sample records representing the random process. The probability distribution $P(x)$ for a random process is defined as (Bendat and Piersol, 1986):

$$P(x) = \int_{-\infty}^{\infty} p(x) dx \quad (4.2)$$

where $p(x)$ is the probability density function (PDF) expressing the probability that the random variable takes a value between x and $x+dx$. A random process $x(t)$ is said to be stationary if for any time t_1, t_2, \dots, t_n , its probability distribution does not depend on time, i.e.

$$P\{x(t_1), x(t_2), \dots, x(t_n)\} = P\{x(t_1 + \tau), x(t_2 + \tau), \dots, x(t_n + \tau)\} \quad (4.3)$$

where τ is an arbitrary time displacement. In practice, low order statistics are employed to describe random process, leading to the definition of the term “weak stationarity” to describe stationarity up to order 2. Under this condition, a stationary random process can be described by the statistical averages up to the second order, computed over the ensemble of N_s sample records, i.e.

- the mean value: $\mu_x = \frac{1}{N_s} \sum_{k=1}^{N_s} x_k(t); \quad (4.4)$

- the mean square value: $\mu_x^2 = \frac{1}{N_s} \sum_{k=1}^{N_s} x_k^2(t); \quad (4.5)$

- the variance: $\sigma_x^2 = \frac{1}{N_s} \sum_{k=1}^{N_s} [x_k(t) - \mu_x]^2; \quad (4.6)$

- the autocorrelation function: $R_{xx}(\tau) = \frac{1}{N_s} \sum_{k=1}^{N_s} x_k(t)x_k(t + \tau); \quad (4.7)$

- the cross correlation function: $R_{xy}(\tau) = \frac{1}{N_s} \sum_{k=1}^{N_s} x_k(t) y_k(t + \tau);$ (4.8)

By definition, the weakly stationary condition implies that the mean value, the mean square value and the variance are constant and independent of time, and that the autocorrelation and cross correlation functions are dependent only on the time displacement τ . If the random process is stationary and the statistical properties as defined in Equation 4.4 to 4.8 do not differ when computed over different sample records k , the random process is said to be ergodic.

A commonly used model of a stationary random process is the Gaussian distribution, which occurs when random signal amplitudes follow the well known ‘bell-shaped’ probability distribution illustrated in Figure 4.4.

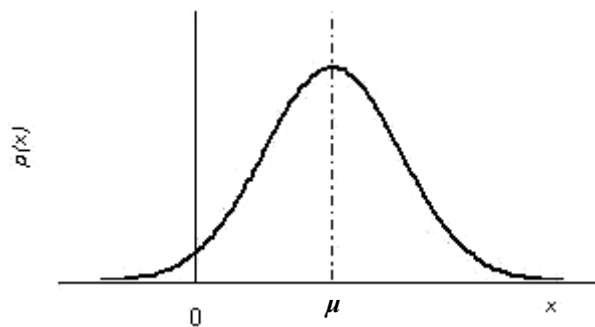


[Figure 4.4] The Gaussian distribution.

In this case the distribution of amplitudes is described by the mathematical expression

$$p(x) = \frac{1}{\sqrt{2\pi}\sigma} \exp^{-\frac{(x-\mu)^2}{2\sigma^2}} \quad (4.9)$$

where $p(x)$ is the probability of occurrence of the amplitude x and where m and σ are constants; the mean value and the variance, respectively. Newland (1993) suggests that the *normal* or *Gaussian* probability distribution is extensively used in random vibration theory to approximate the characteristics of random excitation. The function is symmetric about the mean value μ , where it achieves its maximum value.

A random process $x(t)$ is said to be non-stationary if for any time t_1, t_2, \dots, t_n , its probability distribution depends on time. According to Giacomini et al. (1999) non-stationary signals can be further divided into two categories, mildly non-stationary and

heavily non-stationary. Figure 4.5 presents examples of automobile steering wheel acceleration signals which exhibit stationary, mildly non-stationary and heavily non-stationary characteristics.

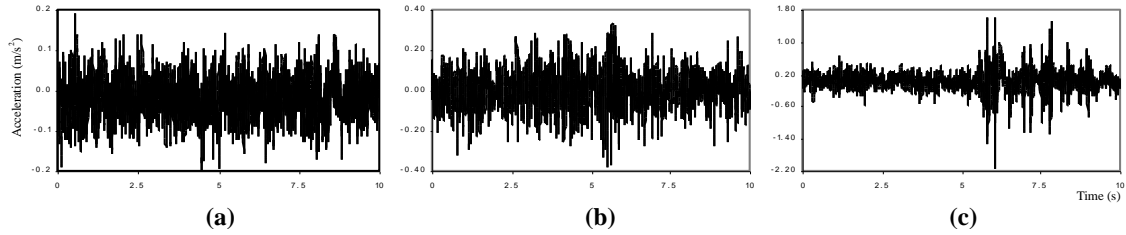


[Figure 4.5] Examples of a stationary and non-stationary time histories: (a) Stationary Gaussian signal (Highway Surface), (b) Mildly non-stationary signal (Speed Circuit Surface) and (c) Heavily non-stationary signal (Bump).

A mildly non-stationary signal is defined by Priestley (1988) as a random process with stable mean, variance and root-mean-square values for most of the record, but with short periods of changed signal statistics due to the presence of transient behaviour. A heavily non-stationary signal is defined in a similar manner to mildly non-stationary signals, but is characterised by the presence of more transient events (Giacomin et al., 2000).

4.3 Global Signal Statistics

Global signal statistics calculated from the time series are commonly used in order to describe data sets and to quantify the extent of any departures from stationary-Gaussian behaviour.

4.3.1 Root Mean Square Value

The root-mean-square (r.m.s.) value, which is a 2nd statistical moment, gives a measure of the overall energy of a signal. For a time series, the r.m.s. is defined as:

$$r.m.s. = \left\{ \frac{1}{N} \sum_{j=1}^N x_j^2 \right\}^{1/2} \quad (4.10)$$

where x_j is the instantaneous value of the sampled process $x(t)$ at time $t = j\Delta t$ and N is the number of the sampled values. The sampling interval Δt is equal to $1/f_s$ where f_s is the sampling frequency of the signal. For a sinusoidal motion of amplitude A the r.m.s. value is $2^{-1/2}A$ (i.e. approximately $0.7071A$).

4.3.2 Skewness

The skewness, which is a 3rd statistical moment, characterizes the degree of asymmetry of a distribution around its mean value. It is dimensionless and it is expressed as:

$$S_{kew} = \frac{1}{N} \sum_{j=1}^N \left(\frac{x_j - \mu_x}{\sigma_x} \right)^3 \quad (4.11)$$

For a symmetrical distribution, such as a harmonic waveform or for a stationary Gaussian process, the value of skewness is zero. Positive skewness indicates a distribution with an asymmetric tail extending toward more positive values. Negative skewness indicates a distribution with an asymmetric tail extending toward more negative values.

4.3.3 Kurtosis

The kurtosis, which is a 4th statistical moment, is highly sensitive to outlying data among the instantaneous values and therefore characterizes the relative peakedness or flatness of a distribution compared to the normal distribution. It is dimensionless and it can be expressed as:

$$K_t = \frac{1}{N} \sum_{j=1}^N \left(\frac{x_j - \mu_x}{\sigma_x} \right)^4 \quad (4.12)$$

The kurtosis is an important metric since it helps quantify the extent of departure from stationary Gaussian distribution, for which the kurtosis value should be close to 3. Any positive deviation from this value indicates a relatively peaked distribution, while a kurtosis less than 3 indicates a relatively flat distribution. For a sinusoidal signal the kurtosis value is, instead, 1.5. For the purpose of hand-transmitted vibration evaluation, an estimate in terms of kurtosis is useful due to the close correspondence between this metric and the 4th power methods, where the 4th power reflects an increased human

sensitivity to high amplitude events (Howarth and Griffin, 1991).

4.3.4 Root Mean Quad Value

The root mean quad (r.m.q.) of a time series is given by

$$r.m.q. = \left\{ \frac{1}{N} \sum_{j=1}^N x_j^4 \right\}^{1/4} \quad (4.13)$$

For a sinusoidal motion of amplitude A the r.m.q. value is $(3/8)^{1/4} A$ (i.e. approximately 0.7825A).

4.3.5 Crest Factor Value

The Crest Factor (CF) is defined as the ratio of the maximum instantaneous value of a sampled signal and the calculated r.m.s. value.

$$CF = \frac{x_{j\max}}{r.m.s.} \quad (4.14)$$

Crest factors can be either positive or negative depending on the sign of the maximum instantaneous value. For a Gaussian distribution the crest factor should normally lie in the range 3.5 to 4.5.

4.4 Frequency Domain Analysis

4.4.1 The Fourier Transform

Spectral analysis is widely used to analyse vibration signals. The mathematical function used to transform a time data series $x(t)$ into the frequency domain is called the Fourier Transform. The Fourier transform is used to convert a non-periodic function of time, $x(t)$, into a continuous function of frequency. The Fourier Transform of $x(t)$ is defined by the expression

$$X(\omega) = \int_{-\infty}^{\infty} x(t) e^{-i\omega t} dt \quad (4.15)$$

where $i = \sqrt{-1}$ and ω is called the frequency variable, which is in units of rad/s in SI units. From a Fourier transformed dataset $X(\omega)$ it is also possible to reverse the

transformation by obtaining its inverse;

$$x(t) = \int_{-\infty}^{\infty} X(\omega) e^{i\omega t} d\omega \quad (4.16)$$

Equations 4.15 and 4.16 are called the Fourier Transform pairs, and they exist if $x(t)$ is continuous and integrable as defined by the admissibility condition

$$\int_{-\infty}^{\infty} |x(t)| dt < \infty \quad (4.17)$$

4.4.2 The Discrete Fourier Transform (DFT)

Frequency analysis is concerned with the estimating of the spectrum of a random process $x(t)$ by analysing the discrete time series obtained by sampling a finite length of the sample function shown in Figure 4.6.

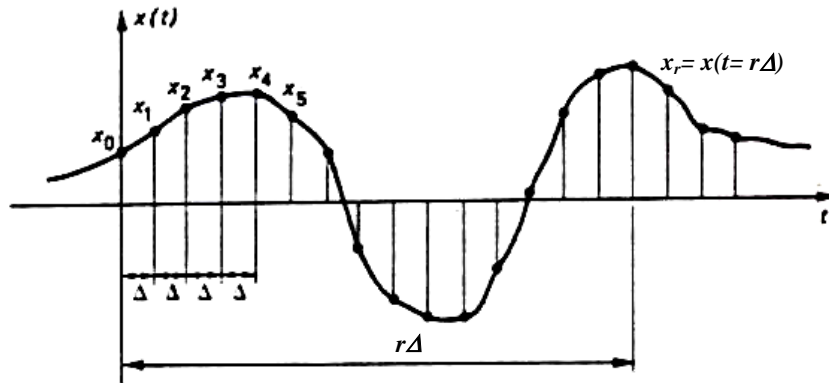


[Figure 4.6] Sampling a continuous function of time at regular intervals (Newland, 1993).

In most applications the Fourier transform is applied to sampled data on a digital computer. The digital interpretation of the Fourier transform is called the Discrete Fourier Transform (DFT) and is defined for N discrete samples of $x(t)$ as

$$X(\omega) = \frac{1}{N} \sum_0^{N-1} x(t) e^{-i\omega t/N} \quad (4.18)$$

for $\omega = 0, 1, 2, \dots, N-1$. The inverse of the discrete Fourier transform is defined by

$$x(t) = \sum_0^{N-1} X(\omega) e^{i\omega t/N} \quad (4.19)$$

for $x = 0, 1, 2, \dots, N-1$. Again, the continuity and differentiability of the underlying processes are necessary conditions for the existence of the transform and of its inverse.

4.4.3 The Fast Fourier Transform (FFT)

The DFT makes possible the computer implementation of the Fourier Transform, but it is not efficient. The number of complex multiplications and additions required to implement Equations 4.18 and 4.19 is proportional to the square of the number of data points N . For every $X(\omega)$ which is calculated, it is necessary to use all $x(0), \dots, x(N-1)$ data points.

It has been shown, however, that the decomposition of Equation 4.18 can be achieved using a number of multiplication and addition operations which is proportional to $N \log_2 N$. The decomposition procedure in question is called the Fast Fourier Transform (FFT) algorithm. The FFT works by partitioning the full sequence x_r into a number of shorter sequences, it then combines together in a way which takes advantage of the symmetry of the matrix of reduction operations so as to yield the full DFT of x_r .

If the full sequence x_r (see Figure 4.7a) is partitioned into two shorter sequences y_r and z_r (Figure 4.7b), two half sequences are yielded. The half sequences are expressed as $y_r = x_{2r}$ and $z_r = x_{2r+1}$ when $r = 0, 1, 2, \dots, (N/2 - 1)$.

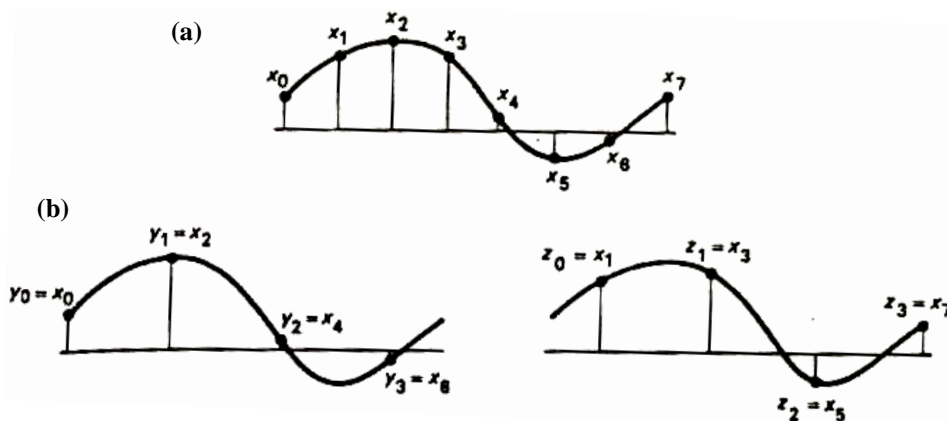


[Figure 4.7] Partitioning the sequences x_r into two half sequences y_r and z_r (Newland, 1993).

The DFT's of these two short sequences, Y_k and Z_k , after simplification of the expression 4.18 are found to be

$$Y_k = \frac{1}{(N/2)} \sum_0^{N/2-1} y_r e^{\frac{i\omega r}{(N/2)}} \quad k = 0, 1, 2, \dots, (N/2 - 1)$$

$$Z_k = \frac{1}{(N/2)} \sum_0^{N/2-1} z_r e^{-\frac{i\omega r}{(N/2)}}$$
(4.20)

Returning to the DFT of the original sequence and considering rearranging the summation into two separate sums similar to those occurring in Equation 4.20, the resultant equation is the heart of the FFT method, mathematically expressed as

$$X_k = \frac{1}{2} \left\{ Y_k + e^{-\frac{i\omega r}{N}} Z_k \right\}$$
(4.21)

A useful representation in the case of random vibration signals is the autospectral density function which is commonly referred to as the Power Spectral Density (PSD) (Bendat and Piersol, 1986). The PSD represents the mean squared value as a function of frequency. It avoids the problem that random signals, producing a continuous frequency spectra, have the signal energy measured within only a certain frequency band (Bendat and Piersol, 1986). Because the Fourier Transform in Equation 4.18 is computed only on one time interval, the spectrum is not typical of the complete time history. Averaging of the spectra from different intervals of the signal is thus necessary in order to obtain a more accurate representation. The PSD of a time series is thus defined as:

$$G_{xx}(f) = \frac{2}{n_d T} \sum_{i=1}^{n_d} |X_i(f, T)|^2 \quad f > 0$$
(4.22)

where $X_i(f, T)$ is the FFT of the signal computed over the i^{th} data interval of duration T and n_d is the number of averages used in the calculation. The segment duration T determines the frequency resolution $\Delta f = 1/T = 1/N_{data} \square f_s$ for the FFT computation, and is normally chosen based on the characteristics of the type of data being analysed.

4.5 Digital Filters

A filter is considered a black box which contains some form of processing that generates outputs from inputs (Winder, 2002). As shown in Figure 4.8 the output can be found mathematically by multiplying the input by the transfer function, which is a frequency dependent equation relating the input and output. The outputs should be more useful than the inputs, thus the purpose of using a filter is to improve the quality of the



outputs and to extract information (Winder, 2002).

[Figure 4.8] A transfer function of input and output (adapted from Winder, 2002).

Digital filters fall into one of two main categories: finite impulse response (FIR) filters and infinite impulse response (IIR) filters. This section provides an introduction to both types of filter.

4.5.1 Finite Impulse Response (FIR) Filters

Finite Impulse Response (FIR) filters are often called nonrecursive filters because the output of the filter is calculated only from the current and previous input values (Bendat and Piersol, 1986; Elliott, 1987; Smith, 2003; Kester, 2003). The equation of an N_{th} order FIR filter is

$$y(n) = \sum_{k=0}^{N-1} h(k)x(n-k) \quad (4.23)$$

where $y(n)$ is the filter output for time n , $x(n-k)$ is the filter input at time $(n-k)$, $h(k)$ is the filter coefficient (k), and N is the number of taps, which defines how many input data points are used to calculate the simple output data point.

If the FIR filter is subjected to a digital impulse defined as

$$k_n = \begin{cases} 1, & \text{if } n = 0 \\ 0, & \text{otherwise} \end{cases} \quad (4.24)$$

the response is called the filter's impulse response, and is a characteristic trait of the filter. If the input is a digital impulse, then

$$X_n = k_n = \begin{cases} 1, & \text{if } n = 0 \\ 0, & \text{otherwise} \end{cases} \quad (4.25)$$

or

$$X_{n-1} = \begin{cases} 1, & \text{if } k = n \\ 0, & \text{otherwise} \end{cases} \quad (4.26)$$

each product of the sum is zero except the product where $n = k$. The impulse response of the FIR filter therefore consists of the coefficients of the filter. The length of the nonzero portion of the impulse response is dictated by the number of coefficients in the filter. Since these filters have at most N nonzero coefficients, the impulse response can be no longer than N . For this reason, the filters have a finite duration (Kester, 2003), thus the use of the name finite impulse response.

When the input to a filter is $x(n) = e^{j\omega n}$ which is equivalent to a sampled sinusoid of frequency ω , Equation 4.23 is to be

$$\begin{aligned} y(n) &= \sum_{k=0}^{N-1} h(k)e^{j\omega(n-k)} \\ &= e^{j\omega n} \sum_{k=0}^{N-1} h(k)e^{-j\omega k} \\ &= x(n)H(e^{j\omega}) \end{aligned} \quad (4.27)$$

The quantity $H(e^{j\omega})$ is the frequency response function of the filter. The frequency response of the filter has an amplitude and a phase (LMS International Inc., 2002; Elliott, 1987)

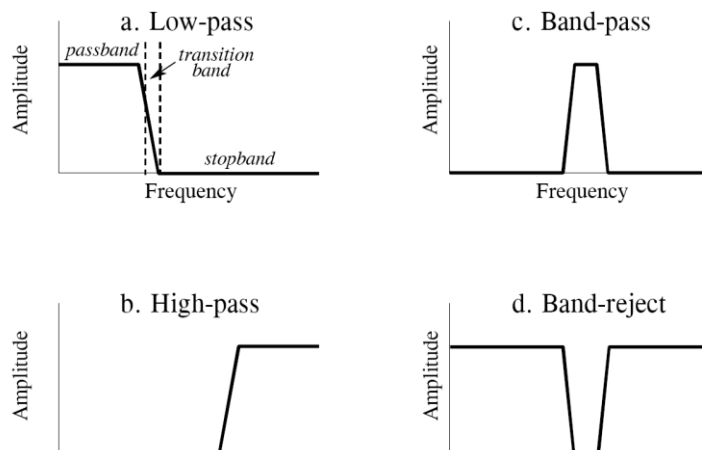
$$H(e^{j\omega}) = |H(e^{j\omega})| \cdot e^{j\theta(\omega)} \quad (4.28)$$

In the case of the filter with a symmetric impulse response [$h(n) = h(N-1-n)$] the filter has a linear phase response (Elliott, 1987). Therefore, the phase response of the filter is

$$\theta(\omega) = -\left(\frac{N-1}{2}\right)\omega, \quad \text{where } -\pi \leq \omega \leq \pi \quad (4.29)$$

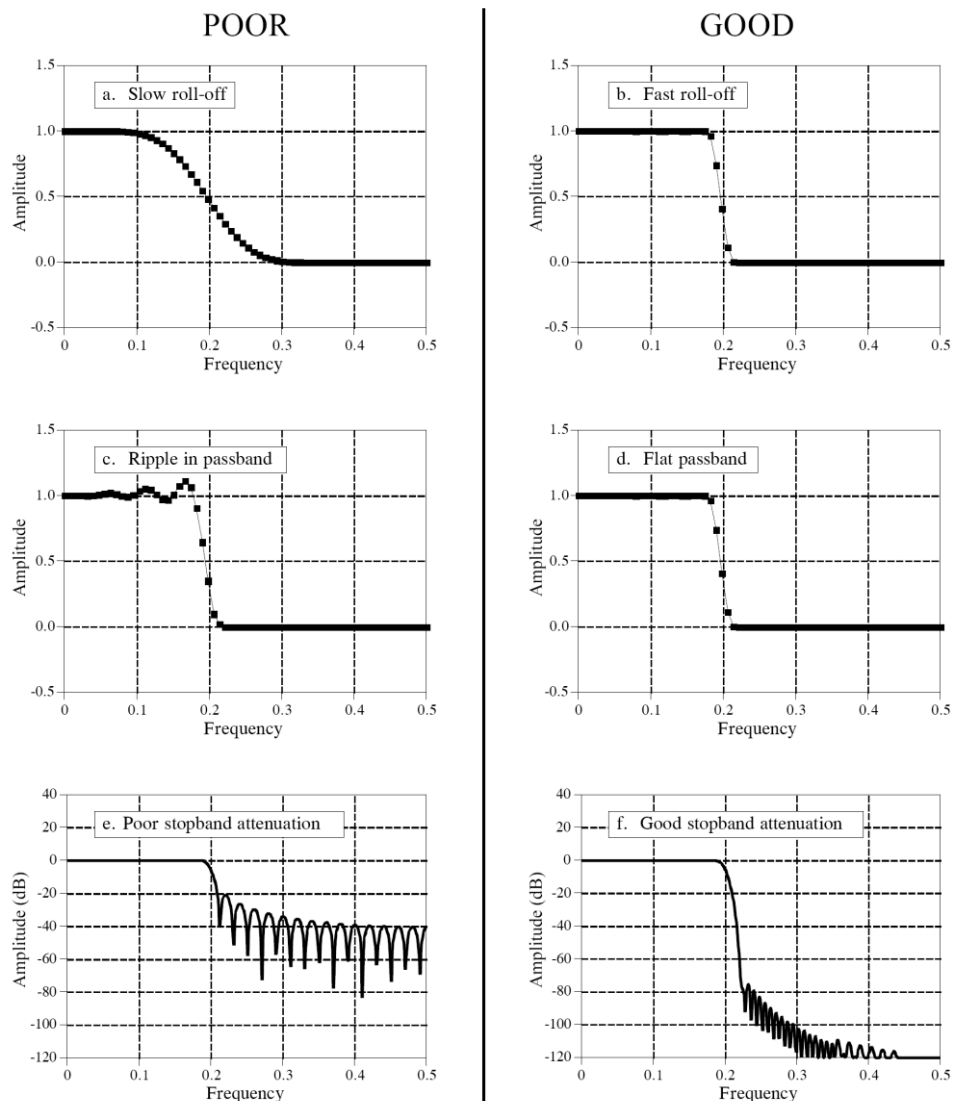
which shows a linear phase filter with a constant group delay of $(N-1)/2$ (Elliott, 1987).

Figure 4.9 shows the four most commonly used frequency responses. A pass-band refers to those frequencies that are passed, while a stop-band contains those frequencies that are blocked. The frequency interval between the pass-band and the stop-band is a transition band, which is related to a filter parameter called the roll-off sharpness.



[Figure 4.9] Four commonly used frequency responses; A (a) low-pass, (b) high-pass, (c) band-pass and a (d) band-stop responses (reproduced from Smith, 2003).

Figure 4.10 shows three filter characteristics which are commonly used to indicate how well a filter performs in the frequency domain. To separate closely spaced frequencies, the filter must have a fast roll-off, as illustrated in (a) and (b). For the pass-band frequencies to move through the filter unaltered, there must be no pass-band ripple, as shown in (c) and (d). Lastly, to adequately block the stop-band frequencies, it is necessary to have good stop-band attenuation, displayed in (e) and (f).



[Figure 4.10] Three filter characteristics which are used to indicate frequency domain performance (reproduced from Smith, 2003).

4.5.1.1 FIR Filter Design

The FIR filter design process consists of determining the impulse response from the desired frequency response, and then quantizing the impulse response to generate the filter coefficients (Kester, 2003). The main FIR filter design methods are the Fourier transform method (Winder, 2002), the Frequency sampling method (Kester, 2003) and the Parks-McClellan method (Winder, 2002; Kester, 2003).

- **Fourier transform method**

The frequency response of a filter can be expanded into the Fourier series.

$$H(e^{j\omega}) = \sum_{n=-\infty}^{\infty} h(n)e^{-j\omega n} \quad (4.30)$$

$$h(n) = \frac{1}{2\pi} \int_{-\pi}^{\pi} H(e^{j\omega})e^{j\omega n} d\omega$$

The coefficients of the Fourier series are identical to the impulse response of the filter. However, when the impulse response is truncated to a reasonable number of N taps it can become a problem since repetition implies a discontinuity, meaning that the input signal is not periodic in time as shown in Figure 4.11. The discontinuity creates a smearing of energy throughout the frequency domain which is called leakage. The solution to the problem of leakage is known as windowing (Kester, 2003). A time window function has value zero at the ends and is large in the middle so that the discontinuity is eliminated.

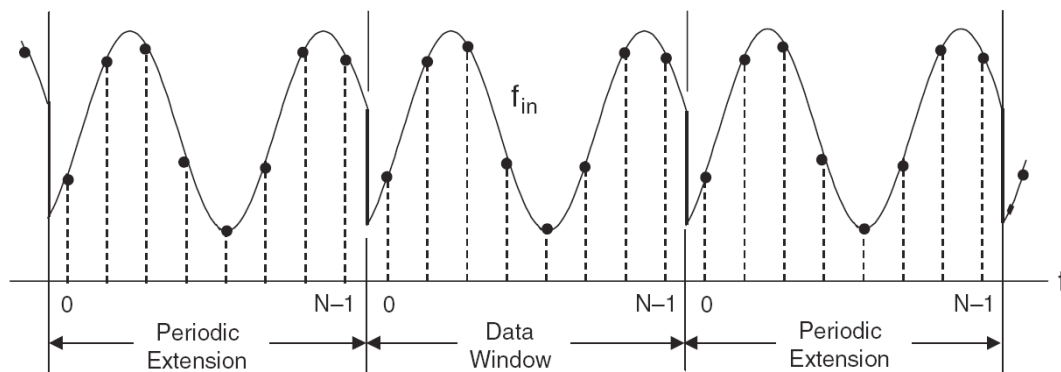


[Figure 4.11] Input signal not periodic in time record (reproduced from Kester, 2003).

After truncation and windowing, an FFT is used to generate the corresponding frequency response which can be modified by choosing different window functions. Some popular window functions (Elliott, 1987; Taylor, 1994) were summarised below:

$$\text{– Rectangular window: } w(n) = \begin{cases} 1 & \text{if } |n| \leq (N-1)/2 \\ 0 & \text{otherwise} \end{cases} \quad (4.31)$$

$$\text{– Triangular window: } w(n) = \begin{cases} 1 - \frac{2|n|}{N-1} & \text{if } |n| \leq \frac{(N-1)}{2} \\ 0 & \text{otherwise} \end{cases} \quad (4.32)$$

$$\text{– Hanning window: } w(n) = \begin{cases} 0.5 + (1-0.5)\cos\left(\frac{2\pi n}{N-1}\right) & \text{if } |n| \leq \frac{(N-1)}{2} \\ 0 & \text{otherwise} \end{cases} \quad (4.33)$$

$$\text{– Hamming window: } w(n) = \begin{cases} 0.54 + (1-0.54)\cos\left(\frac{2\pi n}{N-1}\right) & \text{if } |n| \leq \frac{(N-1)}{2} \\ 0 & \text{otherwise} \end{cases} \quad (4.34)$$

$$\text{– Blackman window: } w(n) = \begin{cases} 0.42 + 0.5\cos\left(\frac{2\pi n}{N-1}\right) + 0.08\cos\left(\frac{4\pi n}{N-1}\right) & \text{if } |n| \leq \frac{(N-1)}{2} \\ 0 & \text{otherwise} \end{cases} \quad (4.35)$$

- **Frequency sampling method**

This method is useful in generating an FIR filter which has an arbitrary frequency response. The desired frequency response $H(k)$ is specified as a series of amplitude and phase points in the frequency domain using the DFT Equation 4.18. The points are then converted into real and imaginary components. The impulse response is obtained by taking the complex inverse FFT of the frequency response. The impulse response is then truncated to N points, and a window function is applied to minimize the effects of truncation. The filter design should then be tested by taking its FFT and evaluating the frequency response. Several iterations may be required to achieve the desired frequency response (LMS International Inc., 2002; Kester, 2003).

- **Parks-McClellan method**

The Parks-McClellan method uses the Remez exchange algorithm (Winder, 2002; Kester, 2003) which tries to generate a set of filter coefficients that will produce the

same response. The algorithm is a curve-fitting method that minimizes the error between the model and the filter in which the final response has equal errors above and below the desired frequency response (Winder, 2002). The filter designer needs to specify the parameters which are the pass-band ripple, the stop-band attenuation and the transition region. When the parameters are specified, the algorithm estimates the number of taps required to implement the filter based on the specifications.

4.5.2 Infinite Impulse Response (IIR) Filters

Infinite Impulse Response (IIR) filters are often called recursive filters because the output of an IIR filter is calculated not only using the input values, but also using previous output values (Bendat and Piersol, 1986; Elliott, 1987; Smith, 2003; Kester, 2003). The equation of an N, M order IIR filter is

$$y(n) = \sum_{k=0}^N a(k)x(n-k) - \sum_{k=1}^M b(k)y(n-k) \quad (4.36)$$

where $y(n)$ is the filter output for time (n) , $x(n-k)$ is filter input at time $(n-k)$, $y(n-k)$ is the filter output at time $(n-k)$, $a(k)$ are the coefficients of the non-recursive component of the filter, $b(k)$ are the coefficients of the recursive component of the filter and N and M are the number of taps. When the digital impulse is applied as input only the $n = k$ term contributes to the non-recursive sum. The impulse response of the IIR filter can remain nonzero for even large indices. The recursive portion continues to generate an output long after the $a(k)$ s are zero. For this reason, the IIR filters have a infinite duration (Kester, 2003).

When the input to an IIR filter is $x(n) = e^{j\omega n}$ then Equation 4.36 becomes

$$y(n) = \sum_{k=0}^N a(k)e^{j\omega(n-k)} + \sum_{k=1}^M b(k)y_{n-1} \quad (4.37)$$

The frequency response function of an IIR filter is thus expressed as $H(\omega)$

$$H(\omega) = \frac{\sum_{k=0}^N a(k)e^{-j\omega k}}{1 - \sum_{k=1}^M b(k)e^{-j\omega k}} \quad (4.38)$$

The frequency response of an IIR filter is thus determined by the weighted sum of the recursive and non-recursive coefficients. The frequency response is the most useful

characterization of both recursive and non-recursive filters, but it only provides information regarding how the filter behaves with exponential inputs. The z-transform shows instead how the filter responds to a broader class of inputs. There exists a direct relationship between the coefficients of a recursive filter and the filter's z transform. From the Equation 4.38 the following equation can be obtain

$$H_z(z) = \frac{\sum_{k=0}^N a(k)z^{-k}}{1 - \sum_{k=1}^M b(k)z^{-k}} \quad (4.39)$$

where z is $e^{j\omega}$. The non-recursive coefficients appear in the numerator while the recursive coefficients appear in the denominator. In the z-domain the transfer function of a digital filter is written as one polynomial divided by another polynomial, the roots of the denominator are the poles of the system, while the roots of the numerator are the zeros (Smith, 2003).

IIR filters are usually more efficient than FIR filters because they have infinite memory, while FIR filters have finite memory (Elliott, 1987). However, when designing IIR filters the designer must pay attention to stability and phase nonlinearity (Elliott, 1987). Therefore if sharp cut-off filters are needed, and processing time is at a premium, IIR filters are a good choice, but if the number of taps is not restrictive, and linear phase is a requirement, the FIR should be chosen (Kester, 2003).

4.5.2.1 IIR Filter Design

Since the transfer function is frequency dependent the frequency response is complex (Winder, 2002). Therefore the frequency response is described in terms of s , where s is $j\omega$, rather than frequency ω and it is called s-domain. Then the analog transfer function becomes $H(s)$ defined by the Laplace transform. A common method for designing IIR filter is to first design the analog equivalent filter and then mathematically transform the analog transfer function $H(s)$ into z-domain, $H(z)$ (Kester, 2003). There are three methods used to convert the Laplace transform into the z-transform: impulse invariant transformation, bilinear transformation and the matched z-transform (Kester, 2003). Only the bilinear transformation provides a general-purpose conversion function that can be used for low-pass, high-pass, band-pass. and band-reject (or band-stop) responses (Winder, 2002). The impulse invariant conversion function (Winder, 2002)

can only be used for low-pass filter while the matched z-transform (Elliott, 1987) can be used for high-pass and band-stop filters. For these reasons, only bilinear transformation is considered below.

- **Bilinear transformation**

Bilinear transform is used to convert the analog frequency response (s-domain) into a digital domain (z-domain) response. Once in the z-domain, the response function can be reorganised and the filter coefficients read off directly (Winder, 2002). The bilinear transform is defined by

$$s = \frac{2}{T} \frac{(z - 1)}{(z + 1)} \tag{4.40}$$

where s is $j\omega$, z is $e^{j\omega T}$ and T is the sampling rate in seconds per sample. However, the bilinear transform approach is an approximation and will not produce the exact frequency response required. The frequency response will be distorted by what is called the warping effect (Winder, 2002). Frequency warping effects can be reduced or altogether eliminated by designing digital filters from a pre-warp analog frequency response shown in Equation 4.41 and Figure 4.12.

$$\omega_a = \tan\left(\frac{\omega_c}{2}\right) \tag{4.41}$$

where ω_a is a analog cut-off frequency and ω_c is a desired filter cut-off frequency. This should be used in the s-domain transfer function before applying the bilinear transform.

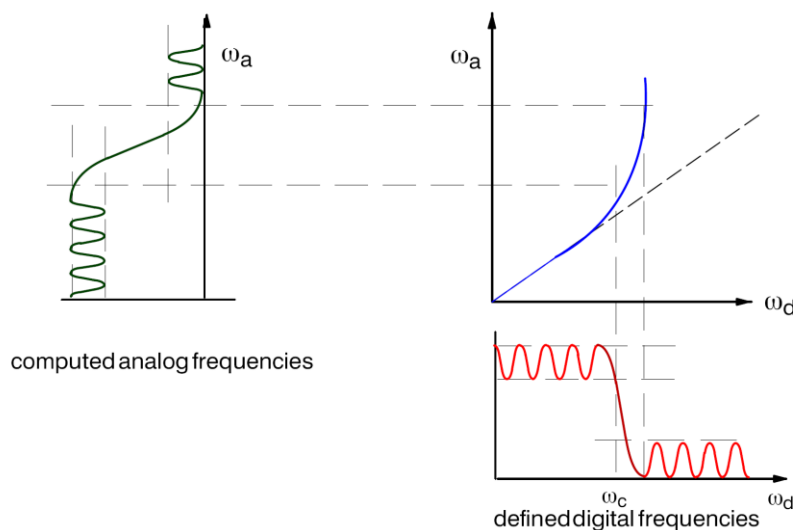


[Figure 4.12] Conversion from digital to analog frequencies (reproduced from LMS

International Inc., 2002).

* ω_a : a analog cut-off frequency, ω_c : a desired filter cut-off frequency, ω_d : a digital cut-off frequency

4.5.2.2 Some Typical IIR Filters

Unlike the FIR filters which have no real analog counterparts, IIR filters have traditional analog counterparts which are Butterworth, Chebyshev, Elliptic and Bessel. This section therefore introduces the characteristics of the analog counterparts commonly used in the field of signal processing.

- **Butterworth filters**

These are characterised by the response being maximally flat in the pass-band and monotonic in the pass-band and stop-band. Maximally flat means as many derivatives as possible are zero at the origin. The squared magnitude response of a Butterworth filter is

$$|H(s)|^2 = \frac{1}{1 + (s/s_c)^{2n}} \quad (4.42)$$

where s is $j\omega$, s_c is $j\omega_c$ (ω_c is a cut-off frequency) and n is the order of the filter. Butterworth filters are all-pole filters i.e. the zeros of $H(s)$ are all when s is infinite. They have magnitude of $1/\sqrt{2}$ when ω/ω_c is 1 i.e. the magnitude response is down 3dB at the cut-off frequency.

- **Chebyshev (typel)**

The Chebyshev (typel) filter, instead, has a faster roll-off than the Butterworth for the same number of poles and has ripple in the pass-band. The formula is

$$|H(\omega)|^2 = \frac{1}{1 + \varepsilon^2 C_n^2(\omega)} \quad (4.43)$$

where $C_n(\omega)$ are the Chebyshev polynomials and ε is the parameter related to the ripple in the pass-band. As the ripple increases the roll-off becomes sharper (Smith, 2003) meaning the optimal concession is required to obtain a desired response. Given the existence of the ripple the transition width of a Chebyshev filter is narrower than for a Butterworth filter of the same order.

- **Elliptical (Cauer)**

The Elliptical (Cauer) filter has poles and zeros, and ripple in both the pass-band and stop-band. This filter has even faster roll-off than the Chebyshev for the same number of poles. These filters are optimum in the sense that for a given filter order and ripple specifications, they achieve the fastest transition between the pass- and the stop-band. They have equiripple stop-bands and pass-bands. The transfer function is given by

$$|H(\omega)|^2 = \frac{1}{1 + \varepsilon^2 R_n^2(\omega L)} \quad (4.44)$$

where ε is a parameter related to the pass-band ripple, $R_n(\omega L)$ is called a Chebyshev rational function and L is a parameter describing the ripple properties of $R_n(\omega L)$. This group of filters is characterised by the property that the group delay is maximally flat meaning the delay is independent of frequency. However this characteristic is not normally preserved by the bilinear transformation and it has poor stop-band characteristics. For a given requirement, this approximation will require a lower order than the Butterworth or the Chebyshev filters. The Elliptical approximation will thus lead to the least costly filter realization, but at the expense of the worst delay characteristics.

- **Bessel (Thompson)**

The Bessel (Thompson) filter is an all-pole filter optimised for pulse response and linear phase but has the poorest roll-off of any of the types discussed for the same number of poles. The goal of the Bessel approximation for filter design is to obtain a flat delay characteristic in the pass-band. The delay characteristics of the Bessel approximation are far superior to those of the Butterworth and the Chebyshev approximations, however, the flat delay is achieved at the expense of the stop-band attenuation which is even lower than that for the Butterworth. The poor stop-band characteristics of the Bessel approximation make it impractical for most filtering applications. Bessel filters have sloping pass- and stop-bands and a wide transition width resulting in a cut-off frequency that is not well defined. The transfer function is given by

$$|H(s)|^2 = \frac{d_0}{B_n(s)} \quad (4.45)$$

where $B_n(s)$ is the n _{th} order Bessel polynomial and d_0 is a normalizing constant.

Chapter 5

Steering Wheel Vibration Measured from Road Testing

5.1 Introduction

This chapter describes the steering wheel acceleration data obtained from several road surfaces and several automobiles which were used in the research presented in this thesis. In particular, signal analysis was applied to quantify the typical statistical variation which occurred in the steering wheel acceleration when driving over different road surfaces.

Variations in the magnitude and frequency content of steering acceleration signals are

primarily caused by variations of the road roughness and by variations of the automobile speed (Gillespie and Sayers, 1983; Rouillard and Sek, 2002), where road roughness has been defined by the ASTM E1364-95 (2005) as “the deviation of a surface from a true planar surface with characteristic dimensions that affect vehicle dynamics, ride quality, dynamic loads, and drainage”. While the data presented in this chapter cannot be considered to be a definitive scientific analysis of road vehicle vibration, the values obtained can be considered to be typical of the automotive vibration problem, thus useful for the purpose of defining specific laboratory-based experiments which can be considered representative of the automobile environment.

5.2 Experimental Vibration Tests

Before performing any laboratory tests of human perception, real stimuli from real automobiles had to be selected which could serve as the base stimuli for use in the research. From a review of the available literature treating automotive vibration, and from a review of the aims and objectives of the planned experimentation, it was decided that the group of steering acceleration signals which could be used to study the human perception should satisfy a set of logical conditions which can be summarised as the following:

- The stimuli should come from normal production automobiles of the most commonly encountered manufacturers such as Ford, Renault, Toyota and Volkswagen and from the most commonly encountered market segments defined by the International Organization of Motor Vehicle Manufacturers, “Organisation Internationale des Constructeurs d’Automobiles” (OICA, 2008).
- The stimuli should have been produced by commonly encountered road surfaces such as city asphalt, pavé, potholes, bumps, country asphalt and smooth motorway surfaces, so as to be representative of ordinary driving conditions (Giacomin and Gnanasekaran, 2005).
- The automobile test speeds should be reasonable values which are commonly used when driving over each specific type of surface (Department of Transport, 2006).

- Where possible, the choices described above should be made in such a way as to be as close as possible to the values used by the testing programmes of the major European automobile manufacturers, given their vast experience in the field of testing.
- Where possible, the choices described above should be made in such a way as to widen the amplitude range, the frequency range and the frequency distribution of the stimuli so as to produce the widest possible operational envelope of test stimuli.

The steering wheel acceleration signals used in the research were provided by MIRA (Motor Industry Research Association), by the Michelin Group, by Honda Motor Company or were directly measured by tests over road surfaces in and around Uxbridge, West London, UK (Berber-Solano, 2009). All acceleration measurements were made at the automotive steering wheel. The measurement point was on the surface of the steering wheel at the 60° position (two o'clock position) with respect to top centre. This location coincides with a typical grip position of the driver's hand when holding an automotive steering wheel (Giacomin and Gnanasekaran, 2005).

In the sections which follow, each of the steering wheel acceleration data sets which was considered and analysed will be described in terms of the test equipment and experimental protocol, and the statistical properties of the acquired signals will be summarised. The order of presentation is based on the source of the data sets, thus the order is: Mira tests, Michelin tests, Honda tests and Uxbridge tests.

5.2.1 Mira Tests

Six steering wheel acceleration signals were measured at MIRA's proving ground in Nuneaton, Warwickshire, UK, which has a comprehensive range of circuits and facilities which are used to carry out a wide range of tests (MIRA Ltd, 2006). All data were measured using an accelerometer which was clamped to the steering wheel measurement position by means of a mounting bracket of sufficient stiffness to guarantee accurate measurements to frequencies in excess of 500 Hz. The steering wheel acceleration time histories were digitally acquired using a PC-based digital data

acquisition system running MIRA's own in-house software. The data acquisition system was placed inside the vehicle, and the data acquisition was triggered by the driver when driving over each road surface at a single constant speed. The sensors used in the road test data acquisition were Kyowa model AS-5GB accelerometers. The calibration of the MIRA measurement equipment was guaranteed by regularly scheduled calibration tests and by an internal quality assurance scheme.

The automobile used by MIRA during the experimental vibration test was an Audi A4 model year 2000, type 4/5S SAL (4 doors, 5-speed manual transmission and saloon sedan). The engine was a turbocharged diesel 4-cylinder 1.8L with an EFi (Electronic Fuel injection) fuel system. The Audi A4 steering system was a rack and pinion Power Assist Steering (PAS). The front suspension was an independent, four-link, double wishbone, and anti-roll bar, while the rear suspension was an independent, trapezoidal link and anti-roll bar. The front and rear tyres specifications were P195/65 R 15 meaning tires from a passenger car (P), nominal section width in mm of 195, an aspect ratio of 65 for the ratio of the height to the total width of the tire, Radial (R) construction of the fabric carcass of the tire and a rim diameter in inches of 15.

The road surfaces used to measure the test stimuli were a Coarse Asphalt, Cobblestone surface, Concrete surface, Low Bump, Slabs surface and a Tarmac surface. Figure 5.1 presents the six road surfaces as viewed from directly above and as seen from a distance as when driving, along with the automobile velocity at which they were measured.

Steering wheel tangential acceleration time histories were measured for the Audi A4 when driving over the six surfaces shown in Figure 5.1. For each road surface a 2 minute data recording was acquired. From each 2 minute recording a 7 second data segment of the tangential direction steering wheel acceleration time history was extracted from each data set to serve as test stimuli. The individual segment for each surface type was selected such that the root mean square value, kurtosis value and power spectral density were statistically close to those of the complete 2 minute recording. Figure 5.2 presents the single 7 second time history segment which was extracted for each of the six test roads.

Coarse Asphalt (vehicle speed 96 km/h)



Cobblestone Road (vehicle speed 30 km/h)



Concrete Road (vehicle speed 96 km/h)



Low Bump (vehicle speed 50 km/h)



Slabs Road (vehicle speed 96 km/h)



Tarmac Road (vehicle speed 96 km/h)

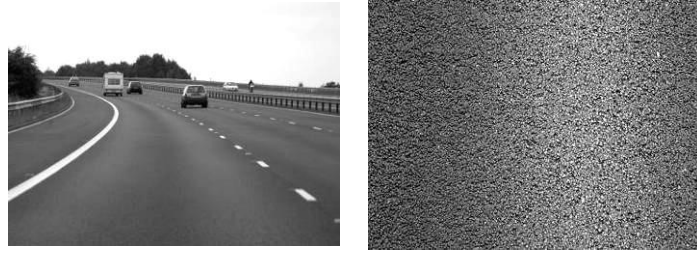


[Figure 5.1] Road surfaces used by MIRA for their steering wheel vibration tests.

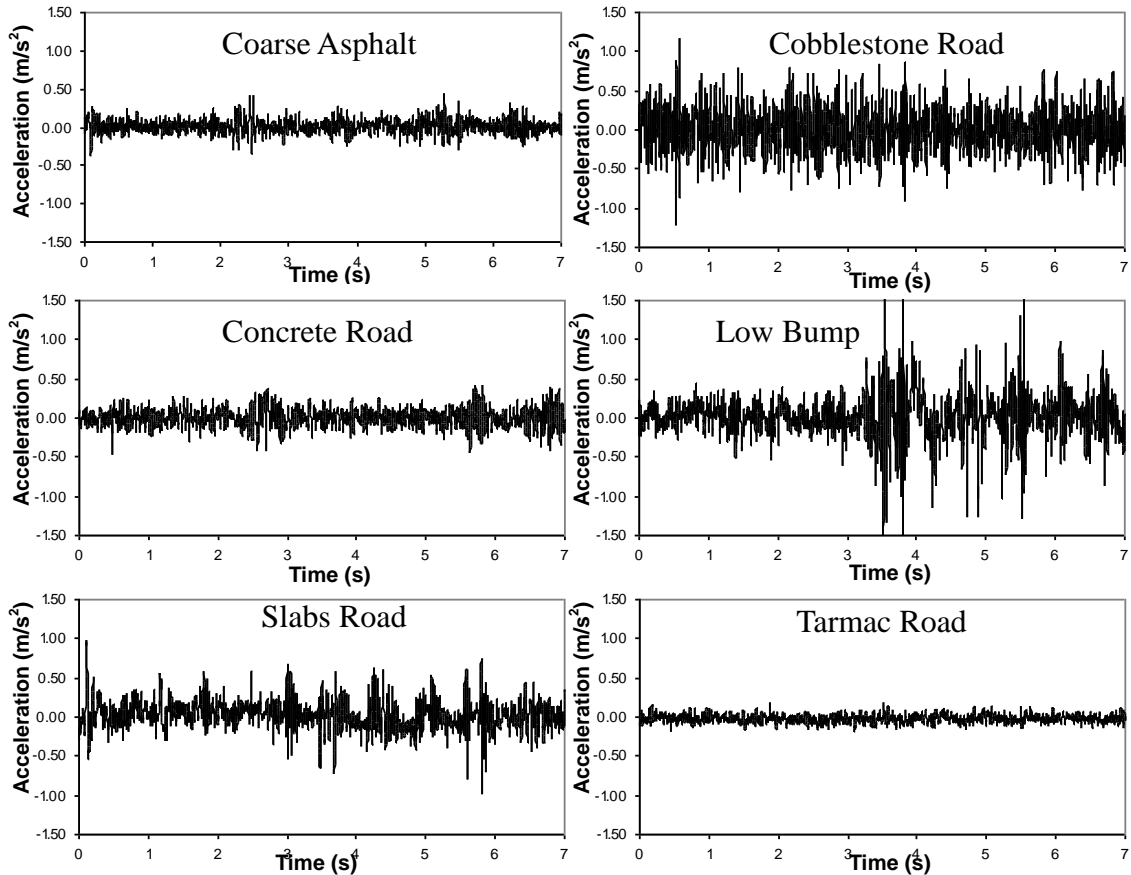


[Figure 5.2] A 7 second segments of the tangential acceleration time history measured at the steering wheel for each of the six road surfaces (The MIRA test).

The global statistical properties calculated for the complete original 2 minute recording of each road surface are presented in Table 5.1 along with the automobile speed used during the measurement. The global statistical properties were calculated by means of the equations of the r.m.s., kurtosis, skewness, crest factor and the r.m.q. described in Chapter 4. Results from Table 5.1 suggest that vibration at the steering wheel achieved root mean square (r.m.s.) acceleration levels from a minimum of 0.056 m/s^2 for the tarmac surface to a maximum of 0.315 m/s^2 for the low bump surface. The kurtosis values were from 3.101 to 8.064 while the skewness values were from -0.22 to 0.133.

The maximum crest factor (CF) was 5.95 for the low bump surface, while the minimum CF was 3.435 for the tarmac surface. The root mean quad (r.m.q.) values were from a minimum of 0.073 m/s² for the tarmac surface to a maximum of 0.509 m/s² for the low bump surface.

[Table 5.1] Global statistical properties of the six road stimuli measured from Mira tests.

Type of road	Global Statistics and Characteristics					
	r.m.s. (m/s ²)	Kurtosis	Skewness	Crest Factor	Speed (km/h)	r.m.q. (m/s ²)
Coarse Asphalt	0.095	4.207	0.177	4.236	96	0.136
Cobblestone	0.278	3.180	0.069	4.336	30	0.377
Concrete	0.117	3.461	-0.001	3.823	96	0.164
Low bump	0.315	8.064	-0.220	5.950	50	0.509
Slabs	0.182	5.275	0.133	5.388	96	0.281
Tarmac	0.056	3.101	0.091	3.435	96	0.073

The power spectral density (PSD) of each of the two minute acceleration signals was calculated and the results are presented as Figure 5.3. Observation of the results suggests that the principal frequency content is mostly in the range from 0 to 80 Hz for all six road surfaces. The frequency distributions suggest that the higher peaks of energy correspond to the typical automobile resonance frequencies (Hamilton, 2000; Kulkarni and Thyagarajan, 2001; Pottinger et al., 1986). The first region of resonance behaviour in the region from 0 to 5 Hz is common in any road data due to rigid body motion of the automobile chassis on the main suspensions. The second broader resonance region covering frequencies from 5 to 13 Hz can be associated with the behaviour of suspension units separately or with the rigid body motion of the engine/transmission unit. The third region resonance behaviour distributed between 13 and 22 Hz may reflect low frequency flexible body modes of the chassis. Finally, the fourth region from 22 to 100 Hz is probably mostly defined by higher-frequency modes of the chassis and by tire resonances (Giacomin and Lo Faso, 1993; Pottinger et al., 1986).

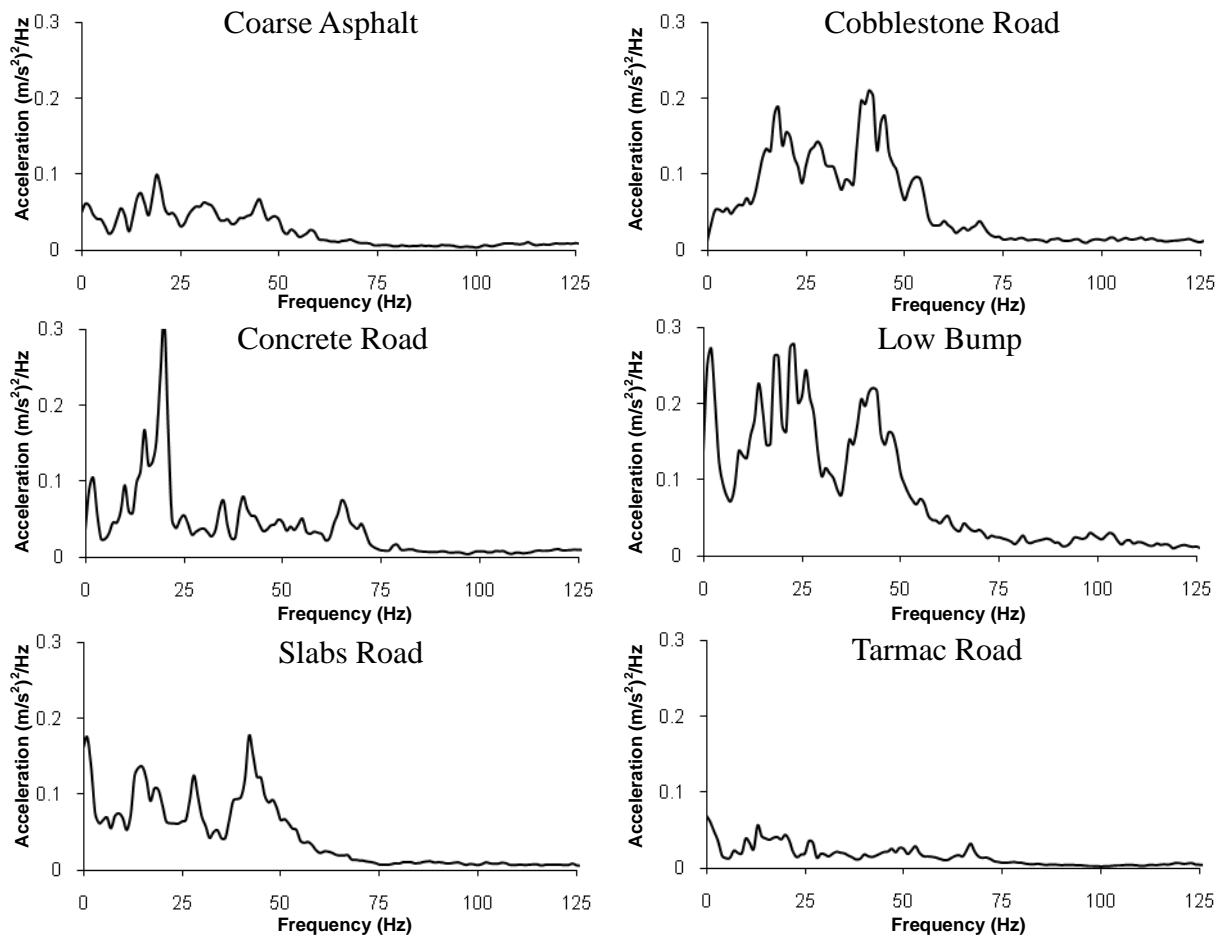


[Figure 5.3] Power Spectral Densities (PSD) calculated from the four tangential acceleration time histories of the 2 minute duration which were measured at the steering wheel.

5.2.2 Michelin Tests

Four of the steering wheel acceleration signals were provided by the Michelin Group. The acceleration measurements were performed at the Claremont-Ferrand proving ground in the province of Auvergne, France, which has a comprehensive range of circuits and facilities which are used to carry out a wide range of tests. The steering wheel vibrations were measured by means of a tri-axial piezoresistive accelerometer

(Entran EGAS3-CM-25). The acceleration signals were amplified by means of an Entran MSC6 signal-conditioning unit, and stored using 6 channels of a Sony PC 216A Digital Audio Tape (DAT) recorder and monitored by a Tektronix TDS 210 digital oscilloscope. The DAT sampling rate chosen for the vibration measurements was 5 kHz. The steering wheel acceleration time histories were digitally acquired using a PC-based digital data acquisition system running Michelin's own in-house software.

The automobile used by Michelin during the acceleration measurements was a Renault Megane 1.9 dTi model year 1996, type 2+2 FHC (Fixed-Head Coupé), with 3 doors and a 5-speed manual transmission. The engine was a turbocharged diesel direct injection system (dTi) 4-cylinder 1.9 L. The Renault steering system was a rack and pinion Power Assist Steering (PAS).

The front suspension was an independent and Macpherson strut, while the rear suspension was an independent. The front and rear tyre specifications were P175/65 R 14. The road surfaces used by Michelin to measure the steering wheel acceleration stimuli were named Harsh surface, Noise surface, Service surface and Gravel surface. Figure 5.4 presents these road surfaces as viewed from directly above, and as seen from a distance as when driving, along with the automobile test velocity.



Service Road (vehicle speed 80 km/h)



[Figure 5.4] Road surfaces used by Michelin for their steering wheel vibration tests.

For each road surface a 1 minute data recording was available from experimental testing. A 7 second data segment of the tangential direction steering wheel acceleration time history was extracted from each data set to serve as test stimuli. The segments were selected such that the root mean square value, kurtosis value and power spectral density were statistically close to those of the complete recording. Figure 5.5 presents the time history segments selected for each of the road surfaces. As expected, different shapes and different acceleration levels are observed from the road surfaces.

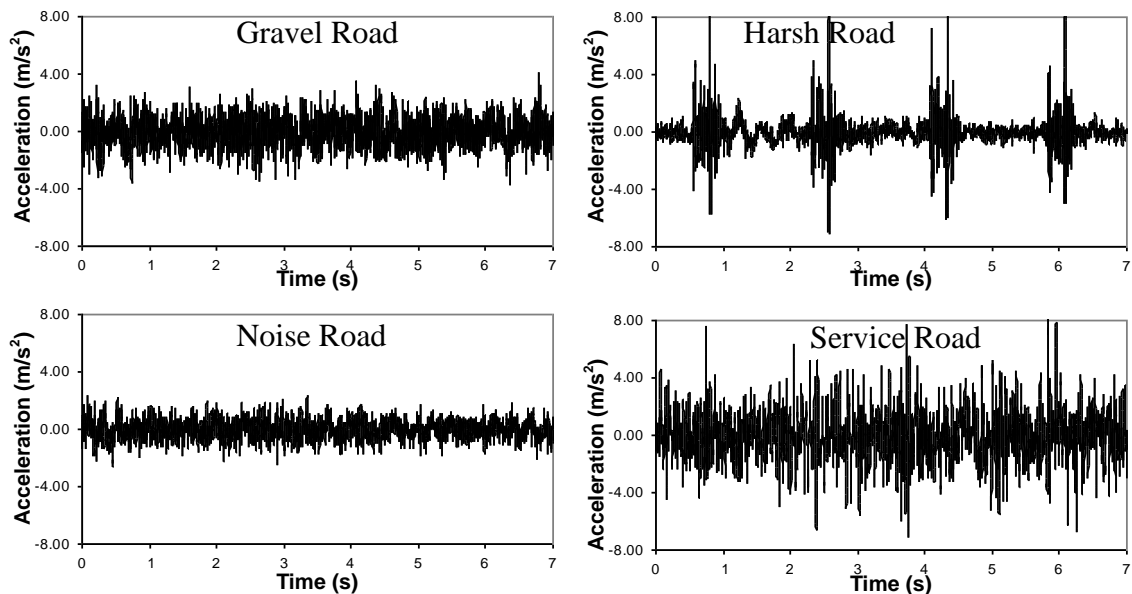


[Figure 5.5] A 7 second segments of the tangential acceleration time history measured at the steering wheel for each of the four road surfaces (The Michelin test).

The global statistical properties calculated for the complete original 1 minute recording over each road surface is presented in Table 5.2 along with the automobile speed used during the measurement. Table 5.2 suggests that vibration at the steering wheel achieved root mean square (r.m.s.) acceleration levels from 0.711 to 1.987 m/s^2 . The

acceleration levels achieved for these road surfaces were higher than those achieved in the MIRA measurements, where the acceleration level achieved by all the road surfaces was below 0.4 m/s^2 . The lowest kurtosis value was 2.925 for the noise surface while the highest kurtosis value was 17.117 for the harsh surface. The noise surface also produced the lowest skewness value of -0.056 which was close to 0.0 while the harsh surface produced a skewness value of 1.047 which was the highest, which suggests that its acceleration data is not Gaussian distributed. The harsh surface also had the higher crest factor (CF) of 6.886 while the noise surface had the lowest CF of 3.55. The root mean quad (r.m.q.) values were from 0.955 to 2.725 m/s^2 which were also higher than those achieved in the MIRA measurements, where the r.m.q. value achieved by all the road surfaces was below 0.6 m/s^2 .

[Table 5.2] Global statistical properties of the four Michelin road stimuli.

Type of road	Global Statistics and Characteristics					
	r.m.s. (m/s^2)	Kurtosis	Skewness	Crest Factor	Speed (km/h)	r.m.q. (m/s^2)
Gravel	1.066	2.998	-0.055	3.687	80	1.415
Harsh	1.320	17.117	1.047	6.886	40	2.523
Noise	0.711	2.925	-0.056	3.550	80	0.955
Service	1.987	3.850	0.169	4.182	80	2.725

The power spectral density (PSD) calculated for each acceleration measurement is presented in Figure 5.6. As with the MIRA road surfaces, the principal frequency content is in the range from 0 to 80 Hz for all the road surfaces. The acceleration power spectral densities were found to be different among these road surfaces, and also different from those of the MIRA road surfaces which were shown in Figure 4.3.

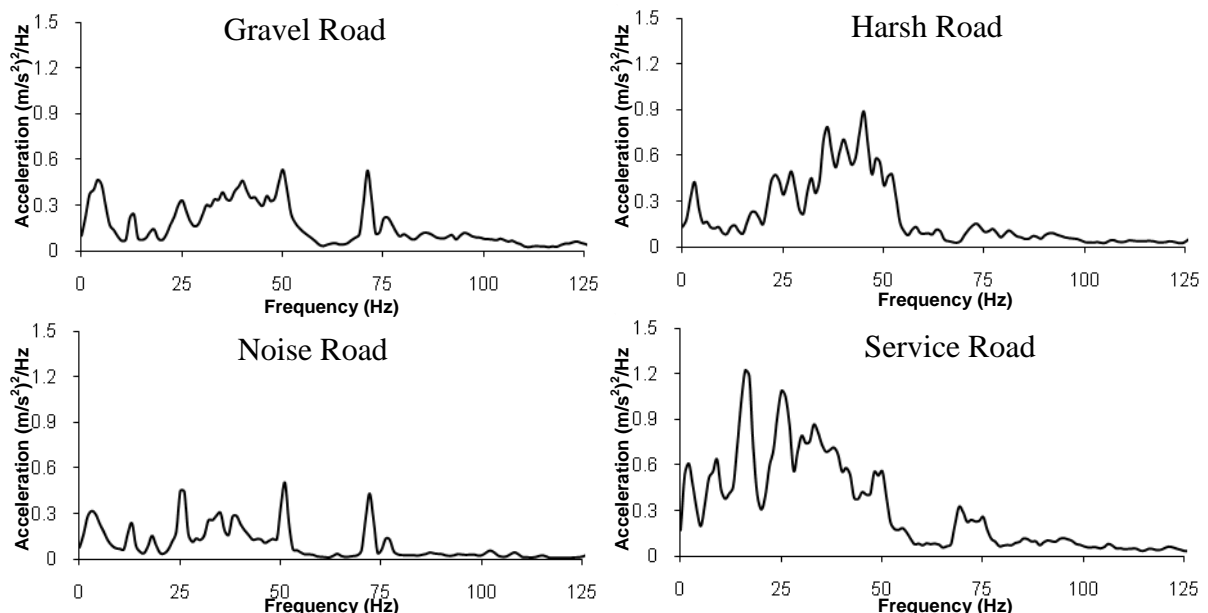


[Figure 5.6] Power Spectral Densities (PSD) calculated from the four tangential acceleration time histories of the 1 minute duration which were measured at the steering wheel.

5.2.3 Honda Tests

Six steering wheel acceleration signals were provided by the Honda Motor Company. The acceleration measurements were performed at the Millbrook proving ground in Millbrook, Bedfordshire, UK, which has a comprehensive range of circuits and facilities which are used to carry out a wide range of tests. The automobile used by Honda Motor Company during the acceleration measurements was a Honda Accord 2.0 i-VTEC SE, 4 door saloon with a 5-speed manual transmission and a petrol 2.0-liter DOHC 4-cylinder engine. The Accord steering system was a rack and pinion Power Assist Steering (PAS). The front suspension was an independent and Double Wishbone, while the rear suspension was an Independent Multi-Link. The front and rear tyre specifications were P195/65 R 15.

The road surfaces used by Honda Motor Company to measure the steering wheel acceleration stimuli were named Broken Road surface, Cats-eye, Expansion Joints, Manhole Cover, Stone on Road and UK City Street surface. Figure 5.7 presents these road surfaces as viewed from directly above, and as seen from a distance as when driving, along with the automobile test velocity.

For each road surface a 1 minute data recording was available from experimental testing. A 7 second data segment of the tangential direction steering wheel acceleration time history was extracted from each data set to serve as test stimuli. The segments were selected such that the root mean square value, kurtosis value and power spectral density were statistically close to those of the complete recording. Figure 5.8 presents the time history segments selected for each of the road surfaces. As expected, different shapes

and different acceleration levels are observed from the road surfaces.

Broken Road (vehicle speed 40 km/h)



Cats-eye Road (vehicle speed 60 km/h)



Expansion Joints (vehicle speed 16 km/h)



Manhole Cover (vehicle speed 60 km/h)



Stone on Road (vehicle speed 20 km/h)



UK City Street (vehicle speed 90 km/h)



[Figure 5.7] Road surfaces used by Honda for their steering wheel vibration tests.

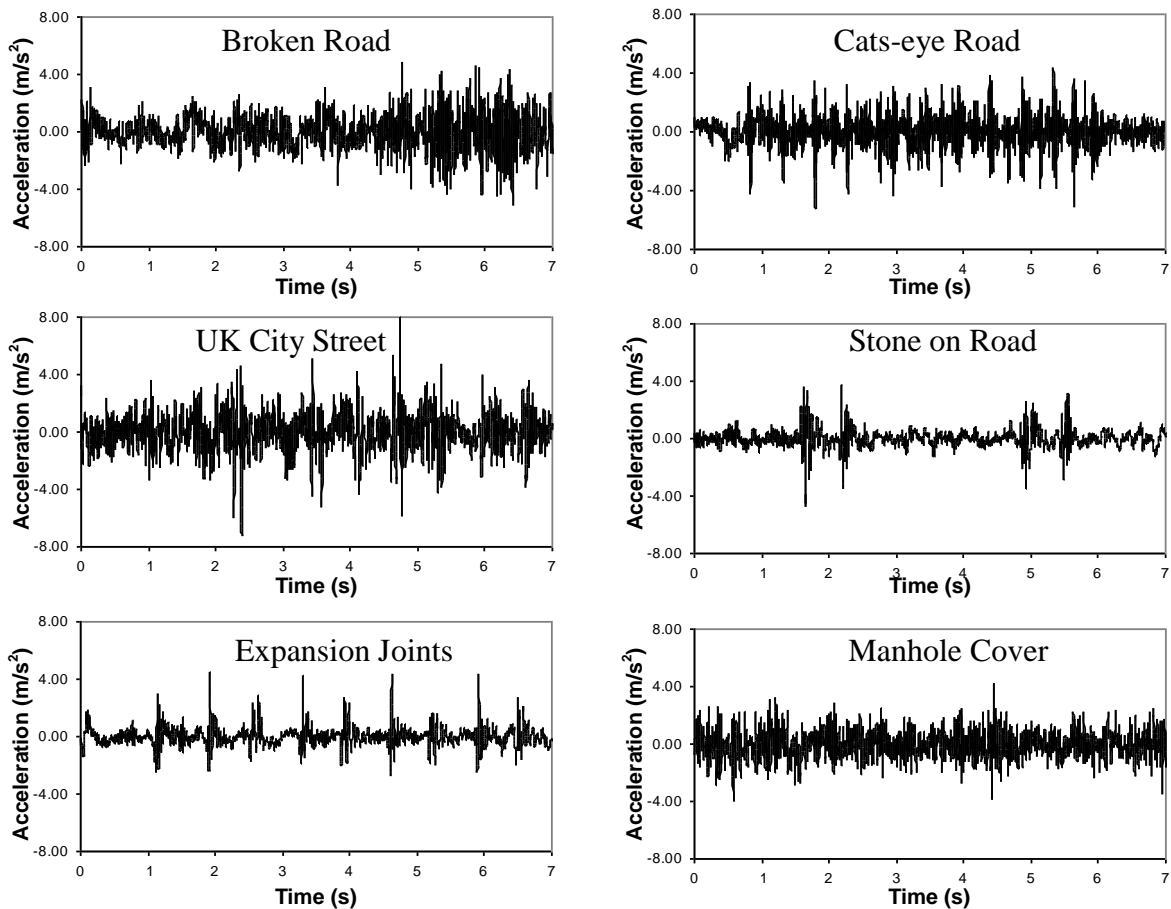


[Figure 5.8] A 7 second segments of the tangential acceleration time history measured at the steering wheel for each of the six road surfaces (The Honda test).

Table 5.3 presents the global statistical properties determined from the data of each of the road surfaces. Root mean square (r.m.s.) acceleration levels from a minimum of 0.665 m/s^2 for the stone on road surface to a maximum of 1.394 m/s^2 for the UK city street surface were found. All the road surfaces produced the higher kurtosis values which were larger than 3.0 from a minimum value of 3.263 for the manhole surface to a maximum value of 11.0 for the stone on road surface. The largest skewness value was found for the expansion joints surface with a value of 1.209, while the remaining road

surfaces had skewness values close to 0.0. The stone on road surface had the highest crest factor (CF) at approximately 6.441. The root mean quad (r.m.q.) values from a minimum of 1.160 m/s² for the stone on road surface to a maximum of 2.047 m/s² for the UK city street surface were found. The root mean square (r.m.s.) acceleration levels and the root mean quad value (r.m.q.) achieved with these six road surfaces were higher than those achieved for the MIRA test but lower than those achieved for the Michelin test.

[Table 5.3] Global statistical properties of the six Honda road stimuli.

Type of road	Global Statistics and Characteristics					
	r.m.s. (m/s ²)	Kurtosis	Skewness	Crest Factor	Speed (km/h)	r.m.q. (m/s ²)
Broken Road	1.218	3.935	-0.062	4.101	40	1.715
Cats-eye	1.132	4.677	-0.158	4.249	100	1.578
Expansion Joints	0.705	10.291	1.209	5.173	16	1.243
Manhole Cover	0.966	3.263	0.011	4.282	60	1.328
Stone on Road	0.665	11.000	-0.016	6.441	20	1.160
UK City Street	1.394	5.119	-0.081	5.488	90	2.047

Figure 5.9 presents the PSD calculated for each acceleration measurement. As with the MIRA and the Michelin road surfaces, the principal frequency content is in the range from 0 to 80 Hz for all the road surfaces. The acceleration power spectral densities were found to be different among these road surfaces, and also different from those produced by the MIRA and the Michelin road surfaces.

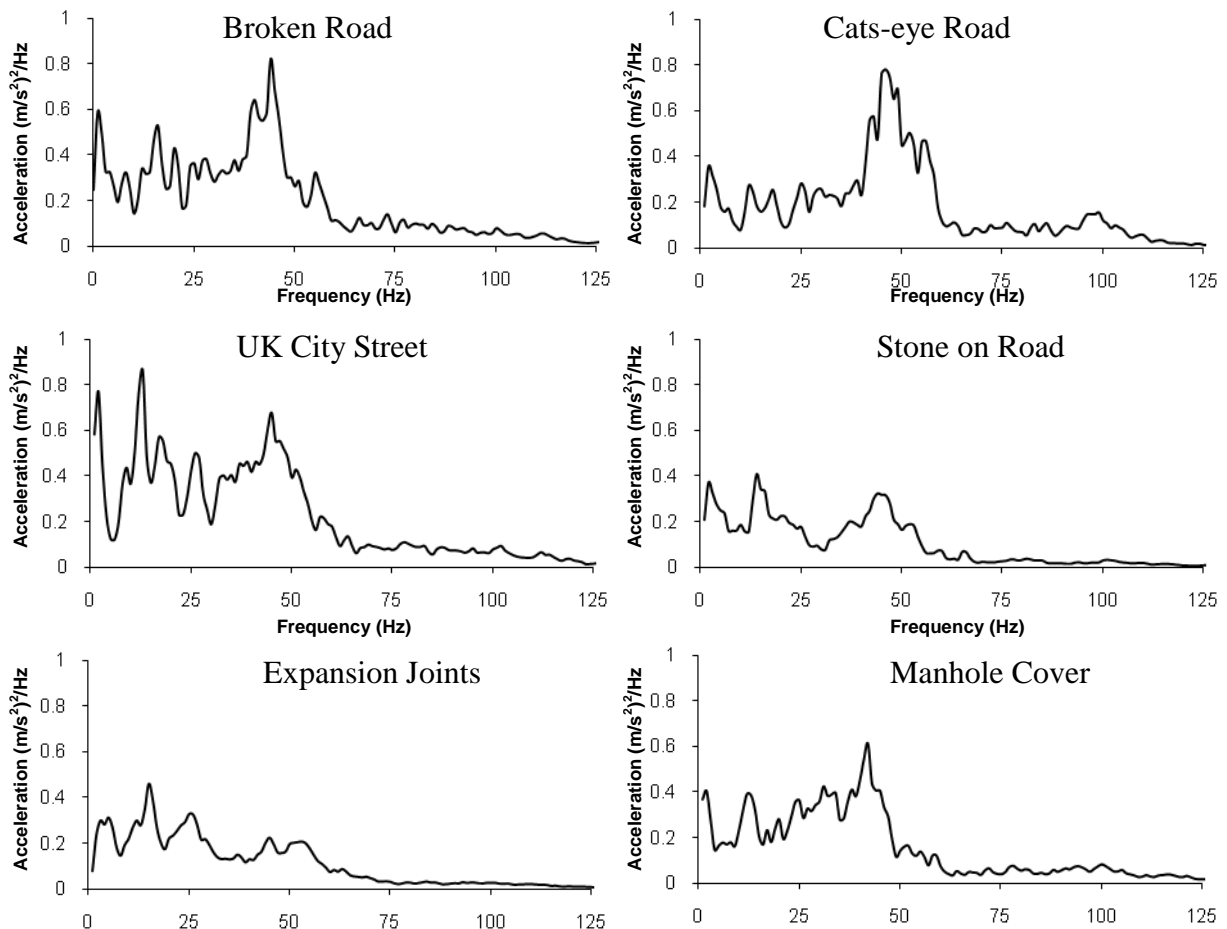


[Figure 5.9] Power Spectral Densities (PSD) calculated from the two tangential acceleration time histories of the 1 minute duration which were measured at the steering wheel.

5.2.4 Uxbridge Tests

In order to provide the widest possible statistical base of steering wheel acceleration signals, a small number of measurements were also performed by the Perception Enhancement Systems research group of Brunel University over local roads whose characteristics differed from those which are typically found at the testing facilities of the motor vehicle manufacturers (Berber-Solano, 2009). The acceleration measurements were performed over road surfaces in and around Uxbridge, West London, UK. The road surfaces were chosen due to their appearance and physical composition, which differed significantly from the road surfaces of the MIRA, Michelin and the Honda.

The steering wheel acceleration was measured by means of a SVAN 947 Sound and Vibration Level Meter and Analyser manufactured by SVANTEK Ltd., which uses a Low Impedance Voltage Mode (LIVM) accelerometer 3055B1. The specifications of the accelerometer and the test equipment are provided in Appendix A. The accelerometer at the steering wheel measurement position was fixed by means of an aluminium clamp and mounting screws which guaranteed sufficient coupling stiffness to perform acceleration measurements in excess of 300 Hz. The geometrical dimensions of the steering wheel clamp are provided in Appendix B. The acceleration signals were stored using the SVAN 947 by means of its fast USB 1.1 interface (with 12MHz clock) which created a real time link for the application of the SVAN 947 as a PC front-end.

The SVAN 947 was run using a battery so as to eliminate electronic noise from vehicle systems. The sampling rate chosen for the acceleration measurements was 1 kHz. The

rate of 1 kHz was sufficient to ensure that the acceleration stimuli were recorded with adequate definition at the maximum frequency of interest of 512 Hz. The maximum analysis frequency of 512 Hz was chosen based on the assumption that the vibrational energy transmitted to the steering wheel can reach frequencies of up to 300 Hz when driving over certain road asperities and that the largest resonances are presented in the frequency range from 20 to 50 Hz (Pottinger et al., 1986). The recorded signals were reacquired and analyzed at the Perception Enhancement Systems Laboratory by means of the T-MON module of the LMS CADA-X 3.5E software (LMS International Inc., 2002), where signals were read as WAV files, transferred and converted to TDF (Test Data File) files into the LMS software. The signals were then resample at 512 Hz.

The automobile used for the steering wheel tangential acceleration acquisition was a VW Golf 1.9 TDI model year 2005, 5 door Hatchback with 5-speed manual transmission. The engine was a turbocharged diesel direct injection (TDI) 4-cylinder 1.9l. The steering system was a rack and pinion Power Assist Steering (PAS). The front suspension was an Independent, Macpherson Strut, Coil Spring with an Anti-Roll Bar, while the rear suspension was an Independent, Torsion Bar, Coil Spring with an Anti-Roll Bar. The front and rear tyres specifications were P205/55 R 16.

The five road surfaces were used for the steering acceleration tests are shown in Figure 5.10. They were named as a Broken Concrete, Broken Lane, Bump, Country Lane and a Motorway surface.

Steering wheel tangential acceleration time histories were measured using a VW Golf automobile which was driven over the five surfaces shown in Figure 5.10. For each road surface a 1 minute data recording was made. Figure 5.11 presents the 7 second data segment which was extracted from the tangential direction steering wheel acceleration time history of each data set so as to serve as test stimuli. The segments were selected such that the root mean square value, the kurtosis and the power spectral density were statistically close to those of the complete recording. From Figure 5.11 it can be observed that each road surface achieved a rather different acceleration level.

Broken Concrete (vehicle speed 50 km/h)



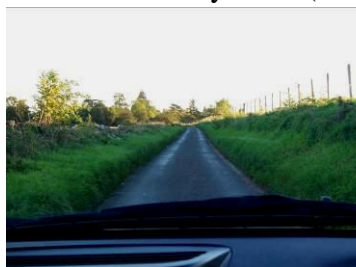
Broken Lane (vehicle speed 40 km/h)



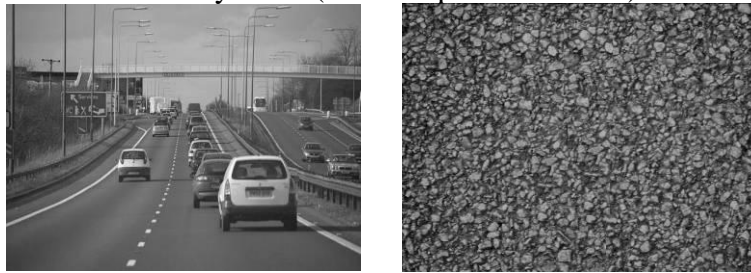
Bump Road (vehicle speed 60 km/h)



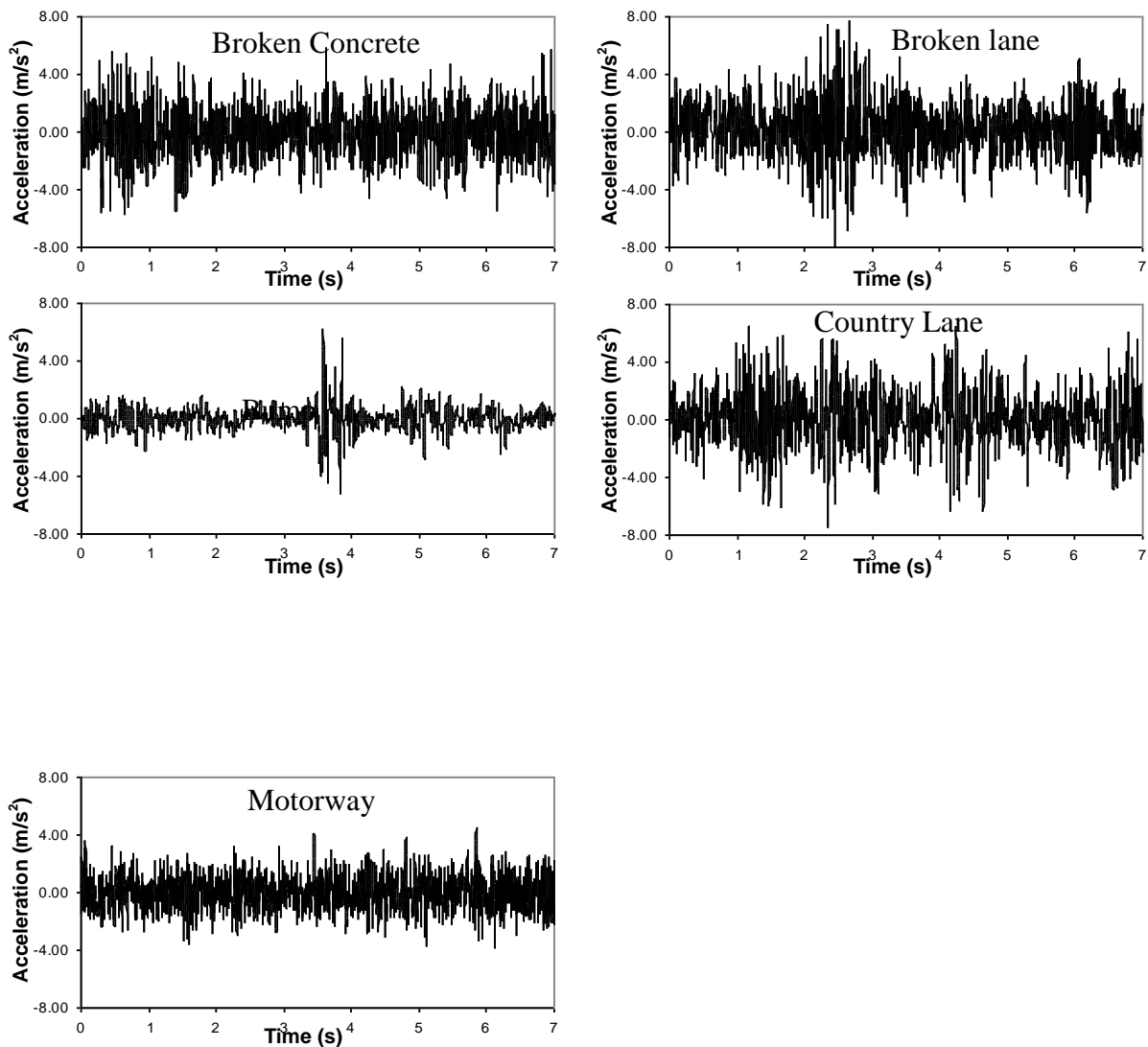
Country Lane (vehicle speed 40 km/h)



Motorway Road (vehicle speed 110 km/h)



[Figure 5.10] Road surfaces for the Uxbridge steering wheel tests.



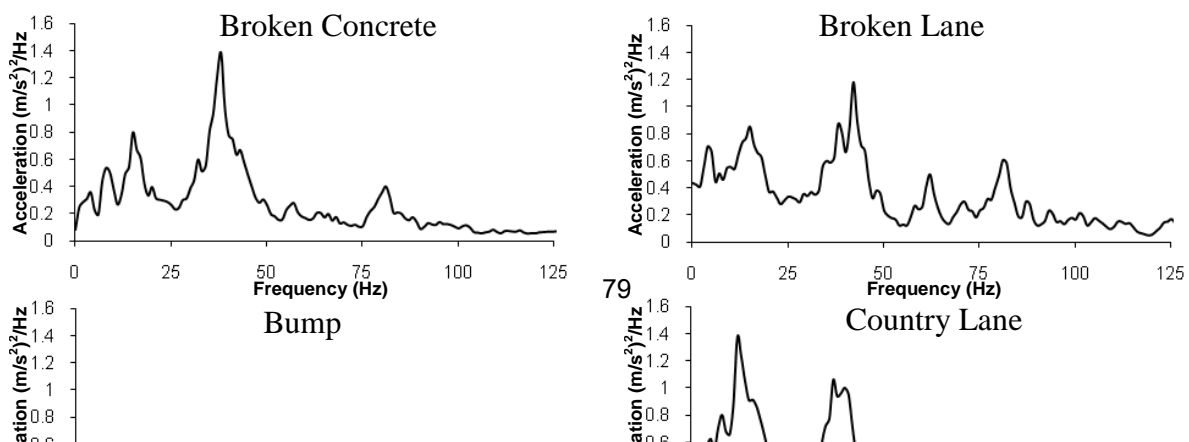
[Figure 5.11] A 7 second segments of the tangential acceleration time history measured at the steering wheel for each of the five road surfaces (The Uxbridge test).

Table 5.4 presents the global statistical properties determined from the data of each of the road surfaces. Root mean square (r.m.s.) acceleration levels from a minimum of 0.916 m/s² for the bump surface to a maximum of 1.982 m/s² for the country lane surface were found. Kurtosis value larger than 3.0 were found for the bump surface which produced an impulsive input to the vehicle subsystems, while the remaining road surfaces had kurtosis values close to 3.0. The largest skewness value was found for the bump surface with a value of 0.158, while the remaining road surfaces had skewness values close to 0.0. The bump had the highest crest factor (CF) at approximately 6.324. The root mean quad (r.m.q.) values from a minimum of 1.514 m/s² for the motorway surface to a maximum of 2.68 m/s² for the country lane surface were found. The root mean square (r.m.s.) acceleration levels and the root mean quad value (r.m.q.) achieved with these five road surfaces were generally higher than those achieved for the MIRA, Michelin and Honda tests.

[Table 5.4] Global statistical properties of the five Uxbridge road stimuli.

Type of road	Global Statistics and Characteristics					
	r.m.s. (m/s ²)	Kurtosis	Skewness	Crest Factor	Speed (km/h)	r.m.q. (m/s ²)
Broken concrete	1.673	3.194	0.013	3.458	50	2.286
Broken lane	1.858	3.799	-0.060	4.225	40	2.529
Bump	0.916	10.164	0.158	6.324	60	1.569
Country lane	1.982	3.438	-0.048	3.534	40	2.680
Motorway	1.132	3.066	0.073	3.706	110	1.514

Power spectral densities (PSD) were calculated for the five acceleration measurements and are shown in Figure 5.12. The principal frequency content is in the range from 0 to 80 Hz as was previously seen in the MIRA, Michelin and the Honda tests. The highest peaks in the PSD energy were found for the broken concrete surface, while the lowest peaks were found for the motorway surface. The acceleration PSDs were found to be different across the seven road surfaces, and also different from those produced by the MIRA, Michelin and the Honda road surfaces.



[Figure 5.12] Power Spectral Densities (PSD) calculated from the four tangential acceleration time histories of the 1 minute duration which were measured at the steering wheel.

5.2.5 Summary of the Road Testing Data

Although the data presented in this chapter cannot be considered to be a definitive scientific analysis of road vehicle vibration, the values obtained can be considered to be typical of the automotive vibration problem, thus useful for the purpose of defining specific laboratory-based experiments which are representative of the automobile environment. The selected group of stimuli respect the five criteria which were established at the beginning of the chapter for the purpose of obtaining steering wheel vibrations for use in the study of the human perception of steering wheel hand-arm vibration.

The global statistical properties of all 21 road surfaces analysed in this chapter suggest that the road surfaces differ between themselves significantly in terms of the root mean square (r.m.s.) and the root mean quad (r.m.q.). Figure 5.13 and 5.14 present the distribution of the 21 road surfaces based on these two statistical properties which suggested that the steering wheel acceleration data from the tests performed in this chapter provided r.m.s. acceleration levels from a minimum approximately of 0.06 m/s^2

to a maximum approximately of 1.99 m/s^2 , and r.m.q. values from a minimum approximately of 0.07 m/s^2 to a maximum approximately of 2.73 m/s^2 .

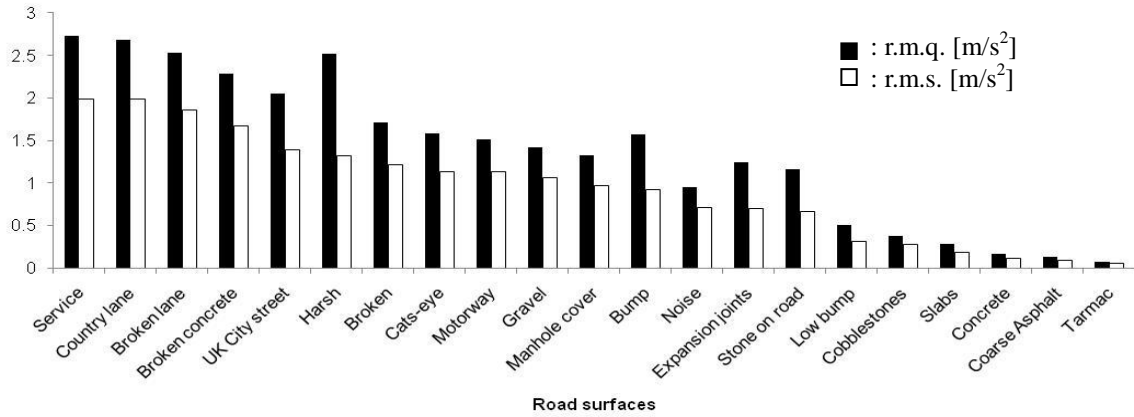


[Figure 5.13] Comparison between the root mean square value and the root mean quad value of the 21 road surfaces.

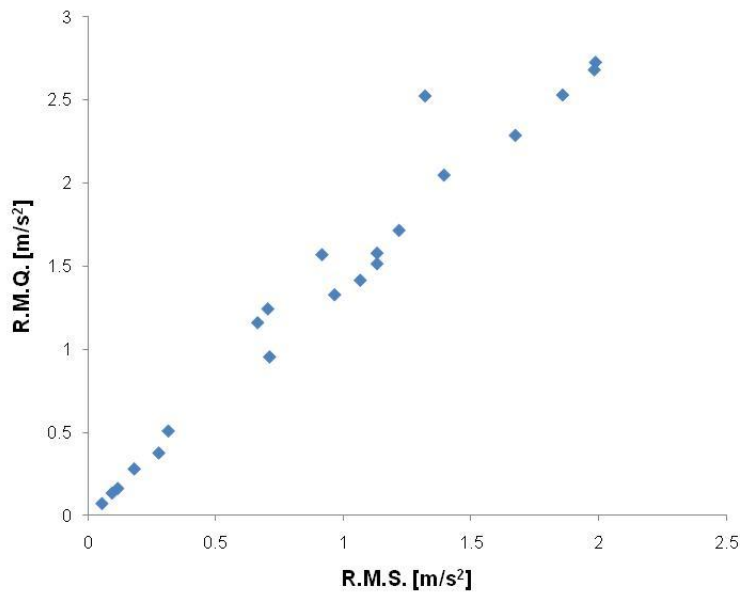


[Figure 5.14] Distribution of the statistical values of the 21 road surfaces: r.m.s. acceleration level against r.m.q. value.

As can be seen in Figure 5.14 the distribution of the 21 road surfaces based on the two metrics suggests that the steering wheel acceleration data from the tests may provide a wide statistical base of steering wheel magnitudes when compared to the vibration

acceleration magnitude ranges from the previous research studies (Giacomin and Woo, 2004; Gnanasekaran et al., 2006; Berber-Solano, 2009). For example, Giacomin and Woo performed psychophysical laboratory experimental tests using steering wheel vibration stimuli with the acceleration magnitude range of 0.05 to 0.27 m/s² r.m.s. while Gnanasekaran et al. performed the psychophysical testing with stimuli in the range of 0.098 to 2.02 m/s² r.m.s. and Berber-Solano performed psychophysical tests with stimuli in the range of 0.056 to 2.355 m/s² r.m.s. and the range of 0.07 to 3.34 m/s² r.m.q.. Thus the acceleration data from the road tests in this chapter can be considered a wide and representative operating envelope for use in laboratory-based experiments of automotive steering wheel vibration.

For the 21 road surface stimuli Figure 5.15 presents the minimum, mean and the maximum amplitudes at each frequency from 0 to 300 Hz. From Figure 5.15 it can be noted that a significant amount of vibrational energy is present in the rotational direction between 5 and 50 Hz ($p < 0.01$), but that vibrational energy was much lower outside this range. However, there was still the perceivable energy in the higher frequencies approximately up to 300 Hz. From this result, it was noted that steering wheel road vibration produced perceptible energy in the frequency range from approximately 5 to 300 Hz.

Based on the steering wheel acceleration signals which are described in this chapter it was considered reasonable to assume that a frequency bandwidth from 5 to 300 Hz, and an amplitude range from 0.06 to 1.99 m/s² r.m.s., are required for laboratory experiments of steering wheel hand-arm vibration.

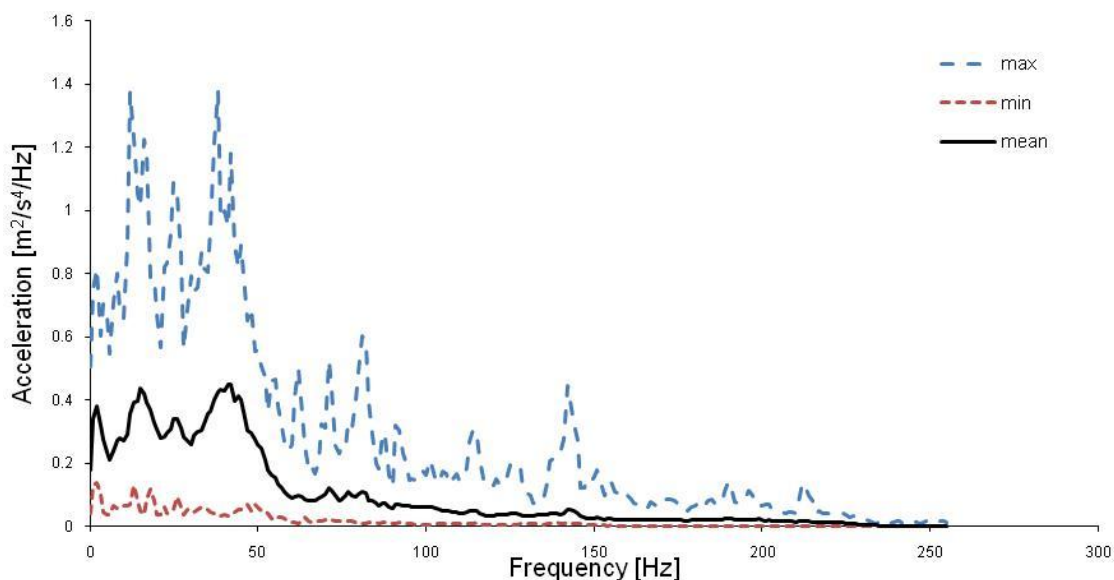


[Figure 5.15] The minimum, mean and the maximum acceleration magnitude for each frequency from 0 to 300 Hz of the 21 road surfaces.

Chapter 6

Human Subjective Response to Steering Wheel Hand-Arm Vibration consisting of Sinusoidal

Vibration

6.1 Introduction

The human subjective response to sinusoidal hand-arm vibration has been investigated in several studies. Equal sensation curves have been established which indicate the combination of sinusoidal frequency and amplitude that produces a similar sensation of perceived intensity.

Miwa (1967) established equal sensation curves for 10 male participants who held their palm flat against a plate which was vibrated sinusoidally in either the vertical or horizontal direction at acceleration amplitudes of either 0.31, 3.1 or 31.1 m/s² r.m.s. over the frequency range from 2 to 300 Hz. Human subjective response to hand-arm vibration was found to decrease almost monotonically as a function of frequency.

Reynolds et al. (1977) established equal sensation curves for 8 male participants who gripped with one hand a handle which was vibrated sinusoidally in either the vertical, axial or horizontal directions at acceleration amplitudes of either 1.0, 10.0 or 50.0 m/s² r.m.s. over the frequency range from 16 to 1000 Hz. The three curves suggested a nonlinear acceleration dependency of the perceived intensity of hand-arm vibration, and a general trend of reduced sensitivity with increasing frequency.

Morioka and Griffin (2006) established a family of equal sensation curves for 12 male participants who gripped with one hand a cylindrical handle which was vibrated sinusoidally in either the vertical, axial or horizontal directions over the frequency range from 8 to 400 Hz. At acceleration magnitudes greater than about 2.0 m/s² r.m.s. the equal sensation curves suggested a decreased sensitivity to hand-arm vibration with increasing frequency, while at lower acceleration magnitudes the curves suggested an increased sensitivity to hand-arm vibration with increasing frequency from 20 to 100 Hz. At all vibration magnitudes, the curves suggested decreased sensitivity with increasing frequency from 8 to 16 Hz.

With respect to automotive steering vibration Giacomin et al. (2004) established equal sensation curves for 15 participants (10 males and 5 females) who held a rigid sinusoidally rotating steering wheel with both hands at two acceleration amplitudes of 1.0 and 1.5 m/s² r.m.s. over the frequency range from 3 to 315 Hz. A constant acceleration dependency was noted from 3 to 5 Hz, and a decrease in the human sensitivity to hand-arm rotational vibration was found with increasing frequency from 5 to 315 Hz.

Amman et al. (2005) established equal sensation curves for 28 participants (gender was not reported) who held an automotive steering wheel with both hands. The study investigated the human subjective response to 1.0 m/s² r.m.s. amplitude sinusoidal vibration applied along either the longitudinal, lateral or vertical over the frequency range from 8 to 64 Hz. The study also investigated the subjective response to vibration along the rotational direction by means of sinusoidal stimuli with acceleration amplitudes of 0.8 and 1.6 m/s² r.m.s. over the frequency range from 8 to 20 Hz. Amman et al.'s equal sensation curves suggested a general trend of decreasing sensitivity to vibration with increasing frequency over the frequency range investigated.

Table 6.1 provides a compilation of the main parameter values considered by the previous researchers when establishing equal sensation curves. This compilation was referenced extensively during the design of the test programme used in the research which is described in this thesis.

[Table 6.1] Test protocol parameters adopted in previous studies of human subjective response sinusoidal hand-arm vibration.

Reference	Subjects [numbers (male, female)]	Psychophysical Method	Semantic word used	Direction	Stimulus Type / Duration	Posture	Vibration Exciter	Reference Frequency [Hz]	Frequency range [Hz]	Amplitude level r.m.s [m/s ²]
Miwa (1967)	10 (10, 0) Non- experienced	Paired Comparison	Vibration Greatness	Vertical Horizontal	Sinusoidal, 3 or 6 sec.*	One hand pressing plate	Electro- dynamic shaker	20	3 ~ 300	0.31, 3.1, 31 1, 10
Reynolds et al. (1977)	8 (8, 0)	Method of Adjustment	Sensation	Vertical Horizontal Axial	Sinusoidal	One hand gripping a handle	Electro- dynamic shaker	100	16 ~ 1000	1, 10, 50
Giacomin, Onesti (1999)	25 (13, 12) Non- experienced	Method of Adjustment	Sensation	Rotational	Sinusoidal, 10 sec.	Both hand gripping a steering wheel	Electro- dynamic shaker	16 or 63	4 ~ 125	1.9 ~ 5.6

Giacomin et al. (2004)	15 (10, 5) Non-experienced	Method of Adjustment	Intensity	Rotational	Sinusoidal, 10 sec.	Both hand gripping a steering wheel	Electro-dynamic shaker	63	3 ~ 315	1, 1.5
Morioka (2004)	12 (12, 0) Non-experienced	Magnitude Estimation	Discomfort	Rotational	Sinusoidal, 2 sec.	Both hand gripping a steering wheel	Electro-dynamic shaker	31.5	4 ~ 250	0.1 ~ 1.58
Amman et al. (2005)	28	Method of Adjustment	Annoyance	Rotational	Sinusoidal	Both hand gripping a steering wheel	Hydraulic shaker	14 25	8 ~ 20 8 ~ 64	0.8, 1.6 1
Morioka, Griffin (2006)	12 (12, 0) Non-experienced	Magnitude Estimation	Discomfort	Vertical Horizontal Axial	Sinusoidal, 2 sec.	One hand gripping a handle	Electro-dynamic shaker	50	8 ~ 400	0.002 ~ 0.126 m/s

* 3 seconds used for above 10 Hz, 6 seconds used for below 10 Hz.

As can be seen in Table 6.1 the equal sensation curves established in most of the studies performed to date represent the average responses of small groups of 8 to 15 people. In addition, the human subjective response to hand-arm vibration stimuli is based mainly upon responses from male participants, despite the fact that since the 1970s the percentage of female drivers has increased in most countries as described in Chapter 1.

From the summary of the previous chapter it was observed that the steering wheel vibrational energy reached up to 300 Hz and the amplitude range was approximately from 0.06 to 2.0 m/s² r.m.s.. However, no previous study has investigated those representative ranges of automobile steering wheel shown in Table 6.1.

The primary objective of the research which is described in this chapter was to establish a family of equal sensation curves for sinusoidal steering wheel rotational vibration by means of the most commonly applied regression models, namely, least squares regression, all possible regression, backward elimination regression and stepwise regression procedure. The equal sensation curves were to be developed for use across the operating envelope of steering wheel vibration stated above. Statistical regression was chosen for summarising the experimental data because it produces relatively simple analytical models (Aleksander, 1995) and because the model coefficients often have obvious physical explanations. The secondary objective was to investigate the effect of gender differences on the shape of the equal sensation curves for hand-arm steering wheel rotational vibration in order to develop the individual family of equal sensation curves.

6.2 Experimental Apparatus

6.2.1 Test Facility

Figure 6.1 presents a schematic representation of the steering wheel rotational vibration test facility used in this research and of the associated signal conditioning and data acquisition systems. The main geometric dimensions of the test rig, which were based on average data taken from a small European automobile, are presented in Table 6.2. The rotational steering system consisted of a 350 mm diameter aluminium wheel attached to a steel shaft which was in turn mounted to two low friction bearings which were encased in a square steel casing. The steering wheel consisted of a 5 mm thick central plate with two cylindrical handles of 25 mm diameter and 3 mm thickness welded at the extremities. The steering wheel was made of aluminium in order to obtain a first natural frequency greater than 350 Hz. Rotational vibration was applied by means of a G&W V20 electrodynamic shaker, which was connected to the shaft by means of a steel stinger rod, and amplified by PA100 amplifier (Gearing and Watson Electronics Limited, 1995) using an Leuven Measurement Systems (LMS) Cada-X 3.5 E software and a 12-channel Difa Systems Scadas III front-end unit (LMS International Inc., 2002). The acceleration obtained at the steering wheel was measured using an Entran MSC6 signal-conditioning unit (Entran Devices Inc., 1991). The acceleration was measured in the tangential direction. The car seat was fully adjustable in terms of horizontal position and back-rest inclination as in the original vehicle. The safety features of the test rig, and the acceleration levels used, conform to the health and safety recommendations outlined by British Standard 7085 (1989).

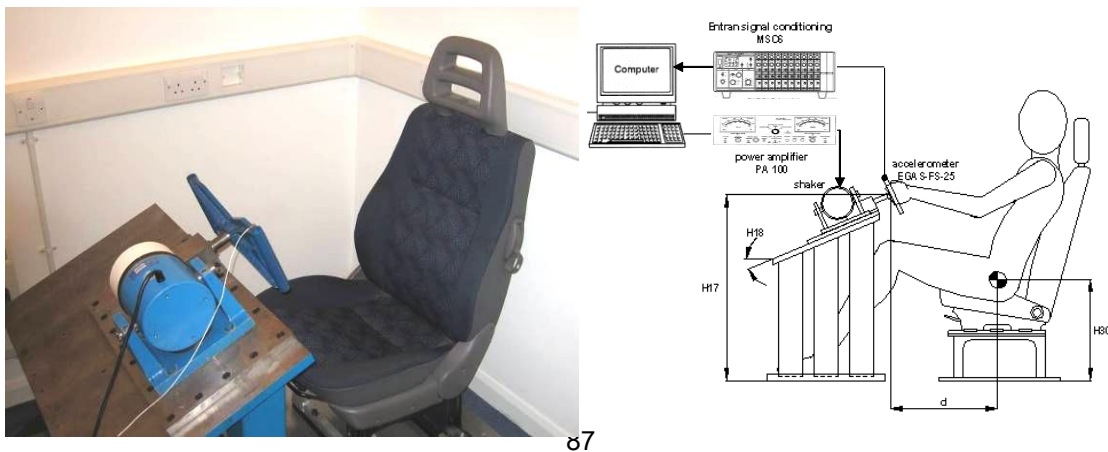


[Figure 6.1] Steering wheel rotational vibration test rig and associated electronics.

[Table 6.2] Geometric dimensions of the steering wheel rotational vibration test rig.

Geometric Parameter	Value
Steering column angle (H18)	23
Steering wheel hub centre height above floor (H17)	710 mm
Seat H point height from floor (H30)	275 mm
Horizontal distance adjustable from H point to steering wheel hub centre (d)	390-550 mm
Steering wheel handle diameter	25 mm
Steering wheel diameter	350 mm

6.2.2 Accuracy of Signal Reproduction

According to the British Standards Institution BS 6840-2 (1993) for sound reproduction fidelity, signal distortion is defined as an error phenomenon that causes the appearance of extraneous signals at the output of a test equipment. These errors are directly based on the frequency content of the input signal. The parameter generally used to evaluate the fidelity of signal reproduction is termed the total harmonic distortion (THD), which is specified by the standard BS EN 60268-5 (1997).

When loaded by a human hand-arm system and tested at frequencies of 4.0, 8.0 16.0 31.5 63.0, 125 and 250 Hz at amplitudes of 0.2, 2.0 and 20.0 m/s² r.m.s., the test bench provided a maximum total harmonic distortion (THD) of 11.15% at 3Hz and 1 m/s². With both increasing frequency and decreasing amplitude the THD dropped to a minimum of 0.01% at 200 Hz and 0.2 m/s². During the tests, which measured the bench tangential direction total harmonic distortion, a linear fore-and-aft direction acceleration measurement was also performed at the same point on the rigid wheel. Unwanted fore-and-aft acceleration was found to be no greater than -50dB with respect to the tangential acceleration in all cases measured.

Beyond the basic measure of total harmonic distortion, a specific evaluation was also performed of the accuracy of the test facility when reproducing target test stimuli. The

accuracy of the signal reproduction was quantified by measuring the maximum r.m.s. error between the target signal and the actual steering wheel motion achieved by means of the LMS software, the front end electronics unit, the shaker, the accelerometer and the signal conditioning unit. Three test subjects were used in the process, and maximum and minimum response r.m.s. acceleration values were obtained. The response r.m.s. values were then expressed as a percentage of the target r.m.s. value, as presented in Table 6.3. The results suggest that the maximum percentage error of the target r.m.s. value was below 11.0%, which compared favourably with the just-noticeable-difference value for human perception of hand-arm vibration of 15 to 18% (Morioka, 1999).

[Table 6.3] Bench steering vibration reproduction error defined as a percentage of the target r.m.s. acceleration level (n = 3 test subjects).

Frequency [Hz]	Target r.m.s. [m/s ²]	Min. response		Max. response	
		[r.m.s. m/s ²]	Error [%]	[r.m.s. m/s ²]	Error [%]
3	0.08	0.073	-9.59	0.079	-1.27
4	1.26	1.14	-10.89	1.29	2.02
5	3	2.8	-7.10	3.22	6.77
6.3	0.45	0.44	-2.95	0.49	6.78
8	0.08	0.075	-6.67	0.086	6.98
10	3.92	3.78	-3.87	3.91	-0.38
12.5	8	7.82	-2.28	8.45	5.28
16	1.26	1.17	-8.23	1.34	5.46
20	2.87	2.67	-7.30	3.04	5.57
25	0.73	0.68	-7.02	0.8	7.92
31.5	0.36	0.35	-4.90	0.39	5.94
40	0.17	0.16	-8.18	0.18	5.49
50	0.08	0.075	-6.67	0.088	9.09
63	0.85	0.83	-3.14	0.93	8.67
80	22	21	-4.76	23.8	7.60
100	0.06	0.055	-9.09	0.067	10.45
125	4.46	4.15	-7.44	4.75	6.02
160	10.31	9.43	-9.33	10.62	2.97

200	4.71	4.65	-1.29	4.94	4.54
250	13.27	12.16	-9.08	13.1	-1.26
315	1.36	1.3	-4.86	1.48	8.36
400	6.35	6.52	2.59	6.98	9.09

6.3 Laboratory Based Experimental Testing using Sinusoidal Vibration

6.3.1 Test Stimuli

In chapter 5 it was shown that steering wheel road vibration stimuli normally contain significant energy over the interval from 5 to 300 Hz. Despite the observation that the steering wheel vibrational energy reached only up to 300 Hz, the maximum frequency was extended to 400 Hz in this research in order to obtain a good interpolation of the asymptotic segment of the equal sensation curves at the highest frequencies. On the other hand the maximum stroke of the test rig shaker unit (± 10 mm) limited the maximum achievable acceleration at the steering wheel which, in turn, limited the minimum test frequency to 3 Hz. For frequencies lower than approximately 3 Hz accurate sinusoidal acceleration signals could not be achieved at the rigid wheel. Based on these considerations, the frequency interval of the test stimuli was chosen to be from 3 Hz to 400 Hz.

The individual test frequencies were chosen to be all 1/3 octave band centre frequencies in the range from 3 to 400 Hz. The 1/3 octave band centre frequencies were chosen because it was felt that octave band analysis would provide a sufficiently fine resolution (Griffin, 1990) and because it was used often in the studies of hand-arm vibration listed in Table 6.1. A total of 22 frequencies (3, 4, 5, 6.3, 8, 10, 12.5, 16, 20, 25, 31.5, 40, 50, 63, 80, 100, 125, 160, 200, 250, 315 and 400 Hz) were thus chosen.

With regard to the steering wheel acceleration magnitudes, the automotive steering wheel vibration summarised in chapter 5 suggested that the maximum amplitude level of each frequency did not reach to the hand-arm vibration annoyance threshold (Miwa, 1967; Reynolds et al., 1977; Giacomini et al., 2004). The maximum amplitude levels defined for the laboratory test were thus extended up to the vicinity of the annoyance threshold. The maximum amplitude level was chosen to be 27 m/s^2 r.m.s. which was

sufficient to cover the annoyance threshold obtained for steering wheel hand-arm vibration (Giacomin et al., 2004).

The minimum amplitude of each frequency was chosen to be in the vicinity of the hand-arm vibration perception threshold (Morioka, 2004). The minimum amplitude level chosen was 0.04 m/s^2 r.m.s. at 160 Hz due to the response of the Pacinian mechanoreceptors, which produces a lowest response in the vicinity of 100 Hz (Verrillo, 1966; Reynolds et al., 1977). This minimum amplitude it was sufficient to cover the minimum amplitude level of all the road surface stimuli which were described in chapter 5.

In order to maximise the signal density in the frequency-amplitude plane while simultaneously also not exceeding a test duration of 60 minutes so as to avoid any learning or fatigue effects (Coolican, 1999), a total of 86 steering wheel rotational sinusoidal vibration stimuli were used in the experiment as illustrated in Figure 6.2 and listed in Table 6.4. Four test amplitudes were used at each frequency, but the highest amplitudes at 300 and 400 Hz were removed since those signals were so powerful as to produce audible sound.

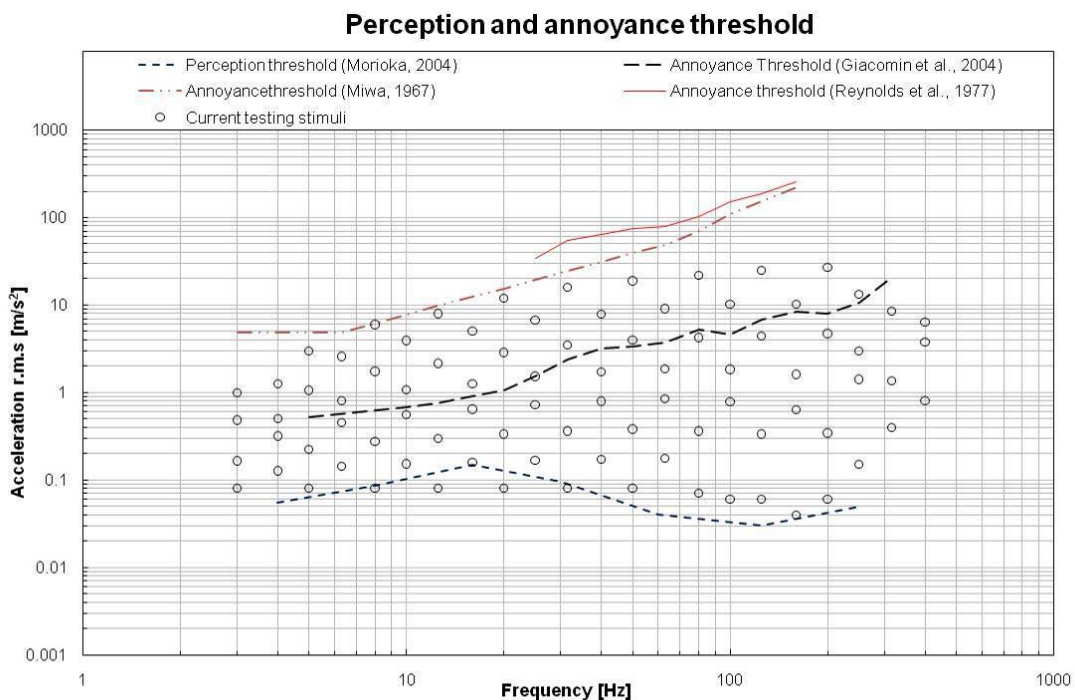


[Figure 6.2] Comparison the 86 sinusoidal rotational steering wheel vibration stimuli with the hand-arm vibration perception threshold (Morioka, 2004) and the hand-arm vibration annoyance threshold (Miwa, 1967; Reynolds et al., 1977; Giacomini et al., 2004).

[Table 6.4] Frequency and amplitude of the 86 sinusoidal rotational steering wheel vibration stimuli.

Frequency [Hz]	Acceleration amplitude [r.m.s. m/s ²]
3	0.08, 0.17, 0.49, 1.0
4	0.13, 0.32, 0.5, 1.26
5	0.08, 0.23, 1.07, 3.0
6.3	0.14, 0.45, 0.81, 2.58
8	0.08, 0.28, 1.75, 6.0
10	0.15, 0.56, 1.07, 3.92
12.5	0.08, 0.3, 2.15, 8.0
16	0.16, 0.63, 1.26, 5.02
20	0.08, 0.34, 2.87, 12.0
25	0.17, 0.73, 1.53, 6.69
31.5	0.08, 0.36, 3.52, 16.0
40	0.17, 0.8, 1.71, 7.91
50	0.08, 0.38, 3.98, 19.0
63	0.18, 0.85, 1.88, 9.09
80	0.07, 0.36, 4.26, 22.0
100	0.06, 0.78, 1.84, 10.2
125	0.06, 0.34, 4.46, 25.0
160	0.04, 0.64, 1.62, 10.31
200	0.06, 0.34, 4.71, 27.0
250	0.15, 1.41, 2.98, 13.27
315	0.4, 1.36, 8.53
400	0.8, 3.78, 6.35

6.3.2 Test Subjects

A total of 40 university students and staff, 20 male and 20 female, were randomly selected to participate in the experiment. An optimum sample size of approximately 25 to 30 participants has been previously proposed for use in experimental research (Coolican, 1999), therefore the use of 40 participants was considered a conservative approach which would ensure representative sample statistics.

A consent form and a short questionnaire were presented to each participant prior to testing, and information was gathered regarding their anthropometry, health and history of previous vibration exposures. Table 6.5 presents a basic summary of the physical characteristics of the group of test participants. The mean values and the standard

deviations of the height and mass of the test participants were close to the 50 percentile values for the U.K. population (Pheasant and Haslegrave, 2005). A statistical t-test performed for the test groups suggested significant physical differences in height and mass between the males and the females ($p < 0.05$), while no significant differences were found in age between the males and the females. All subjects declared themselves to be in good physical and mental health.

[Table 6.5] Mean and standard deviation summary statistics for the test participants.

Test Group	Age [years]	Height [m]	Mass [kg]
Male (n=20)	33.9 (6.2)	1.81 (0.08)	84.2 (14.0)
Female (n=20)	34.3 (6.6)	1.61 (0.06)	56.5 (7.1)
Total (N=40)	34.1 (6.4)	1.71 (0.12)	70.3 (17.8)

6.3.3 Test Protocol

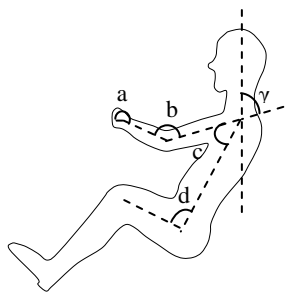
For each test subject, a strict test protocol was adhered to in which a predetermined sequence of events, each of fixed time duration, was performed. Upon arriving in the laboratory, each subject was issued an information and consent form, and was provided an explanation of the experimental methods and of the laboratory safety features. The consent form and the instruction sheet detailing the fixed verbal instructions used during the testing procedure are presented in Appendix C.

Before commencing testing each subject was required to remove any heavy clothes such as coats, and to remove any watches or jewellery that they were wearing. In order to reduce the statistical variance in the test results the driving posture was controlled for each test participant since the body posture is known to effect subjective response (Griffin, 1990). Four postural angles were controlled which were the wrist, elbow, shoulder and back angles (Norkin and White, 2003). For the wrist angle the range from 177 to 190 was chosen while for the elbow, shoulder and back angles the range from 102 to 126, from 23 to 39 and from 95 to 105 were chosen, respectively, based on the range of comfortable postures suggested by the literature (Andreoni et al., 2002; Babbs, 1979; Hanson et al., 2006; Henry Dreyfuss Associates, 2002; Park et al., 1999; Porter and Gyi, 1998; Rebiffé, 1969; Seidl, 1994; Shayaa, 2004; Tilley, 1994; Wisner and Rebiffé, 1963). The chosen data of the ranges for each postural angle were the median

values of the data presented in Table 6.6.

Since grip type and grip strength (Reynolds and Keith, 1977) are also known to effect the transmission of vibration to the hand-arm system, the subjects were asked to maintain a constant palm grip on the steering wheel using both hands. In addition, they were asked to maintain the grip strength which they felt they would use when driving an automobile on a winding country road. The subjects were also asked to wear ear protectors so as to avoid auditory cues. Room temperature was maintained within the range from 20° to 25°C so as to avoid significant environmental effects on the skin sensitivity (ISO 13091-1, 2001).

[unit : degree]

	Research	a	b	c	d
	Andreoni et al. (2002)	-	115 ± 10	32 ± 10	93 ± 6
	Wisner-Rebiffé (1963)	-	80 ~ 90	15 ~ 35	85 ~ 100
	Rebiffé (1969)	170 ~ 190	80 ~ 120	10 ~ 45 *	95 ~ 120
	Babbs (1979)	170 ~ 190	80 ~ 110	15 ~ 35 *	85 ~ 115
	Seidl (1994)	187	126	33	97.9
	Tilley (1994)	-	80 ~ 165	0 ~ 35	95 ~ 100
	Porter and Gyi (1998)	-	121 ± 18	45.1 ± 2.6	100 ± 5.6
	Park et al. (1999)	-	112 ± 11	19.2 ± 5.6	116 ± 6.5
	Shayaa (2004)	214 ± 6.1	139 ± 18.9	38 ± 7	108 ± 7.8
	Hanson et al. (2006)	187 ± 10	128 ± 16	39 ± 15	100 ± 4.4

[Table 6.6] Minimum and maximum angles of the (a) wrist, (b) elbow, (c) shoulder and (d) back which were found to guarantee postural comfort.

* The angle is from shoulder to the vertical (γ).

A Borg CR10 category-ratio scale (Borg, 1998), which was introduced in Chapter 2, was used to estimate the subjectively perceived intensity of the steering wheel rotational vibration. The information describing the experiment was presented to the test participant by the experimenter using the instructions provided by Borg (Borg, 1998) for the scale's administration. The test subjects were further asked to focus their eyes on a board which was placed about 1 meter ahead at eye level, which presented the Borg rating scale. Before starting the experiment a trial run involving three stimuli was performed so as to familiarize the participants with the test procedure.

The 86 test stimuli were repeated three times in three single blocks, for a total of 258 assessment trials for each participant. The mean Borg CR10 values of the three

repetitions, and the standard deviation values, were calculated for each stimulus. In order to minimize any possible bias resulting from learning or fatigue effects, the order of presentation of the test signals was randomised for each subject for each block. A break of 1 minute after the presentation of each block was used to reduce annoyance effects. A 7 second stimulus duration was used so as to provide a vibrotactile stimulus which remained within human short-term memory (Sinclair and Burton, 1996), thus a stimulus which could be judged without reliance upon the long-term storage of stimuli information by the test participant. A complete session required approximately 60 minutes to complete with one participant. The test procedure adhered to the fixed phases and the mean time durations outlined in Table 6.7.

[Table 6.7] Steering wheel rotational vibration testing protocol.

Phase	Tasks Performed and Information Obtained
Consent form and questionnaire (~ 3 minutes)	The participant was asked to read the instructions and intended purpose of the experiments and to sign a consent form. Each subject also completed a questionnaire concerning age, height, mass, health and previous exposure to vibration.
Measurement of postural angles (~ 3 minutes)	The participant was asked to remove heavy clothing, watches and jewellery. Sitting posture angles were measured using a full circle goniometer and adjusted into the standard comfort range so as to minimise individual postural differences.
Preparation for test (~ 1 minute)	The participant was asked to wear ear protectors and to close eyes before gripping the steering wheel. The grip strength was suggested to be that required to drive an automobile over a country road. Once comfortable with grip, the participant was asked to keep it constant during all tests.

Familiarization for test (~ 1 minutes)	The participant was given a verbal introduction to the experiment. The range of experimental frequencies and amplitudes applied so as to familiarise the subject with the stimuli.
Perception testing (~ 45 minutes)	The participant performed psychophysical tests of hand-arm vibration with the combination signals of frequency and amplitude presented in random order so as to avoid learning or fatigue effects. A total of 86 vibration stimuli were repeated three times. Each stimulus lasted 7 seconds to each subject.
Breaks (~ 5 minutes)	A short break of 1 minute was made every 43 stimuli so as to avoid annoyance effects.

6.3.4 Multivariate Regression Methods

There are a large number of multivariate approaches that can be applied to analyzing the correlations between subjective and objective metrics. These include a variety of iterative methods such as genetic algorithms (Goldberg, 1989) and neural networks (Aleksander and Morton, 1995), as well as non-iterative methods such as regression methods (Ezekiel and Fox, 1959) which use statistical techniques such as least squares to establish a system equation whose results can then be rated for accuracy using other statistical measures such as correlation coefficients. A statistical regression analysis was performed using both MATLAB (Mathworks Inc., 2002) and the SPSS software (SPSS Inc., 2004).

The objective was to establish a mathematical model to express the Borg CR10 subjective intensity as a function of the two independent parameters of frequency and magnitude. A linear fitting procedure was chosen since nonlinear fitting methods often suffer from convergence problems (Mathworks Inc., 2002) and since the deviation from linear forms in the current application were not so dramatic as to produce extensive local minima or widely differing multiple solutions. As the most widely used modelling methods, the least squares regression (NIST, 2006), all possible regressions, backward elimination and the stepwise regression procedures (Draper and Smith, 1998) were chosen. Based on the results from a previous study (Ajovalasit and Giacomini, 2009) all the regression models were expressed in logarithmic polynomial form up to either 4th, 5th or 6th order. The use of a logarithmic transformation and of polynomial regression terms from 4th to 6th order for both the frequency and the acceleration values was found in a previous study to provide the most accurate description of the physical phenomena

contained in the dataset (Ajovalasit and Giacomini, 2009).

6.3.4.1 MethodI: Least Squares Regression Procedure

Least squares regression is a mathematical procedure for finding the regression curve which best fits a set of data points. In this method the estimated values are found by minimizing the sum of the squares of the error between each point and curve (Draper and Smith, 1998).

6.3.4.2 MethodII: All Possible Regressions Procedure

This procedure analyzes every possible combination of the independent variables. If there are r independent variables, 2^r equations must be tested (Draper and Smith, 1998).

6.3.4.3 MethodIII: Backward Elimination Procedure

In this technique a regression equation containing all variables is calculated and then the variables are eliminated one by one based on the significance of the variables, until an optimum solution has been found (Draper and Smith, 1998).

6.3.4.4 MethodIV: Stepwise Regression Procedure

The first step of this process is to select and add the most correlated variable into a model. After the variable has been added, the model is checked for significance to determine if any variable should be deleted. If the model is significant, the next predictor variable is added. If the model is not significant, the procedure will be stopped to conclude the model. The procedure is continued until a final model is derived (Draper and Smith, 1998).

6.3.4.5 Selection Criteria

Several methods can be used to rate the quality of the fit of a correlation equation (Hocking, 1976; Pickering, 2005). Four selection criteria are commonly used for choosing an optimal model (Draper and Smith, 1998). These are the residual mean-square (MSE), the coefficient of determination (R^2), the adjusted coefficient of determination (R_a^2) and the total squared error (C_p), i.e.

- the residual mean-square: $MSE = \frac{RSS}{n-p}$; (6.1)

- the coefficient of determination: $R^2 = 1 - \frac{RSS}{TSS}$; (6.2)

- the adjusted coefficient of determination: $R_a^2 = 1 - \frac{(n-1)(1-R^2)}{n-p}$; (6.3)

- the total squared error: $C_p = \frac{RSS}{\sigma^2} + 2p - n$; (6.4)

where RSS is the residual sum of squares, p is the number of parameters in a model, TSS is the total sum of squares and σ^2 is a estimate of the error variance. The term residual refers the difference between the observed value and the estimated value (Draper and Smith, 1998). Therefore the residual sum of squares (RSS) was defined as the sum of squares of the residuals of the model shown in Equation 6.5. The total sum of squares (TSS) is, thus, the sum of the squares of the difference of the variable and its grand mean (Draper and Smith, 1998) shown in Equation 6.6.

- the residual sum of squares: $RSS = \sum_{i=1}^n (Y_i - \hat{Y}_i)^2$; (6.5)

- the total sum of squares: $TSS = \sum_{i=1}^n (Y_i - \bar{Y}_i)^2$; (6.6)

where \hat{Y}_i is the estimated value in the model and \bar{Y}_i is the mean value of the variables.

A baseline value of the R_a^2 equal or greater than 0.95 was chosen for use in the model selection, following the recommendations of Draper and Smith (1998). A baseline value of the MSE of 0.5 was chosen based on the just-noticeable value of the Borg CR10 scale, which in the case of Borg CR10 rated hand-arm vibration is approximately 0.3 (Neely et al., 2001).

From the selection criteria listed above the MSE and the R_a^2 were the only ones which were used in this thesis since the R_a^2 is the only criterion to be maximum when MSE is the minimum (Park, 1993), and since the C_p can be used in a similar way to the R^2 (Gorman and Toman, 1966). Therefore the primary criteria was that the fitted model should produce the highest goodness-of fit as defined by the highest R_a^2 when the MSE is the smallest (Hocking, 1976; Draper and Smith, 1998).

The secondary criteria was that the equal sensation curves which are defined by means of the regression model should present similar frequency dependency characteristics to those found in previous studies on the physiology of vibrotactile perception. Finally, a third criteria was applied which was the consideration that the fitted mathematical equation should be as simple as possible in light of possible practical application.

6.3.5 Results

Table 6.8 presents the mean and one standard deviation values obtained for each frequency and each amplitude tested in the experiment. For each test amplitude the mean Borg CR10 subjective values can be seen to generally decrease with increasing test frequency, suggesting a lower perceived intensity at higher frequencies, as expected from psychophysical theory (Gescheider, 1997) and from previous research (Miwa, 1967; Reynolds et al., 1977; Giacomini et al., 2004; Amman et al., 2005; Morioka, 2004; Morioka and Griffin, 2006). Another feature that can be observed is that the standard deviation was found to generally increase with increasing test amplitude, suggesting a greater difficulty on the part of the test participants to distinguish high amplitude stimuli.

6.3.5.1 Effect of the Multivariate Regression Approach

In order to identify an optimal model with which to represent the equal sensation curves, the goodness-of-fit statistics were evaluated for each polynomial regression expression determined by means of each multivariate regression procedure. Table 6.9 presents the goodness-of-fit statistics for the overall test dataset in the experiment obtained using the four multivariate regression analysis procedures at polynomial orders up to the 6th order. Although the differences in MSE and R_a^2 were small among the different approaches used, the best result was achieved by means of the stepwise regression procedure using terms up to 6th order, which obtained the lowest MSE value (0.084) and the highest R_a^2 value (0.983).

[Table 6.8] Summary of the subjective responses to sinusoidal steering wheel vibration stimuli obtained by means of Borg CR10 scale (n = 40).

Freq.	Acceleration	Subjective	Standard	Freq.	Acceleration	Subjective	Standard
-------	--------------	------------	----------	-------	--------------	------------	----------

[Hz]	[r.m.s. m/s ²]	response	deviation	[Hz]	[r.m.s. m/s ²]	response	deviation
3	0.08	0.7	0.54	40	0.17	0.7	0.56
	0.17	1.53	0.76		0.8	2.09	1.09
	0.49	2.66	1.01		1.71	2.33	0.9
	1	4.13	1.21		7.91	6.34	2.68
4	0.13	0.84	0.72	50	0.08	0.19	0.28
	0.32	1.65	0.83		0.38	1.23	0.69
	0.5	2.41	0.86		3.98	3.91	1.43
	1.26	4.1	1.31		19	7.61	2.95
5	0.08	0.58	0.53	63	0.18	0.83	0.61
	0.23	1.61	0.8		0.85	1.51	0.77
	1.07	4.69	1.75		1.88	2.72	1.43
	3	6.19	1.75		9.09	4.41	1.72
6.3	0.14	1.43	0.8	80	0.07	0.2	0.22
	0.45	2.43	0.94		0.36	1.11	0.63
	0.81	3.97	1.79		4.26	3.6	1.69
	2.58	6.54	1.66		22	6.46	1.95
8	0.08	0.41	0.47	100	0.06	0.09	0.18
	0.28	2.2	0.89		0.78	1.78	1.17
	1.75	4.81	1.25		1.84	1.8	0.82
	6	8.65	2.71		10.2	4.62	2.07
10	0.15	0.99	0.69	125	0.06	0.13	0.22
	0.56	2.22	0.96		0.34	1.27	0.77
	1.07	3.51	1.37		4.46	2.72	1.19
	3.92	6.27	1.31		25	5.48	2.65
12.5	0.08	0.46	0.36	160	0.04	0.04	0.13
	0.3	1.36	0.64		0.64	1.32	0.74
	2.15	5.39	2.16		1.62	2.39	1.14
	8	8.38	1.8		10.31	3.97	1.68
16	0.16	0.73	0.43	200	0.06	0.1	0.18
	0.63	2.52	1.1		0.34	0.88	0.73
	1.26	3.23	0.81		4.71	2.69	1.27
	5.02	6.85	2.4		27	4.43	2.42
20	0.08	0.21	0.22	250	0.15	0.24	0.41
	0.34	1.65	0.79		1.41	1.46	0.84
	2.87	4.62	1.18		2.98	2.27	1.29
	12	8.57	2.77		13.27	3.35	1.65
25	0.17	0.65	0.51	315	0.4	0.5	0.61
	0.73	1.95	1.03		1.36	1.3	0.95
	1.53	4.08	2.08		8.53	3.04	1.81
	6.69	6.21	1.68				
31.5	0.08	0.23	0.33	400	0.8	0.71	0.77
	0.36	1.12	0.68		3.78	2.22	1.69
	3.52	4.49	1.98		6.35	2.31	1.49
	16	8.15	1.94				

[Table 6.9] Goodness of fit statistics obtained for overall data set (n = 40).

Regression method	Polynomial order	Interaction terms	Residual mean square (MSE)	Adjusted coefficient of determination (R_a^2)	Number of regression coefficients
Least-squares procedure	4 th	3 rd	0.107	0.979	12
		4 th	0.088	0.982	15
	5 th	3 rd	0.108	0.978	14
		4 th	0.093	0.981	17
		5 th	0.093	0.980	21
	6 th	3 rd	0.108	0.978	16
		4 th	0.091	0.981	19
		5 th	0.092	0.980	23
		6 th	0.098	0.975	28

Stepwise procedure	4 th	-	0.106	0.979	9
	5 th	-	0.085	0.983	13
	6th	-	0.084	0.983	12
Backward elimination procedure	4 th	-	0.101	0.980	11
	5 th	-	0.099	0.980	11
	6 th	-	0.099	0.981	10
All possible procedure	4 th	-	0.100	0.980	13
	5 th	-	0.106	0.980	17
	6 th	-	0.109	0.979	19

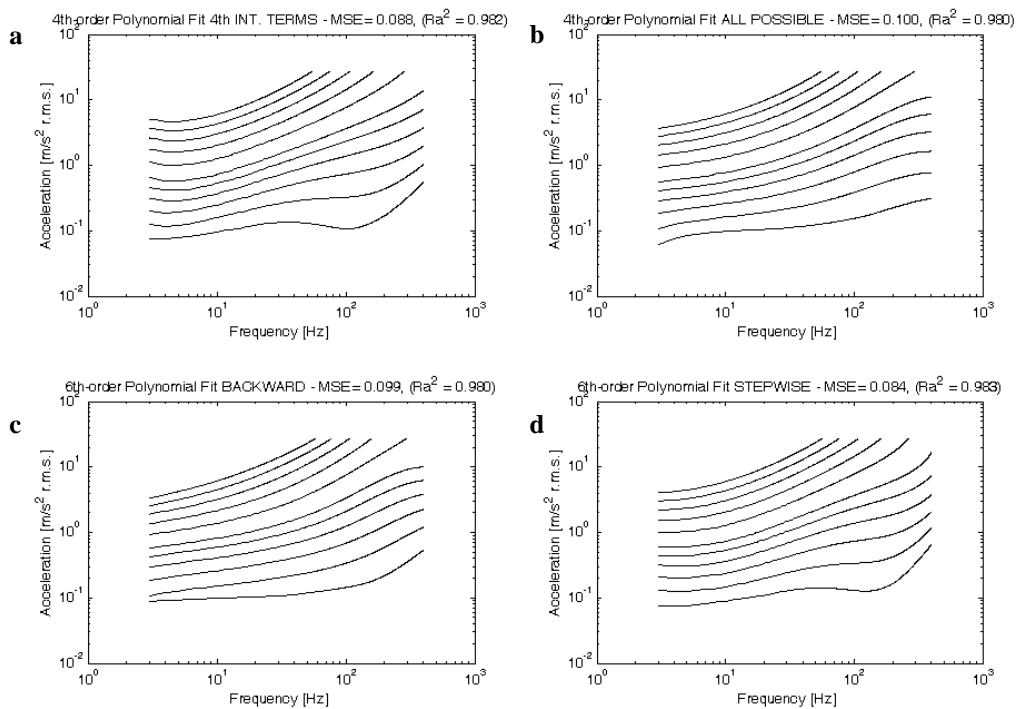


[Figure 6.3] Equal sensation curves obtained for Borg subjective perceived intensity values from 0.5 to 8.0 using the four regression procedures in the experiment ($n = 40$):

(a) Least-square regression procedure, (b) All possible regressions procedure, (c) Backward elimination regression procedure and (d) Stepwise regression procedure.

Figure 6.3 presents the equal sensation curves which achieved the lowest MSE and the highest R_a^2 for each of the different multivariate regression procedures. The curves obtained by means of the stepwise regression procedure suggested a decreased sensitivity with increasing frequency from 6.3 to 400 Hz, a constant sensitivity from 3 to 6.3 Hz, and a dip behaviour in the vicinity of 100 Hz similar to the well known response of the Pacinian mechanoreceptors (Verrillo, 1966; Reynolds et al., 1977). In addition, the 6th order stepwise regression procedure produced a regression model with

only 12 coefficients which was

$$\begin{aligned}
 S = & 3.4268 + 0.7638\log(f) + 2.3058\log(a) + 0.5289\log(a)^2 - 0.2506\log(f)^3 + \\
 & - 0.0978\log(f)^2\log(a) - 0.0881\log(f)\log(a)^2 + 0.0396\log(a)^3 + 0.0523\log(f)^4 + \\
 & - 0.0004\log(f)^6 + 0.0003\log(f)^5\log(a) - 0.0003\log(f)^3\log(a)^3
 \end{aligned} \tag{6.7}$$

where S is the Borg CR10 subjective intensity value which is determined by the fitted model, f is the frequency in units of Hertz and a is the r.m.s. acceleration magnitude in units of meters per second squared.

6.3.5.2 Effect of Gender

Table 6.10 presents the goodness-of-fit statistics obtained for the regression models which were fit separately to the data of only the male test participants ($n = 20$) and of only the female test participants ($n = 20$) using the stepwise regression procedure. The model order which provided the best results for the complete dataset was applied also to the data obtained for each individual gender group. The stepwise regression procedure provided a MSE value of 0.064 and a value of 0.985 for R_a^2 for the males while it produced a MSE value of 0.168 and a value of 0.973 for R_a^2 for the females.

[Table 6.10] Goodness of fit statistics obtained separately for the male test participants data set ($n = 20$) and for the female test participants data set ($n = 20$).

Regression method	Gender	Polynomial order	Residual mean square (MSE)	Adjusted coefficient of determination (R_a^2)	Number of regression coefficients
Stepwise procedure	M	6 th	0.064	0.985	12
	F		0.168	0.973	12

Figure 6.4 presents the equal sensation curves obtained for the male and the female sample groups obtained by means of the stepwise regression procedure. From the results of Figure 6.4 it can be seen that the females provided higher perceived intensity values than the males for the same physical stimulus at most frequencies. At frequencies above approximately 20 Hz the equal sensation curves for the female test group are characterised by a flatter shape than those obtained for the male test group, whereas at frequencies below approximately 20 Hz similar shape was found for both groups.

Gender differences were more marked at acceleration amplitudes above approximately 1.0 m/s^2 r.m.s.. For example, it can be seen in Figure 6.4 that the subjective response of the females for the stimulus with amplitude of 2.0 m/s^2 r.m.s. and frequency of 30 Hz was approximately 4.0 on the Borg CR10 scale, while that of males for the same stimulus was approximately 3.0 on the Borg CR10 scale.

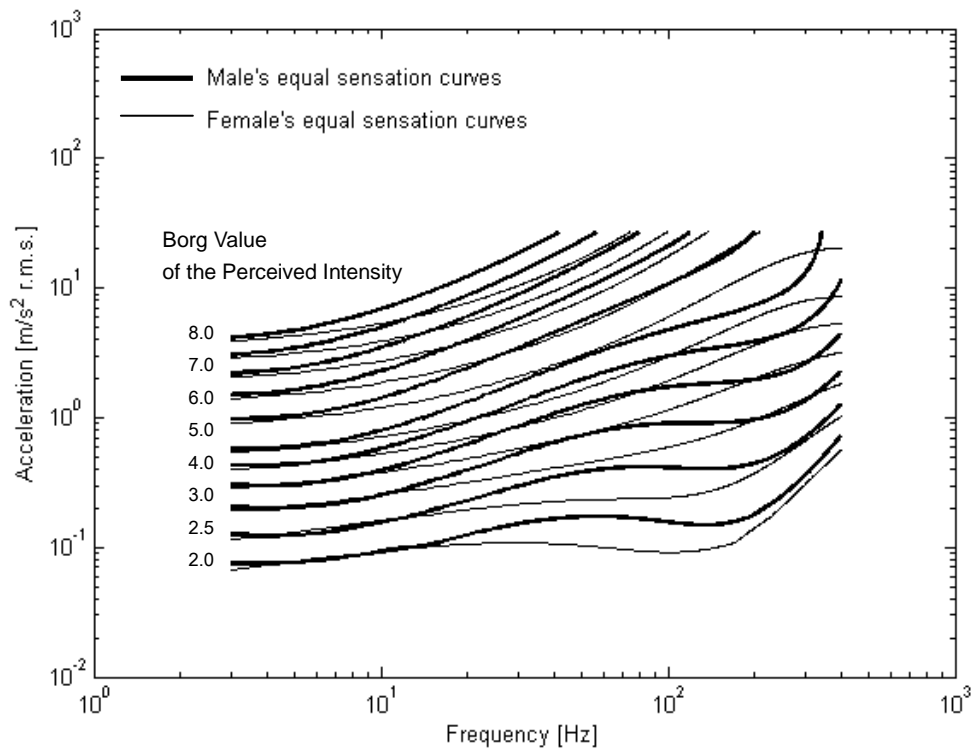


[Figure 6.4] Equal sensation curves obtained separately for the male test participants ($n = 20$) and for the female test participants ($n = 20$), obtained by means of the stepwise regression procedure.

6.4 Discussion

The results of this experiment suggest that the stepwise regression procedure provided the best model of the hand-arm equal sensation curves because the best fit equation provided the lowest MSE of 0.084 and the highest adjusted coefficient of determination R_a^2 of 0.983 using only 12 coefficients. Compared to the other regression procedures used in this research, the equal sensation curves obtained by means of stepwise regression suggested small variations in the shape of the curves at low vibration

amplitudes and more uniform shape at high vibration amplitudes, resembling the curves defined by previous researchers (Reynolds et al., 1977; Gescheider et al., 2004).

A possible explanation of the effectiveness of the stepwise regression procedure may be that only a small number of coefficients were included in the model. Direct support for this can be found in the study of Barrett and Gray (1994) who applied the stepwise regression procedure for constructing a multivariate regression model. They found that the stepwise regression procedure provided a better model using a rather small number of variables as opposed to the approach based on the use of all possible subsets. In addition, the general efficiency of stepwise regression was noted by Wallace (1964), who suggested that the stepwise regression procedure provided a better model because of the reduced bias of the coefficients selection procedure.

The results of this experiment also suggest that the equal sensation curves for steering wheel rotational vibration differed between males and females. These differences are most obvious at intensity levels above approximately 1.0 m/s^2 and at frequencies above approximately 20 Hz. This difference is partially supported by the results of Verrillo (1979) who found that vibratory stimuli at suprathreshold levels are felt more intensely by females than by males, and by those of Neely and Burström (2006) which suggest that females report higher levels of physical intensity and discomfort than males. Similar indications can also be found in the study of steering wheel vibration induced fatigue performed by Giacomini and Abrahams (2000), which found that females reported greater arm region discomfort than males, and by the questionnaire-based investigation of Giacomini and Screti (2005) which found that female drivers reported higher discomfort responses than male drivers for the hand-arm region.

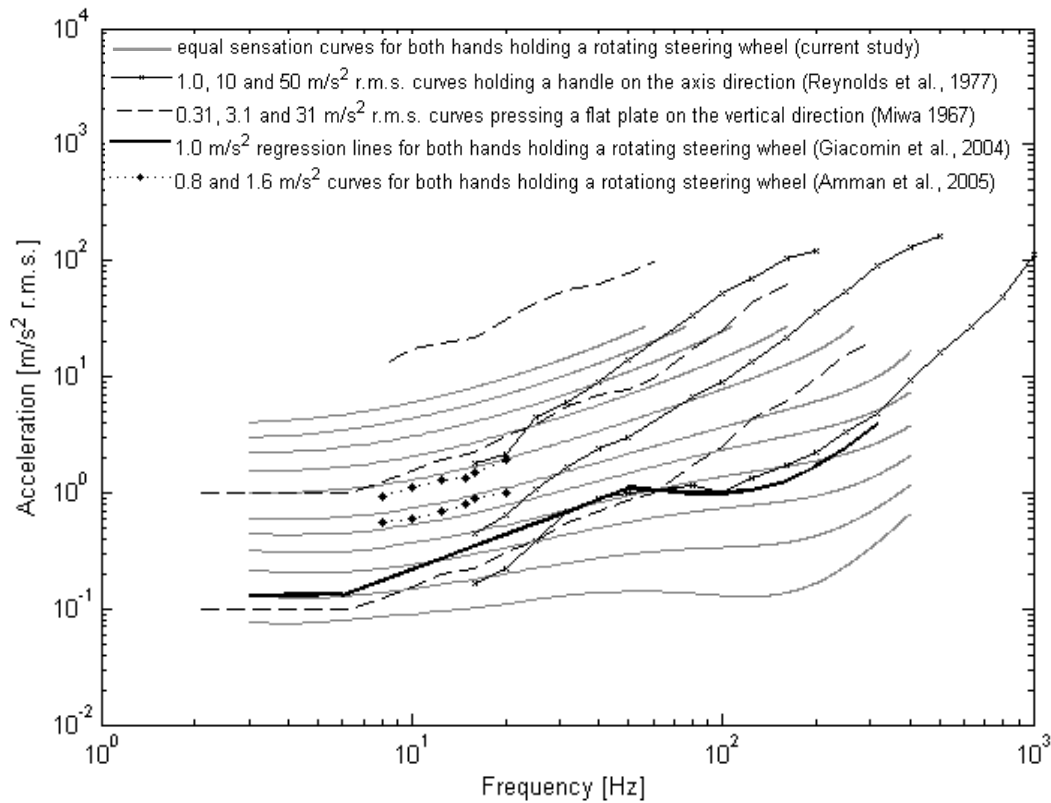


[Figure 6.5] Equal sensation curves obtained in the current study and those obtained in previous studies of hand-arm translational or rotational vibration.

Figure 6.5 presents the best fit equal sensation curves determined in this experiment, the results of Miwa (1967) for hand-arm vibration in the vertical direction ($n = 10$), the results of Reynolds et al. (1977) for hand-arm axial direction vibration ($n = 8$), the results of Giacomin et al. (2004) ($n = 15$) and those of Amman et al. (2005) ($n = 28$) for steering wheel hand-arm rotational vibration. Each of the equal sensation curves shown in Figure 6.5 represents a curve of equal subjective perceived intensity. The equal sensation curves of the current research are interpolations of the Borg values provided by the test subjects. The curves shown in Figure 6.5 are for the Borg values 0.5, 1.0, 1.5, 2.0, 2.5, 3.0, 4.0, 5.0, 6.0, 7.0 and 8.0. The equal sensation curves from the previous research studies are, instead, interpolations of the acceleration data points obtained using magnitude estimation test protocols in the case of Reynolds et al., Giacomin et al. and Amman et al. and a paired-comparison method in the case of Miwa. All the curves suggest a decreased sensitivity of hand-arm vibration with increasing frequency for frequencies above about 6.3 Hz. For frequencies below 6.3 Hz, the curves obtained in this experiment suggest a constant sensitivity as also found in the results of Miwa and of

Giacomin et al.. The reduction in sensitivity was found, however, to be greater in the curves of Miwa than in either those of Reynolds et al. or those of the current research. While difficult to demonstrate without replication of each of the previous studies, a possible explanation for the differences may in part be the use of different psychophysical test methods in the various investigations and the use of only male test participants. As can be seen from Figure 6.4, females were found to provide higher perceived intensity values than males, resulting in a lower equal sensation curve.

It is also evident from Figure 6.5 that at low perceived intensities from 0.5 (just noticeable) to 1.0 (very weak) of the Borg CR-10 scale the equal sensation curves determined in the current experiment show similarities in shape to the well-known vibrotactile perception threshold curves of the human hand. As the perceived intensity increases towards the maximum value of 8.0 found in the current experiment the equal sensation curves assume a more uniform shape, however, resembling the annoyance threshold for the hand-arm system defined by Reynolds et al. (1977). Comparison of the results of Figure 6.5 suggests that while the curves of Miwa and of Amman et al. suggest relatively small dependencies on the vibration amplitude, the equal sensation curves of the current research and those of Reynolds et al. suggest a significant nonlinear response. A possible explanation of these differences may be the use of relatively low reference frequencies in the studies of Miwa and of Amman et al. The use of a low reference frequency has been found to affect the shape of equal sensation curves, especially at frequencies above approximately 50 Hz (Giacomin et al., 2004).

6.5 Summary

Psychophysical response tests of 40 participants (20 males and 20 females) were performed in a steering wheel rotational vibration simulator using the category-ratio Borg CR10 scale procedure for direct estimation of perceived vibration intensity. The equal sensation curves for steering wheel hand-arm rotational vibration were established using multivariate regression analysis procedures. The best fit regression model to describe the equal sensation curves was found to be a 6th order polynomial model having 12 terms, which was obtained by means of a stepwise regression procedure. The results suggest a nonlinear dependency of the subjective perceived intensity on both

frequency and amplitude. The equal sensation curves were found to be characterised by a decreased sensitivity to hand-arm vibration with increasing frequency from 6.3 to 400 Hz, but a constant sensitivity from 3 to 6.3 Hz. The best fit regression models determined for the male test participants and for the female test participants suggest important differences in the frequency range from 20 to 400 Hz, while both sets of curves suggest similar sensitivity at frequencies below 20 Hz. Females were found to be more sensitive to steering wheel rotational vibration than males, particularly at intensity levels above approximately 1.0 m/s^2 r.m.s. and at frequencies above approximately 20 Hz ($p < 0.05$).

Chapter 7

Human Subjective Response to Steering Wheel Hand-Arm Vibration consisting of Random Vibration

7.1 Introduction

In the majority of the previous research studies the equal sensation curves which were established to describe the human subjective response to the hand-arm vibration (Giacomin et al., 2004; Amman et al., 2005; Morioka, 2004; Morioka and Griffin, 2006; Ajovalasit and Giacomin, 2009) were based on the use of sinusoidal vibration due to the great simplicity of the wave form (Bendat and Piersol, 1986). Nevertheless, random vibration is closer in nature to the real vibrational stimuli which are encountered in automobiles (Griffin, 1990).

Miwa (1969) established equal sensation curves for 10 male participants who held their palm flat against a plate which was vibrated in the vertical direction using either one or 1/3 octave band-limited random vibration stimuli at acceleration amplitudes of either 0.31, 1.74 or 0.98 m/s² r.m.s. respectively over the frequency range from 2 to 250 Hz.

Although the equal sensation curves obtained using random vibration showed similarity of shape to those obtained using sinusoidal vibration, differences as large as 3 dB were found below 8 Hz and above 125 Hz. Miwa also investigated the effect of bandwidth by comparing the results of experiments which used one octave wide band-limited random stimuli to those which used 1/3 octave wide band-limited random vibration. In this case, however, no significant differences were found between the two sets of subjective responses.

Reynolds et al. (1977) established equal sensation curves for 8 male participants who gripped with one hand a handle which was vibrated along either the vertical, axial or horizontal directions. The vibration stimuli consisted of 1/3 octave band-limited random vibration at acceleration amplitudes of either 1.0, 10.0 or 50.0 m/s² r.m.s. over the frequency range from 25 to 1000 Hz. The shape of the equal sensation curves was found to be similar in shape to those obtained using sinusoidal vibration. However, the slope of the curves obtained using random vibration was slightly steeper than that obtained using sinusoidal vibration.

The primary objective of the research which is described in this chapter was to determine equal sensation curves for steering wheel hand-arm rotational vibration using random vibration, in order to investigate the effect of the vibrational signal type. The secondary objective was to confirm the effect of gender on the shape of equal sensation curves for hand-arm steering wheel rotational vibration, which was first noted from the results of the experiment which used sinusoidal vibration.

7.2 Laboratory Based Experimental Testing using Random Vibration

The laboratory based experiment which is described in this chapter was performed using the same test facility and the same test protocol which were first described in this thesis in sections 6.2.1 and 6.3.3 respectively.

7.2.1 Test Stimuli

Band-limited random vibration has been used frequently in tests of human response to hand-arm vibration (Miwa, 1969; Reynolds et al., 1977) and to whole-body vibration (Griffin, 1976) because band-limited random vibration can be thought of as containing a

large number of simultaneous sinusoidal functions of similar spectral magnitude (Ministry of Defence, 2007). Thus band-limited random vibration was employed also in the current context to serve as a test signal of the laboratory experimental testing for human perception of hand-arm vibration.

In order to investigate only differences caused by the change of signal type, the same frequency range from 3 to 400 Hz and the same amplitude range from 0.04 to 27 m/s² r.m.s. were used as in the previous experiment for sinusoidal vibration. One-third octave band centre frequencies in the range from 3 to 400 Hz were also chosen to define the position of the test stimuli. Twenty two centre frequencies (3, 4, 5, 6.3, 8, 10, 12.5, 16, 20, 25, 31.5, 40, 50, 63, 80, 100, 125, 160, 200, 250, 315 and 400 Hz) were used in the experiment.

A one-third octave band width was adopted for the test signals of the experiment in order to avoid some errors which may arise when using broad band octave analysis (Griffin, 1990) and because it was used often in the studies of hand-arm vibration consisting of random signals (Miwa, 1969; Reynolds et al., 1977). Therefore 1/3 octave band width test signals centred at the above frequencies were used.

The 1/3 octave band width test signals were obtained by passing a Gaussian white noise signal generated by LMS software, shown in Figure 7.1, through a Butterworth band-pass filter. A Butterworth band-pass filter was chosen for use in constructing the test signals because it produces no ripples in the pass-band or the stop-band (Kester, 2003). An attenuation rate of 48 dB per octave was chosen in order to provide a strong transition between the pass band and the stop band (LMS International Inc., 2002).

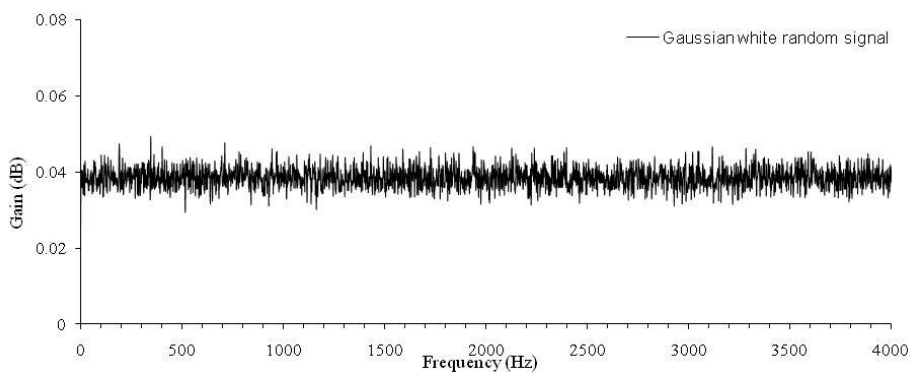


[Figure 7.1] Gaussian white noise signal used to be filtered by applying Butterworth band-pass filter.

In order to maximise the signal density in the frequency-amplitude plane while simultaneously also not exceeding a test duration of 60 minutes, so as to avoid any learning or fatigue effects (Coolican, 1999), a total of 86 steering wheel rotational 1/3 octave band-limited random vibration stimuli were used in the experiment. In order to investigate the differences caused by only the change of signal type, the same amplitude levels were used as in the previous experiment in chapter 6. Figure 7.2 presents the time series and frequency distributions of three of the 1/3 octave band-limited random stimuli which were employed in this experiment.

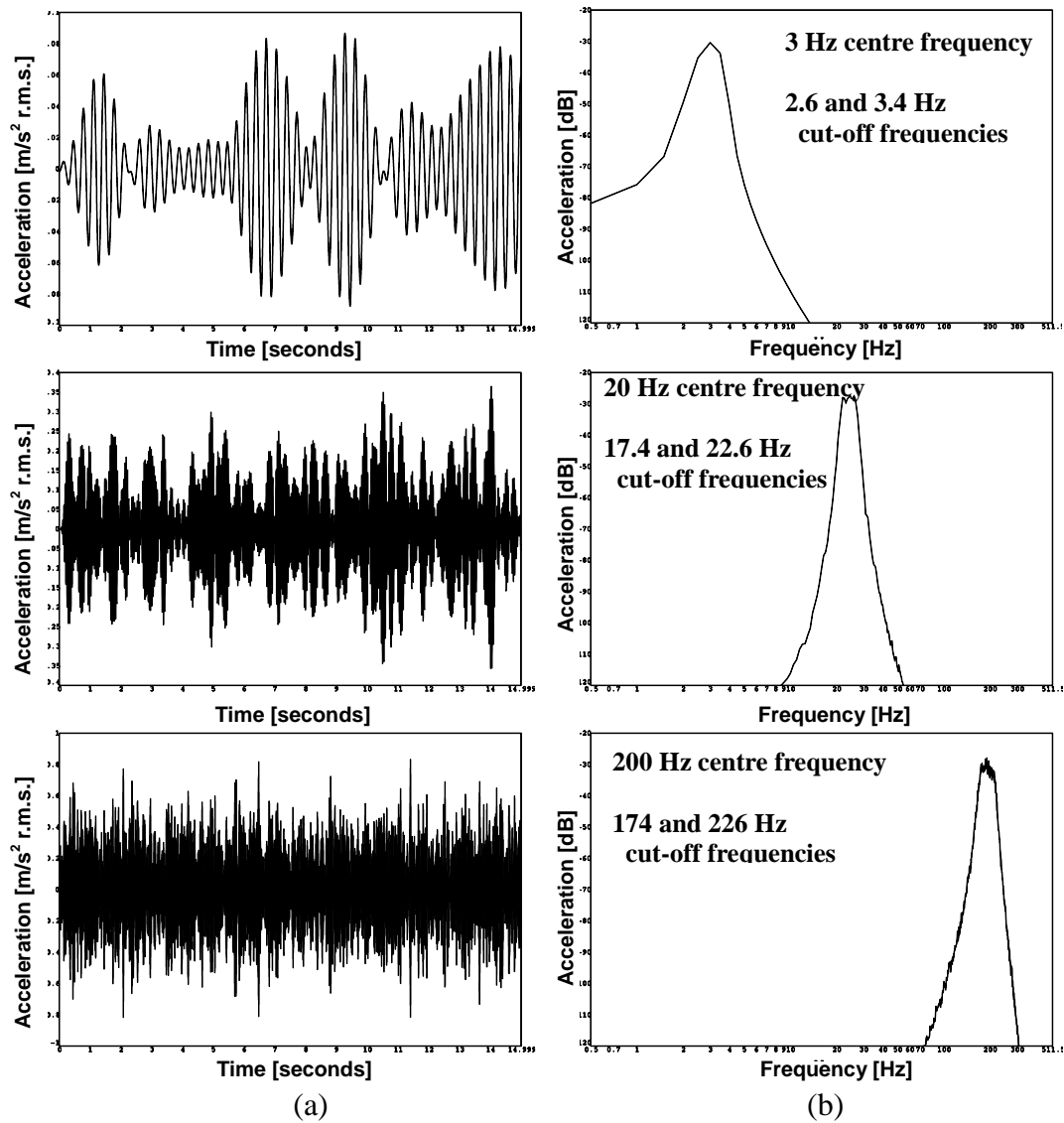


[Figure 7.2] Three examples of the band-limited random signals used in the experiment: (a) time series representation and (b) power spectral density (PSD) representation.

Based on these considerations, a total of 86 steering wheel rotational 1/3 octave band-limited random vibration stimuli in the frequency range from 3 to 400 Hz with the acceleration magnitudes range from 0.04 to 27 m/s² r.m.s. were used in the experiment. Table 7.1 provides the band centre frequency, the lower and upper cutoff frequencies, and the r.m.s. acceleration amplitude of each of the steering wheel test stimuli.

[Table 7.1] Frequency and amplitude of the 86 steering wheel rotational 1/3 octave band-limited random vibration stimuli.

Centred frequency [Hz]	Cut-off frequency [Hz]	Acceleration amplitude [r.m.s. m/s ²]
3	2.6 / 3.4	0.08, 0.15, 0.41, 0.80
4	3.5 / 4.5	0.12, 0.24, 0.34, 0.7
5	4.4 / 5.6	0.08, 0.20, 0.8, 2.0
6.3	5.5 / 7.1	0.13, 0.38, 0.64, 1.79
8	7.0 / 9.0	0.08, 0.26, 1.53, 5.0
10	8.7 / 11.3	0.15, 0.56, 1.07, 3.92
12.5	10.9 / 14.1	0.08, 0.3, 2.15, 8.0
16	13.9 / 18.1	0.16, 0.63, 1.26, 5.02
20	17.4 / 22.6	0.08, 0.34, 2.87, 12.0
25	21.8 / 28.2	0.17, 0.73, 1.53, 6.69
31.5	27.4 / 35.6	0.08, 0.36, 3.52, 16.0
40	34.8 / 45.2	0.17, 0.8, 1.71, 7.91
50	43.5 / 56.5	0.08, 0.38, 3.98, 19.0
63	54.8 / 71.2	0.18, 0.85, 1.88, 9.09
80	69.6 / 90.4	0.07, 0.36, 4.26, 22.0
100	87.0 / 113.0	0.14, 0.78, 1.84, 10.2
125	108.8 / 141.2	0.04, 0.34, 4.46, 25.0
160	139.2 / 180.8	0.1, 0.64, 1.62, 10.31
200	174.0 / 226.0	0.06, 0.34, 4.71, 27.0
250	217.5 / 282.5	0.31, 1.41, 2.98, 13.27
315	274.1 / 355.9	0.4, 1.36, 8.53
400	348.0 / 452.0	0.8, 3.78, 6.35

7.2.2 Test Subjects

A total of 30 university students and staff, 15 male and 15 female, were randomly chosen to participate in the experiment. The use of 30 participants was still considered a conservative approach (Coolican, 1999) as stated in the previous chapter. A consent form and a short questionnaire were presented to each participant prior to testing, and information was gathered regarding their anthropometry, health and history of previous vibration exposures.

Table 7.2 presents a basic summary of the physical characteristics of the group of test

participants. The mean value and the standard deviation of the height and mass of the group of test participants were close to the 50 percentile values for the U.K. population (Pheasant and Haslegrave, 2005). A statistical t-test performed to check for gender based differences suggested significant physical differences in height and mass between the males and the females ($p < 0.05$), while no significant differences were found in age between the males and the females. All subjects declared themselves to be in good physical and mental health.

[Table 7.2] Mean and standard deviation summary statistics for the test participants.

Test Group	Age [years]	Height [m]	Mass [kg]
Male (n=15)	30.1 (6.5)	1.78 (0.06)	77.7 (9.3)
Female (n=15)	31.9 (6.8)	1.61 (0.04)	55.2 (5.3)
Total (N=30)	31.0 (6.6)	1.70 (0.10)	66.4 (13.7)

7.2.3 Results

Table 7.3 presents the mean and one standard deviation values obtained for each frequency and each amplitude tested, for the 30 participants. The general tendency of decreasing Borg CR10 subjective values with increasing frequency for each r.m.s. test amplitude was found to be similar to those obtained by means of sinusoidal vibration stimuli. Another feature that can be observed is that the standard deviation was found to increase with increasing test amplitude, which is also consistent with the results obtained using sinusoidal vibration stimuli, suggesting a greater difficulty on the part of the test participants to distinguish high amplitude stimuli.

The stepwise regression procedure was employed to develop sensation curves using the data from the band-limited random vibration ($n = 30$) tests because it had provided the best fit regression model among other regression procedures presented in the previous chapter ($n = 40$). Table 7.4 presents the goodness of fit statistics obtained for the regression model by means of the stepwise regression procedure implemented by Matlab software (Mathworks Inc., 2002). The same selection criteria as those described in the previous chapter were adopted to rate the quality of the fit of a correlation equation. The stepwise regression procedure lead to a residual mean square (MSE) value of 0.071 and an adjusted coefficient of determination (R_a^2) value of 0.984.

[Table 7.3] Summary of the subjective responses obtained by means of Borg CR10 scale.

Freq. [Hz]	Acceleration [r.m.s. m/s ²]	Subjective response	Standard deviation	Freq. [Hz]	Acceleration [r.m.s. m/s ²]	Subjective response	Standard deviation
3	0.08	1.34	0.80	40	0.17	0.68	0.40
	0.15	1.94	0.93		0.8	2.05	0.84
	0.41	3.3	1.31		1.7	2.32	1.04
	0.8	4.56	1.40		7.91	4.92	1.58
4	0.12	1.41	0.76	50	0.08	0.33	0.35
	0.24	2.42	0.95		0.38	1.26	0.73
	0.34	3.04	1.02		3.98	3.86	1.35
	0.7	4.52	1.74		19	7.13	2.2
5	0.08	0.65	0.54	63	0.18	0.96	0.56
	0.20	2.0	0.9		0.85	1.48	0.76
	0.8	4.55	1.18		1.88	2.36	0.95
	2	6.57	2.13		9.09	4.28	1.41
6.3	0.13	1.05	0.63	80	0.07	0.37	0.34
	0.38	2.32	0.9		0.36	1.21	0.66
	0.64	3.84	1.0		4.26	3.07	1.0
	1.79	6.27	1.71		22	6.03	1.9
8	0.08	0.4	0.32	100	0.14	0.78	0.49
	0.26	1.68	0.67		0.78	1.58	0.76
	1.53	4.98	1.41		1.84	1.62	0.79
	5	8.34	1.65		10.2	3.66	1.28
10	0.15	1.29	0.60	125	0.04	0.29	0.33
	0.56	2.75	0.90		0.34	1.33	0.79
	1.07	3.81	1.35		4.46	2.45	1.07
	3.92	6.94	1.93		25	5.14	2.07
12.5	0.08	0.61	0.40	160	0.1	0.57	0.42
	0.3	1.47	0.56		0.64	1.32	0.81
	2.15	5.4	1.50		1.62	2.14	1.09
	8	8.41	2.06		10.31	4.01	1.69
16	0.16	0.82	0.31	200	0.06	0.21	0.21
	0.63	2.75	0.74		0.34	1.12	0.62
	1.26	4.09	1.43		4.71	2.63	1.14
	5.02	7.02	2.12		27	4.32	1.83
20	0.08	0.38	0.27	250	0.31	0.95	0.62
	0.34	2.11	0.78		1.41	1.58	0.96
	2.87	4.45	1.37		2.98	2.36	1.05
	12	7.66	2.02		13.27	3.37	1.62
25	0.17	0.85	0.48	315	0.4	0.68	0.59
	0.73	2.04	0.78		1.36	1.5	0.83
	1.53	3.17	1.04		8.53	2.83	1.34
	6.69	5.93	1.67				
31.5	0.08	0.28	0.22	400	0.8	0.93	0.66
	0.36	1.08	0.45		3.78	2.15	1.22
	3.52	3.61	1.30		6.35	2.38	1.16
	16	7.24	1.9				

[Table 7.4] Goodness of fit statistics obtained for overall data set (n = 30).

Regression method	Polynomial order	Residual mean square (MSE)	Adjusted coefficient of determination (R_a^2)	Number of regression coefficients
Stepwise procedure	6 th	0.071	0.984	12

The stepwise regression procedure produced a 6th order polynomial regression model with 12 regression coefficients. The best fit model was

$$\begin{aligned}
 S = & 5.843 - 0.2774\log(f) + 2.5245\log(a) + 0.4179\log(a)^2 - 0.2204\log(f)^3 + \\
 & - 0.1289\log(f)^2\log(a) - 0.0676\log(f)\log(a)^2 + 0.0243\log(a)^3 + 0.0517\log(f)^4 + \\
 & - 0.0005\log(f)^6 + 0.0004\log(f)^5\log(a) - 0.0001\log(f)^3\log(a)^3
 \end{aligned} \tag{7.1}$$

where S is the Borg CR10 subjective intensity value which is determined by the fitted model, f is the centre frequency in units of Hertz and a is the r.m.s. acceleration magnitude in units of meters per second squared.

Figure 7.3 presents the family of equal sensation curves which are defined by the regression equation 7.1. From Figure 7.3 it can be noted that there is a decreased sensitivity with increasing frequency over much of the frequency range which was tested, with the exception of the dip behaviour in the vicinity of 100 Hz.

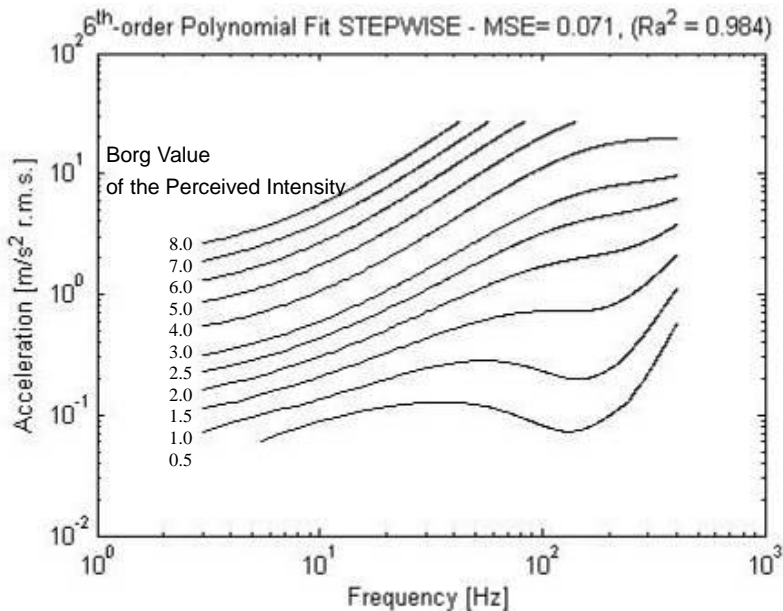


[Figure 7.3] Equal sensation curves obtained for Borg subjective perceived intensity values from 0.5 to 8.0 using the regression formula obtained for the band-limited random vibration.

7.2.3.1 Effect of the Signal Type

Figure 7.4 presents the family of equal sensation curves which were obtained from the sinusoidal vibration tests which were described in the previous chapter ($n = 40$), and those obtained from the tests involving the use of 1/3 octave band-limited random vibration stimuli ($n = 30$). The curves presented for the band-limited random vibration were determined by means of the regression equation 7.1 which was determined by means of stepwise regression procedure which produced the lowest MSE value (0.071) and the highest R_a^2 value (0.984).

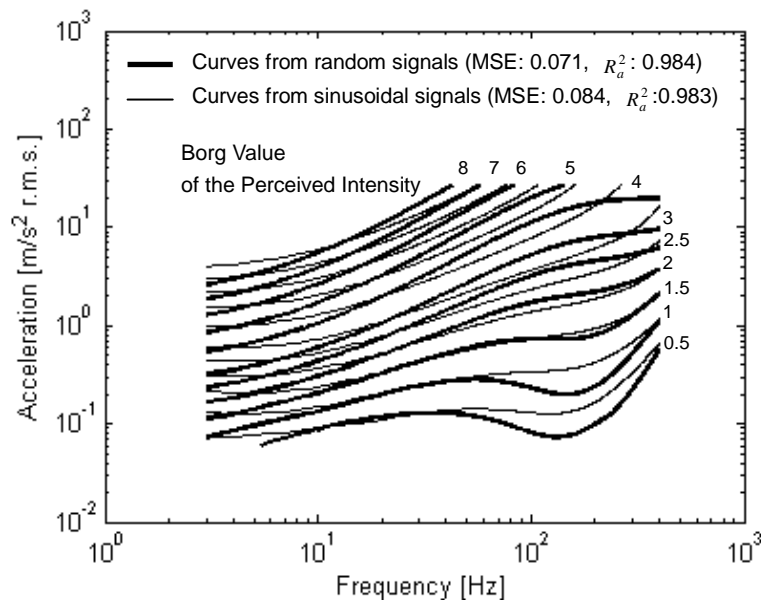


[Figure 7.4] Comparison of the equal sensation curves which were obtained using the band-limited random signals to those obtained using the sinusoidal signals.

With regard to the effect of the test signal type, Figure 7.4 suggests that the subjective responses obtained using band-limited random vibration stimuli were generally steeper in the shape of the equal sensation curves than those obtained using sinusoidal vibration stimuli in the frequency interval from 3 to 400 Hz. This tendency in the shape of the equal sensation curves resembles the results of Reynolds et al. (1977).

The results also suggest that the equal sensation curves obtained using random vibration produced deeper dips in the vicinity of 100 Hz than those obtained using sinusoidal

vibration at acceleration levels below approximately 1.0 m/s^2 r.m.s.. This tendency in the shape of the equal sensation curves resembles the results of Miwa (1969).

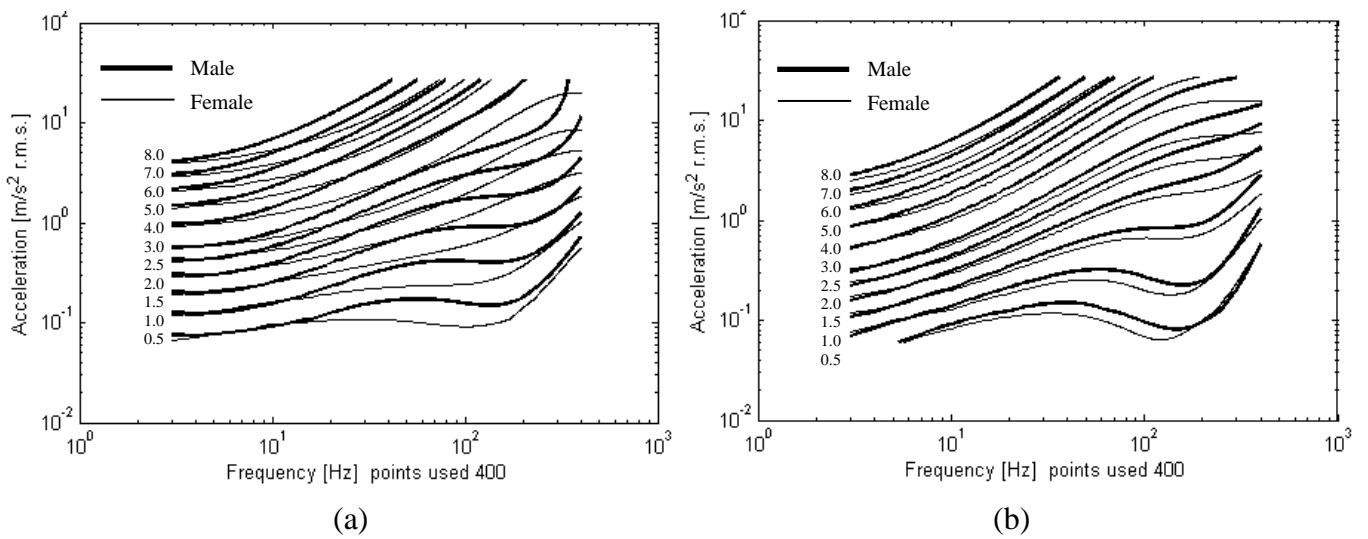
7.2.3.2 Confirming of the Effect of Gender

Table 7.5 presents the goodness-of-fit statistics obtained for the regression models which were fit separately to the data of only the male test participants ($n = 15$) and only the female test participants ($n = 15$) using the stepwise regression procedure. The model order which provided the best results for the complete dataset was applied also to the data obtained of each individual gender group. The stepwise regression procedure provided a MSE value of 0.076 and a value of 0.981 for R_a^2 for the males while it produced a MSE value of 0.101 and a value of 0.979 for R_a^2 for the females.

[Table 7.5] Goodness of fit statistics obtained by fitting to the data of the male test participants ($n = 20$) and the female test participants ($n = 20$) separately.

Regression method	Gender	Polynomial order	Residual mean square (MSE)	Adjusted coefficient of determination (R_a^2)	Number of regression coefficients
Stepwise procedure	M	6 th	0.076	0.981	12
	F		0.101	0.979	12

Figure 7.5 presents a comparison between the equal sensation curves obtained for the male and the female sample groups, using the sinusoidal and the 1/3 octave band-limited random vibration stimuli. All the curves shown in Figure 7.5 were obtained by means of the stepwise regression procedure. The differences between the curves obtained for the two genders using 1/3 octave band-limited random vibration were smaller than those using sinusoidal vibration. However, similar global tendencies are present in both sets of experimental results. For example, the equal sensation curves obtained using 1/3 octave band-limited random vibration suggest that the females provided higher perceived intensity values than the males for the same physical stimulus at frequencies above approximately 20 Hz, which is consistent with the results obtained using sinusoidal vibration.



[Figure 7.5] Equal sensation curves obtained separately for the male test participants and for the female test participants, obtained by means of the stepwise regression procedure using (a) sinusoidal vibration stimuli and (b) band-limited random vibration stimuli.

7.3 Discussion

The results of this experiment suggest a similar general tendency to that noted from the experiment involving sinusoidal vibration, a decreased sensitivity with increasing frequency. However, compared to the previous equal sensation curves obtained using sinusoidal vibration, some differences were found in the shape of the curves.

The shape of the equal sensation curves obtained using the 1/3 octave band-limited random vibration stimuli were generally steeper than those obtained using sinusoidal vibration stimuli and deeper in the vicinity of 100 Hz. This tendency suggests that the perceived vibration magnitude caused by random vibration increases more rapidly with increasing frequency than that caused by sinusoidal vibration. For example, the vibration magnitudes associated with the equal sensation curve of 3.0 Borg CR10 increased from approximately 0.3 to 7.0 m/s² r.m.s. across the frequency range from 3 to 160 Hz for the band-limited random vibration model while those obtained using sinusoidal vibration increased only from approximately 0.6 to 5.0 m/s² r.m.s. across the same frequency range. A possible explanation of the effect of the test signal type may be

that the occasional peak acceleration value of random vibration was well in excess of the r.m.s. value when the crest factor exceeded 3 (Griffin, 1976). The crest factor values of band-limited random vibration used in the experiment were generally in the range from 2.4 to 8.4, which was similar to the values of the real road stimuli which were described in chapter 5. The high peak events may produce more intense response for the human perception of steering wheel hand-arm vibration.

With regard to the effect of gender, the results of this experiment confirm the finding of the sinusoidal vibration tests, that the equal sensation curves for steering wheel rotational vibration differed between males and females. Although the differences found using random vibration were smaller than those found using sinusoidal vibration stimuli, similar tendencies can be noted in the frequencies above approximately 20 Hz, which includes the range of the large resonances of the steering wheel and column (Pottinger et al., 1986). It implies that the gender differences of the subjective responses may occur regardless the type of the signal.

While substantial differences in the perception of hand-arm vibration between males and females appear to be present in the research literature (Verrillo, 1979; Neely and Burström, 2005), the exact cause has yet to be clarified. While gender itself may be a dominant factor, particularly in the trends identified by Verrillo (1979), the actual mechanical mass of the hand-arm system may be the primary cause of the variance found in several research investigations, including this current research. For example, Burström and Lundström (1994) have suggested that the size and mass of the subject's hand and arm greatly affect energy absorption. It was therefore decided that it would prove helpful to investigate the effect of the body mass of the human hand-arm system on the human subjective response to steering wheel rotational vibration.

7.4 Summary

Psychophysical response tests of 30 participants (15 males and 15 females) were performed in a steering wheel rotational vibration simulator using the category-ratio Borg CR10 scale procedure for direct estimation of perceived vibration intensity. The equal sensation curves for steering wheel hand-arm rotational vibration were established

using 1/3 octave band-limited random vibration stimuli by means of a stepwise regression procedure.

The general tendency of decreasing subjective intensity rating with increasing frequency for each r.m.s. test amplitude was found to be similar to that found by means of sinusoidal vibration stimuli. However, the equal sensation curves obtained using band-limited random vibration stimuli were generally steeper in the shape in the frequency interval from 3 to 400 Hz, with deeper dips in the vicinity of 100 Hz than those obtained using sinusoidal vibration stimuli. These differences may be due to the characteristics of random vibration which produce generally higher crest factors than sinusoidal vibration.

With regard to the differences of the equal sensation curves obtained between the males and the females, a similar tendency was found in both the equal sensation curves obtained using band-limited random vibration and those obtained using sinusoidal vibration. Females provided higher perceived intensity values than the males for the same physical stimulus at all frequencies above approximately 20 Hz, which is consistent with the results obtained using sinusoidal vibration.

Chapter 8

Effect of Physical Body Mass Difference on the Subjective Perceived Intensity of Steering Wheel Vibration

8.1 Introduction

From the results of the experiments which were described in the previous two chapters, it was noted that male subjects were less sensitive than female subjects in terms of their subjective response to steering wheel hand-arm vibration. However, it was not possible from those tests to establish whether the differences are sensory or, instead, biomechanical in nature, because the male test participants also differed from the female participants in terms of their body mass ($p < 0.05$). In fact, body mass is one of the principle determinants for the energy absorptions in both whole-body vibration (Wang et al., 2006) and hand-arm vibration (Burström and Lundström, 1994).

This chapter therefore describes an experiment which investigated the effect of physical body mass on the subjective response. A psychophysical experimental was performed in which the test participants were separated into two groups: one consisting of individuals

with small overall body mass and one consisting of individuals of large overall body mass.

8.2 Laboratory Based Experimental Testing of the Effect of Physical Body Mass

The laboratory based experiment described in this chapter was performed using sinusoidal vibration. The test facility, test stimuli and the test protocol were the same as described in this thesis in sections 6.2.1, 6.3.1 and 6.3.3.

8.2.1 Test Subjects

A total of 40 university students and staff, 20 light participants and 20 heavy participants, were randomly selected to participate in the experiment. Those of less than 65 kg of body mass were classified into the light body mass group, while the other participants who were more than 65kg were assigned to the heavy body mass group. The value of 65 kg was used because it was the median value of the subjects who participated in the experiment. Each group consisted of 10 males and 10 females in order to avoid the possible effect of gender.

A consent form and a short questionnaire were presented to each participant prior to testing, and information was gathered regarding their anthropometry, health and history of previous vibration exposures. Table 8.1 presents a basic summary of the physical characteristics of the test participants in terms of the mean value and the standard deviation of the age, height and mass. A statistical t-test performed for the test groups suggested significant differences in height and mass between the light and the heavy test participants ($p < 0.05$), while no significant differences were found in age. All subjects declared themselves to be in good physical and mental health.

[Table 8.1] Mean and standard deviation summary statistics for the test participants.

Test Group	Age [years]	Height [m]	Mass [kg]
Lighter (n=20)	30.6 (7.2)	1.66 (0.08)	57.4 (5.2)
Heavier (n=20)	33.4 (7.1)	1.75 (0.11)	78.5 (12.0)
Total (N=40)	32.0 (7.2)	1.71 (0.10)	68.0 (14.1)

8.2.2 Results for the complete test group

Table 8.2 presents the mean and one standard deviation values obtained for each frequency and each amplitude tested for the complete 40 participants. The results obtained from this experiment were not significantly different from those obtained in the previous experiment for the effect of gender which was described in chapter 6. A t-test performed at a 5% confidence level ($p > 0.05$) found no statistically significant difference, at any frequency or amplitude, between the mean value of the new data set and the results from the experiment which was described in chapter 6.

[Table 8.2] Summary of the subjective response of the complete group of 40 test subjects to sinusoidal steering wheel vibration, obtained by means of Borg CR10 scale.

Freq. [Hz]	Acceleration [r.m.s. m/s ²]	Subjective response	Standard deviation	Freq. [Hz]	Acceleration [r.m.s. m/s ²]	Subjective response	Standard deviation
3	0.08	0.6	0.4	40	0.17	0.72	0.51
	0.17	1.51	0.65		0.8	1.95	0.81
	0.49	2.67	1.03		1.71	2.47	1.03
4	1	4.43	1.3	50	7.91	6.23	2.69
	0.13	0.7	0.55		0.08	0.17	0.18
	0.32	1.58	0.78		0.38	1.11	0.63
	0.5	2.5	0.72		3.98	3.68	1.3
5	1.26	4.06	1.48	63	19	7.46	2.9
	0.08	0.46	0.51		0.18	0.8	0.58
	0.23	1.49	0.8		0.85	1.61	0.87
6.3	1.07	4.55	1.25	80	1.88	2.52	1.09
	3	6.32	1.69		9.09	4.42	1.84
	0.14	1.35	0.71		0.07	0.18	0.2
	0.45	2.24	0.77		0.36	1.16	0.74
8	0.81	3.95	1.26	100	4.26	3.35	1.36
	2.58	6.67	1.65		22	6.62	2.09
	0.08	0.35	0.27		0.06	0.08	0.16
	0.28	2.21	0.81		0.78	1.52	0.67
10	1.75	4.78	1.18	125	1.84	1.85	0.9
	6	8.78	2.03		10.2	4.35	2.12
	0.15	0.84	0.57		0.06	0.12	0.18
	0.56	2.01	0.67		0.34	1.15	0.7
12.5	1.07	3.62	1.38	160	4.46	2.61	1.26
	3.92	6.31	1.41		25	5.25	2.65
	0.08	0.34	0.26		0.04	0.05	0.11
	0.3	1.35	0.61		0.64	1.22	0.72
16	2.15	5.17	1.59	200	1.62	2.18	1.05
	8	8.07	1.93		10.31	3.88	1.73
	0.16	0.69	0.37		0.06	0.1	0.18
	0.63	2.26	0.64		0.34	0.78	0.63
20	1.26	3.17	0.76	250	4.71	2.51	1.19
	5.02	6.86	2.25		27	4.19	2.35
	0.08	0.15	0.17		0.15	0.2	0.27
	0.34	1.5	0.72		1.41	1.4	0.9
25	2.87	4.46	1.3	315	2.98	1.99	1.24
	12	8.44	2.3		13.27	3.24	1.55
	0.17	0.52	0.35		0.4	0.4	0.45
	0.73	1.75	0.89		1.36	1.18	0.93
31.5	1.53	3.35	1.16	400	8.53	2.73	1.7
	6.69	6.1	1.9		0.8	0.65	0.61
	0.08	0.19	0.21		3.78	1.92	1.62
	0.36	1.06	0.56		6.35	2.19	1.31
	3.52	4.12	1.68				
	16	8.15	2.04				

The stepwise regression procedure was again employed to produce equal sensation curves for Borg subjective perceived intensity values from 0.5 to 8.0 obtained from the experiment ($n = 40$) because it again provided the best fit regression model with respect to the other regression procedures presented in chapter 6 ($n = 40$). Table 8.3 presents the goodness of fit statistics obtained for the regression model by means of the stepwise regression procedure implemented by Matlab software (Mathworks Inc., 2002). The same selection criteria were adopted to rate the quality of the fit of the correlation equation. The stepwise regression procedure provided a residual mean square (MSE) value of 0.073 and an adjusted coefficient of determination (R_a^2) value of 0.985.

[Table 8.3] Goodness of fit statistics obtained for overall data set ($n = 40$).

Regression method	Polynomial order	Residual mean square (MSE)	Adjusted coefficient of determination (R_a^2)	Number of regression coefficients
Stepwise procedure	6 th	0.073	0.985	12

For the complete group of 40 test participants the stepwise regression procedure produced a 6th order polynomial regression model with 12 regression coefficients. The best fit model was

$$\begin{aligned}
 S = & 3.8812 - 0.4091\log(f) + 2.3672\log(a) + 0.544\log(a)^2 - 0.218\log(f)^3 + \\
 & - 0.1063\log(f)^2\log(a) - 0.09\log(f)\log(a)^2 + 0.0436\log(a)^3 + 0.0469\log(f)^4 + \\
 & - 0.0004\log(f)^6 + 0.0003\log(f)^5\log(a) - 0.0003\log(f)^3\log(a)^3
 \end{aligned} \tag{8.1}$$

where S is the Borg CR10 subjective intensity value which is determined by the fitted model, f is the frequency in units of Hertz and a is the r.m.s. acceleration magnitude in units of meters per second squared.

Figure 8.1 presents the family of the equal sensation curves defined by equation 8.1, which was determined using sinusoidal vibration obtained data and the stepwise regression procedure. The equal sensation curves obtained for the complete group of 40

participants were not significantly different from those obtained in the previous experiment for the effect of gender which was described in chapter 6.

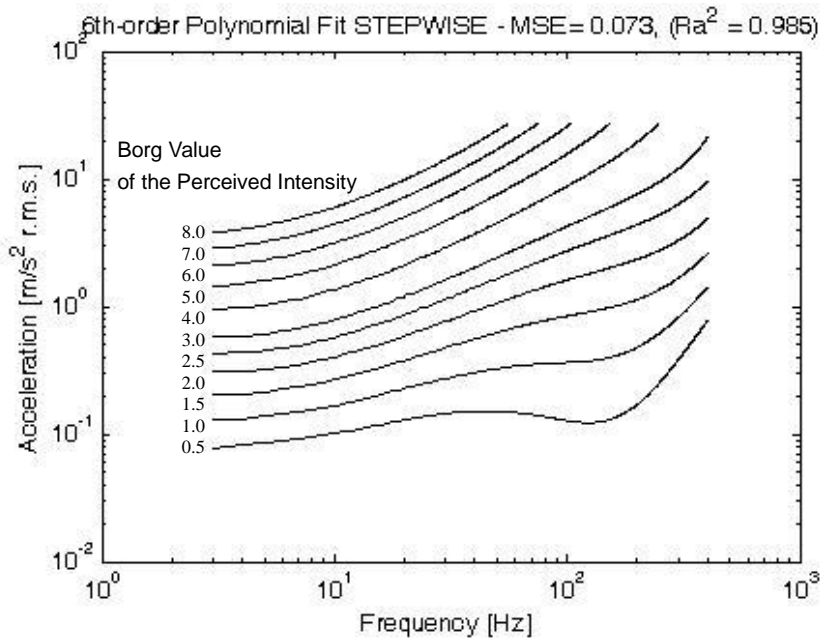


[Figure 8.1] Equal sensation curves for the complete group of 40 participants obtained for Borg subjective perceived intensity values from 0.5 to 8.0 using the regression formula obtained for sinusoidal vibration.

8.2.2.1 Results for the two test groups that were subdivided according to Physical Body Mass

Table 8.4 presents the mean and one standard deviation values obtained for each frequency and each amplitude for the light and heavy body mass groups consisting of 20 test participants respectively. The subjective response values of the light participants were generally higher than those of the heavy participants. Significant differences were found in Borg CR10 values at frequencies from 6.3 to 100 Hz obtained between the subjective responses of the light and heavy participants at a 5 % confidence level ($p < 0.05$).

Table 8.5 presents the goodness-of-fit statistics obtained for the regression models which were fit separately to the data of only the light participants ($n = 20$) and of only the heavy participants ($n = 20$) by means of the stepwise regression procedure. The model order which provided the best results for the complete dataset was applied also to

the data obtained for each individual body mass group. The stepwise regression procedure provided an *MSE* value of 0.147 and a value of 0.975 for R_a^2 for the light test participants, while it produced an *MSE* value of 0.06 and a value of 0.986 for R_a^2 for the heavy test participants.

[Table 8.4] Summary of the subjective response obtained separately for the light test participants data set (n = 20) and for the heavy test participants data set (n = 20) by means of Borg CR10 scale.

Freq. [Hz]	Acceleration [r.m.s. m/s ²]	Lighter		Heavier		Freq. [Hz]	Acceleration [r.m.s. m/s ²]	Lighter		Heavier	
		Borg	SD	Borg	SD			Borg	SD	Borg	SD
3	0.08	0.61	0.35	0.59	0.46	40	0.17	0.85	0.52	0.58	0.47
	0.17	1.72	0.68	1.3	0.56		0.8	2.3	0.86	1.61	0.59
	0.49	2.57	0.81	2.77	1.23		1.71	2.8	1.09	2.14	0.88
4	1	4.54	1.24	4.32	1.37	50	7.91	7.38	3.22	5.09	1.31
	0.13	0.66	0.59	0.73	0.52		0.08	0.16	0.16	0.18	0.2
	0.32	1.45	0.59	1.72	0.92		0.38	1.34	0.74	0.89	0.41
5	0.5	2.53	0.74	2.47	0.72	63	3.98	3.79	1.32	3.57	1.36
	1.26	3.8	1.18	4.33	1.72		19	8.61	3.46	6.32	1.6
	0.08	0.48	0.65	0.44	0.33		0.18	0.93	0.63	0.67	0.51
6.3	0.23	1.33	0.7	1.65	0.88	80	0.85	1.73	0.95	1.49	0.79
	1.07	4.68	1.31	4.42	1.22		1.88	2.79	1.3	2.24	0.76
	3	6.41	1.75	6.23	1.67		9.09	4.84	1.84	4	1.79
8	0.14	1.64	0.73	1.07	0.57	100	0.07	0.2	0.22	0.16	0.17
	0.45	2.4	0.63	2.08	0.88		0.36	1.29	0.77	1.03	0.71
	0.81	4.44	1.17	3.46	1.17		4.26	3.84	1.6	2.85	0.85
10	2.58	6.79	1.74	6.59	1.59	125	22	7	1.98	6.25	2.17
	0.08	0.45	0.29	0.25	0.21		0.06	0.08	0.15	0.09	0.18
	0.28	2.56	0.8	1.86	0.67		0.78	1.69	0.74	1.36	0.56
12.5	1.75	4.77	1.18	4.78	1.22	160	1.84	2.06	0.86	1.64	0.91
	6	9.42	2.19	8.14	1.68		10.2	5.07	2.56	3.64	1.29
	0.15	0.9	0.61	0.78	0.53		0.06	0.12	0.19	0.13	0.17
16	0.56	2.1	0.6	1.91	0.75	200	0.34	1.4	0.84	0.9	0.43
	1.07	4.17	1.46	3.08	1.09		4.46	2.79	1.35	2.43	1.16
	3.92	6.57	1.54	6.06	1.27		25	6	3.26	4.49	1.62
20	0.08	0.36	0.32	0.33	0.2	250	0.04	0.03	0.08	0.07	0.13
	0.3	1.6	0.63	1.1	0.48		0.64	1.27	0.77	1.17	0.69
	2.15	5.56	1.72	4.79	1.39		1.62	2.32	1.2	2.04	0.87
25	8	8.2	2.14	7.95	1.75	315	10.31	3.93	1.72	3.84	1.78
	0.16	0.79	0.42	0.59	0.29		0.06	0.09	0.18	0.11	0.18
	0.63	2.41	0.67	2.12	0.6		0.34	0.78	0.8	0.78	0.42
31.5	1.26	3.28	0.82	3.06	0.7	400	4.71	2.59	1.15	2.44	1.25
	5.02	7.35	2.53	6.37	1.86		27	4.91	2.92	3.48	1.33
	0.08	0.15	0.17	0.16	0.16		0.15	0.2	0.32	0.2	0.23
16	0.34	1.73	0.77	1.26	0.59	250	1.41	1.3	0.92	1.5	0.89
	2.87	4.63	1.49	4.29	1.1		2.98	2.06	1.42	1.92	1.05
	12	9.18	2.56	7.7	1.77		13.27	3.48	1.62	3.01	1.48
25	0.17	0.72	0.35	0.31	0.2	315	0.4	0.36	0.49	0.44	0.41
	0.73	2.06	0.9	1.44	0.78		1.36	1.04	0.97	1.31	0.9
	1.53	3.53	1.26	3.18	1.06		8.53	3.01	2.14	2.44	1.11
31.5	6.69	6.43	2.03	5.77	1.75	400	0.8	0.52	0.53	0.78	0.67
	0.08	0.22	0.24	0.16	0.17		3.78	1.99	2.04	1.85	1.11
	0.36	1.22	0.62	0.91	0.46		6.35	2.21	1.4	2.17	1.24
16	3.52	4.62	1.96	3.62	1.19	16	8.6	2.11	7.71	1.92	
	16	8.6	2.11	7.71	1.92						

[Table 8.5] Goodness of fit statistics obtained separately for the light participants data set (n = 20) and for the heavy participants data set (n = 20).

Regression method	Body mass	Polynomial order	Residual mean square (MSE)	Adjusted coefficient of determination (R_a^2)	Number of regression coefficients
Stepwise procedure	Light	6 th	0.147	0.975	12
	Heavy		0.06	0.986	12

For the light group of 20 test participants the stepwise regression procedure produced a 6th order polynomial regression model with 12 regression coefficients. The best fit model was

$$\begin{aligned}
 S = & 3.7106 + 0.5765\log(f) + 2.3673\log(a) + 0.5571\log(a)^2 - 0.2137\log(f)^3 + \\
 & - 0.1007\log(f)^2\log(a) - 0.0883\log(f)\log(a)^2 + 0.0537\log(a)^3 + 0.0442\log(f)^4 + \\
 & - 0.0004\log(f)^6 + 0.0003\log(f)^5\log(a) - 0.0003\log(f)^3\log(a)^3 \quad (8.2)
 \end{aligned}$$

For the heavy group of 20 test participants the stepwise regression procedure also produced a 6th order polynomial regression model with 12 regression coefficients. The best fit model was

$$\begin{aligned}
 S = & 4.0526 + 0.2414\log(f) + 2.3672\log(a) + 0.5309\log(a)^2 - 0.2222\log(f)^3 + \\
 & - 0.1119\log(f)^2\log(a) - 0.0918\log(f)\log(a)^2 + 0.0336\log(a)^3 + 0.0496\log(f)^4 + \\
 & - 0.0005\log(f)^6 + 0.0003\log(f)^5\log(a) - 0.0002\log(f)^3\log(a)^3 \quad (8.3)
 \end{aligned}$$

Figure 8.2 compares the two families of equal sensation curves obtained for the light test participants (n = 20) and the heavy test participants (n = 20). The light participants rated the subjective intensity generally higher than the heavy participants for the same vibration stimulus, especially in the frequency range from 6.3 to 100 Hz.

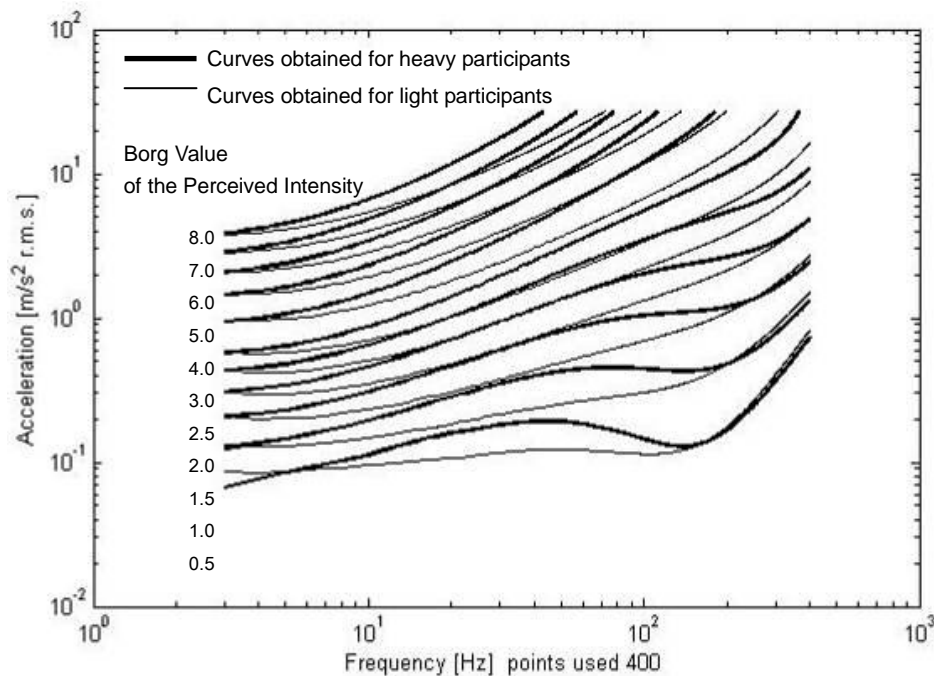


[Figure 8.2] Equal sensation curves obtained separately for the light test participants and the heavy test participants using the regression formulas obtained for sinusoidal vibration.

The differences were found to be similar to the results obtained using the sinusoidal vibration which was described in chapter 6 and the band-limited random vibration which was described in chapter 7. The equal sensation curves of the light participants resemble those of the female test participants, while those of heavy participants resemble those of the male test participants. In all three data sets the female or the light participants produced higher subjective response values than the male or the heavy participants, at frequencies above approximately 6.3 Hz.

8.3 Discussion

When the shapes of the equal sensation curves of Figure 8.2 are compared to those of Figure 7.5 from the two previous experiments it can be observed that the curves of the light test participants resemble those of the female subjects, while the curves of the

heavy test participants resemble those of the male subjects. As previously noted in the tests described in chapter 6 and 7, these differences were most obvious at frequencies in the range from approximately 6.3 to 100 Hz. For example, the subjective response of the light participants for the stimulus with amplitude of 1.0 m/s^2 r.m.s. and frequency of 30 Hz was approximately 2.5 on the Borg CR10 scale, while that of heavy participants for the same stimulus was approximately 2.0 on the Borg CR10 scale as shown in Figure 8.2.

The differences between the light participants and the heavy participants are partially supported by the previous results of Giacomini and Abrahams (2000), who suggested that the light test subjects perceived greater discomfort than the heavy test subjects in their arms for the 4 and 8 Hz test frequencies. Another similar indication supporting the current result is that the size and mass of the subject's hand and arm greatly affect energy absorption (Burström and Lundström, 1994). From the results of this experiment it can therefore be suggested that the equal sensation curves for steering wheel rotational vibration differ mainly due to differences in body size, rather than differences of gender.

8.4 Summary

Psychophysical response tests of 40 test participants (20 lighter and 20 heavier) were performed in a steering wheel rotational vibration simulator using the category-ratio Borg CR10 scale procedure for direct estimation of perceived vibration intensity. The equal sensation curves for steering wheel hand-arm rotational vibration were established using sinusoidal vibration stimuli by means of a stepwise regression procedure.

The results obtained from this experiment were not significantly different at a 5% confidence level ($p > 0.05$) from those obtained in the previous experiment for the effect of gender which was described in chapter 6. The subjective response values of the light participants were generally higher than those of the heavy participants, suggesting that the equal sensation curves of the light test participants resemble those of the female subjects, while the equal sensation curves of the heavy test participants resemble those of the male subjects.

Significant differences were found in Borg CR10 values at frequencies from 6.3 to 100 Hz between the light and heavy participants at a 5 % confidence level ($p < 0.05$). For example, the subjective response of the light participants for the stimulus with amplitude of 1.0 m/s^2 r.m.s. and frequency of 30 Hz was approximately 2.5 on the Borg CR10 scale, while that of heavy participants for the same stimulus was approximately 2.0 on the Borg CR10 scale. From the results of this experiment it can therefore be suggested that the equal sensation curves for steering wheel rotational vibration differ mainly due to differences in body size rather than differences of gender, and that the lighter individuals suffer greater subjective intensity for the same physical intensity of steering wheel vibration.

Chapter 9

Human Subjective Response to Steering Wheel Hand-Arm Vibration consisting of Real Road Stimuli

9.1 Introduction

Current evaluation methods for the estimation of human subjective response to steering wheel rotational vibration in the automotive industry are based on the use of either the original (unweighted) acceleration signal, the ISO W_h frequency weighted acceleration signal or the W_s frequency weighted acceleration signal. Automobile steering system designers and noise, vibration and harshness (NVH) experts apply one of these frequency weightings to the acceleration data which they measure at the steering wheel. However, the estimation using any one of the current evaluation methods applies to all the vibrational data in the measurement regardless of the magnitude of the vibration. Further, it has been continuously suggested by researchers (Morioka and Griffin, 2006; Ajovalasit and Giacomini, 2009) that the use of only one weighting is not optimal to estimate the human perception at all vibrational magnitudes. Therefore the question has been raised regarding how many frequency weightings are necessary for quantifying the

human perception of steering wheel hand-arm vibration.

From both previous research and from the findings described in this thesis it would appear that no single equal sensation curve, thus no single frequency weighting, would prove optimal at each point in time during a vibration measurement. In order to answer the question of how to best select frequency weightings, the research described in this chapter had the following objectives.

- To quantify the human subjective response to representative driving conditions, i.e. real steering wheel road vibration stimuli.
- To use a family of the equal sensation curves to obtain intensity estimates for the same set of representative driving conditions.
- To establish the level of correlation between the subjective responses and the vibration metric obtained by means of the frequency weighting.
- To use the test results to define recommendations regarding the choice of frequency weighting to use in automotive testing.

9.2 Laboratory Based Experimental Testing using Real Road Stimuli

A laboratory based experiment was carried out in order to obtain the subjective response to steering wheel hand-arm vibration using real road stimuli. The test facility was the same as described in this thesis in section 6.2.1. The test protocol was also the same as described in this thesis in section 6.3.3, except for the fact that the total elapsed time of the experiment was approximately 40 minutes rather than 60 minutes, due to use of only 21 road stimuli with three repetitions. The perceived intensity of subjective response was quantified by means of a Borg CR10 scale, as in the previous experiments which used sinusoidal or band-limited random vibration at the steering wheel.

9.2.1 Test Stimuli

The 21 road stimuli presented in chapter 5 can be considered to be typical of the automotive steering vibration problem, thus useful for the purpose of defining laboratory-based experiments which are representative of the automobile environment.

The selected group of stimuli respect the five criteria which were established in chapter 5 for the purpose of obtaining steering wheel vibrations for use in the study of the human perception of steering wheel hand-arm vibration.

Table 9.1 presents the global statistics of the 21 road stimuli. The root mean square (r.m.s.) amplitude levels are from a minimum of 0.056 m/s² for the tarmac surface to a maximum of 1.987 m/s² for the service surface. The kurtosis values are from 2.925 to 17.117 while the skewness values were from -0.22 to 1.209. The maximum crest factor (CF) was 5.95 and was for the low bump surface, while the minimum CF was 3.435 and was for the tarmac surface. The root mean quad (r.m.q.) values varied from a minimum of 0.074 m/s² for the tarmac surface to a maximum of 2.725 m/s² for the service surface.

[Table 9.1] Global statistical properties of the 21 steering wheel rotational road stimuli used the laboratory experimental testing.

Type of road	Global Statistics and Characteristics					
	Speed (km/h)	r.m.s. (m/s ²)	r.m.q (m/s ²)	Kurtosis	Skewness	Crest Factor
Service	80	1.987	2.725	3.85	0.169	4.182
Country lane	40	1.982	2.68	3.438	-0.048	3.534
Broken lane	40	1.858	2.529	3.799	-0.06	4.225
Broken concrete	50	1.673	2.286	3.194	0.013	3.458
UK City Street	90	1.394	2.047	5.119	-0.081	5.488
Harsh	40	1.32	2.523	17.117	1.047	6.886
Broken Road	40	1.218	1.715	3.935	-0.062	4.101
Cats-eye	100	1.132	1.578	4.677	-0.158	4.249
Motorway	110	1.132	1.514	3.066	0.073	3.706
Gravel	80	1.066	1.415	2.998	-0.055	3.687
Manhole Cover	60	0.966	1.328	3.263	0.011	4.282
Bump	60	0.916	1.569	10.164	0.158	6.324
Noise	80	0.711	0.955	2.925	-0.056	3.55
Expansion Joints	16	0.705	1.243	10.291	1.209	5.173
Stone on Road	20	0.665	1.16	11	-0.016	6.441
Low bump	50	0.315	0.509	8.064	-0.22	5.95
Cobblestone	30	0.278	0.377	3.18	0.069	4.336
Slabs	96	0.182	0.281	5.275	0.133	5.388
Concrete	96	0.117	0.164	3.461	-0.001	3.823
Coarse Asphalt	96	0.095	0.136	4.207	0.177	4.236
Tarmac	96	0.056	0.073	3.101	0.091	3.435

The 21 road surface stimuli were repeated three times in three single blocks, for a total of 63 assessment trials for each participant. The mean Borg CR10 values of the three repetitions, and the standard deviation Borg CR10 values, were calculated for each

stimulus. In order to minimize any possible bias resulting from learning or fatigue effects, the order of presentation of the test signals was randomised for each subject for each block. A break of 1 minute after the presentation of each block was used to reduce annoyance effects. A seven second stimulus duration was used so as to provide a vibrotactile stimulus which remained within human short-term memory (Sinclair and Burton, 1996), thus a stimulus which could be judged without reliance upon the long-term storage of stimuli information by the test participant. A complete session required approximately 40 minutes to complete with one participant. The test procedure adhered to the fixed phases and the mean time durations outlined in Table 9.2.

[Table 9.2] Steering wheel rotational vibration testing protocol.

Phase	Tasks Performed and Information Obtained
Consent form and questionnaire (~ 3 minutes)	The participant was asked to read the instructions and intended purpose of the experiments and to sign a consent form. Each subject also completed a questionnaire concerning age, height, mass, health and previous exposure to vibration.
Measurement of postural angles (~ 3 minutes)	The participant was asked to remove heavy clothing, watches and jewellery. Sitting posture angles were measured using a full circle goniometer and adjusted into the standard comfort range so as to minimise individual postural differences.
Preparation for test (~ 1 minute)	The participant was asked to wear ear protectors and to close eyes before gripping the steering wheel. The grip strength was suggested to be that required to drive an automobile over a country road. Once comfortable with the grip, the participant was asked to keep it constant during all tests.
Familiarization for test (~ 1 minutes)	The participant was given a verbal introduction to the experiment. The range of experimental frequencies and amplitudes applied so as to familiarise the subject with the stimuli.
Perception testing (~ 27 minutes)	The participant performed psychophysical tests of hand-arm vibration with the 21 road surface stimuli presented in random order so as to avoid learning or fatigue effects. The 21 road surface stimuli were repeated three times. Each stimulus lasted 7 seconds to each subject.
Breaks (~ 5 minutes)	A short break of 1 minute was made every 21 stimuli so as to avoid annoyance effects.

9.2.2 Test Subjects

A total of 40 university students and staff, 20 light participants and 20 heavy participants, were randomly chosen to participate in this experiment. The participants below 67 kg of body mass were classified into the light body mass group, while the

participants of more than 67kg of body mass were classified as belonging to the heavy body mass group. The value of 67 kg was used as a reference value because it was the median value of the subjects who participated in the experiment. Each body mass group consisted of 10 males and 10 females in order to avoid the possible effect of gender. A consent form and a short questionnaire were presented to each participant prior to testing, and information was gathered regarding their anthropometry, health and history of previous vibration exposures. Table 9.3 presents the mean value and the standard deviation of the age, height and mass of the light body mass group, the heavy body mass group, and of both groups together. A statistical t-test performed for the two test groups suggested significant differences in height and mass between the heavy participants and the light participants ($p < 0.05$), while no significant differences were found in age between the light participants and the heavy participants. All subjects declared themselves to be in good physical and mental health.

[Table 9.3] Mean and standard deviation summary statistics for the test participants.

Test Group	Age [years]	Height [m]	Mass [kg]
Light (n=20)	28.4 (5.9)	1.67 (0.07)	57.0 (6.2)
Heavy (n=20)	31.9 (5.5)	1.75 (0.11)	79.3 (11.8)
Total (N=40)	30.1 (5.9)	1.71 (0.10)	68.1 (14.6)

9.2.3 Results

Each of the 21 road surface stimuli was presented 3 times to each of the 40 test participants. Hence a total of 120 intensity estimates were collected for each driving condition. Table 9.4 presents the mean and standard deviation of the Borg CR10 perceived intensity of steering wheel vibration, as judged by the complete group of 40 test subjects for each of the road surfaces. Table 9.4 also reports the subjective ratings for the light body mass group ($n = 20$) and the heavy body mass group ($n = 20$) individually. The general tendency was that the human subjective response increased with increasing amplitude level of the stimuli, as expected from the results of the previous literature (Verrillo et al., 1969; Wos et al., 1988a; Ajovalasit and Giacomini, 2009) and from the experiments described in this thesis.

It can be observed from the test data that the perceived intensity values spread from 0.2 to 6.3 on the Borg CR10 scale, which represents the range of semantic expressions from

extremely weak to strong. This dynamic range of the perceived intensity for the 21 road surfaces is similar to that reported by Gnanasekaran et al. in their 2006 study of the subjective response to steering wheel vibration.

With regard to the difference between the subjective responses obtained from the light and heavy body mass groups shown in Table 9.4, the subjective responses of the light participants were generally higher than those of the heavy participants, which was consistent with the results of the equal sensation curves obtained for the light and heavy participants investigated in the previous chapters.

[Table 9.4] Mean and standard deviation Borg CR10 subjective intensity values obtained for the complete group of test participants and for the light and heavy subgroups, for each road stimuli.

Road surfaces	Unweighted r.m.s. [m/s ²]	Mean CR10 subjective response (Standard deviation)		
		Complete Group	Light	Heavy
Country lane	1.98	6.3 (1.8)	6.8 (2.0)	5.6 (1.4)
Service	1.99	5.9 (1.7)	6.3 (1.8)	5.2 (1.5)
Broken lane	1.86	5.2 (1.4)	5.5 (1.4)	4.6 (1.0)
Broken concrete	1.67	4.8 (1.4)	5.3 (1.6)	4.0 (0.7)
Bump	0.92	4.7 (1.3)	4.8 (1.3)	4.3 (1.3)
Harsh	1.32	4.6 (1.3)	4.8 (1.6)	4.2 (0.8)
UK City Street	1.39	4.5 (1.3)	4.9 (1.5)	3.9 (0.9)
Motorway	1.13	3.8 (1.0)	4.0 (1.3)	3.5 (0.7)
Broken Road	1.22	3.8 (1.0)	4.0 (1.3)	3.3 (0.5)
Manhole Cover	0.97	3.7 (1.1)	3.9 (1.3)	3.3 (0.8)
Expansion Joints	0.71	3.6 (1.0)	3.5 (1.1)	3.3 (0.9)
Cats-eye	1.14	3.4 (0.9)	3.6 (1.0)	3.0 (0.6)
Gravel	1.07	3.4 (0.8)	3.5 (1.0)	3.1 (0.6)
Stone on Road	0.67	3.0 (0.9)	3.0 (0.9)	2.8 (0.9)
Noise	0.71	2.7 (0.8)	2.7 (0.9)	2.6 (0.6)
Low bump	0.32	1.6 (0.8)	1.5 (0.8)	1.6 (0.8)
Cobblestone	0.28	1.3 (0.6)	1.3 (0.6)	1.3 (0.7)
Slabs	0.18	1.0 (0.7)	0.9 (0.6)	1.1 (0.7)
Concrete	0.12	0.8 (0.6)	0.8 (0.5)	0.9 (0.6)
Coarse Asphalt	0.10	0.4 (0.4)	0.4 (0.3)	0.4 (0.4)
Tarmac	0.06	0.2 (0.2)	0.1 (0.2)	0.2 (0.2)

9.3 Discussion

From the results presented in Table 9.4 it can be observed that the perceived intensity obtained using the 21 road surfaces produced a dynamic range of Borg CR10 scale from 0.2 to 6.3. The range can be split into three segments based on the different semantic expressions of Borg CR10 scale: weak (2.0) for the road surfaces from tarmac to low

bump, moderate (3.0) for the road surfaces from noise to motorway and strong (5.0) for the road surfaces from UK city street to country lane.

Considering the three intensity segments, it can be hypothesised that each may possibly require a different frequency weighting because the results presented in the previous chapters suggest that each level of Borg CR10 scale intensity produces an equal sensation curve of different shape in the frequency and amplitude plane. In practice, the three semantic segments may be connected to the road surface stimuli groups which can be divided based on the acceleration magnitude: low, medium and high. For example, the weak segment of Borg CR10 scale may be connected to the low amplitude group while the moderate segment may be connected to the medium amplitude group and the strong segment may be connected to the high amplitude group. Support for the hypothesis that each amplitude group may require a different frequency weighting can also be found in the previous research (Morioka and Griffin, 2006; Gnanasekaran et al., 2006; Ajovalasit and Giacomini, 2009) which have suggested that different frequency weightings are necessary to estimate human perception at different vibration magnitudes.

9.4 Frequency Weightings developed from the Equal Sensation Curves

In order to construct the frequency weightings from the equal sensation curves, the data of each equal sensation curve was first normalised to the lowest stimuli intensity found on the curve. The frequency weighting was then achieved by taking the reciprocal of each data point on the curve.

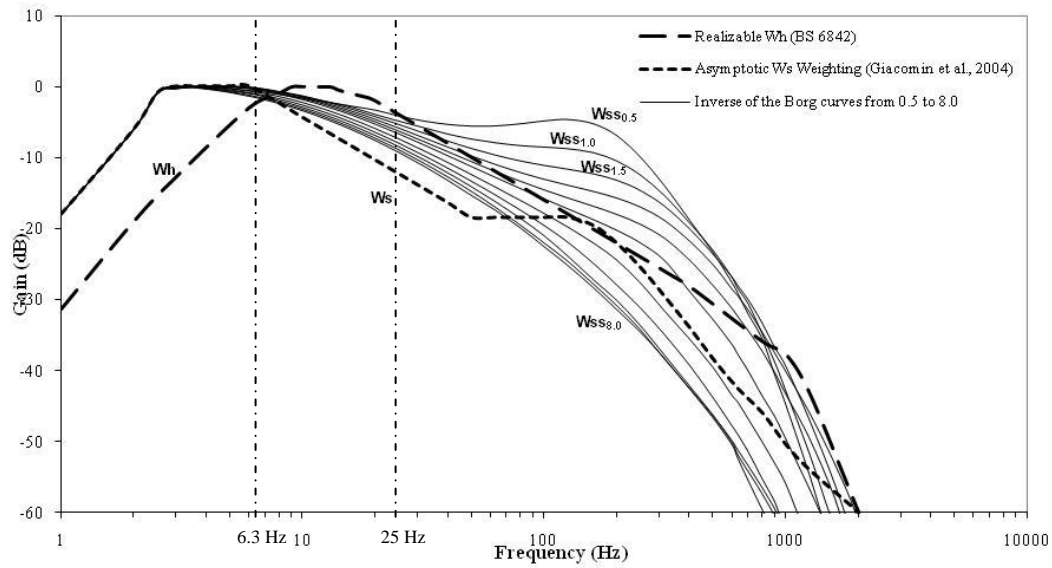
In order for the frequency weighting to accommodate a wide frequency range, extrapolation was performed from 400 Hz to 2000 Hz, which is the recommended frequency range limit for a test of hand-arm vibration as suggested by ISO 8041 (2005). The normalised values of each frequency weighting were extended with a slope of -20 dB per octave in the frequency range from 400 to 2000 Hz. For the extension at frequencies below 3Hz, a slope of -6 dB per octave was chosen based on the slope of the existing frequency weightings W_h (ISO 5349-1, 2001) and W_s (Giacomini et al., 2004) in the frequency range from 1 to 3 Hz. In summary, a total frequency bandwidth from 1 to 2000 Hz was obtained for use in filtering automotive vibration signals. The

frequency weightings were achieved, and checked to be within a 2% accuracy limit in terms of filter gain across the frequency range, within the LMS T-MON software (LMS International Inc., 2002). Appendix D of this thesis provides an example of the procedure which was used to develop each of the frequency weighting filters.

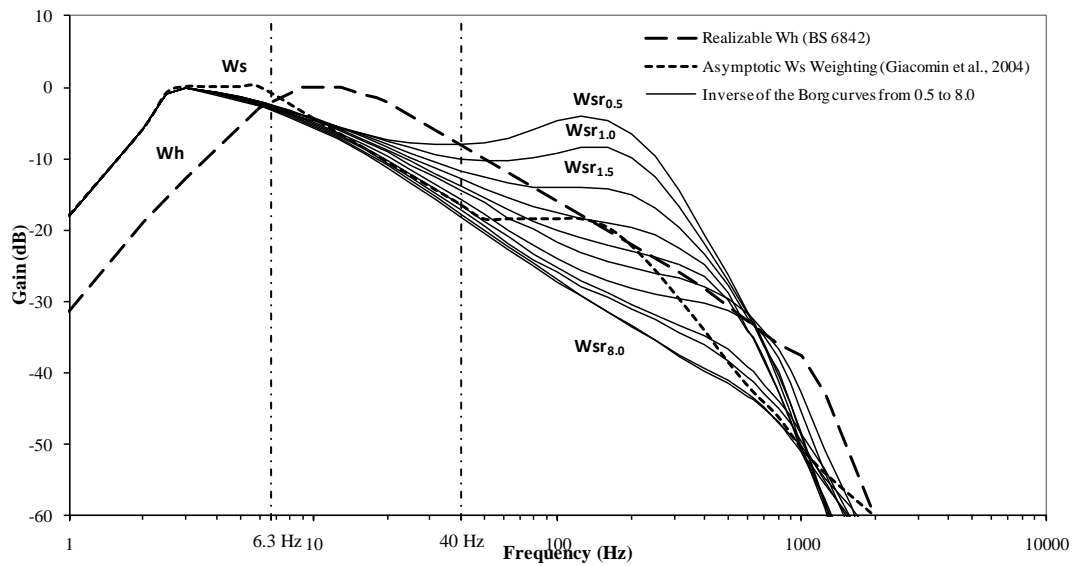
Figure 9.1 presents the frequency weightings which were obtained for the Borg CR10 intensity values of 0.5, 1.0, 1.5, 2.0, 2.5, 3.0, 4.0, 5.0, 6.0, 7.0 and 8.0. The frequency weighting which were defined based on the equal sensation curves from the tests which used sinusoidal stimuli are labelled W_{ss_n} , while those from tests which used random stimuli are labelled W_{sr_n} . The numeral suffixes 'n' in W_{ss_n} and W_{sr_n} indicate the Borg perceived intensity value ($n = 0.5, 1.0, 1.5, 2.0, 2.5, 3.0, 4.0, 5.0, 6.0, 7.0, 8.0$).

Figure 9.1 also compares the families of the W_{ss_n} and W_{sr_n} weightings with the existing W_h weighting and W_s weighting. Like the W_s frequency weighting, all curves of W_{ss_n} and W_{sr_n} have greater gains than the W_h weighting at frequencies below approximately 6.3 Hz. The W_{ss_n} weightings obtained from Borg CR10 0.5 to 3.0 (i.e. from $W_{ss_{0.5}}$ to $W_{ss_{3.0}}$) and the W_{sr_n} weightings obtained from Borg CR10 0.5 to 2.5 (i.e. from $W_{sr_{0.5}}$ to $W_{sr_{2.5}}$) also have greater gains than the W_h weighting at frequencies above approximately 25 Hz and 40 Hz, respectively. In contrast, the W_{ss_n} weightings obtained from Borg CR10 4.0 to 8.0 (i.e. from $W_{ss_{4.0}}$ to $W_{sr_{8.0}}$) and the W_{sr_n} weightings obtained from Borg CR10 3.0 to 8.0 (i.e. from $W_{sr_{3.0}}$ to $W_{sr_{8.0}}$) suggest a lower gain than the W_h weighting at frequencies above approximately 6.3 Hz.

Comparison of the newly defined frequency weightings to the standard W_h weighting suggests that the W_h weighting underestimates human perception of hand-arm vibration at frequencies below approximately 6.3 Hz and above approximately 25 Hz for the low subjective intensities below approximately Borg CR10 2.5. Further, the W_h weighting overestimates human perception of hand-arm vibration at frequencies above approximately 25 Hz for the high subjective intensities above approximately Borg CR10 3.0 or 4.0 for the W_{ss_n} and W_{sr_n} weightings, respectively.



(a)



(b)

[Figure 9.1] Comparisons the existing frequency weightings W_h (ISO 5349-1, 2001) and W_s (Giacomin et al., 2004) to the (a) W_{ss_n} and (b) W_{sr_n} frequency weightings obtained from the equal sensation curves using sinusoidal and band-limited random steering wheel rotational vibration respectively.

9.4.1 Estimates obtained by means of the Frequency Weightings

The LMS T-MON software digital filter implementations of all the frequency weightings W_h , W_s , W_{ss_n} and W_{sr_n} were used to filter the 21 steering wheel stimuli so as to obtain numerical estimates of the subjectively perceived intensity. Table 9.5 presents the r.m.s. acceleration magnitudes of the unweighted, the W_h weighted, the W_s weighted, and both the W_{ss_n} and W_{sr_n} weighted signals.

[Table 9.5] The r.m.s. acceleration magnitudes of the unweighted, the W_h weighted, the W_s weighted and both the W_{ss_n} and W_{sr_n} weighted signals along with the corresponding mean Borg CR10 subjective response value for the stimulus.

Road surfaces	Mean Perceived Intensity	Unweighted	W_h weighted	W_s weighted	W_{ss_n} weighted r.m.s.[m/s ²]											W_{sr_n} weighted r.m.s.[m/s ²]										
	[Borg value]	r.m.s.[m/s ²]	r.m.s.[m/s ²]	r.m.s.[m/s ²]	$W_{SS0.5}$	$W_{SS1.0}$	$W_{SS1.5}$	$W_{SS2.0}$	$W_{SS2.5}$	$W_{SS3.0}$	$W_{SS4.0}$	$W_{SS5.0}$	$W_{SS6.0}$	$W_{SS7.0}$	$W_{SS8.0}$	$W_{SR0.5}$	$W_{SR1.0}$	$W_{SR1.5}$	$W_{SR2.0}$	$W_{SR2.5}$	$W_{SR3.0}$	$W_{SR4.0}$	$W_{SR5.0}$	$W_{SR6.0}$	$W_{SR7.0}$	$W_{SR8.0}$
Country lane	6.3	1.98	1.22	0.75	1.20	1.14	1.11	1.07	1.04	1.01	0.97	0.92	0.88	0.85	0.83	0.86	0.81	0.78	0.76	0.74	0.73	0.70	0.68	0.66	0.65	0.63
Service	5.9	1.99	1.04	0.55	1.05	0.97	0.92	0.89	0.85	0.82	0.78	0.73	0.70	0.68	0.66	0.75	0.68	0.64	0.61	0.59	0.57	0.54	0.52	0.51	0.50	0.48
Broken lane	5.2	1.86	0.94	0.65	1.05	0.97	0.92	0.89	0.86	0.84	0.80	0.76	0.73	0.71	0.69	0.80	0.72	0.67	0.65	0.63	0.62	0.60	0.59	0.57	0.56	0.55
Broken concrete	4.8	1.67	0.80	0.44	0.89	0.80	0.75	0.71	0.68	0.66	0.62	0.58	0.55	0.53	0.51	0.65	0.57	0.52	0.49	0.47	0.45	0.43	0.41	0.40	0.39	0.38
Bump	4.7	0.92	0.60	0.37	0.57	0.55	0.54	0.53	0.51	0.50	0.48	0.45	0.44	0.42	0.41	0.40	0.39	0.39	0.38	0.37	0.37	0.35	0.34	0.33	0.33	0.32
Harsh	4.6	1.32	0.52	0.30	0.66	0.57	0.53	0.50	0.47	0.45	0.42	0.40	0.38	0.36	0.35	0.49	0.42	0.38	0.35	0.33	0.32	0.30	0.29	0.28	0.28	0.27
UK City Street	4.5	1.39	0.70	0.41	0.74	0.68	0.65	0.63	0.60	0.58	0.55	0.53	0.51	0.49	0.48	0.54	0.50	0.47	0.45	0.43	0.42	0.41	0.39	0.38	0.38	0.37
Motorway	3.8	1.13	0.54	0.31	0.59	0.53	0.50	0.47	0.45	0.44	0.41	0.39	0.38	0.36	0.35	0.46	0.39	0.35	0.33	0.32	0.31	0.30	0.29	0.28	0.27	0.27
Broken	3.8	1.22	0.45	0.32	0.51	0.47	0.45	0.44	0.42	0.41	0.39	0.37	0.36	0.35	0.34	0.38	0.35	0.33	0.32	0.32	0.31	0.30	0.29	0.28	0.28	0.28
Manhole Cover	3.7	0.97	0.48	0.26	0.53	0.48	0.45	0.43	0.41	0.39	0.37	0.35	0.33	0.32	0.31	0.38	0.34	0.31	0.29	0.28	0.27	0.26	0.25	0.24	0.23	0.23
Expansion Joints	3.6	0.71	0.38	0.28	0.41	0.39	0.38	0.37	0.36	0.35	0.34	0.32	0.32	0.31	0.30	0.31	0.30	0.29	0.28	0.28	0.27	0.27	0.26	0.26	0.25	0.25
Cats-eye	3.4	1.13	0.38	0.23	0.52	0.45	0.41	0.38	0.36	0.34	0.32	0.30	0.28	0.27	0.27	0.41	0.33	0.29	0.26	0.25	0.24	0.23	0.22	0.21	0.21	0.20
Gravel	3.4	1.07	0.37	0.32	0.56	0.48	0.45	0.42	0.40	0.39	0.37	0.36	0.35	0.34	0.33	0.47	0.39	0.34	0.32	0.31	0.31	0.30	0.29	0.29	0.28	0.28
Stone on Road	3.0	0.67	0.34	0.24	0.37	0.34	0.33	0.32	0.31	0.30	0.29	0.28	0.27	0.26	0.26	0.27	0.26	0.25	0.24	0.24	0.23	0.23	0.22	0.22	0.21	0.21
Noise	2.7	0.71	0.30	0.25	0.41	0.36	0.34	0.33	0.32	0.31	0.30	0.28	0.28	0.27	0.26	0.33	0.29	0.27	0.26	0.25	0.25	0.24	0.23	0.23	0.23	0.23
Low bump	1.6	0.32	0.16	0.10	0.16	0.15	0.15	0.14	0.14	0.13	0.13	0.12	0.12	0.11	0.11	0.12	0.11	0.11	0.10	0.10	0.10	0.09	0.09	0.09	0.09	0.09
Cobblestone	1.3	0.28	0.15	0.07	0.15	0.14	0.13	0.12	0.12	0.11	0.10	0.10	0.09	0.09	0.09	0.11	0.09	0.09	0.08	0.08	0.07	0.07	0.07	0.06	0.06	0.06
Slabs	1.0	0.18	0.10	0.06	0.10	0.09	0.09	0.09	0.08	0.08	0.08	0.07	0.07	0.07	0.07	0.07	0.07	0.06	0.06	0.06	0.06	0.06	0.06	0.06	0.05	0.05
Concrete	0.8	0.12	0.07	0.03	0.06	0.06	0.06	0.05	0.05	0.05	0.05	0.04	0.04	0.04	0.04	0.04	0.04	0.04	0.04	0.04	0.03	0.03	0.03	0.03	0.03	0.03
Coarse Asphalt	0.4	0.10	0.05	0.03	0.05	0.05	0.05	0.04	0.04	0.04	0.04	0.04	0.04	0.04	0.03	0.03	0.03	0.03	0.03	0.03	0.03	0.03	0.03	0.03	0.03	0.03
Tarmac	0.2	0.06	0.03	0.02	0.03	0.03	0.03	0.03	0.03	0.02	0.02	0.02	0.02	0.02	0.02	0.02	0.02	0.02	0.02	0.02	0.02	0.02	0.02	0.02	0.02	0.02

From Table 9.5 it can be observed that the W_{ss_n} and W_{sr_n} weighted acceleration magnitudes for the test road surfaces were generally lower than the W_h weighted acceleration magnitudes. This is due to the greater gain of the W_h weighting at frequencies from approximately 6.3 to 25 Hz.

From Table 9.5 it can also be observed that the subjectively perceived intensity estimates obtained using the W_{ss_n} weightings were generally higher than those obtained using the W_{sr_n} weightings. This is due to the higher gain of the W_{ss_n} weightings at frequencies from approximately 6.3 to 40 Hz.

9.4.2 Selecting the Frequency Weightings

In order to test the hypothesis of section 9.3 that different steering wheel amplitude groups may require different frequency weightings, a series of criteria for selecting frequency weightings was established. Table 9.6 presents a summary of the procedure which was adopted to determine the adequate frequency weighting filters for various amplitude magnitudes of the road surface stimuli by means of correlation analysis. The term adequate is here taken to mean "enough" or "satisfactory" for producing an estimate value which is highly correlated with subjective response.

[Table 9.6] Procedure used to define the adequate frequency weighting.

Step	Procedure
1	The frequency distribution of each steering wheel acceleration signal was subdivided into three intervals based on the use of the characteristics transition points defined by Giacomini et al., (2004). A check was then performed so as to establish which intervals contained energy which was above the threshold of perception.
2	The group of 21 steering wheel acceleration signals was ordered from the lowest r.m.s. to the highest r.m.s. based on the energy content in the frequency range where the signal was mostly greater than the threshold of perception.
3	The group of 21 steering wheel acceleration signals were subdivided into three amplitude groups of "low", "medium" and "high" based on the semantic descriptor of the Borg CR10 scale of subjective perceived intensity, as calculated for the frequency range where the signal was mostly greater than the threshold of perception.
4	Each of the frequency weightings W_{ss_n} and W_{sr_n} was used to filter each of the 21 steering wheel acceleration signals, and a cross-correlation coefficient was calculated between the numerical r.m.s. values provided by the frequency weighting and the experimentally determined Borg CR10 value for the same steering wheel stimuli.

Figure 9.2 compares the amplitude range (minimum amplitude, mean amplitude and

maximum amplitude) of the 21 road surface stimuli with the equal sensation curves obtained using random vibration. From Figure 9.2 it can be noted that the greatest part of the vibrational energy measured at the steering wheel was located in the frequency range from 6.3 to 50 Hz. Further, it can also be noted that the equal sensation curves exhibit changes in shape, due to the changing mechanisms of human hand-arm perception, at approximately the same two frequencies. The range from 6.3 to 50 Hz can therefore be considered the critical interval of the steering vibration perception problem. Finally, it can also be noted that for many roads the vibrational energy above approximately 50 Hz is lower than the threshold curve of human perception, suggesting that the inclusion of the steering wheel energy above 50 Hz in estimations of subjective intensity may prove misleading.

Table 9.7 presents the r.m.s. value of each road surface signal for each frequency range. As can be seen in both Figure 9.2 and Table 9.7 the vibrational energy of the road surface stimuli is uneven across the frequency range from 3 to 400 Hz. For example, 60% of vibrational energy is located in the frequency range from 6.3 to 50 Hz while only 17% and 23% of the energy are located in the frequency ranges from 0 to 6.3 Hz and from 50 to 250 Hz, respectively.

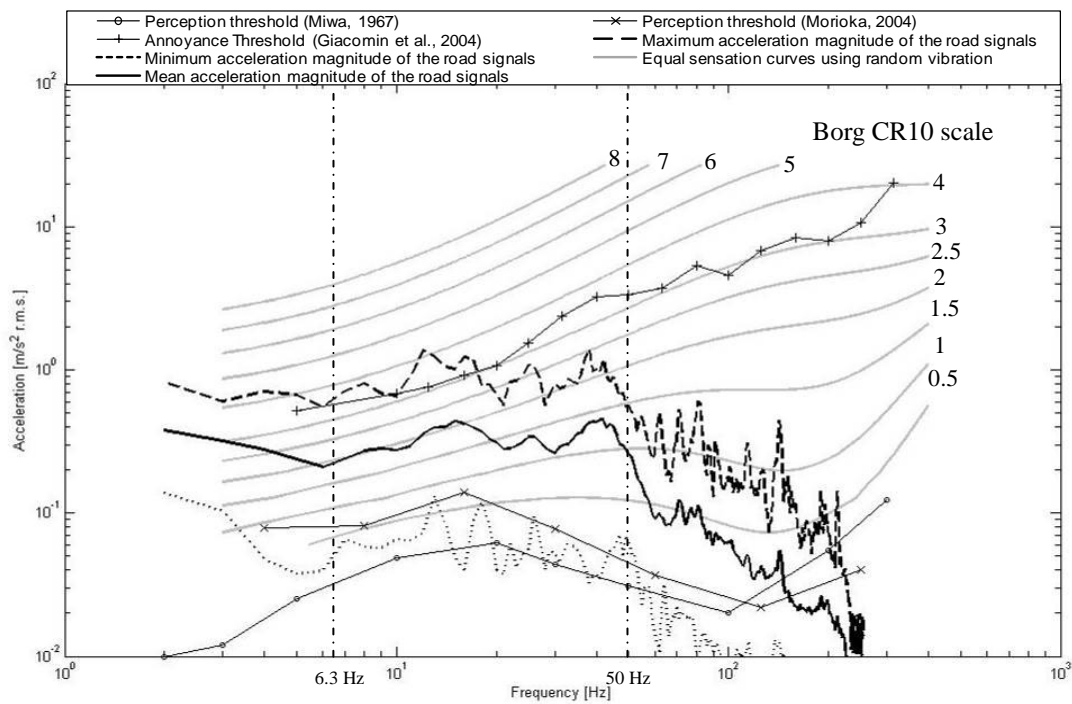


[Figure 9.2] Comparison of the amplitude frequency range of the steering wheel road vibration signals, the equal sensation curves obtained using band-limited random signals and the perception threshold curves defined by Miwa (1967) and by Morioka (2004).

[Table 9.7] The r.m.s. acceleration values of the steering wheel acceleration signals in each frequency range.

Amplitude Group	Road name	Subjective response	R.M.S. value (m/s ²)			
			Global	Frequency range I [0 – 6.3 Hz]	Frequency rangell [6.3 – 50 Hz]	Frequency rangelll [50 – 250 Hz]
Low	Tarmac	0.2	0.06	0.01	0.03	0.02
	Coarse Asphalt	0.4	0.1	0.02	0.06	0.02
	Concrete	0.8	0.12	0.02	0.07	0.03
	Slabs	1	0.18	0.04	0.11	0.03
	Cobblestone	1.3	0.28	0.03	0.20	0.05
	Low bump	1.6	0.32	0.08	0.19	0.05
Medium	Expansion joints	3.6	0.71	0.16	0.30	0.25
	Stone on road	3	0.67	0.17	0.37	0.13
	Noise	2.7	0.71	0.19	0.38	0.14
	Gravel	3.4	1.07	0.21	0.46	0.40
	Cats-eye	3.4	1.13	0.18	0.58	0.37
	Motorway	3.8	1.13	0.16	0.60	0.37
	Manhole cover	3.7	0.97	0.17	0.63	0.17
High	Bump	4.7	0.92	0.17	0.67	0.08
	Broken road	3.8	1.22	0.32	0.65	0.25
	Harsh	4.6	1.32	0.20	0.84	0.28
	UK city street	4.5	1.39	0.30	0.79	0.30
	Broken concrete	4.8	1.67	0.19	1.10	0.38
	Broken lane	5.2	1.86	0.33	0.98	0.55
	Service	5.9	1.99	0.27	1.32	0.40
Country lane	6.3	1.98	0.31	1.33	0.34	
Mean [m/s ² r.m.s.]				0.16	0.56	0.22
Standard deviation				0.1	0.4	0.16
% energy				17%	60%	23%

The 21 road surface stimuli were sorted by r.m.s. amplitude magnitude of the vibrational energy in the frequency range from 0 to 50 Hz, which was above the threshold of perception, as shown in Figure 9.2. The sorted stimuli were then subdivided into three amplitude groups which were low (below 0.46 m/s² r.m.s.), medium (between 0.46 and 0.8 m/s² r.m.s.) and high (above 0.8 m/s² r.m.s.) based on the semantic descriptor of the Borg CR10 scale of subjective perceived intensity as shown in Table 9.7.

Correlation analysis was performed between the weighted r.m.s. values of the 21 road surface stimuli and the subjective responses for each amplitude group, in order to determine the adequate frequency weighting filter. The filter was sought which produced the most accurate estimation, statistically, of the subjective response for each amplitude group.

Matlab software (Mathworks Inc., 2002) was implemented to establish the level of correlation between the two metrics. The coefficient of determination R^2 and the residual mean square MSE were calculated at a 1% confidence level. Table 9.8 presents the correlation coefficient results. The results suggest:

- the $W_{SS_{1.5}}$ and $W_{SR_{1.0}}$ filters provided the best weightings for the low amplitude group of steering vibration signals, providing MSE values of 0.019 and 0.021 respectively, and the same R^2 value of 0.99,
- the $W_{SS_{2.0}}$ and $W_{SR_{1.5}}$ filters provided the best weightings for the medium amplitude group of steering vibration signals, providing MSE values of 0.03 and 0.07 respectively, and R^2 values of 0.92 and 0.84 respectively,
- the $W_{SS_{2.5}}$ and $W_{SR_{2.0}}$ filters provided the best weightings for the high amplitude group of steering vibration signals, providing MSE values of 0.119 and 0.13 respectively, and R^2 values of 0.91 and 0.90 respectively.

[Table 9.8] The correlation coefficients results obtained between the weighted r.m.s. values of the road signals by both (a) the W_{SS_n} and (b) the W_{SR_n} filters and the subjective responses for each amplitude level group.

(a) Correlation coefficients results based on the W_{SS_n} frequency weightings

Amplitude level		Correlation coefficients ($p < 0.01$)										
		$W_{SS_{0.5}}$	W_{SS_1}	$W_{SS_{1.5}}$	W_{SS_2}	$W_{SS_{2.5}}$	W_{SS_3}	W_{SS_4}	W_{SS_5}	W_{SS_6}	W_{SS_7}	W_{SS_8}
Low	R^2	0.98	0.98	0.99	0.99	0.98	0.98	0.98	0.98	0.98	0.98	0.98
	MSE	0.022	0.02	0.019	0.02	0.02	0.02	0.02	0.02	0.021	0.021	0.022
Medium	R^2	0.81	0.89	0.92	0.92	0.91	0.91	0.88	0.86	0.84	0.82	0.8
	MSE	0.07	0.04	0.033	0.03	0.034	0.04	0.05	0.06	0.06	0.07	0.08
High	R^2	0.87	0.9	0.91	0.91	0.91	0.91	0.9	0.9	0.9	0.9	0.89
	MSE	0.16	0.14	0.13	0.123	0.119	0.124	0.13	0.13	0.13	0.13	0.14

(b) Correlation coefficients results based on the W_{SR_n} frequency weightings

Amplitude level		Correlation coefficients ($p < 0.01$)										
		$W_{SR_{0.5}}$	W_{SR_1}	$W_{SR_{1.5}}$	W_{SR_2}	$W_{SR_{2.5}}$	W_{SR_3}	W_{SR_4}	W_{SR_5}	W_{SR_6}	W_{SR_7}	W_{SR_8}
Low	R^2	0.99	0.99	0.99	0.99	0.98	0.98	0.98	0.98	0.98	0.98	0.98
	MSE	0.023	0.021	0.022	0.022	0.023	0.024	0.03	0.03	0.03	0.03	0.03
Medium	R^2	0.59	0.79	0.84	0.84	0.83	0.81	0.78	0.75	0.72	0.70	0.68
	MSE	0.13	0.09	0.07	0.08	0.09	0.10	0.12	0.13	0.14	0.15	0.15
High	R^2	0.85	0.89	0.89	0.9	0.9	0.89	0.89	0.89	0.88	0.88	0.88
	MSE	0.21	0.15	0.14	0.13	0.14	0.14	0.15	0.15	0.16	0.16	0.16

* R^2 : Coefficient of determination, ** MSE : Residual mean square.

Inspection of Figure 9.2 suggests that the frequency weightings from Borg value 1 to 2.5 have amplitude values which are similar to the mean amplitude values of the 21

road spectra used for the analysis. A possible explanation of the high correlation of these frequency weightings is therefore the fact that they were determined using test signals which had similar energy levels to the 21 steering wheel road vibration stimuli, thus leading to a similar degree of nonlinearity in the human psychophysical response.

9.5 Summary

A psychophysical response test of 40 participants (20 light and 20 heavy participants) was performed using the Borg CR10 scale procedure consisting of the 21 road surface stimuli obtained from the road tests described in chapter 5. The test results suggested that the perceived intensity values were from a minimum of 0.2 Borg value for the tarmac road surface to a maximum of 6.3 Borg value for the country lane road surface.

From the results the subjectively perceived intensity of the 21 road surfaces could be classified as falling into one of three semantic regions of the Borg CR10 scale: weak (2.0), moderate (3.0) and strong (5.0). It was hypothesised that each semantic region would benefit from the use of a different frequency weighting because the results presented in the previous experiments suggested that each equal sensation curve of the Borg CR10 scale had a significantly different shape in the frequency and amplitude plane. In practice, the three semantic segments can be associated with groups of road surfaces which are divided based on the steering wheel acceleration magnitude: low, medium and high.

Frequency weightings were defined based on the results obtained from the psychophysical tests which used sinusoidal vibration and were labelled as the W_{ss_n} frequency weightings. Frequency weightings were also defined based on the results obtained from the psychophysical tests which used random vibration and were labelled as the W_{sr_n} frequency weightings. The numeral suffixes 'n' in W_{ss_n} and W_{sr_n} denote the Borg values of perceived intensity ($n = 0.5, 1.0, 1.5, 2.0, 2.5, 3.0, 4.0, 5.0, 6.0, 7.0, 8.0$).

Numerical estimates of the human subjective response to the steering wheel stimuli were obtained by passing the 21 road surface stimuli through the W_h , W_s , W_{ss_n} and W_{sr_n} frequency weightings. Both the W_{ss_n} and W_{sr_n} weighted acceleration magnitudes for the test road surfaces were generally lower than the W_h weighted acceleration

magnitudes. This was due to the lower gains indicated by the W_h weighting at frequencies from approximately 6.3 to 25 Hz. The subjectively perceived intensity estimates obtained using the W_{ss_n} weightings were generally higher than those obtained using the W_{sr_n} weightings due to the higher gain of the W_{ss_n} weightings from approximately 6.3 to 40 Hz.

A method was proposed for selecting an adequate frequency weighting which was based on correlation analysis. The 21 road surface stimuli were split into three frequency segments based on the transition points (6.3 and 50 Hz) of the hand-arm system (Giacomin et al., 2004). The frequency range from 0 to 50 Hz was chosen for use in correlation analysis because the vibrational energy for most of the roads was lower than the human perception threshold above approximately 50 Hz. The 21 road surface stimuli were sorted by the amplitude magnitude in the frequency range from 0 to 50 Hz, and subdivided into three amplitude groups based on the semantic descriptor of the Borg CR10 scale of subjective perceived intensity which were the low (below 0.46 m/s^2 r.m.s.), medium (between $0.46 \sim 0.8 \text{ m/s}^2$ r.m.s.) and high (above 0.8 m/s^2 r.m.s.).

The level of correlation was calculated between the Borg CR10 subjective responses obtained from the psychophysical experiment and the numerical estimates obtained using both the W_{ss_n} and the W_{sr_n} frequency weightings when filtering each of the 21 steering wheel stimuli. For the low amplitude group the $W_{ss_{1.5}}$ and the $W_{sr_{1.0}}$ weightings provided the highest correlation to the subjective responses while the $W_{ss_{2.0}}$ and the $W_{sr_{1.5}}$ weightings provided the highest correlation for the medium amplitude group and the $W_{ss_{2.5}}$ and the $W_{sr_{2.0}}$ weightings provided the highest correlation for the high amplitude group. The possible explanation to support the correlation results is that the vibrational energy of the road surface stimuli was close, statistically, to the acceleration amplitude of the equal sensation curves in the frequency range from 0 to 50 Hz.

Chapter 10

Conclusions and Recommendations for Future Research

10.1 Summary of the Research Findings

The experimental activities described from chapter 6 to chapter 9 of this thesis were performed in order to answer questions about the quantification of the human subjective response to automotive steering wheel vibration, and to use the findings to define a test method for automotive steering wheel hand-arm vibration. This chapter summarises the main findings and attempts to provide answers to the questions posed in chapter 1 in light of the experimental results.

- How do the subjective responses change when the frequency changes?

In all of the tests which were performed the human subjective responses suggest that the human sensitivity decreases when the frequency increases, suggesting a lower perceived intensity at higher frequencies, as expected from psychophysical theory (Gescheider, 1997) and from previous research (Miwa, 1967; Reynolds et al., 1977; Giacomini et al.,

2004; Amman et al., 2005; Morioka and Griffin, 2006). The results also suggest that the equal sensation curves are characterised by a dip behaviour in the vicinity of 100 Hz, similar to the well known response of the Pacinian mechanoreceptors (Verrillo, 1966; Reynolds et al., 1977).

- How do the subjective responses change when the amplitude changes?

In all of the tests which were performed the subjective response magnitude increased when the physical intensity of the vibration increased, which is consistent with the results from previous research (Verrillo et al., 1969). The shape of the equal sensation curves share some similarities with the behaviour of the well-known equal loudness contours for hearing (Zwicker and Fastl, 1990), with the curves becoming flatter and more linear with increases in the vibration amplitude.

- How nonlinear is the human response?

The equal sensation curves obtained from the present research suggest a nonlinear dependency on both the frequency and the amplitude of the test stimulus. At low perceived intensities from 0.5 (just noticeable) to 1.0 (very weak) of Borg CR10 scale the equal sensation curves were found to resemble the general shape of the vibrotactile perception threshold curves of the hand. As the perceived intensity increased towards the maximum value of 8.0, the equal sensation curves assumed a more uniform shape, resembling the annoyance threshold for the hand-arm system defined by Reynolds et al. (1977).

- Is the subjective response dependent on the signal type?

The results obtained in this research suggest that the subjective responses obtained from band-limited random vibration stimuli were generally steeper in the shape of the equal sensation curves than those obtained using sinusoidal vibration stimuli. This tendency in the shape of the equal sensation curves was similar to the behaviour noted by Reynolds et al. (1977). The results also suggest that the equal sensation curves obtained using random vibration produced deeper dips in the vicinity of 100 Hz than those obtained

using sinusoidal vibration at acceleration levels below approximately 1.0 m/s^2 r.m.s.. This tendency in the shape of the equal sensation curves was similar to the results of Miwa (1969). These differences may be due to the characteristics of random vibration which produced generally higher crest factors than the sinusoidal vibration because the crest factor values of band-limited random vibration used in the experiment were generally in the range from 2.4 to 8.4, which was similar to the values of the real road stimuli which were described in chapter 5.

- Is the subjectively perceived intensity for males and females the same when the steering wheel vibration is the same?

From the results of the equal sensation curves obtained separately for each gender it can be seen that the females provided higher perceived intensity values than the males for the same physical stimulus at most frequencies. At frequencies above approximately 20 Hz the equal sensation curves for the female test group are characterised by a flatter shape than those obtained for the male test group, whereas at frequencies below approximately 20 Hz a similar shape was found for both groups. Gender differences were more marked at acceleration amplitudes above approximately 1.0 m/s^2 r.m.s.. These differences were expected from the previous research results of Verrillo (1979) who suggested that vibratory stimuli at suprathreshold levels are felt more intensely by females than by males, and by those of Neely and Burström (2006) who suggested that females report higher levels of physical intensity and discomfort than males. Similar indications can also be found in the study of steering wheel vibration induced fatigue performed by Giacomini and Abrahams (2000), which found that females reported greater arm region discomfort than males, and by the questionnaire-based investigation of Giacomini and Screti (2005) which found that female drivers reported higher discomfort responses than male drivers for the hand-arm region. However, it was not possible from the results to definitively establish whether the differences are sensory or, instead, biomechanical in nature, because the male test participants differed from the female participants in terms of their body mass ($p < 0.05$). The equal sensation curves for steering wheel rotational vibration obtained separately for each body mass test group (light and heavy body mass groups) suggested that the possibility of the cause being due to physical body size rather than gender itself because the equal sensation curves of the

light participants resemble those of the female test participants while those of heavy participants resemble those of the male test participants.

- Is the subjectively perceived intensity for light and heavy individuals the same when the steering wheel vibration is the same?

The results obtained from all the experiments which involved both the light ($n = 20$) and the heavy ($n = 20$) test participants suggest that the subjective responses of the light test participants were greater than those of the heavy test participants, especially in the frequency range from approximately 6.3 to 100 Hz ($p < 0.05$). This tendency was found using the sinusoidal vibration which was reported in chapter 6 and also the band-limited random vibration which was reported in chapter 7. The differences between the light participants and the heavy participants are partially supported by the previous results of Giacomini and Abrahams (2000), who suggested that the light test subjects perceived greater discomfort than the heavy test subjects in their arms for the 4 and 8 Hz test frequencies. Another similar indication supporting the current result is that the size and mass of the subject's hand and arm greatly affect energy absorption (Burrström and Lundström, 1994). From the results of all the experiments which are described in this thesis it can be suggested that the equal sensation curves for steering wheel rotational vibration differ mainly due to differences in body size, rather than differences of gender, and that the lighter individuals suffer greater subjective intensity for the same physical intensity of steering wheel vibration.

- How many frequency weightings are necessary for quantifying human perception of steering wheel hand-arm vibration?

From the results obtained from the experiment which was described in chapter 9, the subjectively perceived intensity of the 21 road surfaces could be classified as falling into one of three semantic regions of the Borg CR10 scale. The three regions were: weak (2.0), moderate (3.0) and strong (5.0). It is hypothesised by the author that each semantic region would benefit from the use of a different frequency weighting because the results presented in the previous experiments suggested that each equal sensation curve of Borg CR10 scale produces significantly different shape in the frequency and

amplitude plane. In practice, the three semantic segments can be associated with groups of road surfaces which are divided based on the steering wheel acceleration magnitude: low, medium and high. For example, the weak segment of Borg CR10 scale may be associated with the low amplitude group while the moderate segment may be associated with the medium amplitude group and the strong segment may be associated with the high amplitude group. The hypothesis that different amplitude groups may require different frequency weightings is supported by previous studies (Morioka and Griffin, 2006; Gnanasekaran et al., 2006; Ajovalasit and Giacomini, 2009) which have suggested that different frequency weightings are necessary to estimate the human perception at different vibration magnitudes.

The 21 road surface stimuli were split into three frequency segments based on the transition points (6.3 and 50 Hz) of the hand-arm system (Giacomini et al., 2004). The frequency range from 0 to 50 Hz was chosen for use in the correlation analysis because the vibrational energy for most of the roads was lower than the human perception threshold above approximately 50 Hz. The 21 road surface stimuli were sorted by the amplitude magnitude in the frequency range from 0 to 50 Hz, and subdivided into three amplitude groups based on the semantic descriptor of the Borg CR10 scale of subjective perceived intensity which were the low (below 0.46 m/s^2 r.m.s.), medium (between $0.46 \sim 0.8 \text{ m/s}^2$ r.m.s.) and high (above 0.8 m/s^2 r.m.s.).

The level of correlation was calculated between the Borg CR10 subjective responses obtained from the psychophysical experiment and the numerical estimates obtained using both the W_{ss_n} and the W_{sr_n} frequency weightings. For the low amplitude group the $W_{ss_{1.5}}$ and the $W_{sr_{1.0}}$ weightings provided the highest correlation to the subjective responses, while the $W_{ss_{2.0}}$ and the $W_{sr_{1.5}}$ weightings provided the highest correlation for the medium amplitude group and the $W_{ss_{2.5}}$ and the $W_{sr_{2.0}}$ weightings provided the highest correlation for the high amplitude group. The possible explanation to support the correlation results is that the vibrational energy of the road surface stimuli was similar (close) to the acceleration amplitude of the equal sensation curves in the frequency range from 0 to 50 Hz for those Borg CR10 values.

From the results of correlation analysis it was suggested that at least three frequency weightings may be necessary to estimate the subjective intensity for road surface stimuli.

10.2 Recommended Test Protocol for Evaluating Automotive Steering Wheel Rotational Vibration

Current evaluation methods used to estimate the human subjective response to steering wheel rotational vibration in the automotive industry are based on the use of either the original (unweighted) acceleration signal, the ISO W_h frequency weighted acceleration signal or the W_s frequency weighted acceleration signal. Automobile steering system designers and noise, vibration and harshness (NVH) experts apply one of these frequency weightings to the acceleration data which they measure at the steering wheel. However, the estimation using any one of the current evaluation methods applies to all the vibrational data in the measurement regardless of the magnitude of the vibration. Further, it has been continuously suggested by researchers (Morioka and Griffin, 2006; Ajovalasit and Giacomini, 2009) that only one weighting is not optimal to estimate the human perception at all vibrational magnitudes. Therefore this section introduces the recommended test protocol for evaluating automotive steering wheel rotational vibration based on the research findings in the present study.

Figure 10.1 presents the test method developed in the present research study. The steering wheel acceleration can be measured by means of a vibration level meter and an accelerometer. The measurement point is suggested to be on the surface of the steering wheel at the 60° position (two o'clock position) with respect to top centre, which is a typical grip position of the driver's hand (Giacomini and Gnanasekaran, 2005). The accelerometer at the steering wheel measurement position should be fixed in such a way as to guarantee sufficient coupling stiffness across the complete frequency range of the intended vibration measurement. An aluminium clamp and mounting screws are often used for this purpose. The acceleration signals can be stored using the vibration level meter. The sampling rate for the acceleration measurements should be chosen to be at least twice the maximum frequency of interest.

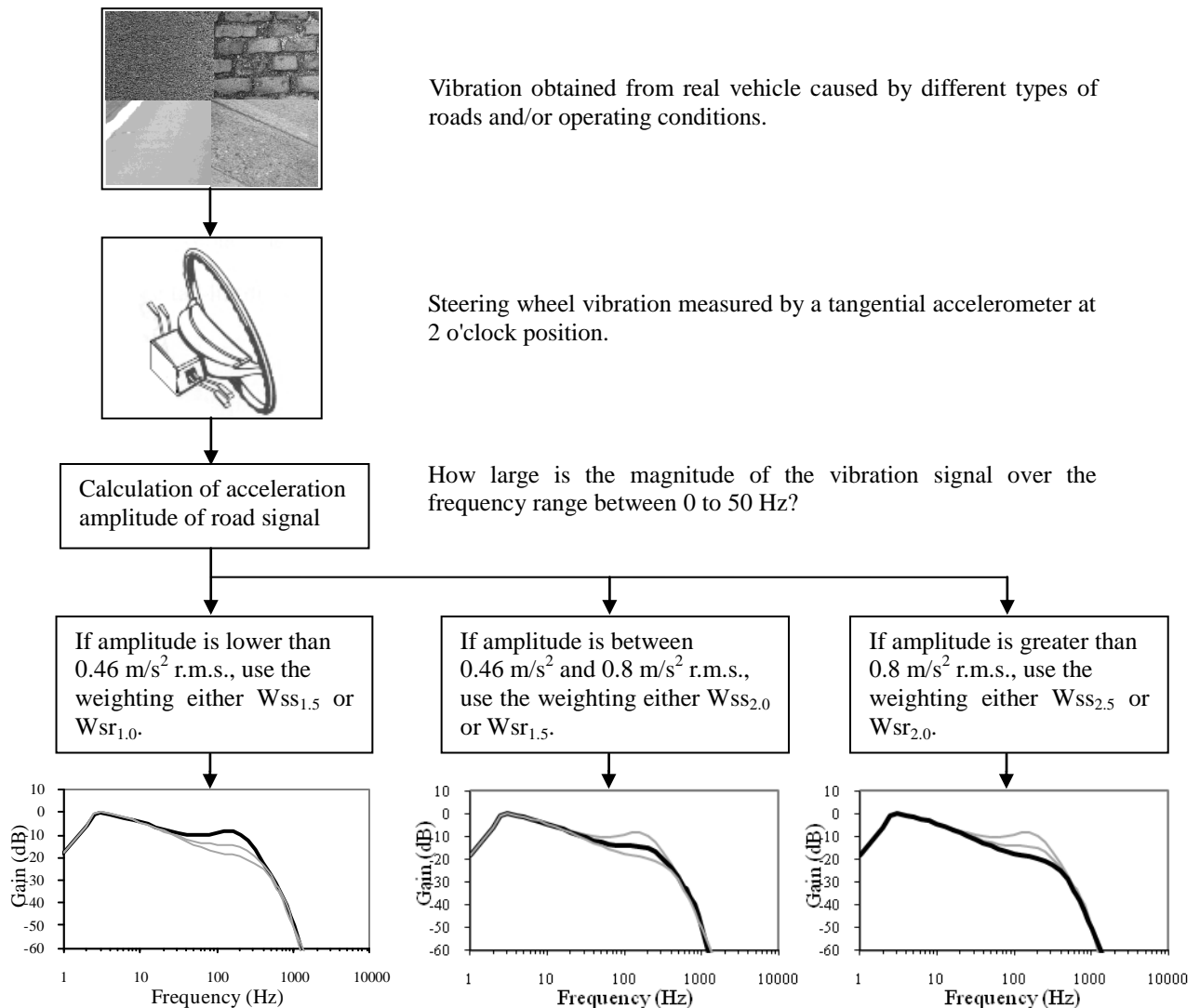


[Figure 10.1] Test method for evaluating steering wheel vibration in automobiles.

Based on the r.m.s. value of the signal in the frequency range from 0 to 50 Hz the signals can be subdivided into three amplitude level groups. The weighted values of subjective response to steering wheel rotational vibration are obtained by passing the signals through either the $W_{ss1.5}$ or the $W_{sr1.0}$ frequency weighting filters for the low, either the $W_{ss2.0}$ or the $W_{sr1.5}$ frequency weighting filters for the medium and either $W_{ss2.5}$ or the $W_{sr2.0}$ frequency weighting filters for the high amplitude group in the case of the present research study.

10.3 Suggested Future Research

The test method proposed in the present research study was developed for the purpose of providing a more accurate estimation of the human subjective response to steering wheel hand-arm vibration, which changes nonlinearly according to vibrational intensity and frequency (Ajovalasit and Giacomini, 2009). Given the nonlinearity of the human subjective response, the frequency weightings developed in the present research study provide better estimations for the human subjective response to steering wheel hand-arm rotational vibration than the existing frequency weightings W_h and W_s .

However, as with all research, there are limitations which should be considered. The following is a summary of the main issues.

The selection method for choosing the adequate frequency weighting was established based on the amplitude of the road signals rather than the frequency contents of the road signals, because of the hypothesis established in the present study that different amplitude groups may require different frequency weightings. However, the frequency contents of road signals can be different even if they have similar acceleration levels. Therefore further research appears necessary in order to clarify this point, while developing a sort of system which can recognise the frequency contents of the signals preferably in real time such as a pattern recogniser. By this it may be possible to select the more accurate frequency weighting to estimate human subjective response in real time than is possible with the current selection method because it may be possible to match a frequency weighting to an individual driving condition rather than a group of signals which have similar amplitude level.

This study attempted to cover the widest possible test envelope in the frequency and amplitude plane. However, due to the physical limitations of the shaker displacement, low frequency signals below 3 Hz could not be achieved. The test apparatus should therefore be upgraded to the necessary specifications for the future research activity, for example, a low frequency shaker, so as to extend the subjective tests to frequencies below 3 Hz and above 400 Hz.

While this research tested some of the most common driving conditions, a limitation of the present study is that the evaluation of the human perception of steering wheel hand-arm vibration was performed using steering wheel stimuli obtained only from European mid-sized passenger cars with four cylinder engines. Since the purpose of the research was to develop a general evaluation method for human perception of steering wheel hand-arm vibration, the limitation of using only four automobiles may be a factor which must be considered when assessing the results.

Another recommendation concerns the variables which were not examined in the current study which might influence the research findings. With regard to the vibration variable, it is useful to investigate the effect of the vibration direction in order to observe the differences compared to the rotational direction. For example, laboratory experiments could be performed which steering wheel vibration in the lateral and for-aft direction. With regard to the subject variable, it would be useful to investigate the effect of driver experience. Experienced subjects have been found to produce higher subjective responses than inexperienced subjects (Wos et al., 1988a) but the current research study did not consider the effect of the experience of the test participants or how it might influence the shape of the equal sensation curves.

References

Ajovalasit, M., 2005, Effect of Fuel Content on the Human Perception of Engine Idle Irregularity, PhD Thesis, Sheffield University.

Ajovalasit, M. and Giacomini, J., 2003, Analysis of variations in diesel engine idle vibration, Proceedings of the IMechE, Part D - Journal of Automobile Engineering, 217 (10), pp 921-933.

Ajovalasit, M. and Giacomini, J., 2005 Human subjective response to steering wheel vibration caused by diesel engine idle, Proceedings of the IMechE, Part D - Journal of Automobile Engineering, 219 (4), pp 499-510.

Ajovalasit, M. and Giacomini, J., 2007, Effect of automobile operating condition on the subjective equivalence of steering wheel vibration and sound, International Journal of Vehicle Noise and Vibration, 3 (2), pp 197-215.

Ajovalasit, M. and Giacomini, J., 2009, Non-linear dependency of the subjective perceived intensity of steering wheel rotational vibration, International Journal of Industrial Ergonomics, 39, pp 58-67.

Aleksander, I. and Morton, H., 1995, An introduction to neural computing, 2nd Edition, International Thompson Computer Press, London.

Amman, S., Meier, R., Trost, K. and Gu, F., 2005, Equal annoyance contours for steering wheel hand-arm vibration, SAE paper 2005-01-2473.

Amman, S., Pielemeier, B., Snyder, D. and Toting, F., 2001, Road vibration investigation using the Ford vehicle vibration simulator, SAE paper 2001-01-1572.

Andreoni, G., Santambrogio, G.C., Rabuffetti, M. and Pedotti, A., 2002, Method for the analysis of posture and interface pressure of car drivers, Applied Ergonomics, 33 (6), pp 511-522.

ASTM E1364 - 95, 2005, Standard Test Method for Measuring Road Roughness by Static Level Method.

Babbs, F. W., 1979, A design layout method for relating seating to the occupant vehicle, Ergonomics, 22 (2), pp 227-234.

Barrett, B.E. and Gray, J.B., 1994, A computational framework for variable selection in multivariate regression, Statistics and Computing, 4, pp 203-212.

- Bekesy, G.v., 1940, The neural terminations responding to stimulation of pressure and vibration, *Journal of Experimental Psychology*, 26, pp 514-519.
- Bellmann, M. A., 2002, Perception of whole-body vibrations: from basic experiments to effect of seat and steering-wheel vibrations on passenger's comfort inside vehicles, PhD Thesis, University of Oldenburg, Oldenburg.
- Bendat, J.S. and Piersol, A.G., 1986, *Random data: Analysis and Measurement procedures*, 2nd Edition, New York: John Wiley & Sons, Inc..
- Berber-Solano, T.P., 2009, Evaluation of the human cognitive detection of road surfaces based on the feedback vibrations provided by the automobile steering wheel, PhD Thesis, Sheffield University.
- Biggs J., and Srinivasan M.A., 2001, Tangential Versus Normal Displacements of Skin: Relative Effectiveness for Producing Tactile Sensations, Proc. 10th Symposium on Haptic Interfaces for Virtual Environment and Teleoperator Systems, HAPTICS 2002, Orlando, USA, pp 121–128.
- Bolanowski Jr., S.J., Gescheider, G.A., Verrillo, R.T. and Checkosky, C.M., 1988, Four channels mediate the mechanical aspects of touch, *Journal of the Acoustical Society of America*, 84(5), pp 1680-1694.
- Borg, G., 1998, Borg's perceived exertion and pain scales, *Human Kinetics*, Illinois.
- British Standards BS 6840-2, 1993, *Sound system equipment: glossary of general terms and calculation methods*, British Standard Institution, London.
- British Standards BS 6842, 1987, *Measurement and evaluation of human exposure to vibration transmitted to the hand*, British Standard Institution, London.
- British Standard BS 7085, 1989, *Safety aspects of experiments in which people are exposed to mechanical vibration and shock*, British Standard Institution, London.
- British Standards BS-EN 60268-5 ,1997, *Sound system equipment: loudspeakers*, British Standard Institution, London.
- Burström, L. and Lundström, R., 1994, Absorption of vibration energy in the hand and arm, *Ergonomics*, 37 (5), pp 879-890.
- Cambridge Advanced Learner's Dictionary, 2008, *Cambridge Dictionary 3rd Edition*, Cambridge: Cambridge University Press.

Checkosky, C.M. and Bolanowski Jr S.J., 1992, The effects of stimulus duration on the response properties of Pacinian corpuscles: Implications for the neural code, *Journal of the Acoustical Society of America*, 91, pp 3372-3380.

Cohen, B. and Kirman, J.H., 1986, Vibrotactile frequency discrimination at short durations, *Journal of General Psychology*, 113(2), pp 179-186.

Coolican, H., 1999, *Research Methods and Statistics in Psychology*, 3rd Edition, Hodder and Stoughton, London.

Coren, S., Ward, L.M. and Enns, J.T., 2003, *Sensation and Perception*, 6th Edition, John Wiley & Sons, Inc..

Craig, J. C., 1985, Tactile pattern perception and its perturbations, *Journal of the Acoustical Society of America*, 77, pp 238-246.

David, H.A., 1988, *The method of paired-comparison*, 2nd Edition, Oxford University Press, New York.

Department of Transport, 2006, *Speed Leaflet 2006*, <http://www.dft.gov.uk>.

Dong, R.G., Welcome, D.E., McDowell, T.W., Wu, J.Z. and Schopper, A.W., 2006, Frequency weighting derived from power absorption of fingers–hand–arm system under zh-axis, *Journal of Biomechanics*, 39, pp 2311–2324.

Draper, N.R. and Smith, H., 1998, *Applied Regression Analysis*, 3rd Edition, New York: John Wiley & Sons, Inc..

Elliott, D.F., 1987, *Handbook of Digital Signal Processing*, Academic Press.

Entran Devices Inc., 1991, *MSC Series Multi-channel Conditioning Unit*, Watford.

Ezekiel, M. and Fox, K.A., 1959, *Methods of Correlation and Regression Analysis: Linear and curvilinear*, 3rd Edition, John Wiley and Sons, Inc., New York.

Fujikawa, K., 1998, Analysis of steering column vibration, *Motion & Control* 4, pp 37-41.

Gearing and Watson Electronics Limited, 1995, *Gearing and Watson Electronics Limited, Power Amplifier Model PA100: GW Vibration Test System Manual*.

Gescheider, G.A., Bolanowski Jr., S.J. and Verrillo, R.T., 2004, Some characteristics of tactile channels, *Behavioural Brain Research*, 148, pp 35-40.

Gescheider, G.A., 1976, Evidence in support of the duplex theory of mechanoreception, *Sensory Process*, 1, pp 68-76.

Gescheider, G.A., 1997, *Psychophysics: The Fundamentals*, 3rd Edition, Lawrence Erlbaum Associates electronics Ltd, Hailsham, East Sussex.

Gescheider, G.A., Bolanowski Jr., S.J. and Hardick, K.R., 2001, The frequency selectivity of information-processing channels in the tactile sensory system, *Somatosensory and Motor Research*, 18, pp 191-201.

Gescheider, G.A., Bolanowski Jr., S.J. and Verrillo, R.T., 2004, Some characteristics of tactile channels, *Behavioural Brain Research* 148, pp 35-40.

Gescheider, G. A., Bolanowski Jr., S. J., Verrillo, R. T., Arpajian, D. J., and Ryan, T. F., 1990, Vibrotactile intensity discrimination measured by three methods, *Journal of the Acoustical Society of America*, 87, pp 330-338.

Gescheider, G.A., Hoffman, K.E., Harrison, M.A., Travis, M.L. and Bolanowski Jr., S.J., 1994, The effects of masking on vibrotactile temporal summation in the detection of sinusoidal and noise signals, *Journal of the Acoustical Society of America*, 95 (2), pp 1006-1016.

Gescheider, G.A., Sklar, B.F., Van Ooren, C.L. and Verrillo, R.I., 1985, Vibrotactile forward masking: psychophysical evidence for a triplex theory of cutaneous mechanoreception, *Journal of the Acoustical Society of America*, 78, pp 534-543.

Gescheider, G.A., Verrillo, R.T., Capraro, A.J. and Hamer, R.D., 1977, Enhancement of vibrotactile sensation magnitude and predictions from the duplex model of mechanoreception, *Sensory Process*, 1, pp 187-203.

Giacomin, J. and Abrahams, O., 2000, Human fatigue due to automobile steering wheel vibration, *SIA Conference on Car and Train Comfort*, 15-16 Nov., LeMans, France.

Giacomin, J. and Gnanasekaran, S., 2005, Driver estimation of steering wheel vibration intensity: questionnaire-based survey, *Journal of the Engineering Integrity Society*, 18, pp 23-29.

Gnanasekaran, S., Ajovalasit, M. and Giacomin, J., 2006, Driver estimation of steering wheel vibration intensity: laboratory-based tests, *Engineering Integrity Society*, 20, pp 25-31.

Giacomin, J. and Lo Faso, 1993, Vibration survey of the Fiat Tempra and Fiat tipo, Fiat Report.

Giacomin J. and Onesti, C., 1999, Effect of Frequency and grip force on the perception of steering wheel rotational vibration, ATA 6th International Conference on the New Role of Experimentation in the Modern Automotive Product Development Process, Firenze, Italy, Nov. 17 –19.

Giacomin, J. and Screti, A., 2005, Upper body discomfort due to driving: effect of driving experience, gender and vehicle age, Zeitschrift für Arbeitswissenschaft, 5, pp 409-418.

Giacomin, J., Shayaa, M.S., Dormegnien, E. and Richard, L., 2004, Frequency weighting for the evaluation of steering wheel rotational vibration. International Journal of Industrial Ergonomics 33, pp 527-541.

Giacomin, J., Steinwolf, A. and Staszewski, W.J., 2000, An algorithm for mildly nonstationary mission synthesis [MNMS], Engineering Integrity, 7, pp 44-56.

Giacomin, J. and Woo, Y.J., 2004, Beyond comfort: Information content and perception enhancement, Journal of the Engineering Integrity Society, 16 July, pp 8-16.

Gillespie, T.D. and Sayers, M.W., 1983, Measuring Road Roughness and its Effects on User Cost and Comfort: A Symposium, Symposium on Roughness Methodology, 7th Dec. 1983, Bal Harbour, Florida, ASTM International.

Gnanasekaran, S., Ajovalasit, M. and Giacomin, J., 2006, Driver estimation of steering wheel vibration intensity: laboratory-based tests, Engineering Integrity, 20, pp 25-31.

Goldberg, D., 1989, Genetic Algorithms in Search, Optimization and Machine Learning, Addison-Wesley, Reading, Massachusetts.

Gorman, J.W. and Torman, R.J., 1966, Selection of Variables for Fitting Equations to Data, Technometrics, 8 (1), pp 27-51.

Griffin, M.J., 1976, Subjective equivalence of sinusoidal and random whole-body vibration, Journal of the Acoustical Society of America, 60 (5), Nov., pp 1140-1145.

Griffin, M.J., 1990, Handbook of human vibration, Academic Press, London.

Guilford, J.F., 1954, Psychometric Methods, 2nd Edition, McGraw-Hill, New York.

Gurram, R., Rakheja, S. and Brammer, A.J., 1995, Driving point mechanical impedance of the human hand-arm system: synthesis and model development subject to sinusoidal and stochastic excitations. *Journal of Sound and Vibration*, 180, pp 439-458.

Hamer, R.D., Verrillo, R.T. and Zwislocki, J.J., 1983, Vibrotactile masking of Pacinian and non-Pacinian channels, *Journal of the Acoustical Society of America*, 73 (4), pp 1293-1303.

Hamilton, D., 2000, Frequency domain considerations in vehicle design for optimal structural feel, SAE paper 2000-01-1344.

Hanson, L., Sperling, L and Akselsson, R., 2006, Preferred car driving posture using 3-D information, *International Journal of Vehicle Design*, 42(1-2), pp 154-169.

Henry Dreyfuss Associates, 2002, *The measure of man & woman*, revised edition, John Wiley & Sons, New York.

Hocking, R.R., 1976, The analysis and selection of variables in linear regression, *Biometrics* 32, pp 1-49.

Hollins, M. and Roy, E.A., 1996, Perceived intensity of vibrotactile stimuli: the role of mechanoreceptive channels, *Somatosensory and Motor Research*, 13 (3-4), pp 273-286.

Hong, S.I., Jang, H.K., Kim S.H., 2003, Determination of Frequency Weighting Curves for the Evaluation of Steering Wheel Vibration, *Transactions of KSAE*, 11(4), 165-172.

Howarth, H.V.C. and Griffin, M.J., 1991, Subjective reaction to vertical mechanical shocks of various waveforms, *Journal of Sound and Vibration*, 147 (3), pp 395 – 408.

International Standard ISO 5349-1, 2001, *Mechanical Vibration: Measurement and assessment of human exposure to hand-transmitted vibration, Part 1: General guidelines*, International Organization for Standardization, Geneva.

International Standard ISO 8041, 2005, *Human Response to Vibration - Measuring Instrumentation*, International Organization for Standardization, Geneva.

International Standard ISO 13091-1, 2001, *Mechanical Vibration: Vibrotactile perception thresholds for the assessment of nerve dysfunction, Part 1: Methods of measurement at the fingertips*, International Organization for Standardization, Geneva.

Isomura, A., Hara, T and Kamiya, K., 1995, Human factors on driver's steering wheel operation: Three parameters evaluating characteristics of driver's steering wheel operations, *JSAE Review*, 16, 383-410.

Iwata, H., Dupuis, H. and Hartung, E., 1972, Übertragung von horizontalen Sinusschwingungen auf die oberen Extremitäten bei Halbpronationsstellung und Reaktion des M. biceps, *Int. Arch. Arbeitsmed*, 30, pp 313-328.

Johansson, R.S., Landström, U. and Lundström, R., 1982, Responses of mechanoreceptive afferent units in the glabrous skin of the human hand to sinusoidal skin displacements, *Brain Research*, 244, pp 17-25.

Kandel, E.R., Schwartz, J.H. and Jessell, T.M., 1991, *Principles of Neural Science*, International Edition, 347.

Kester, W., 2003, *Mixed-Signal and DSP Design Techniques*, Newnes (Elsevier), Burlington, U.S.A..

Kim, J.H., Jung, S.G. and Kim, S.S., 1985, An investigation of the steering wheel vibration and its reduction in passenger cars, SAE paper 852267, 685-694.

Knibestol, M. and Vallbo, A.B., 1970, Single unit analysis of mechanoreceptor activity from the human glabrous skin, *Acta Physiologica Scandinavica*, 80, pp 178-195.

Knudson, V., 1928, Hearing with the sense of touch, *Journal of General Psychology*, 1, 320-352.

Kulkarni, K.B. and Thyagarajan, R.S., 2001, Optimizing the effects of body attachment stiffness on steering column in- vehicle modes, SAE paper 2001-01-0041.

Labs, S.M., Gescheider, G.A., Fray, R.R. and Lyons, C.H., 1978, Psychophysical tuning curves in vibrotaction, *Sensory Process*, 2, pp 231-247.

Lamoré, P.J.J. and Keemink, C.J., 1988, Evidence for different types of mechanoreceptors from measurements of the psychophysical threshold for vibrations under different stimulation conditions, *Journal of the Acoustical Society of America*, 83 (6), pp 2339-2351.

LMS International Inc., 2002, *LMS Cada-X Fourier Monitor Manual*, Revision 3.5F, Leuvan.

Lundström, R. and Burström, L., 1989, Mechanical impedance of the human hand-arm system, *International Journal of Industrial Ergonomics*, 3, pp 235-242.

Mansfield, N.J. and Marshall, J.M., 2001, Symptoms of musculoskeletal disorders in stage rally drivers and co-drivers, *British Journal of Sports Medicine*, 36, 314-310.

Mansfield, N.J., 2005, Human response to vibration, CRC Press, London.

Martin, J.H. and Jessell, T.M., 1999, Modality coding in the somatic sensory system, in Principles of neural science, E.R. Kandel, J.H. Schwartz, and T.M. Jessell, Editors, Appleton and Lange. V, pp 341-351.

Masmejean, E.H., Chavane, H., Chantegret, A., Issermann, J.J. and Alnot, J.Y., 1999, The wrist of the formula one driver, British Journal of Sports Medicine, 33, pp 270-273.

Mathworks Inc., 2002, Statistical Toolbox for use with Matlab.

Ministry of Defence, 2007, Design and Airworthiness Requirements for Service Aircraft Part 7 - Rotorcraft Section 5, Defence Standard 00-970 Part 7, Issue 2.

MIRA Ltd, 2006, <http://www.mira.co.uk/Facilities/TestFacilitiesProvingGround.htm>.

Mishoe, J.W. and Suggs, C.W., 1977, Hand arm vibration Part II: Vibrational responses of the human hand, Journal of Sound and Vibration, 53, pp 545-558.

Miura, T., Morioka, M., Kimura, K. and Akuta, A., 1959, On the occupational hazards by vibrating tools (Report IV) - On the vibration of vibrating tools and the tentative threshold limit value of vibration, Journal of Science of Labour, 35, pp 760-767.

Miwa, T., 1967, Evaluation methods for vibration effect, Part 3: Measurements of threshold and equal sensation contours on hand for vertical and horizontal sinusoidal vibration, Industrial Health, 5, pp 213-220.

Miwa, T., 1968, Evaluation methods for vibration effect, Part 7: The vibration greatness of the pulses, Industrial Health, 7, pp 143-164.

Miwa, T., 1969, Evaluation methods for vibration effect. Part 8: The vibration greatness of random waves, Industrial Health, 7, pp 89-115.

Moore, B.C.J., 1997, An Introduction to the Psychology of Hearing, 4th Edition, London: Academic Press.

Morioka, M., 1999, Effect of contact location on vibration perception thresholds in the glabrous skin of the human hand, Proceedings of the 34th UK Group Meeting on Human Responses to Vibration, Ford Motor Company, Dunton, Essex, UK, 22-24 Sep. 1999.

Morioka, M., 2001, Sensitivity of Pacinian and non-Pacinian receptors: effect of surround and contact location, In 36th United Kingdom Group Meeting on Human Responses to Vibration, Centre for Human Science, QinetiQ, Farnborough, UK, 12-14 Sep. 2001, pp 266-276.

Morioka, M., 2004, Magnitude dependence of equivalent comfort contours for vertical steering wheel vibration, 39th Meeting of the UK Group on Human Response to Vibration, Ludlow, UK, 15-17 Sep., 2004.

Morioka, M. and Griffin, M.J., 2006, Magnitude-dependence of equivalent comfort contours for fore-and-aft, lateral and vertical hand-transmitted vibration, *Journal of Sound and Vibration*, 295, pp 633-648.

Mountcastle, V.B, LaMotte, R.H. and Carli, G., 1972, Detection thresholds for stimuli in humans and monkeys: comparison with threshold events in mechanoreceptive afferent fibres innervating the monkey hand, *Journal of Neurophysiology*, 35, pp 122-136.

National Statistics, 2006, *Social Trends*, Chapter 12: Transport, 36-2006 Edition, pp 176-188.

National Travel Survey, 2005, Department for Transport: Road Casualties Great Britain 2005.

Neely, G. and Burström, L., 2006, Gender differences in subjective responses to hand-arm vibration, *International Journal of Industrial Ergonomics*, 36, pp 235-140.

Neely, G., Burström, L., and Johansson, M., 2001, Subjective Responses to Hand-Arm Vibration: Implications for frequency-weighting and gender differences, The 17th annual meeting of the International Society for Psychophysics, Leipzig, Germany, pp 553-558.

Neely, G., Ljunggren, G., Sylven, C. and Borg, G., 1992, Comparison between the visual analogue scale (VAS) and the category ratio scale (CR) for the evaluation of leg exertion. *International Journal of Sports Medicine*, 13, pp 133-136.

Newland, D.E., 1993, *Random vibrations, spectral and wavelet analysis*, 3rd Edition, Longman Scientific and Technical, England.

NIST (National Institute of Standards and Technology), 2006, *Engineering Statistics Handbook*, U.S. department of commerce, <http://www.itl.nist.gov/div898/handbook/dea/dea.htm>.

Norkin, C. C. and White, D. J., 2003, *Measurement of joint motion: A guide to goniometry*, 3rd Edition, F.A Davis Company, Philadelphia.

OICA, 2007, World Motor Vehicle Production: World Ranking of Manufacturers 2007, <http://oica.net/wp-content/uploads/world-ranking-2007.pdf>.

Oppenheim A.V., Schafer R.W. and Buck J.R., 1999, Discrete-Time Signal Processing, 2nd Edition, Upper Saddle River, New Jersey 07458, Prentice-Hall.

Pak, C.H., Lee, U.S., Hong, S.C., Song, S.K., Kim, J.H. and Kim, K.S., 1991, A study on the tangential vibration of the steering wheel of passenger car, SAE paper 912565, pp 961-968.

Park, S.H., 1993, Regression analysis (revised version), Min Young Sa, (in Korean).

Park, J., Lee, J-W., Kwon, K.S., Kim, C-B. and Kim, H-K., 1999, Preferred driving posture and driver's physical dimension, Proceedings of Human Factors and Ergonomic Society, 43rd annual meeting, Santa Monica, USA, Vol. V, pp 742-746.

Peruzzetto, P., 1988, Assessing the relative importance of hand vibration with respect to whole-body vibration, The U.K and French joint meeting on human resources to vibration, I.N.R.S., Vandoeuvre, France, 26-28 Sep. 1988, pp 1-11.

Pheasant, S. and Haslegrave, C.M., 2005, Bodyspace: Anthropometry, Ergonomics and the Design of work, 3rd Edition, U.S.A., Taylor & Francis.

Phillips, J.R., Johansson, R.S. and Johansson, O., 1992, Responses on human mechanoreceptive afferents to embossed dot array scanned across fingerpad skin, Journal of Neuroscience, 12, pp 827-839.

Pickering, S.G., 2005, The application of multivariate correlation techniques to vehicle driveability analysis, PhD Thesis, University of Bath.

Piersol, A.G., 1992, Data Analysis, in Noise and Vibration Control Engineering: Principles and Applications, L.L.a.V. Bernarek, I.L., Editor. John Wiley & Sons, Inc.: New York.

Pollack, I., 1952, The information of elementary auditory displays, Journal of the Acoustical Society of America, 24, pp 745 – 749.

Porter, J.M. and Gyi, D.E., 1998, Exploring the optimum posture for driver comfort, International Journal of Vehicle Design, 19 (3), pp 255-266.

Pottinger, M.G., Marshall, K.D., Lawther, J.M. and Thrasher, D.B., 1986, A review of tire/pavement interaction induced noise and vibration, In Pottinger, M.G. and Yager, T.J. (Editors), ASTM STP929 The Tire Pavement Interface, ASTM, Philadelphia, pp 183-287.

Priestley, M.B., 1988, Non-linear and non-stationary time series analysis, London: Academic Press.

Pyökkö, I., Färkkilä, M., Toivanen, J., Korhonen, O. and Hyvärinen, J., 1976, Transmission of vibration in the hand-arm system with special reference to changes in compression force and acceleration, Scandinavian Journal of Work, Environment and Health, 2, pp 87-95.

Rebiffé, R., 1969, Le siege du conducteur: son adaptation aux exigences fonctionnelles et anthropométriques, Ergonomics, 12 (2), pp 246-261.

Reynolds, D.D. and Angevine, E.N., 1977, Hand-arm vibration Part II: Vibration transmission characteristics of the hand and arm, Journal of Sound and Vibration, 51 (2), pp 255-265.

Reynolds, D.D. and Keith, R.H., 1977, Hand-arm vibration, Part I: Analytical model of the vibration response characteristics of the hand. Journal of Sound and Vibration 51, pp 237-253.

Reynolds, D.D. and Soedel, W., 1972, Dynamic response of the hand-arm system to a sinusoidal input, Journal of Sound and Vibration, 21, pp 339-353.

Reynolds, D.D., Standlee, K.G. and Angevine, E.N., 1977, Hand-arm vibration, Part III: Subjective response characteristics of individuals to hand-induced vibration, Journal of Sound and Vibration, 51, pp 267-282.

Roulliard, V. and Sek, M.A., 2002, A statistical model for longitudinal road topography, Road and Transport Research, 11 (3).

Schröder, F. and Zhang, T., 1997, Objective and subjective evaluation of suspension harshness, In 6th European Automobile cooperation International Congress, Cernobbio, Italy, Paper 97A068, pp 63-72.

Seidl, A., 1994, The man model RAMSIS: Analysis, Synthesis and Simulation of Three-dimensional Human Posture, Technical University of Munich, Germany, Doctoral thesis.

Shayaa, M.S., 2004, Human perception on rotating steering wheel vibration. MPhil Thesis, The University of Sheffield.

Sinclair, R.J. and Burton, H., 1996, Discrimination of vibrotactile frequencies in a delayed pair comparison task, *Perception & Psychophysics*, 58 (5), pp 680-692.

Smith, S.W., 2003, *Digital Signal Processing: A Practical Guide for Engineers and Scientists*, Newnes (Elsevier), Burlington, U.S.A..

Society of Automotive Engineers Standard SAE J670e, 1976, Vehicle dynamics terminology, SAE International, Warrendale, Pennsylvania.

Sörensson, A. and Burström, L., 1997, Transmission of vibration energy to different parts of the human hand-arm system, *International Archives of Occupational and Environmental Health*, 70, pp 199-202.

Sörensson, A. and Lundström, R., 1992, Transmission of vibration to the hand, *Journal of low frequency noise and vibration*, 11 (1), pp 14-22.

SPSS Inc., 2004, SPSS 13.0 for Windows.

Stelling, J. and Dupuis, H., 1996, Different acute effects of single-axis and multi-axis hand-arm vibration, *International Archives of Occupational and Environmental Health*, 68, pp 236-242.

Stevens, S.S., 1966, A metric for the social consensus, *Science*, 151, 530-541.

Stevens, S.S., 1986, *Psychophysics: introduction to its perceptual, neural and social prospects*, G. Stevens, New Brunswick, U.S.A., Transaction Books.

Talbot, W.H., Darien-Smith, I., Kornhuber, H.H. and Mountcastle, V.B., 1968, The sense of flutter-vibration: Comparison of the human capacity with response patterns of mechanoreceptive afferents from the monkey hand, *Journal of Neurophysiology*, 31, pp 301-304.

Taylor, F.J., 1994, *Principles of Signals and Systems*, McGraw-Hill Series in Electrical and Computer Engineering: Communications and Signal Processing, McGraw Hill, New York.

Teghtsoonian, M. and Teghtsoonian, R., 1983, Consistency of individual exponents in cross-modal matching, *Perception and Psychophysics*, 33, 203 - 214.

Thomas M. and Beaucamp Y., 1998, Development of a new frequency weighting filter for the assessment of grinder exposure to wrist-transmitted vibration, *Computers & Engineering*, 35 (3-4), 651-654.

Thurstone, L.L., 1959, *The measurement of values*, University of Chicago Press, Chicago.

Tilley, A. R., 1994, *Le misure dell'uomo e della donna: dati di riferimento per il progetto*, Henry Dreyfuss Associates – New York – Be-ma ed. Milan, Italy.

Tominaga, Y., 2005, New frequency weighting of hand-arm vibration, *Industrial Health*, 43, 509-515.

Torgerson, W.S., 1958, *Theory and method of scaling*, John Wiley and Sons, New York.

Venillo, R.T., 1965, Temporal summation in vibrotactile sensitivity, *Journal of the Acoustical Society of America*, 37 (5), pp 843-846.

Verrillo, R.T., 1966, Vibrotactile sensitivity and the frequency response of the Pacinian corpuscle, *Psychonomics Science* 4, pp 135-136.

Verrillo, R.T., 1979, Comparison of vibrotactile threshold and suprathreshold responses in men and women, *Perception & Psychophysics* 26(1), pp 20-24.

Verrillo, R.T., 1985, Psychophysics of vibrotactile stimulation, *Journal of the Acoustical Society of America*, 77 (1), pp 225-232.

Verrillo, R.T., Fraioli, A.J. and Smith, R.L., 1969, Sensation magnitude of vibrotactile stimuli, *Perception & Psychophysics*, 6, pp 366-372.

Verrillo, R.T. and Gescheider, G.A., 1977, Effect of prior stimulation on vibrotactile thresholds, *Sensory Process*, 1, pp 292-300.

Wallace, T.D., 1964, Efficiencies for stepwise regressions, *Journal of the American Statistical Association*, 59(308), pp 1179-1182.

Wang, W., Rakheja, S. and Boileau, P.-É, 2006, The role of seat geometry and posture on the mechanical energy absorption characteristics of seated occupants under vertical vibration, *International Journal of Industrial Ergonomics*, 36, pp 171-184.

Wanhammar, L., 1999, *DSP Integrated Circuits*, Academic Press.

Warren, R.M., 1981, *Measurement of sensory intensity, The behavioral and brain sciences*, Cambridge University Press, 4, pp 175-223.

Winder, S., 2002, Analog and Digital Filter Design, 2nd Edition, Newnes (Elsevier), Woburn, U.S.A..

Wisner, A., and Rebiffé, R., 1963, L'utilisation des données anthropométriques dans la conception du poste de travail, *Le Travail Humain* XXVI, pp 193-217.

Wos, H., Marez, T., Noworoi, C. and Borg, G., 1988b, The reliability of self-ratings based on Borg's Scale for hand-arm vibrations of short duration, Part II, *International Journal of Industrial Ergonomics*, 2, pp 151-156.

Wos, H., Wangenheim, M., Borg, G. and Samuelson, B., 1988a, Perceptual rating of local vibration: A psychophysical study of hand-arm vibration of short duration, Part I, *International Journal of Industrial Ergonomics*, 2, pp 143-150.

Zwicker, E. and Fastl, H., 1990, *Psychoacoustic: Facts and Models*, Springer-Verlag, Berlin.

Zwislocki, J.J., 1960, Theory of temporal auditory summation, *Journal of the Acoustical Society of America*, 32, pp 1046-1060.

Appendix A

Technical Specifications of Equipment

A.1 Technical Specifications of the equipment used in the measurement of the steering wheel vibration for the Uxbridge tests.

The technical specifications of the SVAN 947 Sound and Vibration Level Meter and Analyser manufactured by SVANTEK Ltd. are presented in Figures A.1 and A.2. The technical specifications of the Low Impedance Voltage Mode (LIVT™) accelerometer 3055B1 are presented in Figures A.3 and A.4.

SVAN 947 Sound & Vibration Analyser

The SVAN 947 is all digital, Type 1 sound level & vibration meter and analyser. It is intended for general acoustic measurements, environmental noise monitoring, occupational health and safety monitoring.

Three acoustic or vibration profiles can be measured in parallel with independently defined filters and RMS detector time constants (e.g. concurrent Impulse, Fast and Slow measurements are possible).

All required weighting filters (e.g.: A, C, W-Bxy, W-Bz or H-A) including the latest ISO 2631-1 standard are available with this instrument. RMQ detector enables direct measurement of the Vibration Dose Value.

The SVAN 947, using computational power of its digital signal processor, can perform real time 1/1 & 1/3 octave analysis including statistical calculations.

The high resolution FFT and pure tone detection options further extend the capabilities of this unit.

Fast USB 1.1 interface (with 12 MHz clock) creates real time link for the application of the SVAN 947 as a PC front-end.

Measurement results can be stored in large (8, 16 or 32 MB), non-volatile memory and easily downloaded to any PC using USB 1.1 or RS 232 interface and SvanPC software.

The SVAN 947 can be used in hard environmental conditions over the whole work day thanks to built-in rechargeable battery and robust, lightweight construction.

FEATURES

Sound Level Meter & Analyser

- noise measurements (Spl, Leq, SEL, Lden, TaktMax and statistics) with Type 1 accuracy
- parallel Impulse, Fast and Slow detectors for the measurements with A, C or Lin filters
- one measurement range 24 dB_A RMS - 140 dB_A PEAK in the SLM mode
- 1/1 and 1/3 octave real time analysis parallel to the SLM operation (optional)
- FFT calculation (1920 lines in real time up to 22.4 kHz) spectra parallel to the SLM operation (optional)

Vibration Meter & Analyser

- vibration measurements according to ISO 2631-1 with Type 1 accuracy (ISO 8041)
- parallel Peak, RMS (incl. MTVV) and RMQ (incl. VDV) measurements
- 1/1 and 1/3 octave real time analysis (optional)
- FFT calculation (1920 lines in real time up to 22.4 kHz) spectra parallel to the SLM operation (optional)

General

- internal buffer for logging more than two weeks of 1 sec RMS / Max / Peak results (8, 16 or 32 MB of non-volatile memory)
- USB 1.1 and RS 232 interfaces
- built-in rechargeable battery (operational time > 8 h)
- handheld, robust case
- light weight (only ca 600 grams)

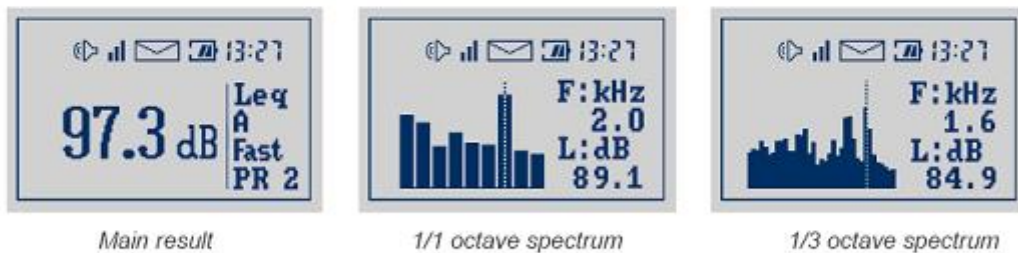


INSTRUMENTATION FOR SOUND & VIBRATION
MEASUREMENTS

[Figure A.1] SVAN 947 Sound and Vibration Level Meter and Analyser manufactured by SVANTEK Ltd. used for the experimental steering vibration measurements.

TECHNICAL SPECIFICATIONS

Sound Level Meter	Type 1: IEC 651, IEC 804 and IEC 61672-1 L _{eq} , L _{max} , L _{min} , L _{Peak} , Spl, SEL, L _{den} , L _{m3} , L _{m5} , statistics: L _n (L ₁ -L ₉₉), Time History for all A, C, Lin (Z) filters in parallel
Vibration Meter	Type 1: ISO 8041 RMS, Peak, Max, Min, MTVV, VDV (RMQ), Time History
Sound & Vibration Analyser	Real time 1/1 & 1/3 octave (optional) analysis with statistics (spectra logging speed down to 2 ms), 1920-line FFT spectra calculated in the real time for 22.4 kHz and sub-bands with Hanning window (optional)
Input	TNC with IEPE power supply for the microphone preamplifier or accelerometer
Microphone Preamplifier Measurement Range	SV 12L From 22 dB _A RMS (with 5 dB margin from noise) to 140 dB _A PEAK or 0.1 ms ⁻² – 10000 ms ⁻² (with 3220B accelerometer)
Dynamic Range	120 dB (in the SLM mode), 100 dB (in the Vibration and Analyser mode), A/D conversion: 2 x 20 bits
Frequency Range	10 Hz – 20 kHz for sound and 1 Hz – 20 kHz for vibration, sampling rate: 48 kHz
Weighting Filters	A, C and Lin (Type 1: IEC 651, IEC 804 and IEC 61672-1) and W-Bxy, W-Bz, W-Bc, H-A, W _k , W _c , W _d , W _j (ISO 8041 and ISO 2631-1)
1/1 Octave Filters	15 filters with centre frequencies 1 Hz – 16 kHz, Type 1- IEC 1260 (optional)
1/3 Octave Filters	45 filters with centre frequencies 0.8 Hz – 20 kHz, Type 1- IEC 1260 (optional)
RMS & RMQ Detectors	Digital True RMS & RMQ with Peak detection, resolution 0.1 dB, integration time programmable up to 24 h Time Constants: Slow, Fast, Impulse (in parallel) in SLM mode; from 100 ms to 10 s in the Vibration Meter mode (any three in parallel)
Microphone Accelerometer	SV 22 prepolarised 1/2" condenser microphone, sensitivity 50 mV/Pa 3220B (3.5 grams, 1 mV/ms ²) for the Hand Arm measurements; other IEPE accelerometers optional
Display	LCD 97x32 pixels plus icons with backlighting
Memory	8, 16 or 32 MB non-volatile (Flash type)
Analogue Output	AC 0.5 V _{RMS}
Interfaces	USB 1.1 and RS 232
Power Supply	Built-in rechargeable battery 4.8 V / 1.6 Ah External power supply 8 - 15 V _{DC} / 600 mA Internal battery operating time > 8 h
Environmental Conditions	Temperature from -10 °C to 50 °C Humidity up to 90 % RH, non condensed
Dimensions	328 x 82 x 42 mm (with microphone and preamplifier)
Weight	Approx. 0.6 kg with battery



Continuous product development and innovation is the policy of our company. Therefore, we reserve the right to change the specifications without prior notice.

SVANTEK Sp. z o.o., ul. Ks. Jana SITNIKA 1/68, 01-410 WARSAW, POLAND
 phone/fax (+48 22) 828 80 39, (+48 22) 827 25 36
<http://www.svantek.com> e-mail: office@svantek.com.pl

[Figure A.2] SVAN 947 Sound and Vibration Level Meter and Analyser manufactured by SVANTEK Ltd. used for the experimental steering vibration measurements.

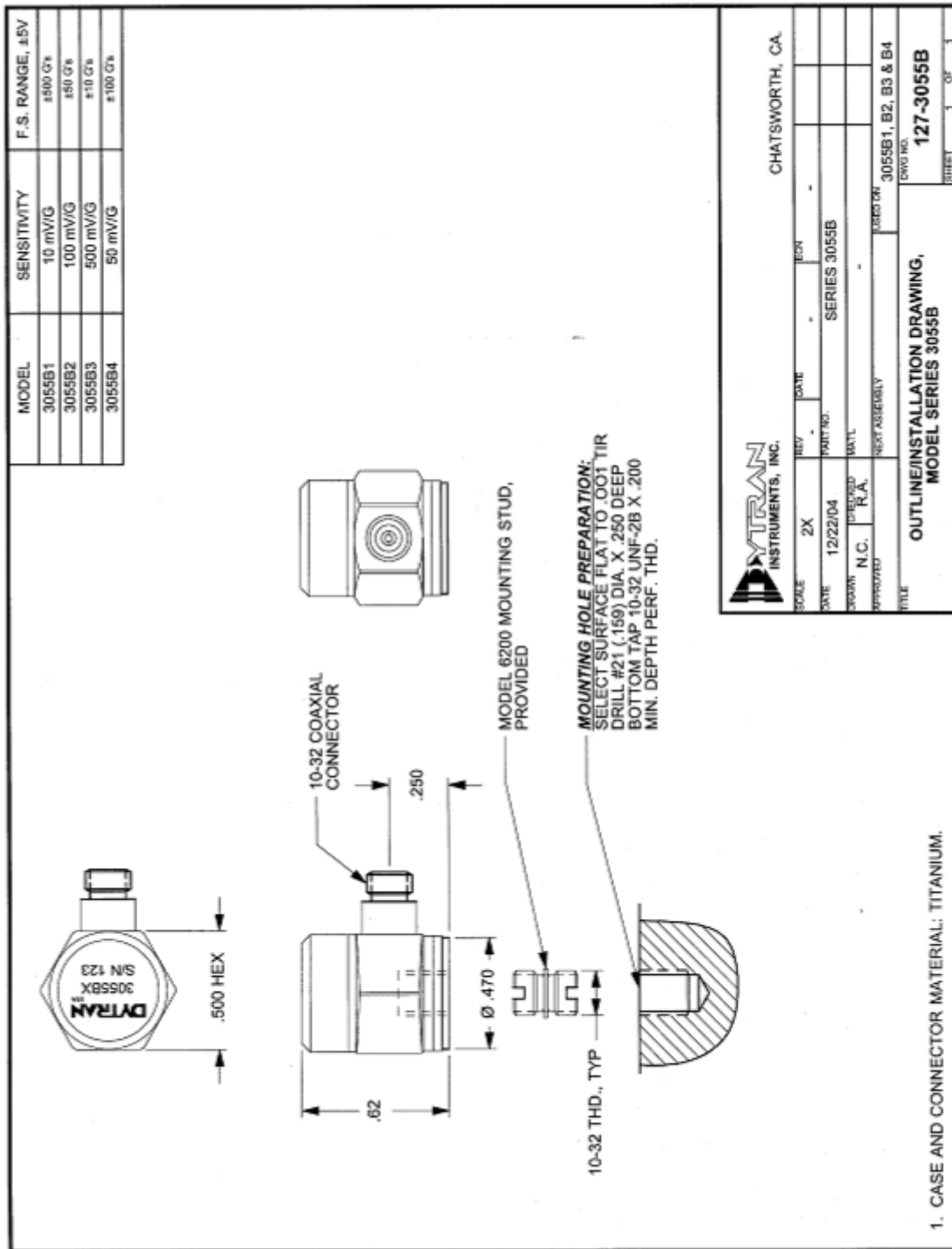


[Figure A.3] Technical specifications for the LIVT™ accelerometer Series 3055B1 used for the experimental steering vibration measurements.

SPECIFICATIONS
MODEL SERIES 3055B LIVM ACCELEROMETERS

SPECIFICATION	VALUE	UNITS			
PHYSICAL					
WEIGHT	10	Grams			
SIZE, HEX x HEIGHT	.50 x 0.62	Inches			
MOUNTING PROVISION	10-32 X .150 DEEP TAPPED HOLE				
CONNECTOR, RADially MOUNTED	10-32	Coaxial			
MATERIAL, BASE, CAP & CONNECTOR	TITANIUM				
SEISMIC ELEMENT TYPE	CERAMIC, PLANAR SHEAR				
PERFORMANCE					
	MODELS				
	3055B1	3055B2	3055B3	3055B4	
SENSITIVITY, ± 5% [1]	10	100	500	50	mV/g
RANGE F.S. FOR ± 5 VOLTS OUTPUT	± 500	±50	±10	±100	g's
FREQUENCY RANGE, ± 5% (all models)	1 to 10,000				Hz
RESONANT FREQUENCY, NOM. (all models)	35				kHz
ELECTRICAL NOISE FLOOR (25Hz-25kHz)	.0002	.00006	.00005	.0005	g's RMS
(1Hz-10kHz)	.0004	.0001	.0001	.0010	g's RMS
LINEARITY [2] (all models)	±2				% F.S.
TRANSVERSE SENSITIVITY, MAX. (all models)	±2				%
ENVIRONMENTAL					
	3055B1	3055B2	3055B3	3055B4	
MAXIMUM VIBRATION/SHOCK	600/3000	400/2000	200/1000	500/2000 ±	g's/g's PK
TEMPERATURE RANGE (all models)	-60 to +250				°F
SEAL, HERMETIC	Glass-to-metal/welded				
COEFFICIENT OF THERMAL SENSITIVITY	.06				%/°F
ELECTRICAL					
SUPPLY CURRENT/COMPLIANCE VOLTAGE RANGE [3]	2 to 20/+18 to +30				mA/Volts
OUTPUT IMPEDANCE, TYP.	100				Ohms
BIAS VOLTAGE, +10.5 VOLTS NOM.	+9 to +12				VDC
DISCHARGE TIME CONSTANT, NOM.	0.5				Sec
OUTPUT SIGNAL POLARITY FOR ACCELERATION TOWARD TOP	Positive				Positive
ELECTRICAL ISOLATION, CASE GROUND TO MOUNTING SURFACE	10 Meg Ω, min.				

Accessories supplied: (1) Model 6200 mounting stud.

[1] Measured at 100 Hz, 1 G RMS per ISA RP 37.2.

[2] Measured using zero-based best straight line method, % of F.S. or any lesser range.

[3] Do not apply power to this device without current limiting, 20 mA MAX. To do so will destroy the integral IC amplifier.

[Figure A.4] Technical specifications for the LIVT™ accelerometer Series 3055B1 used for the experimental steering vibration measurements.

A.2 Technical Specifications of the equipment used in the experimental laboratory test.

The monoaxial accelerometer which was placed on the rotational steering wheel test rig is presented in Figure A.5. Technical specifications of the accelerometer are presented in Figure A.6, while its certificate of calibration is presented in Figure A.7 in which is described the properties of the single axis of measurement. The technical specification for the multi-channel signal conditioning MSC6 is presented in Figure A.8, while the technical specification for the power amplifier PA100E and the shaker V20 are presented in Figure A.9.

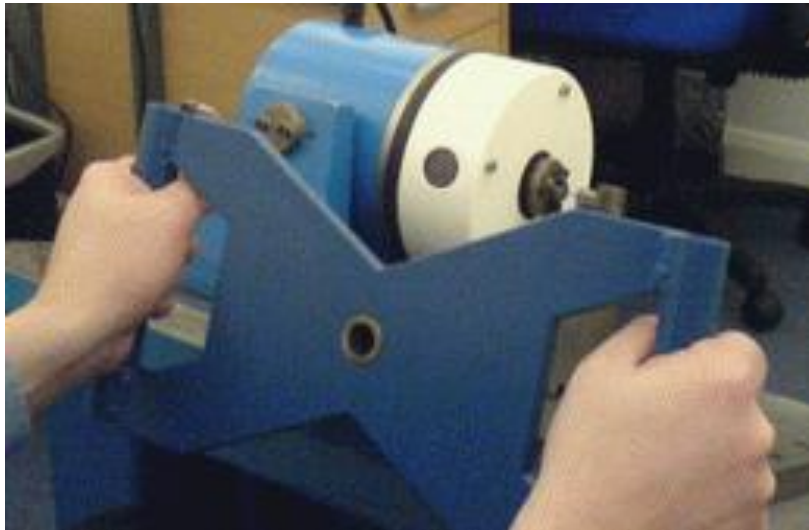


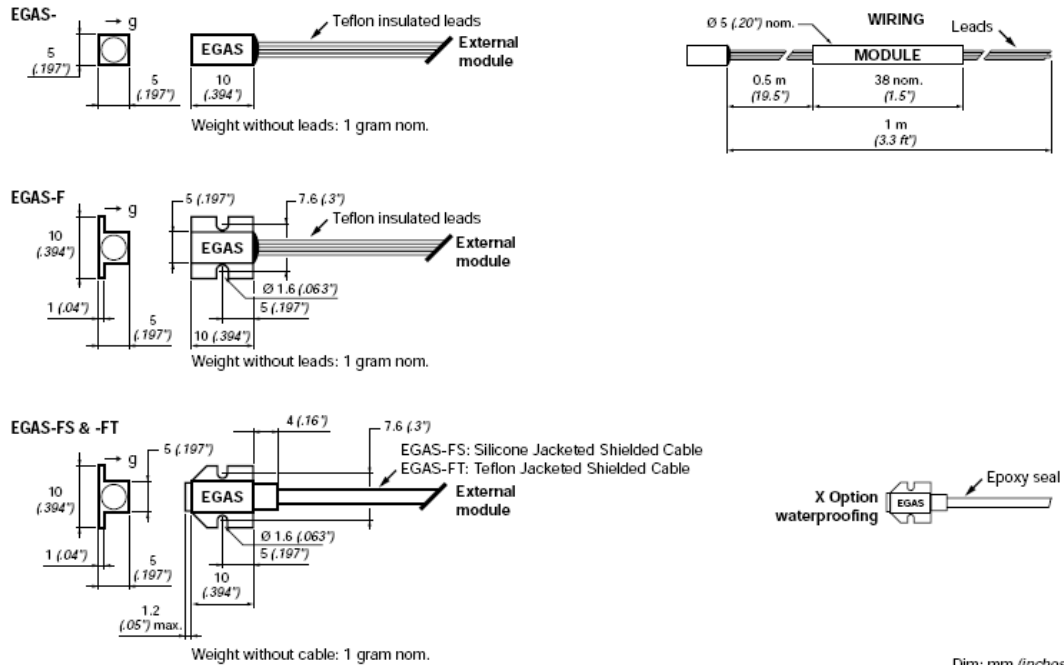
[Figure A.5] Accelerometer position at the rotational steering wheel test rig, located on the top left side of the wheel.

EGAS Series Accelerometers



Miniature - Rugged

EGAS, EGAS-F, EGAS-FS & EGAS-FT



EGAS Series

g RANGES "FS"	g OVERRANGE LIMIT	FREQUENCY RESPONSE $\pm 1/2$ dB nom./min.	NATURAL FREQUENCY nom.	SENSITIVITY mV/g nom.	OUTPUT "FSO" mV nom.
± 5	± 500	0 to 150/80 Hz	300 Hz	20	± 100
± 10	± 1000	0 to 200/120 Hz	400 Hz	10	± 100
± 25	± 2500	0 to 400/240 Hz	800 Hz	4	± 100
± 50	± 5000	0 to 600/350 Hz	1200 Hz	2	± 100
± 100	± 10000	0 to 900/500 Hz	1800 Hz	1	± 100
± 250	± 10000	0 to 1300/750 Hz	2600 Hz	0.4	± 100
± 500	± 10000	0 to 1750/1000 Hz	3500 Hz	0.2	± 100
± 1000	± 10000	0 to 2500/1500 Hz	5000 Hz	0.1	± 100
± 2500	± 10000	0 to 3500/2000 Hz	7000 Hz	0.04	± 100

EXCITATION: 15VDC
 IMPEDANCE IN: 1300 Ω nom. typ.
 IMPEDANCE OUT: 1500 Ω nom.
 COMB. NON-LINEARITY & HYSTERESIS: $\pm 1\%$
 TRANSVERSE SENSITIVITY: 2% max
 DAMPING RATIO AT 20°C (70°F): 0.7 nom. (0.5 to 0.9)
 OVERRANGE STOPS: Integral
 THERMAL ZERO SHIFT: ± 1 mV/50°C (± 1 mV/100°F)
 THERMAL SENSITIVITY SHIFT (TSS): $\pm 2.5\%/50^\circ\text{C}$ ($\pm 2.5\%/100^\circ\text{F}$)
 OPERATING TEMPERATURE: -40°C to 120°C (-40°F to 250°F)
 COMPENSATED TEMPERATURE: 20°C to 80°C (70°F to 170°F)
 ZERO OFFSET AT 20°C (70°F): ± 15 mV typ.

 www.entran.com	EGAS ACCELEROMETERS Miniature Rugged	Entran Sensors & Electronics USA: Fairfield, NJ UK: Garston, Watford, Herts, England Europe: Les Clayes-sous-Bois, France		
		SPECIFICATION	ISSUE	PAGE
		EGASS001U	PB0	1 of 2

[Figure A.6] Technical specifications for the monoaxial EGAS accelerometer used for the experimental laboratory tests.

CERTIFICATE OF CALIBRATION

Property of :

P.O. :

Entran PO : 21138

PLEASE READ OPERATING INSTRUCTIONS BEFORE POWERING UNIT

Model : EGAS-PT*-25-/L02M Axis : S/N : 889329
 Type : ACCELEROMETER
 Range : 25 g Do Not Exceed : 2500 g
 Compensated Range : 20 to 80 °C Operating Range : -40 to 120 °C
 Specifications : *: DIN type 7 pin connector to be wired to sensor for MSC.

Other characteristics according to : EGASS001E-A

CALIBRATION DATA

¹Non linearity : ± ¹Hysteresis : ± ¹CNL&H : ± 1.00 %FSO
¹Th. zero shift : ± 1.00 mV/50°C ¹Thermal Sens. Shift : ± 2.50 %/50°C
¹Zero (typ.) : ± 15 mV
 Ref. Temp. : 22 °C (72°F)
 Shunt Cal : with : KG across :
 Sensitivity : 3.681 mV/g with Excitation : 15.0 V Max. : 18.0 V
 Natural frequency : 740 Hz Damping : 0.66
 Input ohms : 1368 Ω Output ohms : 1562 Ω
 Cal Equip. : M65
 Notes : ELECTROMAGNETIC COMPATIBILITY,
 RESIDENTIAL, COMMERCIAL AND LIGHT INDUSTRY.

WIRING

Connector : DIN 7b. Transducer to Comp. Module : Total length :
 +In. : 1 +Out. : 5 Common mode : V output
 -In. : 2 -Out. : 4 referenced to -Input =

¹The calibrated values do not exceed the data sheet specifications, value shown is the data sheet value.
²Value given by manufacturing design.

The above instrument has been calibrated against a working standard which is directly traceable to a National standard.
 All data interpreted per Entran Instruction Manuals unless otherwise indicated.

Control : S. COSTE



Date : 08/11/99

DQVLEP

Entran Devices, Inc
 FAIRFIELD, NJ 07604 - USA
 (973) 227 1002

Entran European Headquarters
 F-78340 LES CLAYES-BOIS
 33 (0) 1 30 79 33 00

Entran Limited
 WATFORD - WD2 6LQ - England
 44 (01823) - 593 599

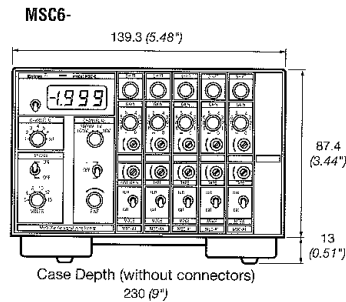
Entran Sensoren GmbH
 D-8700 LUZERN
 49 (0029) 63515-0

[Figure A.7] ENTRAN Certificate of calibration and specifications for the monoaxial EGAS accelerometer used to measure the steering wheel vibration test rig along the z-axis.

Specifications



MSC6



Dim: mm (inches)

Chassis with Power Supply

FOR A1 AMPLIFIERS:
FOR A2 AMPLIFIERS (Also accepts A1 amplifiers):
NUMBER OF CHANNELS:
POWER:
DISPLAY:
EXCITATION TO SENSOR (Common to all Channels):
INTERNAL CALIBRATION:

MSC6
Not Available
6
115/220VAC ($\pm 10\%$, 45-440Hz) Switch Selectable (Optional 12/24 VDC)
3 1/2 DIGIT LED, 1.999V or 19.99V Switchable
Switchable: 5V, 6V, 8V, 10V, 12V and 15V
 $\pm 1\text{mV}$ through $\pm 10\text{V}$ continuously adjustable

Signal Conditioning Channels A1 & A2


OUTPUT:	A1	A2
AMPLIFIER GAIN (Switchable with fine control):	$\pm 10\text{V}$ or $\pm 2\text{V}$	4-20mA and $\pm 10\text{V}$ or $\pm 2\text{V}$
AMPLIFIER BANDWIDTH (-1dB):	1 to 2000	10 to 10000
ZERO OFFSET:	0 to 50KHz	0 to 1.5KHz
	$\pm 40\text{mV}$ at input	$\pm 10\text{mV}$ at input
INPUT RANGE:	5mV to 1.0V	
INPUT MODE:	Full, Half or 1 Arm Bridge. Internal Bridge Completion	
INPUT IMPEDANCE:	1M Ω Differential	
OUTPUT TYPES:	Tape and Galvo	
OUTPUT IMPEDANCE FOR TAPE:	0.5 Ω	
OUTPUT FOR GALVOS:	$\pm 10\text{mA}$ into 120 Ω	
OUTPUT LINEARITY:	0.05%	
OPERATING TEMPERATURE:	0 $^{\circ}\text{C}$ to 40 $^{\circ}\text{C}$ (32 $^{\circ}\text{F}$ to 104 $^{\circ}\text{F}$)	
INPUT CONNECTORS:	DIN Type 7 Pin. with unwired mate	
OUTPUT CONNECTORS:	D Type with unwired mate	
CE CONFORMANCE:	EN61010-1, EN 50081-1, EN 50082-1	

	TITLE MSC INSTRUMENTATION Multi-Channel Signal Conditioning		Entran [®] ENGLAND EUROPEAN HEADQTRS Garston, Watford, Herts Les Clayes-sous-Bois, FRANCE	
	SPECIFICATION NUMBER	ISSUE	PAGE	
	MSCS0001E	01	1 of 2	

[Figure A.8] Technical specification for the multi-channel signal conditioning MSC6.

Specifications

Parameter	Units	V2	V4	V20	V20
Power Amplifier		PA30E	PA30E	PA30E	PA100E
Sine force peak	N	9	17.8	53	100
Random force rms	N	3	5.9	17.6	33
Acceleration peak	g	91	91	32	60
Velocity peak	m/s	1.05	1.49	1.14	1.51
Displacement p-p	mm	2.5	5	10	10
Armature mass	kg	0.01	0.02	0.17	0.17
Armature diameter	mm	Spigot	Spigot	38	38
Suspension stiffness	kgf/mm	0.32	0.45	1.14	1.14
Cooling		Natural	Natural	Natural	Natural
System power utility	VA	100	100	100	200
Parameter	Units	V20	V55	V55	V55
Power Amplifier		PA300E	PA100E	PA300E	DSA1-1K
Sine force peak	N	155	142	310	444
Random force rms	N	58	50	110	160
Acceleration peak	g	90	28.9	63	90
Velocity peak	m/s	1.78	0.81	1.14	1.52
Displacement p-p	mm	10	12.7	12.7	12.7
Armature mass	kg	0.17	0.5	0.5	0.5
Armature diameter	mm	38	76.2	76.2	76.2
Suspension stiffness	kgf/mm	1.14	1.79	1.79	1.79
Cooling		Forced air	Natural	Forced air	Forced air
System power utility	VA	600	200	600	1000

<p>Options</p> <ul style="list-style-type: none"> * Beryllium copper spiders for V2 and V4 shakers to reduce axial stiffness. * Trunnions for models V4, V20 and V55. * Constant current drive for modal applications. * Three axis testing configurations for models V20 and V55. * Metric/Imperial/American table threads. 	<p>Three Axis Testing with Small Shakers</p> 
--	--

Gearing & Watson Electronics Ltd

South Road, Hailsham, East Sussex, BN27 3JJ, United Kingdom
 Tel +44 (0)1323 846464 Fax +44 (0)1323 847550
 E mail: sales@gearing-watson.com Web: www.gearing-watson.com

[Figure A.9] Technical specification for the power amplifier PA100E and the shaker V20 used during the experimental laboratory tests.

Appendix B

Geometrical Dimensions of Clamp for Vibration Measurement

The geometrical dimensions of the steering wheel clamp are presented in Figure B.1 to Figure B.3.

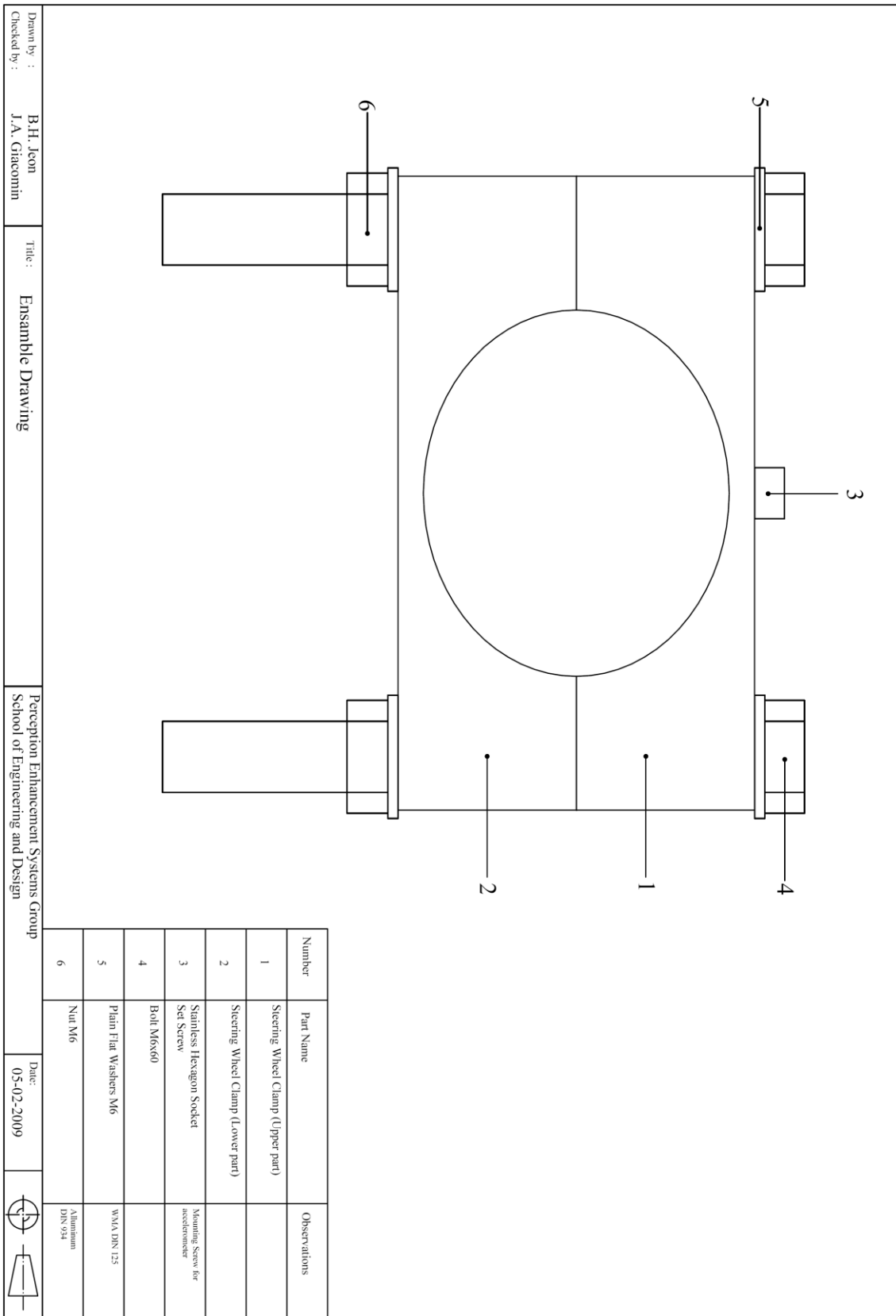


[Figure B.1] Ensemble drawing of the steering wheel clamp used to measure the steering wheel vibration for the Uxbridge test.

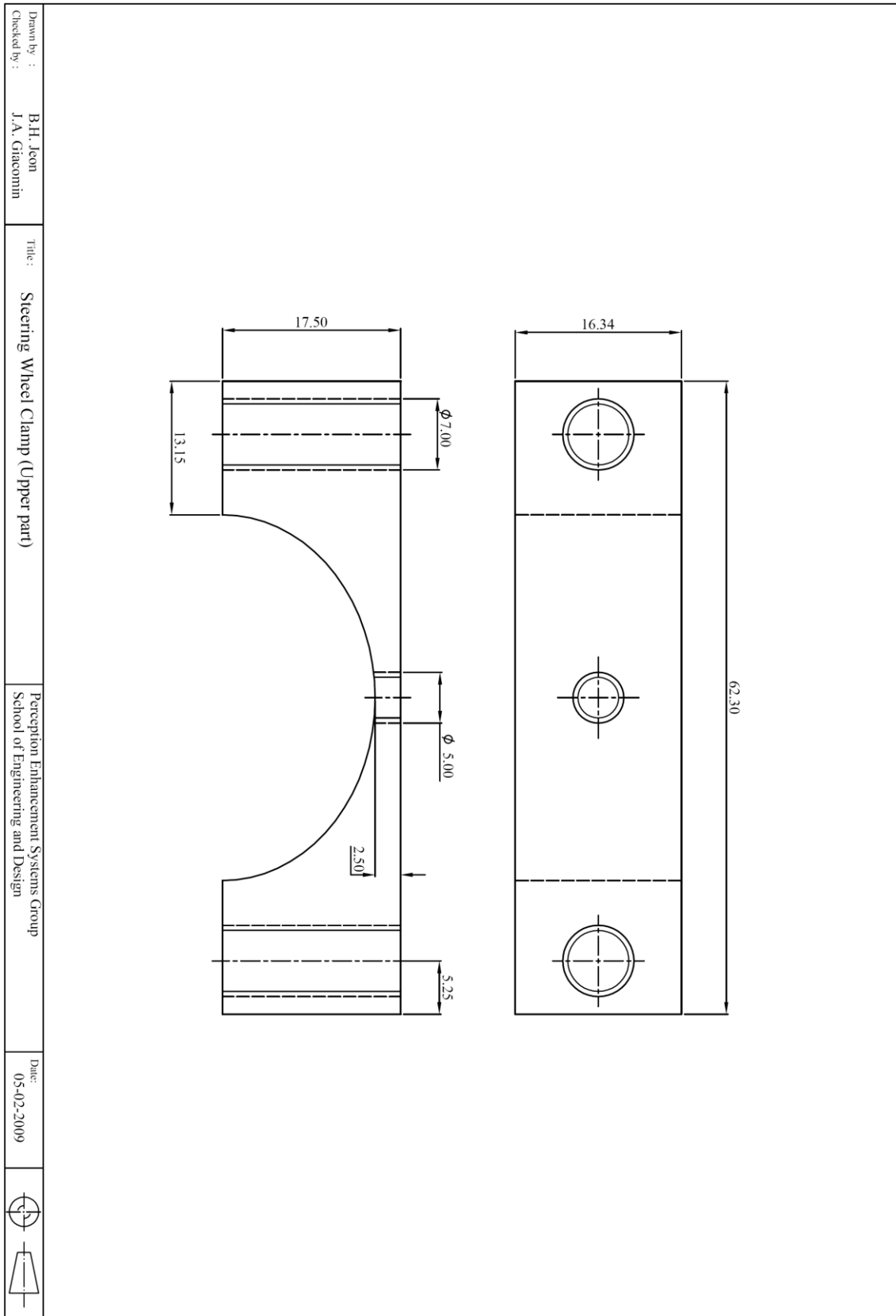


[Figure B.2] Geometrical dimensions of the upper part of the steering wheel clamp used to measure the steering wheel vibration for the Uxbridge test.

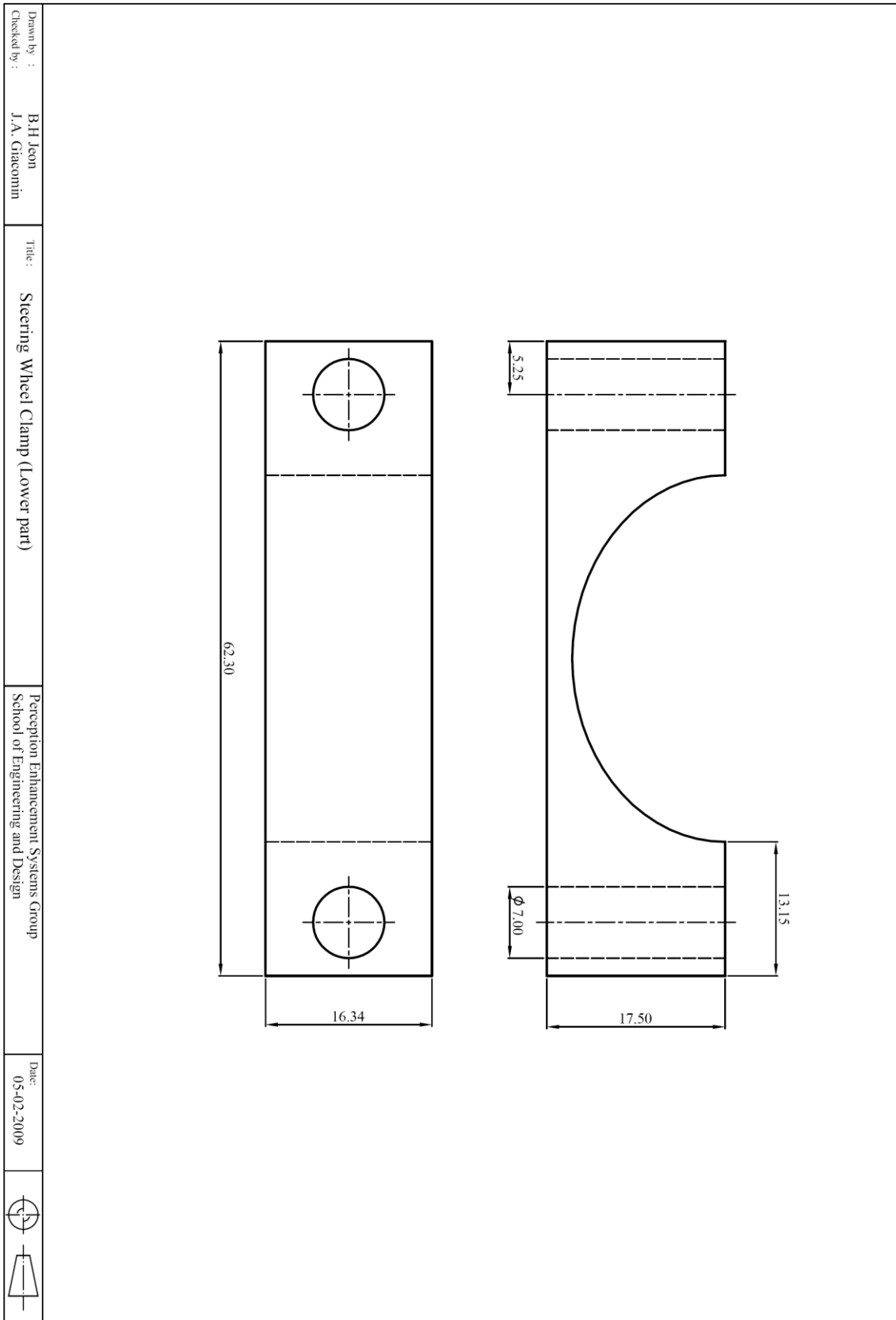


[Figure B.3] Geometrical dimensions of the lower part of the steering wheel clamp used to measure the steering wheel vibration for the Uxbridge test.

Appendix C

Laboratory Test Sheets

Laboratory test sheets used in psychophysical experimental tests for the test participants are presented. A consent form is presented in Figure C.1, a test participant information form is presented in Figure C.2, a test instruction is presented in Figure C.3 and an example of the answer tables is presented in Figure C.4.



Consent to test of Human Perception of Steering Wheel Vibration

Please read carefully the information below which summarises the experiment which you are being requested to perform. Please tick appropriate box and indicate your agreement to participate by providing your signature and the date at the bottom.

The purpose of this experiment is to investigate the human perception of hand-arm vibration. You will be asked to sit in a specially-designed simulator where you will be exposed to rotational steering wheel vibrations similar in level to those experienced in automobiles. The simulator is equipped with hardware and software systems which limit the vibration of the equipment in accordance with the health and safety guidelines specified by *British Standard 7085 Safety aspects of experiments in which people are exposed to mechanical vibration*.

The experiment will last approximately 60 minutes, in which time you will be exposed to a set of vibration stimuli. Each trial consists of a vibration exposure lasting 7-seconds. You will be asked to indicate the perceived intensity of the steering wheel vibration using a rating scale. All information will be used for statistical analyses only and will remain strictly confidential.

		Please tick appropriate box	
		YES	NO
Have you read the Research Participant Information Sheet ?		<input type="checkbox"/>	<input type="checkbox"/>
Have you had an opportunity to ask questions and discuss this study ?		<input type="checkbox"/>	<input type="checkbox"/>
Have you received satisfactory answers to all your questions ?		<input type="checkbox"/>	<input type="checkbox"/>
Do you understand that you will not be referred to by name in any report concerning the study ?		<input type="checkbox"/>	<input type="checkbox"/>
Do you understand that you are free to withdraw from the study:			
- at any time ?		<input type="checkbox"/>	<input type="checkbox"/>
- without having to give a reason for withdrawing ?		<input type="checkbox"/>	<input type="checkbox"/>
I agree to participate in the vibration perception experiment which has just been described to me both verbally and in writing.			
Signature: _____	Date : _____ / _____ / 2009		

Experimenter's detail: Mr Byung-Ho Jeon, PhD Researcher.
Perception Enhancement Systems Research Group, School of Engineering and Design, Brunel University.
Laboratory Room TA043, telephone: ext. 76012, e-mail: byung-ho.jeon@brunel.ac.uk

[Figure C.1] A consent form used in the psychophysical laboratory tests for the test participants.

Test Participant Information Form

Section A - Personal Details

Full Name: _____ Age (years): _____

Sex: Male Female

Height (m): _____ Weight (kg): _____

Section B - Information About You...

1. Do you drive a vehicle on a regular basis?

Yes No

2. Are you often exposed to vibrations, or do you regularly use vibration-producing tools as part of work or hobbies (i.e. tractors, drills)?

Yes No

If Yes, please specify: _____

3. Do you have any physical condition which you feel may affect your vibration test responses?

Yes No

If Yes, please specify: _____

4. Did you consume alcohol or coffee in the last hour before the experiment?

Yes No

If Yes, please specify: _____

If you would be prepared to participate in future research, your contact details would be greatly appreciated:

Email address: _____

[Figure C.2] A test participant information form used in the psychophysical laboratory tests for the test participants.

Test Instructions

- Welcome**, thank you for taking part in this experiment.
- The **purpose** of this experiment is to investigate the human perception of hand-arm steering wheel vibration in automobile. The experiment will be performed using the steering wheel **simulator** that you see in front of you. This simulator consists of a rigid frame, a rigid steering wheel, an automobile seat, an electrodynamic shaker unit, a power amplifier and a signal generator.
- The simulator has **numerous features / which guarantee your safety**. The control software has built-in safety limits which restrict the maximum vibration output to safe values. The power amplifier has similar limiting circuits, and the vibrator is incapable of physically exceeding health and safety limits.
- If at any time before or during the experiment you should decide that you wish to **stop**, please state this and the procedure will be brought to a halt.
- I would like now to ask if you can please read **carefully** and complete a **consent form** and a **personal data form** for the experiment. It's particularly important that you provide a signature to authorize your participation in my research study.
- Please now remove any articles of **heavy clothing**, any **watches** and any **jewellery, glasses** or other items, which might effect your perception of hand-arm vibration.
- Please now sit in the simulator and adjust the **sitting posture** to the **same position** as you are driving. Please don't touch the simulator frame with your legs or feet.
- Please now **hold the steering wheel in the middle of the hand grips** using both hands, avoiding touching the lower or upper arms. Please pay particular attention to the **arm position**, meaning the elbow and wrist angles. You should try to adopt a posture which is as close as possible to the one you use in your own automobile. Please **maintain a constant palm grip** on the steering wheel similar to that adopted when driving your own automobile over on a winding country road during the complete time of the test.
- Ok, now I will explain **how to use the rating scale**.
- Please use the scale which is shown on the board in front of you to rate your perception of the intensity of the vibration signals. By intensity, I mean how large you perceive the vibration to be.
- As you can see from the board, the scale stretches from "nothing at all" (0) to "absolute maximum"
- **"Extremely strong—Max P"** (10) is used to represent the strongest perception of the intensity of the vibration that YOU have ever experienced in your life in any situation. Use that feeling as your 10 point score. P is for perception.
 - **"Absolute maximum"**: is indicated by a dot "•", provides an opportunity for estimating the intensity of any test stimuli which exceed YOUR biggest past experience. If you consider that one of the test stimuli feels larger than 10, you may use any number above 10, such 11, 12 or even higher.
 - **"Extremely weak"** which corresponds to a value of 0.5 on the scale is something just noticeable, i.e., something that is on the boundary of what is possible to perceive.
- Please use the scale in the following way:
1. Always start by looking at the verbal expressions.
 2. Then choose a number.
 3. If your perception corresponds to "very weak", say 1. If it is "moderate", say 3, and so on.
 4. You may use whatever numbers you wish such as half values like 1.5 or 3.5, or decimals, e.g., 0.3, 1.7, 5.6, or 11.5.
 5. It is very important that you answer what you perceive and not what you might feel pressured to answer.
 6. Please be as honest as possible and try not to overestimate or underestimate the perceived vibration. It is your own perception of intensity that is important, not how it compares to other people's. What other people think is not important.
 7. Please remember to start by looking at the verbal expressions before every rating, and then decide a number.
- In order to familiarise with the test procedure you will now be asked after the calibration to judge 3 trial stimuli which are examples of a high intensity stimulus, a low intensity stimulus and an intermediate intensity stimulus of the type used in all the experiments.
- Do you have any questions before the formal testing starts?
- On each trial a 7-second vibrational signal will be presented at the steering wheel simulator. After each stimuli please express your judgement of perceived intensity by using the rating scale. There will be a 5 second gap between each stimulus, which should provide enough time for choosing an intensity value.
- The whole test contains **3 sets of 44 stimuli** each. The total test duration is approximately 30 minutes. **After every 11 stimuli** you will have a pause of **5 seconds** to relax your hands, and **after each set of 44 stimuli** you will have a pause of **1 minute**.
- Please position the ear protectors until they completely cover your ears. This measure is taken to ensure that your responses to the vibration stimuli are not affected by any sounds that you might hear. During the whole period of testing **it is very important that you do not shift your eyes around the room**. Please keep your eyes on the scale in front of you.
- Are you ready?
- Ok, now the **testing is complete**. Thank you very much for having taken part in this experiment.

[Figure C.3] An example of a test instruction for the test participants.

Name : _____ date : _____
 Nb : _____ time : _____
 Test order : _____ trial : _____

Sinusoidal stimuli

	Playlist 1			Playlist 2			Playlist 3		
	Frequency (Hz)	Acceleration r.m.s (m/s ²)	Subjective response	Frequency (Hz)	Acceleration r.m.s (m/s ²)	Subjective response	Frequency (Hz)	Acceleration r.m.s (m/s ²)	Subjective response
1	6.3	0.454		25	0.732		8	0.080	
2	16	1.263		10	3.921		20	0.080	
3	20	2.867		8	1.748		16	0.159	
4	8	1.748		31.5	0.364		25	6.694	
5	16	0.159		25	6.694		12.5	0.298	
6	31.5	0.364		6.3	0.454		31.5	0.364	
7	6.3	2.579		16	0.159		16	1.263	
8	20	0.080		12.5	0.298		12.5	8.000	
9	12.5	0.298		20	2.867		25	0.732	
10	10	3.921		16	1.263		6.3	0.454	
11	25	6.694		31.5	16.000		20	2.867	
12	8	0.080		20	0.080		10	3.921	
13	10	0.560		8	0.080		8	1.748	
14	12.5	8.000		6.3	2.579		6.3	2.579	
15	31.5	16.000		10	0.560		31.5	16.000	
16	25	0.732		12.5	8.000		10	0.560	
17	40	1.710		63	9.088		100	1.841	
18	100	1.841		400	6.347		63	9.088	
19	63	9.088		5	3.000		200	4.713	
20	125	4.461		40	1.710		40	0.172	
21	400	0.800		3	0.080		50	0.080	
22	125	0.060		125	4.461		4	0.318	
23	5	3.000		400	0.800		200	0.060	
24	40	0.172		63	0.853		50	3.981	
25	200	0.060		160	0.642		400	0.800	
26	200	4.713		250	1.411		5	3.000	
27	3	0.486		40	0.172		80	0.362	
28	4	0.318		200	0.060		40	1.710	
29	5	0.225		100	1.841		250	13.265	
30	80	0.362		3	0.486		3	0.080	
31	63	0.853		125	0.060		63	0.853	
32	400	6.347		50	0.080		100	0.060	
33	50	0.080		80	22.000		160	0.642	
34	3	0.080		50	3.981		5	0.225	
35	315	1.360		4	0.318		400	6.347	
36	4	1.263		80	0.362		3	0.486	
37	80	22.000		160	10.307		125	4.461	
38	160	10.307		250	13.265		315	1.360	
39	250	1.411		5	0.225		125	0.060	
40	100	0.060		100	0.060		250	1.411	
41	50	3.981		315	1.360		80	22.000	
42	160	0.642		4	1.263		4	1.263	
43	250	13.265		200	4.713		160	10.307	
44									

Name : _____ date : _____
 Nb : _____ time : _____
 Test order : _____ trial : _____

Sinusoidal stimuli

	Playlist 4			Playlist 5			Playlist 6		
	Frequency (Hz)	Acceleration r.m.s (m/s ²)	Subjective response	Frequency (Hz)	Acceleration r.m.s (m/s ²)	Subjective response	Frequency (Hz)	Acceleration r.m.s (m/s ²)	Subjective response
1	12.5	0.080		31.5	0.080		31.5	3.521	
2	20	12.000		12.5	0.08		8	0.275	
3	6.3	0.810		10	1.071		6.3	0.810	
4	16	0.634		6.3	0.810		16	0.634	
5	31.5	3.521		25	0.167		8	6.000	
6	10	0.153		16	5.017		20	0.335	
7	6.3	0.143		25	1.530		16	5.017	
8	25	0.167		8	0.275		20	12.000	
9	8	0.275		20	12.000		12.5	2.146	
10	10	1.071		31.5	3.521		25	1.530	
11	12.5	2.146		12.5	2.146		10	0.153	
12	31.5	0.080		20	0.335		12.5	0.080	
13	8	6.000		8	6.000		31.5	0.080	
14	16	5.017		16	0.634		25	0.167	
15	25	1.530		10	0.153		10	1.071	
16	20	0.335		6.3	0.143		6.3	0.143	
17	40	0.795		63	1.876		3	1.000	
18	315	8.529		125	25.000		250	0.150	
19	4	0.127		5	1.065		200	27.000	
20	100	0.782		40	7.906		125	0.336	
21	63	0.176		250	2.977		80	4.255	
22	400	3.782		4	0.127		63	1.876	
23	3	0.165		160	0.040		40	0.795	
24	200	27.000		400	3.782		100	10.197	
25	80	4.255		315	8.529		40	7.906	
26	50	0.382		3	0.165		160	1.620	
27	4	0.503		80	4.255		63	0.176	
28	63	1.876		5	0.080		80	0.070	
29	125	25.000		315	0.400		160	0.040	
30	5	1.065		200	27.000		50	0.382	
31	250	0.150		63	0.176		100	0.782	
32	100	10.197		80	0.070		315	0.400	
33	160	1.620		200	0.344		4	0.503	
34	315	0.400		3	1.000		200	0.344	
35	40	7.906		40	0.795		5	1.065	
36	3	1.000		100	10.197		4	0.127	
37	250	2.977		50	19.000		250	2.977	
38	200	0.344		160	1.620		400	3.782	
39	160	0.040		4	0.503		5	0.080	
40	125	0.336		100	0.782		3	0.165	
41	80	0.070		250	0.150		125	25.000	
42	50	19.000		125	0.336		50	19.000	
43	5	0.080		50	0.382		315	8.529	
44									

[Figure C.4] An example of the subjective response answer sheets.

Appendix D

Weighting Filters

The LMS TMON (2002) software was applied to implement constructing the frequency weighting filters by means of the FIR multi window methods which uses the design technique known as frequency sampling (LMS International Inc., 2002). In the LMS TMON software system implementation, the exact shape of the frequency weighting filters is a function of the type of window, the number of taps, the number of grid points and the sampling frequency. The term grid points used in LMS TMON software refers the cut-off break points which specify the shape of the filter. These break points are interpolated onto a dense and evenly spaced grid. Since the FIR multi window filter is not one of the standard types presented in Figure 4.9 the shape of the filter is specified as a number of grid points. Figure D.1 shows the example of 512 grid points which use a value that is a power of 2 (LMS International Inc., 2002).

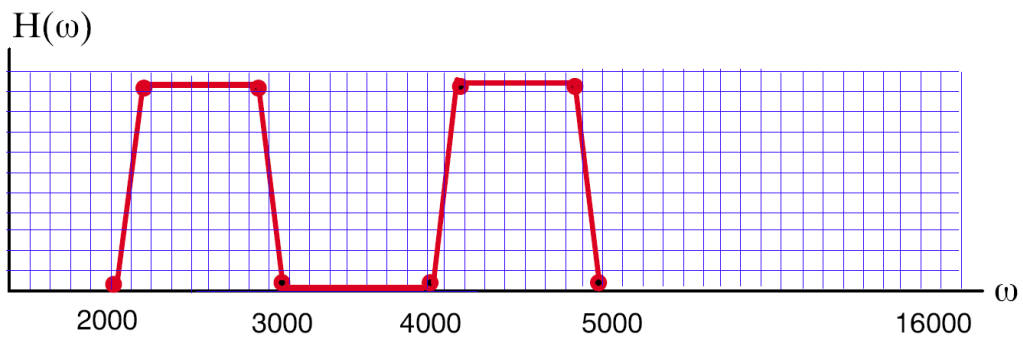


[Figure D.1] Grid points used in the FIR multi window filter (reproduced from LMS International Inc., 2002).

A rectangular window was chosen since some transient input can be reduced the level by using other types of window. A 2048 taps and 30478 grid points were assigned which were sufficient to construct filters when comparing the typical suggestion values of LMS software (LMS International Inc., 2002) suggesting 200 taps and 512 grid points. The assigned sampling frequency of 8192 Hz was also sufficient to ensure that the maximum frequency of interest of 2000 Hz for hand-arm vibration (ISO 8041, 2005).

D.1 W_h weighting filter

Figure D.2 presents the W_h frequency weighting for hand-arm vibration as described in the standards such as the International Organization for Standardization ISO 5349-1 (2001) and the British Standards Institution BS 6842 (1987). The values of the frequency weightings and tolerances shown in Table D.1 were used to check the accuracy of the filter and whether the filtered signals were within the tolerance limits a Gaussian white noise signal was filtered by applying the W_h frequency weighting. Figure D.3 presents the random W_h filtered signal to be within the tolerance limits specified.

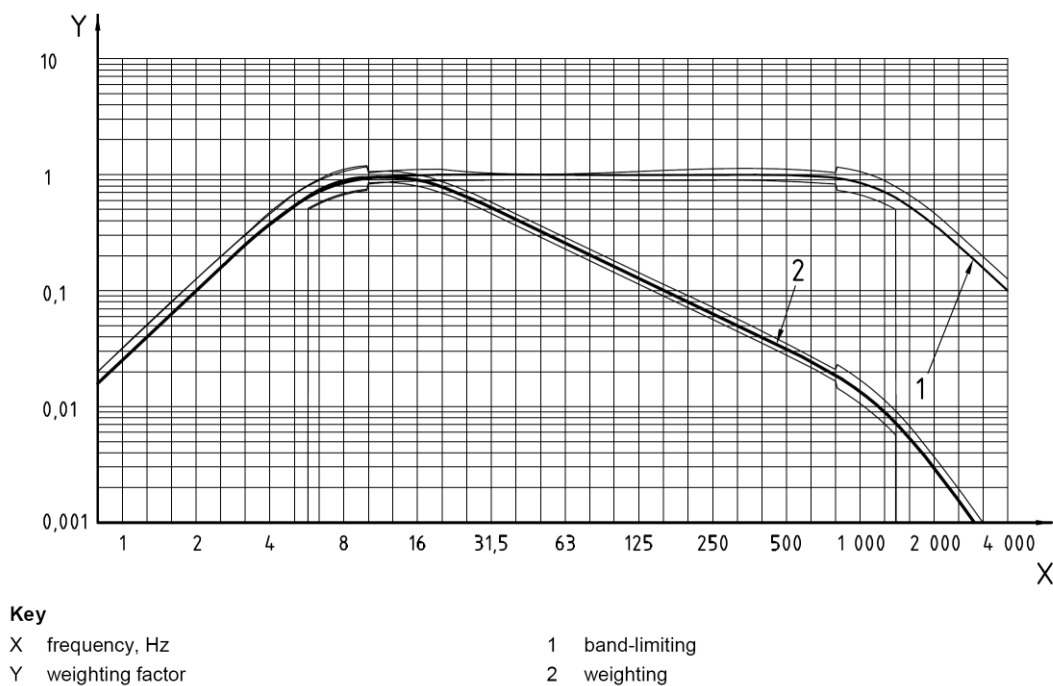


[Figure D.2] Magnitude of frequency weighting W_h for hand-arm vibration, all directions based on ISO 5349-1 (reproduced from ISO 8041, 2005).

[Table D.1] Frequency weighting W_h for hand-arm vibration, all directions (reproduced from ISO 8041, 2005).

n	Frequency Hz		Band-limiting			Weighting, W_h			Tolerance		
	Nominal	True	Factor	dB	Phase degrees	Factor	dB	Phase degrees	%	dB	$\Delta\varphi_0$ degrees
-1	0,8	0,794 3	0,015 85	-36,00	169,7	0,015 86	-36,00	168,1	+26/-100	+2/-∞	+∞/-∞
0	1	1	0,025 11	-32,00	167	0,025 14	-31,99	165	+26/-100	+2/-∞	+∞/-∞
1	1,25	1,259	0,039 78	-28,01	163,5	0,039 85	-27,99	161	+26/-100	+2/-∞	+∞/-∞
2	1,6	1,585	0,062 97	-24,02	159,1	0,063 14	-23,99	155,9	+26/-100	+2/-∞	+∞/-∞
3	2	1,995	0,099 5	-20,04	153,4	0,099 92	-20,01	149,3	+26/-100	+2/-∞	+∞/-∞
4	2,5	2,512	0,156 5	-16,11	146,1	0,157 6	-16,05	140,8	+26/-100	+2/-∞	+∞/-∞
5	3,15	3,162	0,243 6	-12,27	136,4	0,246 1	-12,18	129,7	+26/-100	+2/-∞	+∞/-∞
6	4	3,981	0,369 9	-8,64	123,7	0,375 4	-8,51	115,2	+26/-100	+2/-∞	+∞/-∞
7	5	5,012	0,533 6	-5,46	107,9	0,545	-5,27	96,7	+26/-21	+2/-2	+12/-12
8	6,3	6,31	0,707 1	-3,01	89,59	0,727 2	-2,77	74,91	+26/-21	+2/-2	+12/-12
9	8	7,943	0,845 7	-1,46	71,3	0,873 1	-1,18	51,74	+26/-21	+2/-2	+12/-12
10	10	10	0,929 1	-0,64	55,36	0,951 4	-0,43	29,15	+12/-11	+1/-1	+6/-6
11	12,5	12,59	0,969 9	-0,27	42,62	0,957 6	-0,38	7,81	+12/-11	+1/-1	+6/-6
12	16	15,85	0,987 7	-0,11	32,76	0,895 8	-0,96	-12,05	+12/-11	+1/-1	+6/-6
13	20	19,95	0,995	-0,04	25,14	0,782	-2,14	-29,71	+12/-11	+1/-1	+6/-6
14	25	25,12	0,998	-0,02	19,15	0,6471	-3,78	-44,37	+12/-11	+1/-1	+6/-6
15	31,5	31,62	0,999 2	-0,01	14,34	0,519 2	-5,69	-55,89	+12/-11	+1/-1	+6/-6
16	40	39,81	0,999 7	0,00	10,38	0,411 1	-7,72	-64,78	+12/-11	+1/-1	+6/-6
17	50	50,12	0,999 9	0,00	7,027	0,324 4	-9,78	-71,7	+12/-11	+1/-1	+6/-6
18	63	63,1	0,999 9	0,00	4,065	0,256	-11,83	-77,27	+12/-11	+1/-1	+6/-6
19	80	79,43	1	0,00	1,33	0,202 4	-13,88	-81,94	+12/-11	+1/-1	+6/-6
20	100	100	1	0,00	-1,33	0,160 2	-15,91	-86,06	+12/-11	+1/-1	+6/-6
21	125	125,9	0,999 9	0,00	-4,065	0,127	-17,93	-89,92	+12/-11	+1/-1	+6/-6
22	160	158,5	0,999 9	0,00	-7,027	0,100 7	-19,94	-93,75	+12/-11	+1/-1	+6/-6
23	200	199,5	0,999 7	0,00	-10,38	0,079 88	-21,95	-97,8	+12/-11	+1/-1	+6/-6
24	250	251,2	0,999 2	-0,01	-14,34	0,063 38	-23,96	-102,3	+12/-11	+1/-1	+6/-6
25	315	316,2	0,998	-0,02	-19,15	0,050 26	-25,97	-107,5	+12/-11	+1/-1	+6/-6
26	400	398,1	0,995	-0,04	-25,14	0,039 8	-28,00	-113,8	+12/-11	+1/-1	+6/-6
27	500	501,2	0,987 7	-0,11	-32,76	0,031 37	-30,07	-121,7	+12/-11	+1/-1	+6/-6
28	630	631	0,969 9	-0,27	-42,62	0,024 47	-32,23	-131,8	+12/-11	+1/-1	+6/-6
29	800	794,3	0,929 1	-0,64	-55,36	0,018 62	-34,60	-144,7	+12/-11	+1/-1	+6/-6
30	1 000	1 000	0,845 7	-1,46	-71,3	0,013 46	-37,42	-160,8	+26/-21	+2/-2	+12/-12
31	1 250	1 259	0,707 1	-3,01	-89,59	0,008 94	-40,97	-179,2	+26/-21	+2/-2	+12/-12
32	1 600	1585	0,533 6	-5,46	-107,9	0,005 359	-45,42	-197,5	+26/-21	+2/-2	+12/-12
33	2 000	1995	0,369 9	-8,64	-123,7	0,002 95	-50,60	-213,5	+26/-100	+2/-∞	+∞/-∞
34	2 500	2512	0,243 6	-12,27	-136,4	0,001 544	-56,23	-226,2	+26/-100	+2/-∞	+∞/-∞
35	3 150	3162	0,156 5	-16,11	-146,1	0,000 787 8	-62,07	-235,9	+26/-100	+2/-∞	+∞/-∞
36	4 000	3981	0,099 5	-20,04	-153,4	0,000 397 8	-68,01	-243,3	+26/-100	+2/-∞	+∞/-∞

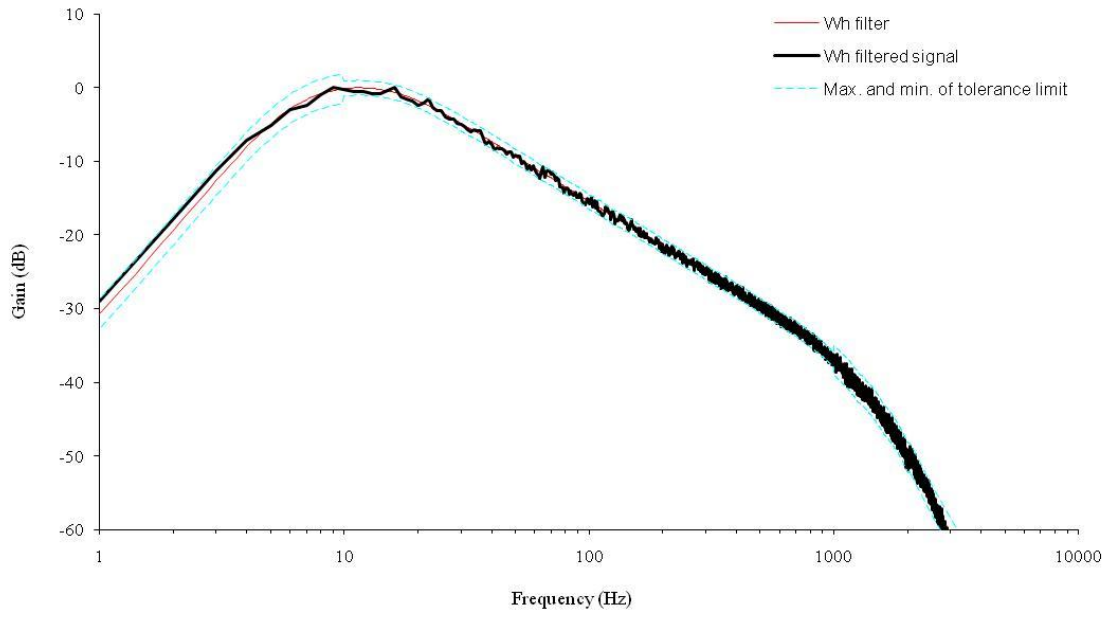


[Figure D.3] Comparison the W_h frequency weighting filter with the W_h filtered Gaussian white noise signal implemented in LMS TMON software within the maximum and minimum tolerance limits.

D.2 W_s weighting filter

Figure D.4 presents the asymptotic approximations of the W_s frequency weighting for steering wheel rotational vibration as proposed by Giacomini et al. (2004). The values of the frequency weighting shown in Table D.2 were used to construct the W_s filter digitally on LMS TMON software. To check the accuracy of the filter the Gaussian white noise signal was also filtered by applying the W_s frequency weighting. Figure D.5 presents the comparison of random W_s filtered signal and the weighting filter implemented in LMS TMON software with the maximum and minimum tolerance limits. For consistency the tolerance limits similar to those required for W_h by ISO 5349-1 and BS 6842 were adopted.

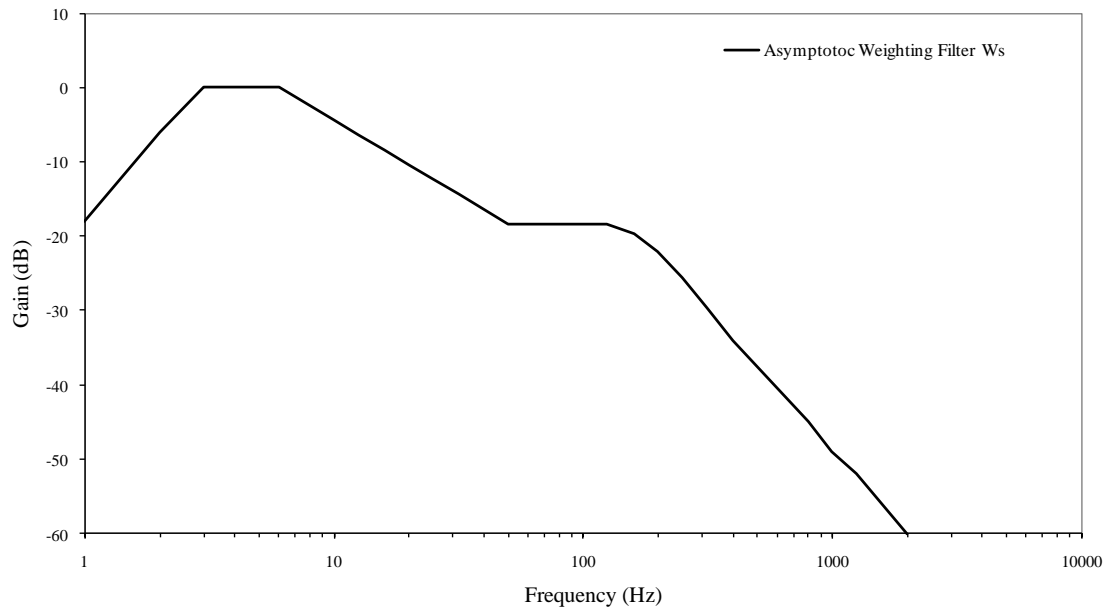


[Figure D.4] The asymptotic frequency weighting W_s for steering wheel hand-arm vibration (reproduced from Giacomini et al., 2004).

[Table D.2] Frequency weighting W_s for steering wheel rotational hand-arm vibration (adapted from Giacomini et al., 2004).

Frequency Hz	W_s weighting		Tolerance dB
	Factor	dB	
0	0	-32.01	+1/-1
1	0.126	-18	+1/-1
2	0.501	-6	+1/-1
2.5	0.9	-0.915	+1/-1
3	1	0	+1/-1
3.5	1	0	+1/-1
4	1	0	+1/-1
5	1	0	+1/-1
6	1	0	+1/-1
8	0.751	-2.482	+1/-1
10	0.602	-4.41	+1/-1
12.5	0.482	-6.34	+1/-1
16	0.377	-8.478	+1/-1
20	0.302	-10.41	+1/-1
25	0.241	-12.34	+1/-1
31.5	0.192	-14.35	+1/-1
40	0.151	-16.42	+1/-1
50	0.119	-18.47	+1/-1
63	0.119	-18.47	+1/-1
80	0.119	-18.47	+1/-1
100	0.119	-18.47	+1/-1
125	0.119	-18.47	+1/-1
160	0.105	-19.62	+1/-1
200	0.078	-22.12	+1/-1
250	0.053	-25.5	+1/-1
315	0.033	-29.6	+1/-1
400	0.02	-34	+1/-1
500	0.012	-38.42	+1/-1
630	0.008	-42.5	+1/-1
800	0.005	-46.02	+1/-1
1000	0.003	-50.46	+2/-2
1250	0.002	-53.98	+2/-2
2000	0.001	-60	+2/-2

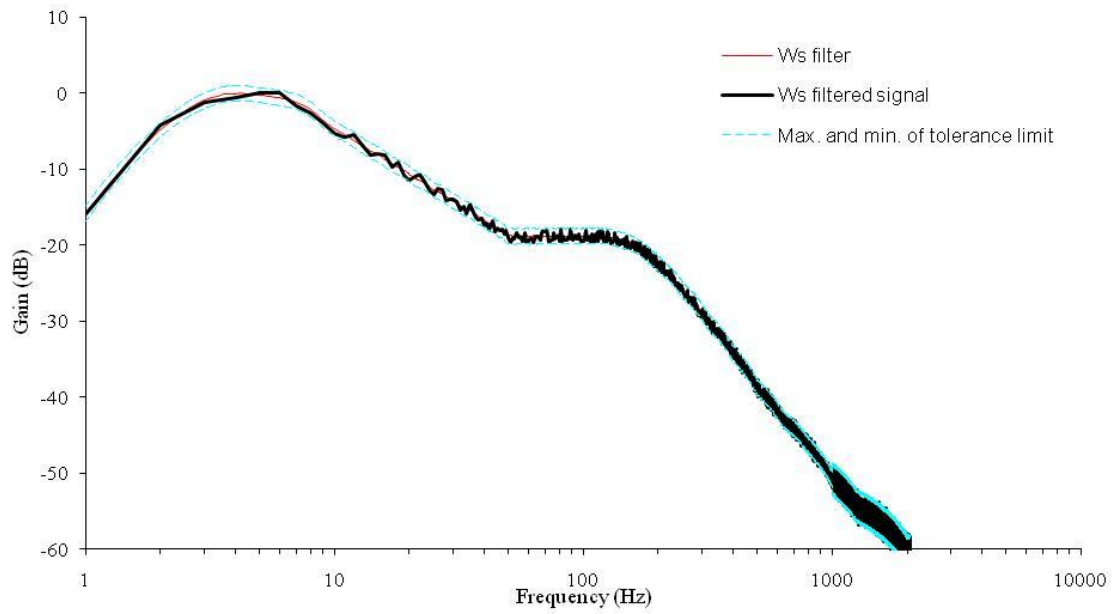


[Figure D.5] Comparison the W_s frequency weighting filter with the W_s filtered Gaussian white noise signal implemented in LMS TMON software within the maximum and minimum tolerance limits.

D.3 W_{ss_n} weighting filters

Figure D.6 presents the W_{ss_n} frequency weightings for steering wheel rotational vibration as developed from the equal sensation curves using sinusoidal vibration in the present research study. The numeral suffixes 'n' next to the letter Wss represents the Borg values of perceived intensity ($n = 0.5, 1.0, 1.5, 2.0, 2.5, 3.0, 4.0, 5.0, 6.0, 7.0, 8.0$). The values of the frequency weightings shown in Table D.3 were used to construct the W_{ss_n} filters digitally also on LMS TMON Software. The accuracy of the filters was also checked by filtering the Gaussian white noise signal by means of each W_{ss_n} frequency weighting. Figure D.7 presents the comparisons of the $W_{ss_{0.5}}$ filtered signals and the $W_{ss_{0.5}}$ weighting filters with the maximum and minimum tolerance limits which also adopted to those required for the W_h weighting while Figure D.8 presents the same comparisons of all the W_{ss_n} filtered signals and all the W_{ss_n} weighting filters with their maximum and minimum tolerance limits.

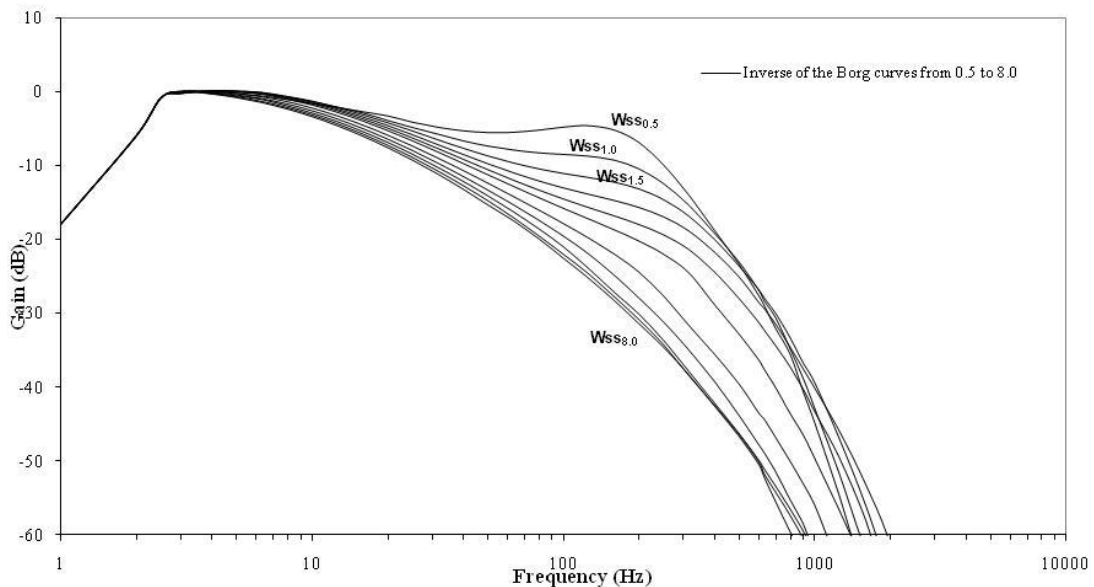


[Figure D.6] The W_{ss_n} frequency weightings obtained from equal sensation curves using band-limited random steering wheel rotational vibration.

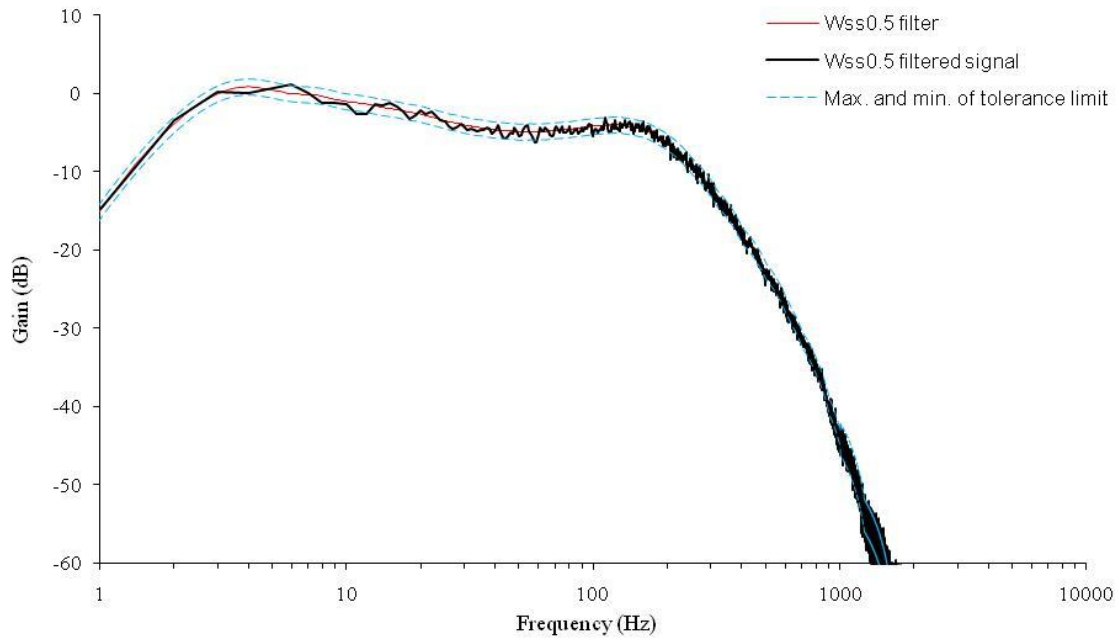


[Figure D.7] Comparison the $W_{ss0.5}$ frequency weighting filter with the $W_{ss0.5}$ filtered Gaussian white noise signals implemented in LMS TMON software within the maximum and minimum tolerance limits

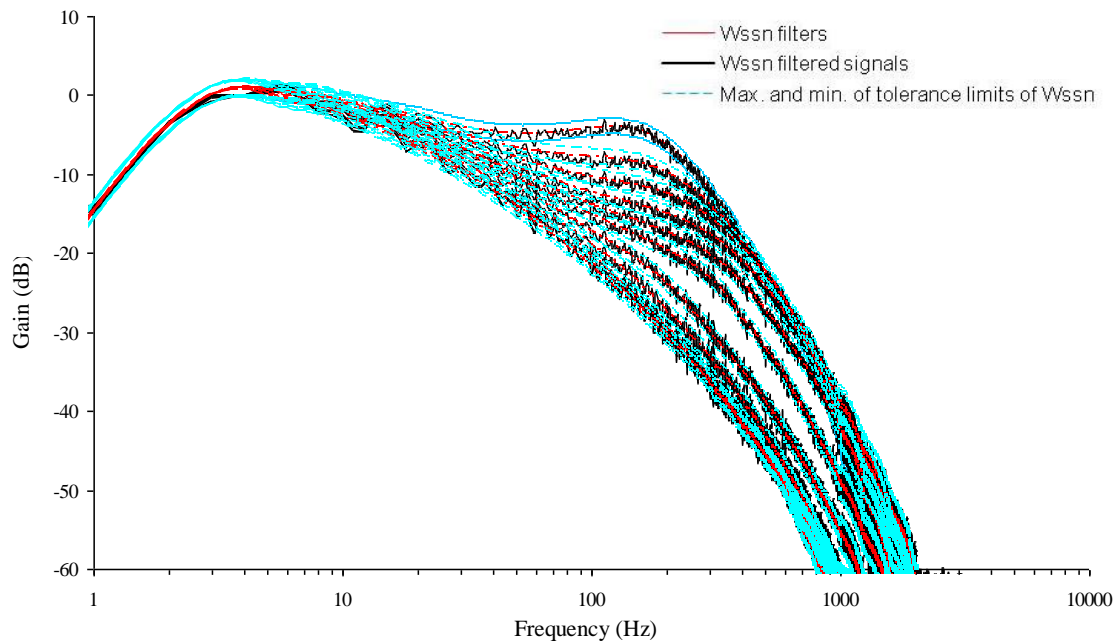


[Figure D.8] Comparison the W_{ss_n} frequency weighting filters with the W_{ss_n} filtered Gaussian white noise signals implemented in LMS TMON software within the maximum and minimum tolerance limits

D.4 W_{sr_n} weighting filters

Figure D.9 presents the W_{sr_n} frequency weightings for steering wheel rotational vibration as developed from the equal sensation curves using band-limited random vibration in the present research study. The values of the frequency weightings shown in Table D.4 were used to construct the W_{sr_n} filters digitally also on LMS TMON Software. The accuracy of the filters was also checked by filtering the Gaussian white noise signal by means of each W_{sr_n} frequency weighting. Figure D.10 presents the comparisons of the $W_{sr_{0.5}}$ filtered signals and the $W_{sr_{0.5}}$ weighting filters with the maximum and minimum tolerance limits which also adopted to those required for the W_h weighting while Figure D.11 presents the same comparisons of all the W_{sr_n} filtered signals and all the W_{sr_n} weighting filters with their maximum and minimum tolerance limits.

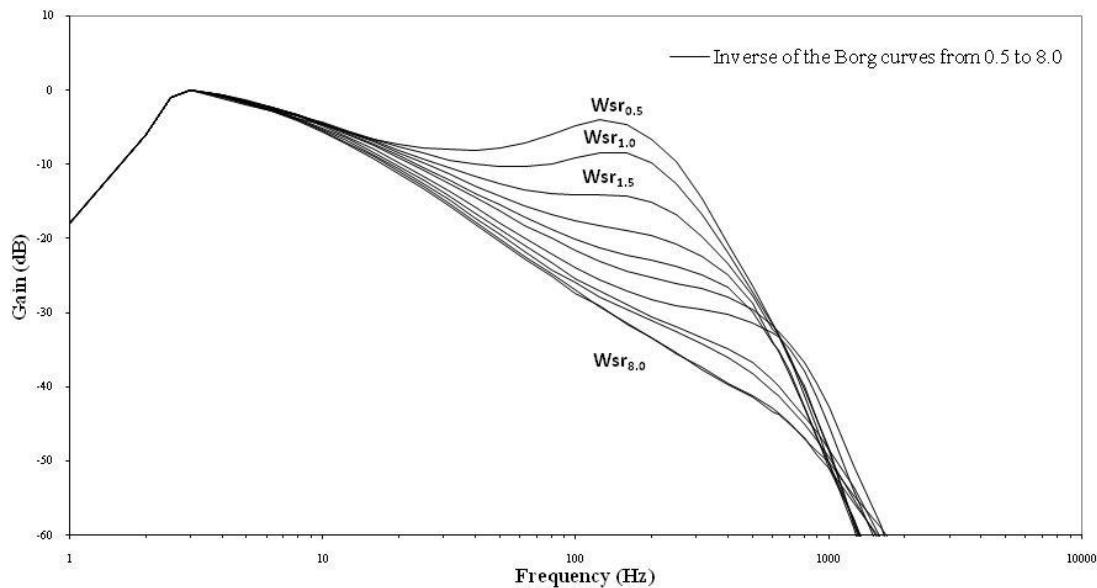


[Figure D.9] The W_{sr_n} frequency weightings obtained from equal sensation curves using band-limited random steering wheel rotational vibration.

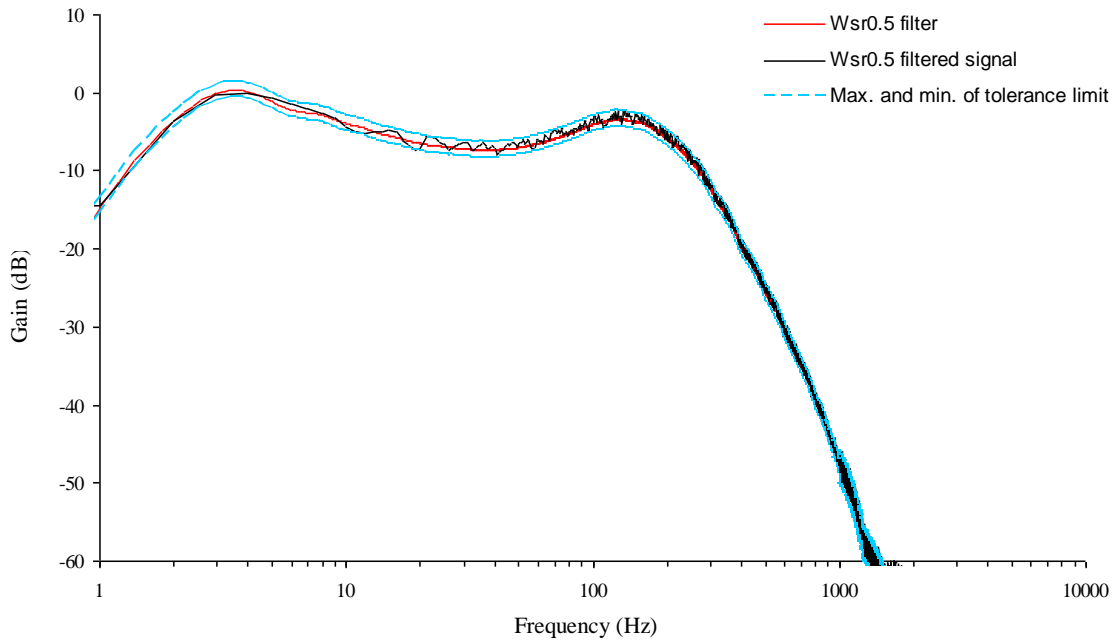


[Figure D.10] Comparison the $W_{sr_{0.5}}$ frequency weighting filters with the $W_{sr_{0.5}}$ filtered Gaussian white noise signals implemented in LMS TMON software within the maximum and minimum tolerance limits

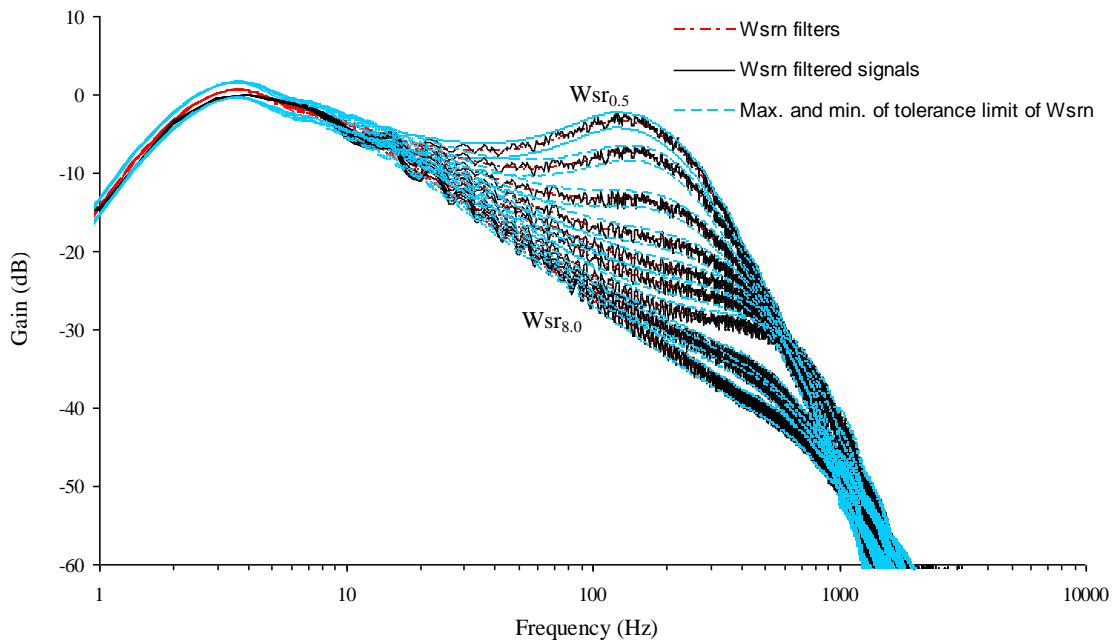


[Figure D.11] Comparison the W_{sr_n} frequency weighting filters with the W_{sr_n} filtered Gaussian white noise signals implemented in LMS TMON software within the maximum and minimum tolerance limits.

[Table D.3] Frequency weightings W_{ss_n} for steering wheel rotational hand-arm vibration.

Frequency	W _{ss_n} weightings																						Tolerance
	W _{ss0.5}		W _{ss1}		W _{ss1.5}		W _{ss2}		W _{ss2.5}		W _{ss3}		W _{ss4}		W _{ss5}		W _{ss6}		W _{ss7}		W _{ss8}		
Hz	Factor	dB	Factor	dB	Factor	dB	Factor	dB	Factor	dB	Factor	dB	Factor	dB	Factor	dB	Factor	dB	Factor	dB	Factor	dB	dB
0	0	-32	0	-32	0	-32	0	-32	0	-32	0	-32	0	-32	0	-32	0	-32	0	-32	0	-32	+1/-1
1	0.126	-18	0.126	-18	0.126	-18	0.126	-18	0.126	-18	0.126	-18	0.126	-18	0.126	-18	0.126	-18	0.126	-18	0.126	-18	+1/-1
2	0.501	-6	0.501	-6	0.501	-6	0.501	-6	0.501	-6	0.501	-6	0.501	-6	0.501	-6	0.501	-6	0.501	-6	0.501	-6	+1/-1
2.5	0.9	-0.915	0.9	-0.92	0.9	-0.92	0.9	-0.92	0.9	-0.92	0.9	-0.92	0.9	-0.92	0.9	-0.92	0.9	-0.92	0.9	-0.92	0.9	-0.92	+1/-1
3	1	0	1	0	1	0	1	0	1	0	1	0	1	0	1	0	1	0	1	0	1	0	+1/-1
4	1	0	0.889	-1.02	0.917	-0.75	0.928	-0.65	0.923	-0.69	0.925	-0.68	0.922	-0.71	0.918	-0.74	0.914	-0.78	0.909	-0.83	0.905	-0.87	+1/-1
5	0.975	-0.218	0.811	-1.82	0.837	-1.55	0.851	-1.4	0.851	-1.4	0.854	-1.37	0.847	-1.44	0.84	-1.51	0.833	-1.59	0.825	-1.67	0.818	-1.74	+1/-1
6.3	0.937	-0.562	0.737	-2.65	0.755	-2.44	0.77	-2.28	0.773	-2.23	0.77	-2.27	0.761	-2.38	0.75	-2.49	0.74	-2.62	0.73	-2.73	0.721	-2.84	+1/-1
8	0.885	-1.059	0.668	-3.51	0.675	-3.41	0.687	-3.26	0.681	-3.34	0.678	-3.38	0.665	-3.54	0.652	-3.72	0.639	-3.89	0.628	-4.05	0.617	-4.19	+1/-1
10	0.830	-1.616	0.607	-4.34	0.603	-4.4	0.603	-4.39	0.597	-4.48	0.591	-4.56	0.575	-4.81	0.559	-5.05	0.545	-5.27	0.533	-5.46	0.523	-5.64	+1/-1
12.5	0.784	-2.113	0.533	-5.47	0.528	-5.55	0.526	-5.58	0.516	-5.75	0.507	-5.9	0.488	-6.24	0.471	-6.54	0.456	-6.81	0.444	-7.05	0.434	-7.26	+1/-1
16	0.732	-2.711	0.466	-6.62	0.457	-6.8	0.446	-7	0.432	-7.29	0.42	-7.53	0.398	-8	0.381	-8.39	0.366	-8.73	0.354	-9.01	0.344	-9.26	+1/-1
20	0.687	-3.263	0.419	-7.55	0.396	-8.05	0.381	-8.39	0.363	-8.79	0.35	-9.13	0.326	-9.73	0.308	-10.2	0.295	-10.6	0.284	-10.9	0.275	-11.2	+1/-1
25	0.623	-4.106	0.376	-8.5	0.344	-9.26	0.323	-9.82	0.303	-10.4	0.288	-10.8	0.263	-11.6	0.246	-12.2	0.234	-12.6	0.224	-13	0.216	-13.3	+1/-1
31.5	0.576	-4.787	0.34	-9.38	0.299	-10.5	0.272	-11.3	0.249	-12.1	0.233	-12.7	0.209	-13.6	0.193	-14.3	0.181	-14.8	0.172	-15.3	0.165	-15.6	+1/-1
40	0.544	-5.288	0.315	-10	0.261	-11.7	0.227	-12.9	0.203	-13.9	0.188	-14.5	0.162	-15.8	0.148	-16.6	0.138	-17.2	0.13	-17.7	0.125	-18.1	+1/-1
50	0.530	-5.513	0.304	-10.4	0.234	-12.6	0.194	-14.2	0.168	-15.5	0.155	-16.2	0.128	-17.9	0.115	-18.8	0.106	-19.5	0.1	-20	0.095	-20.5	+1/-1
63	0.532	-5.488	0.304	-10.3	0.213	-13.4	0.167	-15.6	0.139	-17.2	0.121	-18.3	0.1	-20	0.09	-20.9	0.081	-21.8	0.076	-22.4	0.073	-22.7	+1/-1
80	0.550	-5.186	0.32	-9.9	0.201	-13.9	0.145	-16.7	0.115	-18.8	0.101	-19.9	0.079	-22.1	0.068	-23.3	0.062	-24.2	0.058	-24.7	0.056	-25.1	+1/-1
100	0.576	-4.787	0.348	-9.16	0.197	-14.1	0.131	-17.6	0.099	-20.1	0.083	-21.6	0.063	-24	0.054	-25.3	0.05	-26	0.045	-27	0.043	-27.3	+1/-1
125	0.590	-4.584	0.379	-8.42	0.196	-14.1	0.121	-18.3	0.087	-21.2	0.07	-23.1	0.052	-25.6	0.044	-27.2	0.04	-27.9	0.035	-29.2	0.035	-29.1	+1/-1
160	0.550	-5.199	0.377	-8.47	0.193	-14.3	0.113	-19	0.078	-22.2	0.061	-24.4	0.044	-27.2	0.036	-28.9	0.033	-29.5	0.027	-31.4	0.027	-31.5	+1/-1
200	0.453	-6.877	0.322	-9.85	0.176	-15.1	0.104	-19.6	0.071	-22.9	0.055	-25.2	0.039	-28.2	0.03	-30.5	0.028	-31	0.021	-33.5	0.021	-33.4	+1/-1
250	0.320	-9.891	0.235	-12.6	0.144	-16.8	0.092	-20.7	0.065	-23.8	0.05	-26	0.035	-29.1	0.025	-31.89	0.023	-32.60	0.017	-35.50	0.017	-35.43	+1/-1
315	0.201	-13.95	0.145	-16.8	0.104	-19.7	0.075	-22.5	0.057	-24.9	0.046	-26.8	0.033	-29.7	0.021	-33.39	0.019	-34.30	0.013	-37.44	0.013	-37.73	+1/-1
400	0.115	-18.80	0.081	-21.9	0.068	-23.4	0.057	-24.9	0.047	-26.5	0.04	-27.9	0.031	-30.2	0.018	-34.84	0.016	-36.12	0.011	-39.49	0.010	-39.71	+1/-1
500	0.068	-23.35	0.044	-27.20	0.041	-27.82	0.036	-28.81	0.032	-29.91	0.033	-29.58	0.027	-31.35	0.014	-36.78	0.012	-38.25	0.009	-41.15	0.008	-41.45	+1/-1
630	0.036	-28.97	0.022	-33.10	0.022	-33.09	0.017	-35.26	0.018	-35.08	0.024	-32.50	0.022	-33.29	0.010	-39.89	0.009	-41.23	0.007	-43.46	0.006	-43.75	+1/-1
800	0.017	-35.59	0.009	-41.18	0.010	-39.86	0.007	-42.79	0.007	-42.73	0.015	-36.76	0.013	-37.94	0.006	-44.05	0.006	-45.00	0.004	-46.98	0.005	-46.93	+1/-1
1000	0.006	-44.80	0.003	-50.39	0.003	-48.38	0.003	-50.40	0.003	-50.93	0.007	-42.78	0.005	-45.33	0.004	-48.48	0.003	-49.50	0.003	-50.17	0.003	-51.08	+2/-2
2000	0.000	-70.48	0.000	-82.09	0.000	-86.62	0.000	-74.83	0.000	-77.87	0.000	-69.16	0.000	-70.52	0.000	-66.55	0.000	-66.58	0.001	-63.46	0.001	-65.06	+2/-2

[Table D.4] Frequency weightings W_{sr_n} for steering wheel rotational hand-arm vibration.

Frequency Hz	W_{sr_n} weightings																						Tolerance dB
	$W_{sr_{0.5}}$		W_{sr_1}		$W_{sr_{1.5}}$		W_{sr_2}		$W_{sr_{2.5}}$		W_{sr_3}		W_{sr_4}		W_{sr_5}		W_{sr_6}		W_{sr_7}		W_{sr_8}		
	Factor	dB	Factor	dB	Factor	dB	Factor	dB	Factor	dB	Factor	dB	Factor	dB	Factor	dB	Factor	dB	Factor	dB	Factor	dB	
0	0	-32	0	-32	0	-32	0	-32	0	-32	0	-32	0	-32	0	-32	0	-32	0	-32	0	-32	+1/-1
1	0.126	-18	0.126	-18	0.126	-18	0.126	-18	0.126	-18	0.126	-18	0.126	-18	0.126	-18	0.126	-18	0.126	-18	0.126	-18	+1/-1
2	0.501	-6	0.501	-6	0.501	-6	0.501	-6	0.501	-6	0.501	-6	0.501	-6	0.501	-6	0.501	-6	0.501	-6	0.501	-6	+1/-1
2.5	0.9	-0.915	0.9	-0.92	0.9	-0.92	0.9	-0.92	0.9	-0.92	0.9	-0.92	0.9	-0.92	0.9	-0.92	0.9	-0.92	0.9	-0.92	0.9	-0.92	+1/-1
3	1	0	0.962	-0.339	0.961	-0.347	0.967	-0.294	0.976	-0.209	0.984	-0.141	1	0	1	0	1	0	1	0	1	0	+1/-1
4	0.873	-1.182	1	0	1	0	1	0	1	0	1	0	1	0	0.986	-0.120	0.975	-0.216	0.966	-0.297	0.959	-0.366	+1/-1
5	0.8	-1.938	0.994	-0.048	1	0	0.997	-0.028	0.991	-0.076	0.985	-0.133	0.974	-0.226	0.952	-0.423	0.935	-0.585	0.920	-0.721	0.908	-0.837	+1/-1
6.3	0.727	-2.766	0.963	-0.326	0.980	-0.177	0.975	-0.222	0.955	-0.399	0.955	-0.399	0.925	-0.676	0.897	-0.944	0.884	-1.069	0.856	-1.349	0.841	-1.508	+1/-1
8	0.649	-3.76	0.910	-0.823	0.919	-0.735	0.907	-0.847	0.895	-0.968	0.881	-1.104	0.855	-1.357	0.823	-1.692	0.797	-1.968	0.776	-2.202	0.758	-2.402	+1/-1
10	0.585	-4.651	0.848	-1.436	0.856	-1.348	0.838	-1.534	0.822	-1.699	0.806	-1.877	0.776	-2.199	0.742	-2.588	0.715	-2.910	0.693	-3.183	0.675	-3.417	+1/-1
12.5	0.521	-5.66	0.782	-2.139	0.777	-2.186	0.758	-2.407	0.741	-2.609	0.722	-2.832	0.690	-3.217	0.656	-3.658	0.629	-4.023	0.607	-4.331	0.589	-4.598	+1/-1
16	0.469	-6.573	0.709	-2.987	0.689	-3.234	0.666	-3.533	0.645	-3.808	0.626	-4.074	0.593	-4.535	0.560	-5.035	0.534	-5.446	0.513	-5.796	0.496	-6.098	+1/-1
20	0.432	-7.282	0.632	-3.986	0.610	-4.287	0.584	-4.673	0.561	-5.015	0.541	-5.335	0.508	-5.874	0.477	-6.430	0.453	-6.888	0.433	-7.276	0.416	-7.612	+1/-1
25	0.411	-7.731	0.567	-4.921	0.539	-5.370	0.507	-5.902	0.483	-6.323	0.462	-6.703	0.430	-7.331	0.400	-7.952	0.377	-8.462	0.359	-8.897	0.344	-9.273	+1/-1
31.5	0.397	-8.031	0.512	-5.807	0.470	-6.552	0.436	-7.215	0.410	-7.739	0.389	-8.197	0.357	-8.939	0.329	-9.644	0.308	-10.22	0.291	-10.71	0.277	-11.14	+1/-1
40	0.395	-8.06	0.460	-6.746	0.411	-7.732	0.372	-8.581	0.345	-9.237	0.324	-9.795	0.292	-10.68	0.266	-11.50	0.246	-12.17	0.231	-12.74	0.218	-13.23	+1/-1
50	0.409	-7.769	0.425	-7.436	0.365	-8.758	0.323	-9.820	0.294	-10.63	0.272	-11.30	0.241	-12.37	0.216	-13.33	0.197	-14.10	0.183	-14.77	0.171	-15.35	+1/-1
63	0.442	-7.084	0.399	-7.971	0.327	-9.700	0.281	-11.03	0.250	-12.03	0.228	-12.86	0.196	-14.16	0.172	-15.29	0.154	-16.23	0.141	-17.03	0.134	-17.45	+1/-1
80	0.503	-5.966	0.382	-8.360	0.298	-10.52	0.247	-12.16	0.214	-13.40	0.190	-14.43	0.158	-16.05	0.134	-17.44	0.118	-18.59	0.105	-19.55	0.101	-19.95	+1/-1
100	0.577	-4.778	0.373	-8.571	0.278	-11.13	0.222	-13.09	0.186	-14.60	0.161	-15.85	0.128	-17.86	0.105	-19.57	0.089	-21.00	0.079	-22.02	0.075	-22.55	+1/-1
125	0.627	-4.048	0.363	-8.797	0.261	-11.66	0.201	-13.92	0.164	-15.72	0.137	-17.24	0.103	-19.75	0.080	-21.91	0.064	-23.85	0.059	-24.57	0.055	-25.17	+1/-1
160	0.583	-4.683	0.340	-9.363	0.242	-12.33	0.182	-14.81	0.143	-16.91	0.115	-18.78	0.079	-22.03	0.057	-24.92	0.044	-27.20	0.041	-27.81	0.038	-28.33	+1/-1
200	0.468	-6.598	0.297	-10.54	0.218	-13.23	0.163	-15.73	0.125	-18.06	0.097	-20.28	0.060	-24.45	0.040	-27.97	0.031	-30.12	0.029	-30.85	0.027	-31.43	+1/-1
250	0.332	-9.579	0.237	-12.51	0.185	-14.66	0.141	-16.99	0.107	-19.44	0.079	-22.05	0.041	-27.66	0.028	-31.18	0.021	-33.64	0.019	-34.23	0.019	-34.55	+1/-1
315	0.188	-14.54	0.169	-15.42	0.143	-16.88	0.114	-18.90	0.085	-21.42	0.059	-24.55	0.026	-31.63	0.018	-34.96	0.013	-37.83	0.012	-38.38	0.012	-38.27	+1/-1
400	0.091	-20.78	0.109	-19.26	0.099	-20.07	0.081	-21.79	0.060	-24.51	0.036	-28.91	0.017	-35.59	0.011	-39.30	0.008	-42.16	0.008	-42.46	0.007	-42.55	+1/-1
500	0.048	-26.38	0.070	-23.12	0.066	-23.65	0.056	-25.11	0.040	-28.07	0.023	-32.86	0.010	-39.59	0.006	-43.86	0.005	-46.26	0.005	-46.38	0.005	-46.62	+1/-1
630	0.023	-32.82	0.038	-28.38	0.040	-27.97	0.034	-29.39	0.024	-32.35	0.013	-37.63	0.006	-44.38	0.004	-48.93	0.003	-51.06	0.003	-51.71	0.002	-52.15	+1/-1
800	0.010	-40.35	0.018	-34.92	0.021	-33.37	0.019	-34.65	0.014	-37.34	0.007	-43.65	0.003	-50.13	0.002	-55.34	0.001	-56.52	0.001	-57.36	0.001	-59.58	+1/-1
1000	0.004	-48.65	0.007	-42.87	0.011	-39.40	0.010	-40.13	0.007	-43.36	0.003	-49.67	0.002	-56.02	0.001	-62.28	0.001	-62.54	0.001	-64.10	0.001	-64.44	+2/-2
2000	0.000	-74.33	0.000	-87.56	0.001	-65.86	0.001	-61.18	0.000	-68.07	0.000	-70.59	0.000	-69.57	0.000	-70.24	0.000	-68.56	0.000	-68.19	0.000	-67.54	+2/-2

